SOME STUDIES IN OPTIMUM AND SELF-ADAPTIVE CONTROL SYSTEMS

by

K.K. Murthy, B.E., M.E.

A thesis submitted to the University of Warwick for the degree of Doctor of Philosophy

School of Engineering Science

June, 1967.

CONTAINS PULLOUTS

C O N T E N T S

ACKNOWLEDGEMENTS

The author wishes to acknowledge with gratitude the continual guidance and encouragement of Professor J.L. Douce and Dr. K.C. Ng and expresses his appreciation of the many helpful discussions with his colleagues, during the course of the work described in this thesis. The author is also grateful to the Commonwealth Scholarship Commission in the United Kingdom for the Scholarship award and to the Board of Governors of the Regional Engineering College, Durgapur, for the grant of leave of absence for the duration of this work.

PREFACE

This thesis presents the results of a three year research project carried out by the author from October, 1964 to June, 1967 while a Commonwealth Scholar in this country.

The contents of the thesis are divided into three parts.

Part I describes the analytical and experimental studies on a second-order bang-bang servo under non-ideal operating conditions. The sensitivity and stability of the bang-bang system have been investigated. This work was carried out during 1964-65 while a research scholar at the Queen's University of Belfast.

Part II of the thesis is entitled "Self-optimisation using Pseudo-Random Binary Sequences". In this part, the performance of the original hill-climbing system which employs discontinuous parameter adjustment and of the modified system using continuous parameter adjustment is described. It is shown that the system with continuous parameter adjustment has a superior performance. A novel analogue running averager has been developed which is simple and inexpensive.

Part III describes an investigation into the frequency response of a sample-and-hold element at certain sampling frequencies.

As a result of the work described, three papers have been published and a fourth one has been accepted for publication.

1. "A Note on the Performance of the Second-order Maximum Effort Controller", K.K. Murthy, International Journal of Control, Vol.2, No.3, September, 1965.

2. "An Electro-Mechanical Running Averager", K.C. Ng and K.K. Murthy, Electronic Engineering, March, 1967.

3. "Recent Advances in a Hill-climbing System", K.C. Ng, K.K. Murthy, D.H. Stockwell and K.R. Morris, Second I.E.E. Convention on Advances in Computer Control, Bristol, April, 1967.

(Paper 1 is based on Part I and papers 2 and 3 are based on part II)

4. "Frequency Response of Linear Sampled-Data Control Systems", J.L. Douce, K.C. Ng and K.K. Murthy. This paper has been

accepted for publication in 'Control'.

(This paper is based on part III)

All the published papers are enclosed in the thesis.

P A R T I

PERFORMANCE OF THE SECOND-ORDER RELAY SERVO UNDER NON-IDEAL OPERATING CONDITIONS

SUMMARY

The behaviour of a second-order bang-bang control system when the system parameters are varied is investigated. For non-ideal operating conditions, the response of the bang-bang servo is compared with that of a saturating servo. The sensitivity of the bang-bang servo for variations in the system dynamics has been examined. The stability of the system in the presence of additional time delays and time lags is investigated. Analogue computer results agree with the theoretical predictions.

LIST OF PRINCIPAL SYMBOLS

θ_i = Input position and input signal.

θ_o = Output position and output signal.

x, x_1 = $\theta_o - \theta_i$ = θ_e = Error signal.

$\dot{\theta}_o$ = x_2 = y = Output velocity.

u, u_1 = Control signal.

a = Maximum developed torque.

ω_o = $\frac{1}{T}$ = Undamped resonance frequency.

T_1 = Motor field build-up time constant.

T_D = Delay time.

T_R = Response time.

T_{AB} = Time taken to travel over the phase path AB.

K_v = Gain factor of the stabiliser.

K_1 = Gain factor of the error processing non-linearity.

S = Switching function.

h_o = Initial position x(o).

K_f = Coefficient of viscous friction damping.

C = Cost function.

$\underline{w}$ = Plant parameter vector.

w_o = Nominal design value of motor acceleration.

w_p = Actual motor acceleration.

S^R = Relative sensitivity.

S^M = Maximum value of relative sensitivity.

$G(p)$ = Transfer function of the process.

$N(m)$ = Describing function.

ϕ = Phase angle of describing function.

R = Magnitude of describing function.

λ = Output signal of the relay.

1. INTRODUCTION

There are essentially two approaches to the optimal control problem. One is concerned with optimising the responses of the controlled variable to disturbances of the system to be controlled. For a single variable system, at each instant there is a known desired value of the controlled variable. The control engineer is primarily concerned with keeping the maximum error to a minimum, and then with such other aspects of the response as the number of oscillations in the transients due to step disturbances, the magnitudes of overshoots and undershoots, and their durations. He is interested in the entire response and thus simultaneously in many indexes of performance. Reduction of the maximum system error cannot normally be achieved regardless of the magnitude of a step change, over the reduction that can be attained with linear control functions. Tests have shown that simple non-linear control functions definitely improve system response.

The early control engineers intuitively assumed that any control system error which did not demand the maximum control effort could be corrected faster

if the maximum available control effort were applied. Thus, when the control signal is constrained to take on only its maximum or minimum values, it is called a 'Steering Function'. Minimum response time is obtained only if the sign of the steering function is caused to change in the proper manner.

A 'Switching Function' is the function of the controlled variable and its derivatives that defines all the instants at which the steering or control function must change sign for minimum response time.

A lot of work has been done on these optimum switched systems. Minimum response time control was obtained for an Aircraft engine propeller system as early as 1944 by Oldenberger[1]. In 1950, Mcdonald[2] published a paper on the on-off time optimal control of second-order systems with bounded inputs. This was followed in 1951 by phase plane, topological and analogue computer studies of the same system by Hopkin[3], Uttley and Hammond[4]. Flugg-Lotz[5] published a book in 1951 on the bang-bang control of second-order systems with linear switching functions. West et al[6] in 1954 proposed a method of mechanising the bang-bang control of a second-order system. Many

authors have derived optimum switching functions for higher order control systems[7,8].

The second approach to the optimal control problem is essentially a mathematical one. Bushaw[14] in 1953, originated this approach. In 1956, Bellman et al[9] gave a general treatment of the optimal problem. In 1957, the Russian mathematician Pontryagin published his maximum principle explained in 1959 by Rosonoer[10]. Lasalle[11] proved that an on-off control system is the time optimal system. Since then, various authors have reported further work on the mathematics of optimal systems.

In the work being reported in this thesis, the first essentially engineering approach is taken.

The simplest example of a bang-bang servo is the relay actuated servo motor position controller. In all relay or bang-bang control systems, the system always operates under maximum actuating torque conditions. For half the time, maximum accelerating torque is developed and for the other half maximum deceleration torque is developed. In other words, the direction of the torque is reversed at exactly half way following an initial disturbance from the

state of rest. The switching trajectories for this ideal second-order system are half parabolas in the second and fourth quadrants passing through the origin. The switching from acceleration to deceleration takes place on this parabolic switching curve. Such an optimum switching can be achieved by a suitably designed non-linear error processing device[6] to actuate the relay.

The operation of such a switched relay servo system has been obtained under the following assumptions:

(i) Inputs limited to step functions.

(ii) Instantaneous switching on the change-over boundary.

(iii) No time delays present in the system.

(iv) Accurate knowledge of the motor dynamics.

The limitation on the admissible inputs is in general, severe. Bushaw[12] has shown that for the response to be optimal, only steps and ramps are admissible as inputs to the pure inertia servo and only steps are admissible inputs for the servo with inertia plus Coulomb or viscous friction. Nevertheless, West and Nikiforuk[13] have obtained the frequency

response and shown that considerable improvement in performance can be achieved for sinusoidal inputs also.

The other two assumptions tend to be in general, idealistic. In practice, instantaneous switching on the reversal curve cannot take place and finite time delays have to be taken into account. In addition, relay hysteresis, contact spacing, etc., tend to deteriorate the performance of the system. Time delays have the effect of permitting the state of the system to over-travel the switching trajectory, reverse, over-travel again and so forth. Thus the trajectory may approach a terminal limit cycle. The effect of inputs other than the ones considered in the initial system concept, can also have disturbing consequences.

These remarks emphasize the fact that the on-off control system can be extremely sensitive to variations in system parameters. The qualitative nature of the deterioration in performance under the non-ideal conditions is investigated in this work. It is compared with the performance of a saturating servo system with a small linear regime and shown that the performance of the saturating servo is superior to that of

the relay servo. The stability of the relay servo is investigated in the presence of time delays and additional lag. The sensitivity of the system for variations in the motor dynamics is examined. If the range of variations of the system parameter is known, it is shown that by suitably designing the switching curve, the response can be made to be least sensitive to these variations.

2. THE OPTIMUM SYSTEM

The system used for the analysis is schematically shown in Fig.1. The torque limited servo motor is actuated by a relay so that the motor always develops maximum torque the direction of which depends upon the position of the relay or the sign of the control signal u. Frictional forces in the motor are neglected. The transfer function can then be represented by $G(p) = 1/T^2p^2$.

The Equations of the switching curves or trajectories on which the polarity of the control signal is reversed is to be derived, since these are necessary for synthesising the controller. Either a differential equation approach or a matrix notation can be used. The matrix notation is particularly suitable for higher order systems.

For the system under consideration,

$$\ddot{e}_o = u_1 \qquad \ldots\ldots (1)$$

By defining

$$x_1 = e_o$$

$$x_2 = \dot{x}_1 = \dot{e}_o$$

the system Equation can be written in the matrix form

$$\dot{\underline{x}} = A\,\underline{x} + B\,\underline{u} \qquad \ldots\ldots (2)$$

where

A is an n x n matrix, B is an n x m matrix ($m \leq n$), $\underline{x}$ is an n-vector and $\underline{u}$ an m-vector.

In our case,

$$A = \begin{bmatrix} 0 & 1 \\ 0 & 0 \end{bmatrix}, \quad B = \begin{bmatrix} 0 \\ 1 \end{bmatrix}, \quad \underline{x} = \begin{bmatrix} x_1 \\ x_2 \end{bmatrix}, \quad \underline{u} = \begin{bmatrix} u_1 \end{bmatrix}$$

The solution of Equation (2) is obtained by the method of variation of parameters, and is given by Bellman[9] as

$$\underline{x} = Q \int_0^t Q^{-1} B\,\underline{u}\, dt + Q\,\underline{x}_0 \qquad \ldots\ldots (3)$$

where the matrix Q is defined in such a way as to satisfy the Equation

$$\dot{Q} = A\,Q \qquad \ldots\ldots (4)$$

and $$Q(0) = I = \begin{bmatrix} 1 & 0 \\ 0 & 1 \end{bmatrix} \qquad \ldots\ldots (5)$$

and $\underline{x}_0$ is $\underline{x}$ at $t = 0$. ($\underline{x}_0$ lies on the last phase of the trajectory)

Equation (4) represents four simultaneous differential equations:

$$\dot{q}_{11} = q_{21} \; ; \quad \dot{q}_{12} = q_{22} \; ; \quad \dot{q}_{21} = 0 \; ; \quad \dot{q}_{22} = 0 \qquad \ldots\ldots (6)$$

The solution of this set of equations with the constraints of Equation (5) yields

$$Q = \begin{bmatrix} 1 & +t \\ 0 & 1 \end{bmatrix} \qquad \ldots\ldots (7)$$

$$Q^{-1} = \begin{bmatrix} 1 & -t \\ 0 & 1 \end{bmatrix} \qquad \ldots\ldots (8)$$

When $t = T$, origin is reached and from Equation (3) we get

$$\underline{x}_o = - \int_o^T Q^{-1} B \, \underline{u} \, dt \qquad \ldots\ldots (9)$$

Solving the two simultaneous equations represented by (9), we get

$$x_{o_1} = \frac{u_1 T^2}{2} \; , \quad x_{o_2} = - u_1 T$$

Eliminating T between these two Equations, the switching function S is given by

$$S = x_1 - \frac{x_2^2}{2u_1} = 0 \qquad \ldots\ldots (10)$$

Equation (10) defines the curve in the phase plane at which the control function u_1 must change sign for optimal response. On the phase plane (x_1=x, x_2=y), Equation (10) becomes

$$S = x - \frac{y^2}{2u_1} = 0 \qquad \ldots\ldots (11)$$

which is the Equation of a Parabola.

For the system of Fig.1,

$$u_1 = \ddot{\theta}_o = \pm \frac{a}{T^2}$$

where 'a' is the maximum torque developed by the motor.

Hence Equation (11) can be written as

$$S = y^2 \mp \frac{2ax}{T^2} = 0 \qquad \ldots\ldots (12)$$

positive sign in Region (i) and negative sign in Region (ii).

Equation (12) can also be written as

$$S = y\,|y| + \frac{2ax}{T^2} = 0 \qquad \ldots\ldots (13)$$

for $S<o$, the output of the relay is positive

for $S>o$, the output of the relay is negative

In Fig.2, ABC is a typical trajectory. With correct reversal from acceleration to deceleration on the critical trajectory, the response will be optimum. This means that for minimum time of response, all the constant acceleration trajectories from different initial conditions must change over to the same critical decelerating trajectory through the origin.

At the point of change-over B,

$$\left.\begin{aligned} x_B &= -h_o/2 \\ y_B &= (ah_o/T)^{1/2} \end{aligned}\right\} \qquad \ldots\ldots (14)$$

The optimum change-over can be achieved by mechanising Equation (13) using a non-linear error processing device and a linear velocity feedback stabilisation term which has been called the SERME system by West[6] et al.

2.1. The Total Response Time

The total time of response can be calculated easily from the above equations.

It is assumed that no over-shoot is to occur at C.

$$\ddot{e} = a/T^2 \qquad \text{in Region (i)}$$

Integrating,

$$\dot{e}_o = at/T^2$$

At B, $\dot{e}_o = y_B = at_B/T^2$

Hence $$T_{AB} = y_B T^2/a$$

Substituting for y_B from Equation (14), we get

$$T_{AB} = (h_o T^2/a)^{1/2}$$

Since the change-over takes place at the half-way point

$$T_R = 2T_{AB} = (4h_o T^2/a)^{1/2} \qquad \ldots\ldots (15)$$

Thus from Equation (15), it is seen that the response time is dependent on the magnitude of the input step only since 'a', the maximum torque developed is a constant for a given servo motor. The response time versus the input step magnitude characteristic is shown in Fig.10.

3. EFFECT OF DEPARTURES FROM IDEAL SWITCHING CONDITIONS

It is again emphasised that the response of the system is optimal only when the assumptions of Section 1 (page 7) are valid. In this Section, some of the common practical departures from the ideal conditions and their effect on the system response are considered.

3.1. Errors in the Switching Locus

When the switching trajectory is mechanised, the actual realisation of the switching curve may not follow the ideal parabolic curve exactly. Let us first consider the effect when the actual switching curve is nearer to the error axis than the ideal curve. This is shown in Fig.3(a). Any representative point P moves along the acceleration trajectory till it meets the change-over boundary at P_1 at which the relay reverses the torque. The system must then follow a deceleration trajectory. The switching locus itself is not a deceleration trajectory, so the state point tries to follow the deceleration trajectory $P'P''$ which passes through P_1. This causes the relay to reverse again and follow an acceleration trajectory parallel to PP_1. Thus, the state point follows the

switching locus to the origin with the relay chattering at high frequency. This response of the system is slower than the ideal response.

On the other hand, if the actual switching trajectory is nearer to the y-axis than the ideal, the motion is shown in Fig.3(b). Relay reverses at P_1, follows the deceleration trajectory through P_1, reverses again at P_2 and so on. Thus, the system has overshoots and undershoots and the amplitude of successive oscillations decreases and the frequency increases until the system reaches the origin.

3.2. Effect of Friction

The effect of friction on the ideal trajectory has been studied by Kazda[15], Stout[16], Flugge-lotz[5] and others. In principle, the presence of Coulomb friction results in bringing the error rate to zero but not the error when the steady state is reached. This is not true in practice. In the presence of friction, in practice, end-point oscillations (a kind of convergent hunting) as shown in Fig.4(a) are observed. This results in a larger time to reach the steady state. If the magnitude of the Coulomb friction torque is known, by delaying the instant of

switching from acceleration to deceleration, improved performance can be obtained. With this modification the Equation of the switching trajectory in the fourth quadrant becomes

$$S = y^2 - \frac{2a}{T^2}\left(1 + \frac{a_c}{a}\right) x$$

instead of Equation (12) where a_c is the magnitude of Coulomb friction torque.

If the effect of viscous friction has to be taken into account properly, new switching trajectories must be derived by solving the Equation

$$\ddot{e}_o + k_f \dot{e}_o = u_1$$

instead of solving Equation (1).

The solution of this yields the Equation of the switching trajectory

$$S = x + \frac{y}{k_f} + \frac{u_1}{k_f^2} \ln\left(1 - \frac{k_f y}{u_1}\right) = 0$$

It is seen that the Equation of the switching trajectory depends upon the damping constant k_f.

3.3. Relay Hysteresis and Threshold

The presence of Hysteresis and Threshold in the relay characteristic delays the change-over from acceleration to deceleration. The delayed trajectories are shown in Fig.4(a). The delayed trajectories are also parabolic. Because of the delayed trajectory not passing through the origin, terminal limit cycles are observed[17]. These limit cycle oscillations can be stable or unstable. The system thus performs wasteful gyrations resulting in an increase in response time.

3.4. Time Lags and Time Delays

Time delays and time lags are inevitably present in any practical system. The effect is again to delay the change-over from acceleration to deceleration. The effect of time delay is shown in Fig.4(b). These may produce terminal limit cycles. If the time constant of the lag and the delay times are known, the magnitude and frequency of the limit cycle can be calculated by the method of Section 5.

4. SENSITIVITY OF THE OPTIMAL SYSTEM

In any successful optimal design, the achievement of the desired response and its relative insensitivity to system parameter changes or for small component imperfections is one of the basic requirements. In many applications, the invariability of the response or the insensitivity to parameter changes is even more important than nominal behaviour.

Consider the general control process described by the Equation

$$\dot{\underline{x}} = f\left[\, \underline{x}(t),\ \underline{u}(t),\ \underline{w} \,\right] \qquad \ldots\ldots (16)$$

where

$\underline{x}$ is the state vector

$\underline{u}(t)$ is the control vector

$\underline{w}$ is the plant parameter vector

If

$$C = \int_0^T \phi(\underline{x},\underline{u})\, dt \qquad \ldots\ldots (17)$$

is the performance index on the basis of which the optimum $\underline{u}$ is determined, then by solving Equations (16) and (17), $\underline{u}_{opt}$, in general, can be determined.

Let

$$\underline{u}_{opt} = \underline{\Psi}\left[\ \underline{x}(t),\ \underline{w}_o(t),\ t\ \right] \qquad \ldots\ldots (18)$$

The plant parameter vector $\underline{w}$ which appears in Equation (16) seldom corresponds to the value of $\underline{w}_o$ in Equation (18) due to component inaccuracies, environment effects, etc. Hence if $\underline{w}_p$ is the actual value of the plant vector, then from Equations (16) and (18), we have

$$\dot{\underline{x}} = f\left[\ \underline{x}(t),\ \left\{\underline{\Psi}\left[\ \underline{x}(t),\ \underline{w}_o(t),\ t\ \right]\right\},\underline{w}_p\ \right]$$

Optimum operation requires that $\underline{w}_o = \underline{w}_p$.

For every actual plant parameter value $\underline{w}_p$, a best value of $\underline{w}_o$ exists such that the performance index C has an optimum value. Under such conditions, when $\underline{w}_p$ is varying, C can be considered as a function of $\underline{w}_o$ and $\underline{w}_p$. Therefore variations in C due to small parameter variations is given by

$$\Delta C = C(\underline{w}_o,\ \underline{w}_p) - C(\underline{w}_o,\ \underline{w}_o)$$

Analytical solution for the evaluation of ΔC is in general, difficult[18].

One possible criterion of performance based on the insensitivity to parameter changes would be to minimise the maximum deviation from the optimal behaviour. This can be achieved by evaluating the "Relative sensitivity" and choosing the control parameter such that the maximum value of the relative sensitivity is a minimum[19].

Relative sensitivity for the control $\underline{u}(t)$ is defined[19] to be the difference between the actual value of the performance index $C(\underline{w}_o, \underline{w}_p)$ and that which would be obtained if the control were the optimal for the plant parameter $\underline{w}_p$, $C(\underline{w}_p, \underline{w}_p)$ divided by the optimal performance index for normalisation.

$$S^R = \frac{C(\underline{w}_o, \underline{w}_p) - C(\underline{w}_p, \underline{w}_p)}{|C(\underline{w}_p, \underline{w}_p)|} \qquad \ldots\ldots (19)$$

It is seen from Equation (19) that the relative sensitivity S^R is always a positive number and that the optimal value of S^R is zero, regardless of the value of the performance index itself.

The relative sensitivity function can now be evaluated for the bang-bang system considered in Section 2.

From Equation (1), the plant considered in Section 2 is described by

$$\ddot{\theta}_o = \pm \frac{a}{T^2} = w_p u \ , \quad \text{where } |u| \leq 1$$

The control signal u is given by

$$u = - \text{sign} \left[x^{1/2} + \frac{y}{(2w_o)^{1/2}} \right]$$

where

$$w_o = \frac{1}{2} \left[\frac{K_1}{K_v} \right]^2$$

When $w_p = w_o$, the system is optimal.

For a given range of variation in w_p (i.e. in 'a') a suitable value of w_o (i.e. K_v) can be chosen such that the maximum relative sensitivity is a minimum thus resulting in a system which is relatively insensitive to these variations.

The performance index for this system is the time to reach the optimum from any initial point in the phase plane. From Equation (15), the response time of the optimal system is given by

$$T_R = C(\underline{w}_p, \underline{w}_p) = 2(h_o/w_p)^{1/2} \qquad \ldots\ldots (20)$$

Let us consider the normalised system in which $h_o=1$, and nominal $w_p=1$. w_p is assumed to vary in the range $0.7 \leq w_p \leq 1.3$. That is a variation of ± 30 percent from the nominal value.

When $w_p > w_o$, as discussed in Section 3.1, the system chatters to the origin along the switching curve and the response time can be shown to be given by (Appendix A.1)

$$T_R = C(w_o, w_p) = \left[\frac{2(1 + \frac{w_p}{w_o})}{w_p}\right]^{\frac{1}{2}}, \quad w_p > w_o$$

$\ldots\ldots (21)$

However, when $w_p < w_o$, again as discussed in Section 3.1, an infinite number of switchings are required for the state point to reach the origin and the response time can be derived as (Appendix A.2)

$$T_R = C(w_o, w_p) = \frac{2\sqrt{2}}{\left[w_p(1+\frac{w_p}{w_o})\right]^{1/2}\left[1-(\frac{w_o-w_p}{w_o+w_p})\right]^{1/2}} \qquad w_p < w_o$$

$\ldots\ldots (22)$

From Equations (20), (21) and (22), the relative sensitivity S^R is given by

$$S^R = \frac{1}{\sqrt{2}} \left[1 + \frac{w_p}{w_o} \right]^{1/2} - 1 , \quad w_p > w_o$$

$$= \frac{\sqrt{2}}{(1+\frac{w_p}{w_o})^{1/2} \left[1-(\frac{w_o-w_p}{w_o+w_p}) \right]^{1/2}} - 1 , \quad w_p < w_o \qquad \ldots\ldots (23)$$

Equation (23) is plotted in Fig.5 as a function of w_p over the assumed range of w_p for different values of w_o. The value of w_o is to be chosen such that the maximum relative sensitivity S^M is a minimum. From Fig.5 it is seen that

$$S^M (0.7, 1.3) = 0.2$$

$$S^M (1.3, 0.7) = 1.45$$

$$S^M (1, 0.7) = 0.89$$

and so on. Hence $w_o = 0.7$ gives the minimum value for S^M. Thus, when w_o is chosen as 0.7, the response time will be within $\frac{2}{\sqrt{0.7}} = 2.35$ seconds for a variation of w_p in the range $0.7 \leq w_p \leq 1.3$. Hence by choosing the switching curve corresponding to $w_o = 0.7$, the best system from the sensitivity considerations can be obtained.

5. STABILITY OF THE SYSTEM

In this Section, the stability of the relay servo considered in Section 2 is discussed. As stated in Section 3, presence of time delays, lags, etc. are inevitable in practice and their presence gives rise to non-ideal switching trajectories. The object of stability analysis for the bang-bang servo is to determine the magnitude and frequency of the limit cycle that may be present due to the non-optimum operating conditions that may exist.

The system of Section 2 can be represented by the block diagram of Fig.6(a). The stability analysis of the system of Fig.6(a) is difficult since the two non-linearities are not in simple cascade. Since the purpose of the non-linearity N_1 and the velocity feedback signal is to satisfy Equation (13), these can be replaced by a single non-linearity satisfying the boundary Equation (13). The equivalent system is shown in Fig.6(b). The control computer obeys Equation (13) and generates the control signal e_c. Now since N_1' and N_2 are in simple cascade, stability analysis is possible by the describing function technique. The non-linearity N_1' is frequency dependent

and N_2 is only amplitude dependent. The frequency dependent describing function of N_1' can be evaluated from Equation (13). It is assumed that the system has sufficient low-pass filtering effect so that the harmonics above the fundamental may be neglected.

The non-linearity N_2 is of zero memory type and does not introduce a phase shift to the describing function. But N_1' contributes a phase shift to the describing function which can be evaluated (Fig.7).

Let N(m) be the describing function of the two non-linearities in cascade. Let

$$N(m) = R \exp(j\phi) \qquad \ldots\ldots (24)$$

If $x = m \cos \omega t$,

the output of N_2 is a square wave of magnitude $\pm a$.

Hence the magnitude R of the describing function is

$$R = \frac{4a}{\pi m} \qquad \ldots\ldots (25)$$

The phase shift ϕ is calculated by considering the control computer.

The control computer in Fig.6(b) evaluates the control signal e_c.

$$e_c = y\,|y| + \frac{2ax}{T^2}$$

if $e_c > 0$, $\lambda = -a$ and if $e_c < 0$, $\lambda = +a$.

The phase shift is found by evaluating the instant at which e_c goes through zero (Fig.7). Considering the one half-cycle in which y does not change sign,

$$e_c = \frac{2am}{T^2}\cos \omega t - m^2\omega^2 \sin^2 \omega t$$

$$e_c = 0$$

when

$$\frac{2am}{T^2}\cos \omega t - m^2\omega^2 \sin^2 \omega t = 0 \qquad \ldots\ldots (26)$$

Solving Equation (26) for cos ωt, we get

$$\cos \omega t = \cos \theta = \frac{1}{\omega^2 m}\left\{ - \frac{a}{T^2} + \left[\left(\frac{a}{T^2}\right)^2 + (\omega^2 m)^2 \right]^{\frac{1}{2}} \right\}$$

The phase angle ϕ of the describing function = the phase angle at which x passes through zero - the phase angle θ.

Therefore

$$\phi = \frac{\pi}{2} - \theta = \sin^{-1}\left[\frac{1}{\omega^2 m}\left\{ - \frac{a}{T^2} + \left[\left(\frac{a}{T^2}\right)^2 + (\omega^2 m)^2 \right]^{\frac{1}{2}} \right\} \right]$$

$$N(m) = \frac{4a}{\pi m} \exp\left\{ j \sin^{-1}\left[\frac{1}{\omega^2 m}\left\{ \frac{-a}{T^2} + \left[\left(\frac{a}{T^2}\right)^2 + (\omega^2 m)^2 \right]^{\frac{1}{2}} \right\} \right] \right\} \quad \ldots\ldots (27)$$

The amplitude and phase of N(m) as a function of m are plotted in Fig.8.

If $G(j\omega)$ is the transfer function of the control process, then by Nyquist stability criterion, the limit cycle must adjust itself to satisfy the Equation

$$-N(m) = \frac{1}{G(j\omega)} \quad \ldots\ldots (28)$$

The limit cycle may give rise to stable or unstable oscillations. This can be easily checked by plotting $\frac{1}{G(j\omega)}$ and $-N(m)$. Since $-N(m)$ is frequency dependent, a family of N(m) curves for different values of ω are to be plotted in the $G(j\omega)$ plane. The point of intersection of $\frac{1}{G(j\omega)}$ and $-N(m)$ that corresponds to the same frequency on both the curves gives the magnitude and frequency of the limit cycle. Alternatively, an analytical solution can be obtained by equating the amplitudes and phase angles in Equation (28).

Simple Lag :-

If a simple lag representing the motor field build-up time constant which was neglected earlier, is included with the process of Section 2,

$$G(p) = \left[\frac{1}{T^2 p^2 (1+T_1 p)} \right]$$

where T_1 is the time constant of the lag.

$$G(j\omega) = \left[- \frac{1}{T^2 \omega^2 (1+jT_1 \omega)} \right]$$

$$\text{or} \quad G(j\omega) = - \frac{1}{T^2 \omega^2 (1+\omega^2 T_1^2)^{1/2}} \exp \left[j \tan^{-1}(-\omega T_1) \right]$$

Hence from Equation (28), we have

$$\frac{4a}{\pi m} \exp \left\{ j \sin^{-1} \left[\frac{1}{\omega^2 m} \left\{ \frac{-a}{T^2} + \left[\left(\frac{a}{T^2} \right)^2 + (\omega^2 m)^2 \right]^{\frac{1}{2}} \right\} \right] \right\}$$

$$= \omega^2 T^2 (1 + \omega^2 T_1^2)^{\frac{1}{2}} \exp \left[j \tan^{-1}(\omega T_1) \right] \qquad \ldots\ldots (29)$$

The amplitude and frequency of the limit cycle are obtained by equating the magnitudes and phase angles in Equation (29) and solving for ω and m.

This results in

$$\left.\begin{aligned} \omega &= \frac{0.447}{T_1} \\ m &= 5.61\ a\ \left(\frac{T_1}{T}\right)^2 \end{aligned}\right\} \quad \ldots\ldots (30)$$

From Equation (30) the amplitude and frequency of the limit cycle can be calculated. It is seen that the period of the limit cycle is proportional to T_1 and the amplitude proportional to $(T_1/T)^2$.

Time Delay :-

If a pure time delay of magnitude T_D is present instead of a lag of time constant T_1, proceeding in a similar way, it can be shown that

$$\left.\begin{aligned} \omega &= \frac{0.485}{T_D} \\ m &= 5.42\ a\ \left(\frac{T_D}{T}\right)^2 \end{aligned}\right\} \quad \ldots\ldots (31)$$

Thus the period and amplitude of the limit cycle are again proportional to T_D and $(T_D/T)^2$ respectively.

Time Delay and Time Lag :-

If both the time delay and the lag are present, the same method can be applied to derive expressions for m and ω.

It can be shown that

$$\left.\begin{aligned}\omega^2 &= \frac{-(T_1+T_D)(\pi^2+8)+\left\{\pi^4(T_1+T_D)^2+16\pi^2\left[T_1^2+(T_1+T_D)^2\right]\right\}^{\frac{1}{2}}}{2(T_1+T_D)\left[\pi^2T_1^2-4(T_1+T_D)^2\right]}\\ m &= \frac{2a(T_1+T_D)}{\omega T^2\left[1-\omega^2(T_1+T_D)^2\right]}\end{aligned}\right\} \quad \ldots\ldots (32)$$

From Equation (32), ω and m can be evaluated for any given T_1 and T_D.

6. ANALOGUE COMPUTER STUDIES

As pointed out in Sections 3 and 4, the bang-bang system is sensitive to departures from ideal operating conditions and parameter variations. The deterioration in the performance of the ideal system under these operating conditions is studied by simulating the system on the analogue computer. For comparison of the performance under these different operating conditions, a common performance index is necessary. The time required to bring the state point to the origin from an initial state in the phase plane is chosen as the performance index. The response time (T_R) is defined to be the time taken for both the error and error rates to become zero simultaneously following an initial step disturbance to the system. In the presence of terminal limit cycles, the error and error rates cannot become zero. Hence response time is reckoned as the time required to bring the error and error rates into a small region around the origin. This region is chosen to be a small rhombus enclosing the origin.

The performance of the bang-bang controller is compared with that of a saturating system. The

parameter chosen for variation is the gain factor of the stabilising network. When the stabiliser gain factor is adjusted to have the critical value, the bang-bang system has the optimal response and the state point reaches the origin without any overshoot. It ia easily seen that the critical value of the gain factor is given by

$$K_v(\text{critical}) = \frac{K_1}{\sqrt{2a}}$$

where K_1 is the gain factor of the error processing non-linearity.

The effect of additional lags representing field build-up time constant of the motor on both the bang-bang system and the saturating system are studied. The magnitude and frequency of the terminal limit cycle when the additional time lag and time delay are present are measured and compared with the calculated values using Equation (32).

The block diagram of the analogue computer set-up is shown in Fig.9. The non-linear units are built using biased diode circuits. The bang-bang characteristic has negligible hysteresis and threshold effects. Response time is measured by measuring the output voltage of an integrator to the input of which

a constant D.C. voltage is applied at the same instant as the input step is applied to the system. The time delay is simulated using fourth order Pade' approximation[58]. In the simulation, the saturation characteristic had a slope of 10 and the time constant of the additional lag $\frac{1}{10}$ the integrator time constant.

6.1. Discussion of Results

The results of the computer studies are shown in Figs. 10 and 11. It is seen that, from Fig.10, the theoretical and the practical response time characteristics agree very closely for the system, under the ideal conditions. It is seen that the saturating system with the stabiliser gain set to correspond to critical damping takes about 5 percent more time to reach the origin than the bang-bang system with critical stabiliser gain. Fig.11 shows the response time characteristics for the different non-ideal conditions. The bang-bang system is more sensitive to changes in stabiliser gain than the saturating system as can be seen from Figs.11(a) and 11(b). The response time increases by about 32 percent when the gain is reduced from the best (critical)

value by 10 percent in the case of bang-bang system, as compared to an increase of about 13 percent only for the saturating system. The magnitude of the overshoot or undershoot for the bang-bang system can be calculated from the expression

$$x_{o.s.} = \frac{h_o \left[\frac{K_1^2}{2a} - K_v^2 \right]}{\left[\frac{K_1^2}{2a} + K_v^2 \right]}$$

where h_o is the magnitude of the step input.

The inclusion of the additional lag introduces terminal limit cycles. The response time for the bang-bang system increases by about 45 percent with the lag as compared to an increase of only 3 to 4 percent for the saturating system, as can be seen from Figs. 11(c) and (d).

When both a time delay and a lag are included, the magnitude and frequency of the resulting limit cycle in the bang-bang system has been measured. Fig.12 shows that the measured values agree closely with the values calculated using Equation (32).

7. CONCLUSIONS

From experimental studies on the Analogue computer, it has been shown that the performance of the bang-bang controller is optimum only when the conditions obtainable are ideal. In the presence of switching curve errors, time lags and time delays the saturating servo has a better performance. The bang-bang servo is more sensitive to parameter variations and non-ideal conditions than the saturating servo. The linear operating regime in the saturating servo is also extremely useful in eliminating terminal limit cycles.

The stability of the SERME system has been studied and expressions for the magnitude and frequency of the limit cycle have been derived. Experimental values agree closely with the theoretically predicted values.

When the motor dynamics vary, if the range of these variations are known, it has been shown that by suitably altering the switching curve it is possible to obtain a system response which is least sensitive to these variations.

8. APPENDICES

A.1. Derivation of Response Time when $w_p > w_o$

When the motor dynamics are such that $w_p > w_o$, the nature of the response is similar to the case when the switching curve is nearer the error axis than the ideal curve as discussed in Section 3.1. The state point reaches the origin along the switching curve, the relay chattering at high frequency. For the calculation of response time, it can be assumed that the system moves to the origin along the switching curve. A typical trajectory is shown in Fig.13(a).

The system Equation is given by

$$\ddot{x} = w_p u_1$$

The time required for the path PP_1 [Fig.13(a)] is given by

$$T_{pp_1} = \frac{y_{p_1}}{-w_p} \qquad \ldots\ldots \text{(A.1)}$$

The motion along the path PP_1 is described by

$$y_{p_1}^2 - y_o^2 = -2w_p (x_{p_1} - h_o)$$

or

$$y_{p_1}^2 = -2w_p (x_{p_1} - h_o) \qquad \ldots\ldots \text{(A.2)}$$

As point P_1 is on the deceleration trajectory passing through the origin, y_{p_1} is also given by

$$y_{p_1}^2 = + 2w_o\, x_{p_1} \qquad \ldots\ldots (A.3)$$

From Equations (A.2) and (A.3), we get

$$y_{p_1} = - \frac{(2w_p h_o)^{1/2}}{(1+ \frac{w_p}{w_o})^{1/2}} \qquad \ldots\ldots (A.4)$$

Hence

$$T_{pp_1} = \frac{(2h_o)^{1/2}}{\left[w_p(1+ \frac{w_p}{w_o})\right]^{1/2}} \qquad \ldots\ldots (A.5)$$

The response time for the path P_1O is given by

$$T_{p_1o} = - \frac{y_{p_1}}{w_o} = \frac{(2w_p h_o)^{1/2}}{w_o(1+ \frac{w_p}{w_o})^{1/2}}$$

The total response time is hence

$$T_R = T_{pp_1} + T_{p_1o} = \frac{(2h_o)^{1/2}(1+ \frac{w_p}{w_o})^{1/2}}{w_p^{1/2}} \qquad \ldots\ldots (A.6)$$

A.2. Derivation of Response Time when $w_p < w_o$

When $w_p < w_o$, the nature of response is similar to the case when the switching curve is nearer the y-axis than the ideal curve. There will be more than one intersection of the state point with the switching curve as shown in Fig.13(b). There will be overshoots and undershoots and the number of switchings depends on the initial position and w_p. The total response time is derived considering that an infinite number of switchings take place and computing the time for each switching[59]. Hence

$$T_R = T_{pp_1} + T_{p_1p_2} + T_{p_2p_3} + \ldots \infty$$

As derived in Equation (A.5)

$$T_1 = T_{pp_1} = \frac{(2h_o)^{1/2}}{\left[w_p(1+\frac{w_p}{w_o})\right]^{1/2}} \qquad \ldots\ldots (A.7)$$

Time required for path P_1P_2 is given by

$$T_{p_1p_2} = \frac{y_{p_2} - y_{p_1}}{w_p} \qquad \ldots\ldots (A.8)$$

y_{p_2} is obtained by solving Equations (A.9) and (A.10)

$$y_{p_2}^2 - y_{p_1}^2 = 2w_p (x_{p_2} - x_{p_1}) \quad \ldots\ldots (A.9)$$

$$y_{p_2}^2 = -2w_o x_{p_2} \quad \ldots\ldots (A.10)$$

Solving Equations (A.9) and (A.10) and substituting for y_{p_1} and x_{p_1} from Equations (A.4) and (A.3) gives

$$y_{p_2} = \frac{(2w_p h_o)^{1/2} (1 - \frac{w_p}{w_o})^{1/2}}{(1 + \frac{w_p}{w_o})} \quad \ldots\ldots (A.11)$$

From Equations (A.8), (A.11) and (A.4), we get

$$T_2 = T_{p_1 p_2} = \frac{(2h_o)^{1/2}}{\left[w_p(1 + \frac{w_p}{w_o})\right]^{1/2}} \left[1 + \left[\frac{1 - \frac{w_p}{w_o}}{1 + \frac{w_p}{w_o}}\right]^{1/2}\right] \quad \ldots\ldots (A.12)$$

Proceeding on similar lines the response times for the paths P_2P_3, P_3P_4, ... can be derived as

$$T_3 = T_{p_2 p_3} = \frac{(2h_o)^{1/2}}{\left[w_p(1 + \frac{w_p}{w_o})\right]^{1/2}} (1 + \alpha)\alpha$$

$$T_4 = T_{p_3p_4} = \frac{(2h_o)^{1/2}}{\left[w_p(1+\frac{w_p}{w_o})\right]^{1/2}} (1+\alpha)\alpha^2$$

. . .

. . .

. . .

$$T_n = T_{p_{n-1}p_n} = \frac{(2h_o)^{1/2}}{\left[w_p(1+\frac{w_p}{w_o})\right]^{1/2}} (1+\alpha)\alpha^{n-2} \qquad \ldots\ldots \text{(A.13)}$$

where $\alpha = \left[(1-\frac{w_p}{w_o}) \Big/ (1+\frac{w_p}{w_o}) \right]^{1/2}$

Hence the total response time is

$$T_R = \sum_{n=1}^{\infty} T_n = \frac{(2h_o)^{1/2}}{\left[w_p(1+\frac{w_p}{w_o})\right]^{1/2}} \left[1+(1+\alpha)(1+\alpha+\alpha^2+\ldots\infty)\right]$$

or

$$T_R = \frac{(2h_o)^{1/2}}{\left[w_p\left(1+\frac{w_p}{w_o}\right)\right]^{1/2}} \cdot \frac{2}{1-\frac{\left(1-\frac{w_p}{w_o}\right)^{1/2}}{\left(1+\frac{w_p}{w_o}\right)^{1/2}}}$$

..... (A.14)

A.3. The Published Paper

Reprinted from
INTERNATIONAL JOURNAL OF CONTROL, Vol. 2, No. 3, p. 255, September 1965

A Note on the Performance of the Second-order Maximum Effort Controller†

By K. K. MURTHY
Department of Electrical Engineering, Queen's University of Belfast, Belfast

[Received June 18, 1965]

ABSTRACT

The paper shows experimentally how the second-order maximum effort (bang-bang) servo system performance deteriorates when the system parameters are varied. With reference to a particular criterion, it experimentally demonstrates the superiority of the torque limited saturating servo as compared to the relay servo when the system parameters are varied. The magnitude and the frequency of the resulting limit cycle for the bang-bang system are calculated.

List of Principal Symbols

θ_i = input position and input signal.
θ_0 = output position and output signal.
$x = \theta_0 - \theta_i$ = error signal.
$\dot{\theta}_0 = y$ = output velocity.
e_c = control signal.
λ = output signal of the relay.
a = maximum developed torque.
$\omega = 1/T$ = undamped resonant frequency.
T_1 = motor field build-up time constant.
t_r = response time.
K_v = gain factor of the stabilizer.
$N(m)$ = describing function.
$G(p)$ = transfer function of the process.
K_1 = gain of the error processing non-linearity.

§ 1. INTRODUCTION

FOR a second-order servo system it has been shown by West *et al.* (1954), Mcdonald (1950), Neiswander and Macneal (1953) and by many other authors that the 'optimum' controller is the 'bang-bang' or the relay system. Such a controller is considered optimum since it takes minimum response time to reach the quiescent state following an applied input disturbance. The admissible input disturbances are steps and ramps, in general, though West and Nikiforuk (1956) have shown that considerable improvement in performance could be achieved for sinusoidal inputs also.

† Communicated by the Author.

The simplest example of a bang-bang servo is the relay actuated servomotor position controller. In all the relay or bang-bang systems, the system always operates under maximum actuating torque conditions. For half the time, maximum acceleration torque is developed and for the other half maximum decelerating torque is developed. In other words, the direction of the torque is to be reversed at exactly half way following an initial disturbance from the state of rest. The switching trajectories for the ideal second-order system are half parabolas in the second and fourth quadrants passing through the origin. The switching from acceleration to deceleration is to take place on this parabolic switching trajectory. Such an optimum switching can be achieved by a suitably designed non-linear error processing device (West *et al.* 1954) to actuate the relay.

Fig. 1

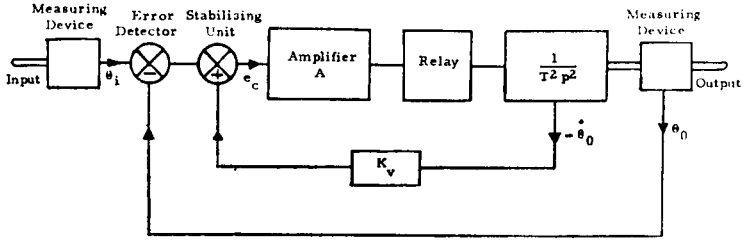

The general system.

The operation of such an optimum relay switching system is derived under the following assumptions.

(i) Inputs limited to step functions.

(ii) Instantaneous switching on the change-over boundary.

(iii) No time delays present in the system.

These ideal conditions are seldom satisfied in practice and the system, in general, will have to be modified even to give very nearly optimum response. Such modifications to give nearly optimum response under the non-ideal conditions cannot easily be derived, analytically.

The purpose of this paper is to show the qualitative nature of the deterioration in performance of the bang-bang system under non-ideal conditions and to demonstrate the superiority of the saturating servo under such conditions. The magnitude of the resulting limit cycle in the case of the bang-bang servo under such conditions is calculated.

§ 2. The Optimum System

The system used for analysis is shown schematically in fig. 1. The torque limited servo motor is actuated by a relay so that the motor always develops maximum torque, the direction of which depends upon the

position of the relay or the sign of the control signal. The control signal which actuates the relay is given by:

$$e_c = A(\theta_i - \theta_0 - K_v\dot{\theta}_0)$$

or

$$e_c/A = -x - K_v y \text{ on the phase plane.} \quad (x = \theta_0,\ y = \dot{\theta}_0).$$

The position of the relay which turns on maximum acceleration in one direction or other depends on the sign of $(-x - K_v y)$.

Fig. 2

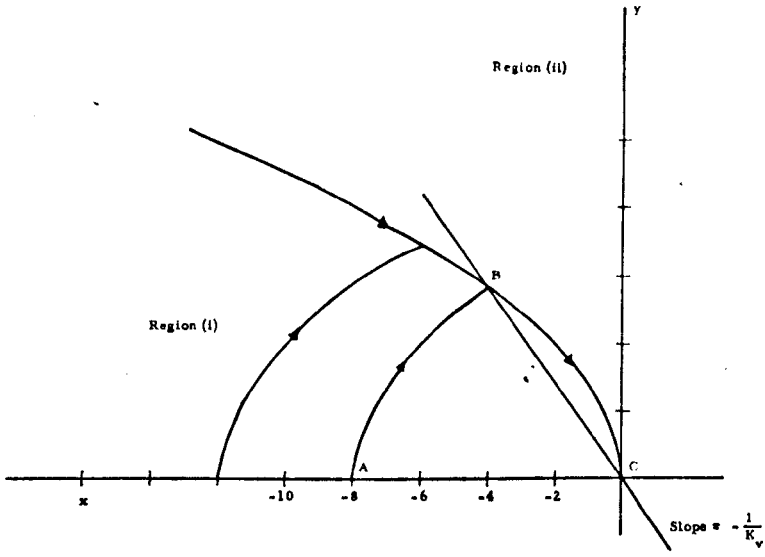

The optimum switching boundary.

If a is the maximum torque developed by the motor, then maximum acceleration is a/T^2:

$$\left.\begin{aligned} \ddot{\theta}_0 &= \pm a/T^2 = (a/T^2)\,\text{sign}\,(e_c) \\ \text{or} \qquad y\frac{dy}{dx} &= (a/T^2)\,\text{sign}\,(e_c). \end{aligned}\right\} \quad (1)$$

Integrating, we get:

$$y^2 - y_0^2 = (2a/T^2)(x - x_0)\,\text{sign}\,(e_c). \quad (2)$$

Equation (2) represents a family of parabolas on the phase-plane.

In fig. 2, ABC is a typical trajectory on the phase-plane. If the response is not to overshoot, then eqn. (2) becomes:

$$y^2 = \pm 2ax/T^2; \quad (3)$$

+ve sign in region (i) and −ve sign in region (ii).

Equation (3) can be written as:

$$-y|y| = 2ax/T^2$$

or

$$S = y|y| + 2ax/T^2 = 0. \qquad (4)$$

Equation (4) is the parabolic switching curve;

for $S < 0$, the output of the relay is + ve.

for $S > 0$, the output of the relay is − ve;

At the point of change over B (fig. 2),

$$x_B = -h_0/2, \qquad y_B = (ah_0/T)^{1/2}. \qquad (5)$$

Thus the change-over from acceleration to deceleration takes place on the curve $S = 0$, at the point $x_B = -h_0/2$, for step inputs.

This optimum change-over can be achieved by mechanizing eqn. (4) by a non-linear error processing device and a linear velocity feedback stabilization term which has been called the SERME system by West *et al.* (1954).

Fig. 3

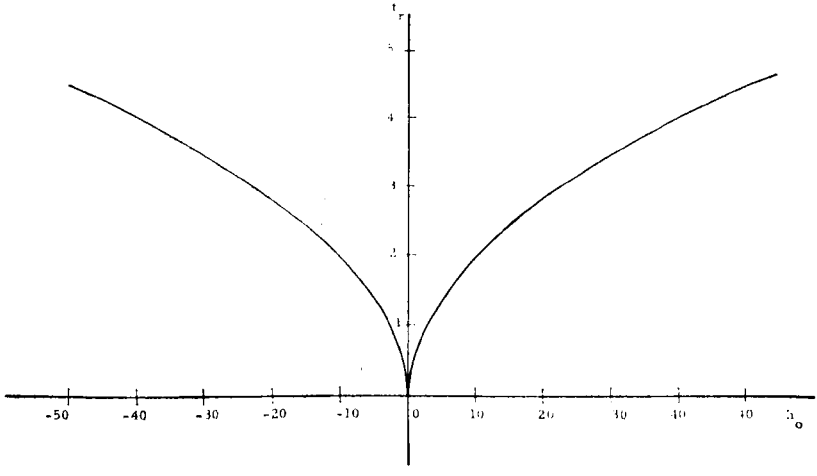

Variation of response time with input.

The Total Response Time

The total response time can be calculated easily from the above equations. It is assumed that no overshoot is to occur (at C):

$$\ddot{\theta}_0 = +a/T^2 \quad \text{in region (i)}$$

integrating,

$$\dot{\theta}_0 = at/T^2.$$

At B, $\dot{\theta}_0 = y_B = at_B/T^2$. Hence $t_B = y_B T^2/a$.

Substituting for y_B from eqn. (5) we get:

$$t_B = (h_0 T^2/a)^{1/2}.$$

The total time taken to reach the origin is:

$$2t_B = t_r = (4h_0T^2/a)^{1/2}. \tag{6}$$

Thus, from eqn. (6), it is seen that the response time is dependent on the magnitude of the input step only since a, the maximum torque developed is a constant for a given servo motor. The response time versus input step magnitude characteristic is shown in fig. 3.

§ 3. Sensitivity of the Optimum System

In any successful optimum design the achievement of the desired response and its relative insensitivity to system parameter changes or for small component imperfections is one of the basic requirements. In many applications the invariability of the response is even more important than nominal behaviour. Analysis and synthesis procedures must take account of these requirements, as far as possible.

Consider the general control process described by the equation:

$$\dot{\mathbf{x}} = f[\mathbf{x}(t), \mathbf{u}(t), \mathbf{w}], \tag{7}$$

where $\dot{\mathbf{x}}$ and $\mathbf{x}$ are state vectors,

$\mathbf{u}(t)$ is the control variable vector,

$\mathbf{w}$ is the plant parameter vector.

If

$$C = \int_0^T F(\mathbf{x}, \mathbf{u})\, dt \tag{8}$$

is the performance index, on the basis of which the optimum $\mathbf{u}$ is determined, then by solving eqns. (7) and (8), $\mathbf{u}_{opt}$, in general, can be determined.

Let

$$\mathbf{u}_{opt}(t) = \Psi[\mathbf{x}(t), \mathbf{w}(t), t]. \tag{9}$$

The plant parameter vector $\mathbf{w}$ which appears in (7) seldom corresponds to the value of $\mathbf{w}$ used in (9), due to component inaccuracies, environment effects, etc.

From (7) and (9) we have:

$$\dot{\mathbf{x}} = f[\mathbf{x}(t), \{\Psi[\mathbf{x}(t), \mathbf{w}_0(t), t]\}, \mathbf{w}]; \tag{10}$$

optimum operation requires that $\mathbf{w} = \mathbf{w}_0$.

Variations in C due to parameter variations is given by:

$$\Delta C = C(\mathbf{w}_0, \mathbf{w}) - C(\mathbf{w}_0, \mathbf{w}_0). \tag{11}$$

ΔC cannot be evaluated easily in general, even for small parameter variations analytically (Dorato 1963).

By experimental analysis the effect of parameter variations and other departures from the ideal conditions can be qualitatively observed.

First, let us consider some of the common departures from the ideal conditions for the system of § 2.

3.1. *Effect of Friction*

The effect of friction on the ideal trajectory has been studied by Kazda (1953), Stout (1953), Flugg-Lotz (1953), and many others. Ideally, the presence of coulomb friction must result in bringing the error rate to zero but not the error when the steady state is reached. But it is observed experimentally that this is not true. In the presence of friction, or under highly over damped conditions, end-point oscillations as shown in fig. 4 are observed. This results in a larger settling time required to reach the steady state.

Fig. 4

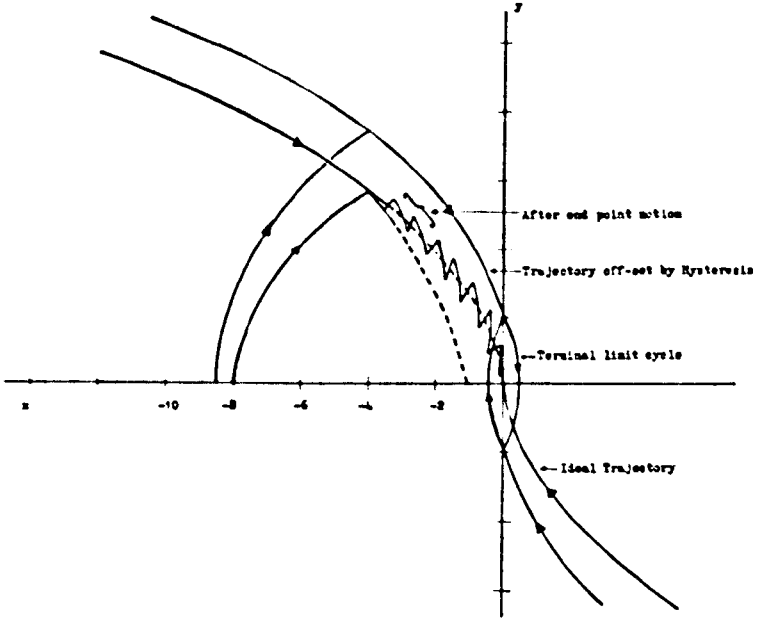

Effect of friction and hysteresis on the switching curve.

3.2. *Relay Hysteresis and Threshold*

The presence of hysteresis and threshold in the relay characteristic delays the change-over from acceleration to deceleration. The delayed trajectories are shown in fig. 4. Because of the non-optimum trajectory not passing through the origin, terminal limit cycles are observed (Graham and McRuer 1961). Limit cycles are by definition continuous oscillations and they can be either stable or unstable. When the hysteresis and threshold effects are small, these oscillations are stable. But the effect of such limit cycling is to increase the response time since the system has to undergo wasteful gyrations.

3.3. *Time Lags and Time Delays*

Presence of an additional time lag (as for example the motor field build-up time constant in the system of § 2) or a pure time delay results in delayed switching and may produce terminal limit cycling. If the time constant of the lag or the magnitude of the time delay is known, the magnitude and frequency of the limit cycle can be calculated as shown in § 4.

Fig. 5

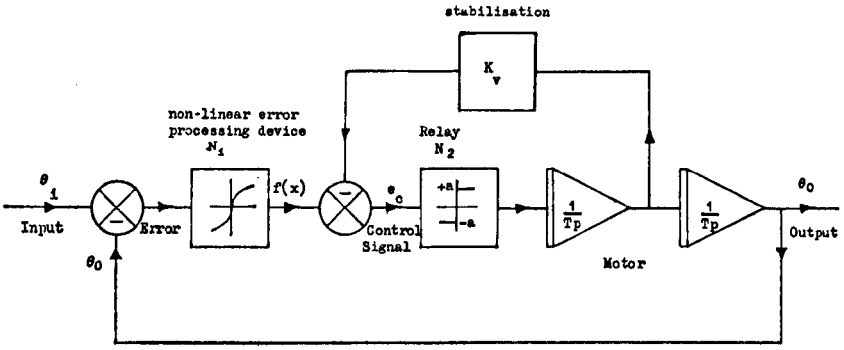

The optimum system.

§ 4. Stability Analysis

The optimum system of § 2 can be represented by the block diagram of fig. 5.

The stability analysis of the system of fig. 5 is difficult since the two non-linearities N_1 and N_2 are not in simple cascade. Since the purpose of N_1 and the velocity feed-back stabilization is to satisfy eqn. (4), for purposes of stability analysis, these can be replaced by a single non-linearity satisfying the boundary eqn. (4). The equivalent system is shown in fig. 6. The non-linearity N_1' can be thought of as a control computer satisfying eqn. (4). Now since N_1' and N_2 are in simple cascade, stability analysis is possible by the describing function technique (Douce 1963).

Fig. 6

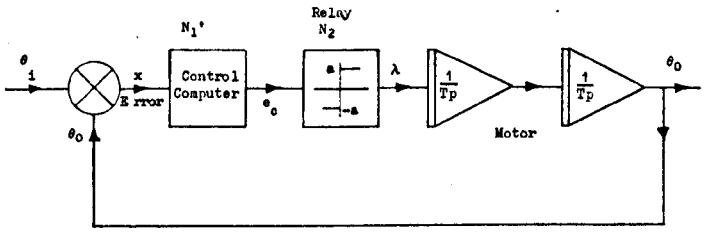

The equivalent system.

The object of the stability analysis for the bang-bang servo is to determine the magnitude and frequency of the limit cycle that may be present due to non-optimum operating conditions that may exist.

In this section, the magnitude and frequency of the limit cycle due to the presence of an additional lag with the process of § 2 are calculated. It is assumed that the system has sufficient low-pass filtering effect so that the harmonics above the fundamental may be neglected.

The describing function of the two non-linearities N_1' and N_2 is evaluated considering them in cascade. The non-linearity N_1' introduces a phase shift to the describing function, whereas N_2 does not contribute to the phase shift. Let $N(m)$ be the describing function of the two non-linearities in cascade. Let

$$N(m) = R\exp(j\phi). \tag{12}$$

If $x = m\cos\omega t$, the output of N_2 is a square wave of magnitude $\pm a$. Hence the magnitude R of the describing function is:

$$R = \frac{4a}{\pi m}. \tag{13}$$

The phase shift ϕ is calculated by considering the control computer.

The control computer in fig. 6 evaluates the control signal e_c:

$$e_c = y|y| + 2ax/T^2,$$
$$\text{if} \quad e_c > 0, \quad \lambda = -a,$$
$$\text{if} \quad e_c < 0, \quad \lambda = +a.$$

The phase shift is found by evaluating the instant at which e_c goes through zero. Considering one-half cycle in which y does not change sign,

$$e_c = 2am/T^2\cos\omega t - m^2\omega^2\sin^2\omega t,$$
$$e_c = 0, \quad \text{when} \quad 2am/T^2\cos\omega t - m^2\omega^2\sin^2\omega t = 0 \tag{14}$$

or
$$m^2\omega^2\cos^2\omega t + 2am/T^2\cos\omega t - m^2\omega^2 = 0. \tag{15}$$

Solving (15) for $\cos\omega t$ we get:

$$\cos\omega t = \cos\theta = 1/\omega^2 m\{-a/T^2 + [(a/T^2)^2 + (\omega^2 m)^2]^{1/2}\}. \tag{16}$$

The phase angle ϕ of the describing function =

phase angle at which x passes through zero − phase angle θ.

$$\therefore \quad \phi = \frac{\pi}{2} - \theta = \sin^{-1}\{1/\omega^2 m[-a/T^2 + \{(a/T^2)^2 + (\omega^2 m)^2\}^{1/2}]\}.$$

Hence

$$N(m) = (4a/\pi m)\exp\{j\sin^{-1}[1/\omega^2 m\{-a/T^2)^2 + [(a/T^2)^2 + (\omega^2 m)^2]^{1/2}\}]\}. \tag{17}$$

If $G(j\omega)$ is the transfer function of the control process, then by Nyquist stability criterion, the limit cycle must adjust itself to satisfy the equation:

$$-N(m) = 1/G(j\omega). \tag{18}$$

Simple Lag

If a simple lag representing the motor field build-up time constant which was neglected earlier, is included in the process of § 2,

$$G(p) = [1/\{T^2p^2(1+T_1p)\}], \tag{19}$$

$$G(j\omega) = [1/\{-T^2\omega^2(1+jT_1\omega)\}] \tag{20}$$

or
$$G(j\omega) = -(1/T^2\omega^2)(1/1+\omega^2T_1^2)^{1/2}\exp\{j\tan^{-1}(-\omega T_1)\}. \tag{21}$$

Hence from (18) we have :

$$(4a/\pi m)\exp\{j\sin^{-1}[(1/\omega^2 m)\{-a/T^2+[(a/T^2)^2+(\omega^2 m)^2]^{1/2}\}]\}$$
$$= \omega^2T^2(1+\omega^2T_1^2)^{1/2}\exp\{j\tan^{-1}(\omega T_1)\}. \tag{22}$$

The amplitude and frequency of the limit cycle are obtained by equating the magnitudes and phase angles in (22) and solving for ω and m.

This results in :

$$\omega = 0{\cdot}45/T_1, \tag{23}$$

$$m = 5{\cdot}61\,a\,(T_1/T)^2. \tag{24}$$

Equations (23) and (24) give the frequency and amplitude of the limit cycle, respectively.

It is seen that the period of the limit cycle is proportional to T_1 and the amplitude proportional to $(T_1/T)^2$.

If a pure time delay T_D is present instead of the lag of time constant T_1, proceeding in a similar way we can show that

$$\omega = 0{\cdot}485/T_D$$

and
$$m = 5{\cdot}42\,a(T_D/T)^2.$$

Thus the period and amplitudes of the limit cycle are proportional to T_D and $(T_D/T)^2$ respectively.

§ 5. Analogue Computer Studies

As has been observed in § 3 the bang-bang system is very sensitive to parameter variations. The deterioration in the performance of the ideal system for parameter variations is studied by simulating the system on an analogue computer. For comparison of the performances under these different operating conditions, a common performance index is necessary. In these studies the total response time required to bring the system to rest for different magnitudes of input step disturbances is chosen as the index. Since the ideal bang-bang system is the minimum response time controller, this performance index is chosen. The response time (t_r) is defined to be the time taken for both the error and the error rates to become zero simultaneously following an initial step input disturbance to the system. Since it is difficult, in the presence of terminal limit cycles and end-point oscillations, to precisely estimate the instant when both the error and error rates become exactly zero, it is considered adequate to reckon response time as the time required to bring the error and error rates into a small region around the origin. This region is chosen to be a small square enclosing the origin.

The ideal second-order bang-bang system shown in fig. 5 is simulated on the analogue computer. The gain factor of the stabilizer K_v is adjusted to have the critical value. When the stabilizer gain factor has the critical value the change-over from acceleration to deceleration takes place at exactly the half-way point, resulting in a response running into the steady state without any over-shoot. It is easily seen that the critical value of the gain factor is given by:

$$K_v \text{ (critical)} = K_1/2a,$$

where K_1 is the gain of the error processing non-linearity. The response time is measured for different magnitudes of input step.

Fig. 7

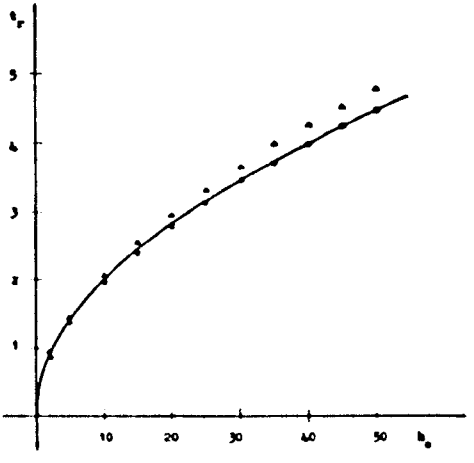

Variation of response time with input.
— Theoretical bang-bang.
○ Practical bang-bang.
△ System with limiter.

The parameter chosen for variation is the gain factor of the stabilizer. The response time is measured for gain factors other than the critical.

Additional time lag representing the field build-up time constant of the motor is included and the response time is measured with the stabilizer gain factor unchanged at the critical value.

The same studies are repeated on the system with the bang-bang non-linearity replaced by a saturating non-linearity or a ' limiter ' with a small linear regime.

The results are shown in figs. 7 to 9. It is seen from fig. 7 that the theoretical and the practical response time characteristics agree very closely for the system, under the ideal conditions. It is seen that the saturating system with the stabilizer gain factor set to correspond to critical damping takes about 5% more response time than the bang-bang system with

Fig. 8

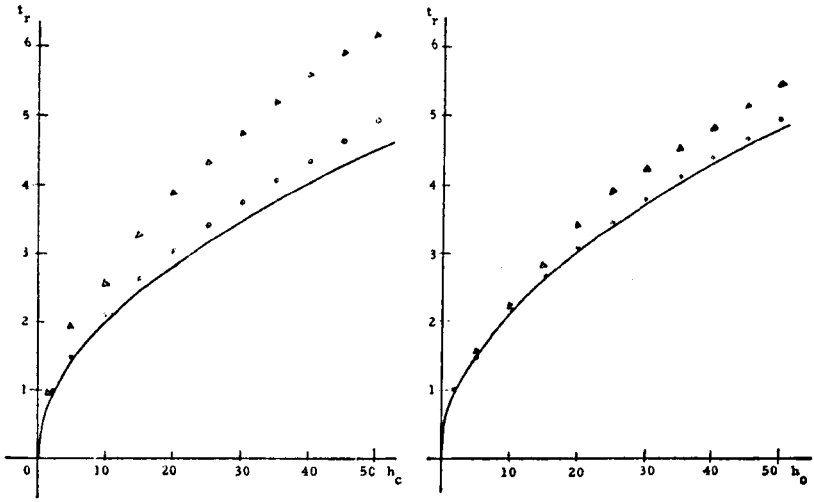

(*a*) (*b*)

Variation of response time with input.
(*a*) Bang-bang controller. (*b*) Controller with limiter.
— Critical gain factor for stabilizer.
⊙ Critical gain factor+10%.
△ Critical gain factor−10%.

Fig. 9

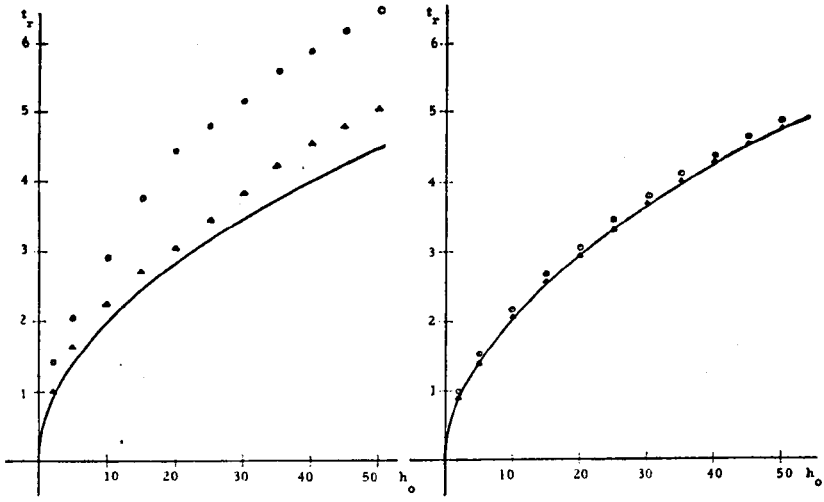

(*a*) (*b*)

Variation of response time with input.
(*a*) Bang-bang controller. (*b*) Controller with limiter.
— Ideal response.
⊙ With a lag $\frac{1}{1+T_1 p}$ with the motor.
△ With a lag $\frac{1}{1+T_1 p}$ with the error detector.

critical stabilizer gain. Figures 8 and 9 show the response time characteristics for the different non-ideal conditions considered. It is seen that the bang-bang system is more sensitive to changes in the stabilizer gain factor than the system with the limiter. The response time shows an increase of about 30 to 35% in the case of the bang-bang system as compared to an increase of only 12 to 15% for the system with the limiter, when the stabilizer gain factor is reduced from the best (critical) value by 10%. The inclusion of the additional lag results in terminal limit cycles of considerable magnitude in addition to the great increase in the response time as can be seen from fig. 9 (*a*). For different values of the motor field build-up time constant T_1, the measured values of the magnitude and frequency of the limit cycle agree very closely with the calculated values using eqns. (23) and (24). Thus, for any departures from the ideal conditions, the performance of the bang-bang controller is seen to deteriorate more, both qualitatively and quantitatively.

§ 6. Conclusions

By experimental studies on an analogue computer, it has been shown that the performance of the bang-bang controller is optimum only when the conditions obtainable are ideal. For situations where there is a likelihood of the existence of time lags and parameter variations, the saturating system gives a better response as far as the total response time is concerned. With the additional time lag, the magnitude and frequency of the resulting limit cycle for the bang-bang system have been calculated. The calculated and the observed values agree closely.

The percentage over-shoot observed is larger for the bang-bang system than for the saturating system, under the changed operating conditions, except in the overdamped case. From fig. 9 (*a*) and (*b*) it is seen that when the extra lag is added with the motor, the response time increases by nearly 45 to 50% for the bang-bang system as compared to the increase of only 3 to 4% for the saturating system.

Acknowledgments

The author is grateful to Dr. J. L. Douce for his constant guidance and encouragement during the course of this work. The author is also grateful to the Commonwealth Scholarship Commission of U.K. for having provided the opportunity to undertake research in this country.

References

Dorato, P., 1963, *Trans. Amer. Inst. elect. electron. Engrs*, **AC 8**, 256.

Douce, J. L., 1963, *An Introduction to Mathematics of Servomechanisms* (English Universities Press).

Flugg-Lotz, I., 1953, *Discontinuous Automatic Control* (Princeton University Press).

Graham, D., and McRuer, D., 1961, *Analysis of Non-linear Control Systems* (John Wiley).

KAZDA, L. F., 1953, *Trans. Amer. Inst. elect. Engrs*, **72**, 323.
MACDONALD, D., 1950, *Proc. National Electronics Conference*, **6**, 400.
NEISWANDER, R. S., and MACNEAL, R. H., 1953, *Trans. Amer. Inst. elect. Engrs*, **72**, 262.
STOUT, T. M., 1953, *Trans. Amer. Inst. elect. Engrs*, **72**, 329.
WEST, J. C., DOUCE, J. L., and NAYLOR, R., 1954, *Proc. Instn elect. Engrs*, **101**, 166.
WEST, J. C., and NIKIFORUK, P. N., 1956, *Trans. Amer. Inst. elect. Engrs*, **75**, 235.

PART II

SELF-OPTIMISATION USING PSEUDO-RANDOM BINARY SEQUENCES

SUMMARY

In this part of the thesis, self-optimisation of control systems by the Hill-climbing technique using pseudo-random binary sequences as the perturbation signal is studied. Two methods of closing the adaptive loop are examined.

In the first method, adjustments to the parameter are made discontinuously once every period of the binary sequence. The step change in parameter after every adjustment sets up transients in the response of the process which will in general be correlated with the perturbing signal. The correlation of the transient with the perturbation signal produces errors in the measured gradient during the subsequent periods. It is shown that this error produces dissimilar adaptive loop response from each side of the optimum.

In the second method of closing the loop, the parameter is adjusted continuously. It is shown that

by using a running averager*, the gradient can be measured continuously, thus resulting in a system with continuous adjustment. Theoretical and experimental responses for the two systems have been obtained. It is shown that continuous parameter adjustment reduces the effect of the transient to a great extent resulting in similar forms of loop response from either side of the optimum.

The response of the system with continuous adjustment is shown to be superior in regard to response time, stability and errors due to output noise disturbances when compared with the response of the system with discontinuous adjustment.

An analogue running averager is developed which is novel and inexpensive. The principle of operation and performance of this running averager is described.

In a search for new uncorrelated periodic binary sequences with a desired auto-correlation function, two methods of synthesising these sequences are discussed. Some new sequences have been derived.

---

* A running averager is defined as giving a response $r(t) = \int_{t-T_1}^{t} x(s)\,ds$ where $x(t)$ is the applied signal.

LIST OF PRINCIPAL SYMBOLS

$y(t)$ = Response function of the controlled process.

$x(t)$ = The perturbation signal (PRBS).

$h(\tau)$ = Impulse response of the process from parameter to performance measure.

$\phi_{xy}(\tau)$ = Cross-correlation function between $x(t)$ and $y(t)$ for a delay of τ.

K = Parameter being adjusted in the adaptive system.

$\phi_{xx}(\tau)$ = Auto-correlation function of $x(t)$ for a delay of τ.

$\frac{dP}{dK}$ = Gradient of the parameter-performance characteristic.

λ = Clock period of the PRBS, Basic clock interval.

T = Period of the chain code.

ω_c = Repetition frequency of the PRBS.

N = Number of bits in the chain code or binary sequence.

$S(t)$ = Slope or gradient at time t.

$S(T)$ = Slope evaluated at intervals T.

$r(t)$ = Running average of $x(t)$.

$Z(t)$ = Output signal of the integrator.

$Z_1(t)$ = The component of the measured gradient

due to the transient in y(t).

$Z'(t)$ = Output signal of the second running averager RA2.

$Z_1'(t)$ = Error term in the measured gradient in the system with continuous adjustment.

ΔK_r = rth adjustment step.

$\alpha, \alpha_n, \alpha'$ = Transient factors in the system with discontinuous adjustment.

g = Gradient at the working point.

$q(t)$ = Unit step response from parameter to performance index.

T_i = Time constant of an integrator.

T_1 = Time over which running average is taken.

T_o = Time constant of the plant.

T_m = Measurement time.

$\emptyset$ = Phase angle of the running average wave-form.

β, β_k = Transient factors in the system with continuous adjustment.

δK_r = rth step change in parameter.

G = Loop gain.

σ_{cc}^2 = Mean square value of the chain code.

σ_{nn}^2 = Mean square value of the signal n(t).

$n(t)$ = Gaussian noise signal.

$\phi_{HH}(\tau)$ = $\int_{-\infty}^{+\infty} H_\eta(t)\, H_\eta(t+\tau)\, d\tau$ = Auto-correlation function of the impulse response $H_\eta(t)$ of a linear transfer function $H(p)$.

$H_\eta(t)$ = $H(t)$ for $o \leqslant t < \eta$.

= 0 otherwise.

$Z_\nu(t)$ = Output signal of the multiplier due to noise.

$\frac{1}{T_f}$ = Noise signal band-width.

D^2 = Variance.

$\rho_{ii}(\tau)$ = Normalised auto-correlation function of $i(t)$.

$L(t)$ = Gaussian input signal to the non-linearity.

$X(t)$ = Two-level sequence.

$Y(t)$ = Impulse train.

$u(t)$ = Unit step function.

$\delta(t)$ = Unit impulse function.

μ = Constant of square law device.

$\frac{1}{T_r}, \frac{1}{T_r}$, = Gain of the running averager.

B = A constant determining the amplitude of the fundamental component of $r(t)$.

C', C_s, G_1', G_1 = Constants.

1. INTRODUCTION

One of the main problems confronting the control engineers is the design of suitable controllers and compensators for processes whose properties are unknown and may be subject to extraneous disturbances and environmental changes under operating conditions. To overcome this difficulty, the technique of adaptive control has been developed and is the subject of several publications[20,21]. Adaptation is a highly developed biological process possessed by all living organisms. Adaptation is the mechanism by which the interaction of a system with its environment actuates some changes in the system which is in some sense an improvement to the performance of the system.

An 'Adaptive' or 'Self-optimising' system may be defined as a system in which one or more parameters are automatically adjusted to achieve and maintain a defined ideal standard of performance. Many techniques for automatic optimisation have been proposed[20,21,22,23] which vary in complexity and the nature of application. These methods can be classified broadly into open-loop and closed-loop techniques. Open-loop techniques are not dependent on the measurement of system

performance. They perform the optimisation in a pre-programmed manner on the basis of information about the structure and parameters of the system to achieve the best value for the chosen performance criterion. These techniques are limited in their application since considerable 'a priori' knowledge about the process is required for their implementation.

Closed-loop techniques, on the other hand, achieve optimisation based only on the direct measurement of a criterion of performance. They do not in general, need much 'a priori' information about the process. Among the principle difficulties of closed-loop optimisation are the definition and measurement of a meaningful performance criterion of the system. In many situations, the criterion can only be defined in a statistical sense. Then automatic optimisation must be performed using only estimates of the criterion. In such cases, the effect of noise introduces additional measurement difficulties due to statistical errors.

There are different methods of closed-loop optimisation proposed by various authors which have particular advantages and applications.

Anderson et al[24] determine the impulse response

of the overall system by injecting white noise and measuring the cross-correlation function between input and output. The parameters of the controller are adjusted so that the ratio between positive and negative areas of the impulse response attains its desired value. Margolis and Leondes[25] and Popov[26] describe the use of a learning model. In this method the learning model and the physical process are subject to the same input signals. Their outputs are compared and the resulting error is fed to the adjusting mechanism where some function of this error is used to adjust the parameters of the learning model. Draper and Li[27], Grensted and Jacobs[28] and Feldbaum[29] have proposed methods of iterative search which can be performed in many ways. In the discrete step method the parameter is adjusted successively by a fixed amount as long as the performance or error measure continues to decrease, otherwise a reverse step is taken. Variants of this method have been proposed by Gibson[30], Norkin[31] and others.

In the gradient method or the hill-climbing technique, the adjustment of the parameter is made proportional to the gradient of the parameter - performance index characteristic. The most practical method of

measuring the gradient is the technique of Parameter perturbation. Grensted and Jacobs[28], McGrath and Rideout[32], Blackman[33] and others[34,35] have described systems using sinusoidal perturbation signals. Douce and King[36] and others[37,38,45] have described systems using square-wave perturbation signals. Square-wave (or ON - OFF) perturbation has the advantage of easy mechanisation. Douce and Bond[39] have shown that the use of a sample-and-hold eliminates parameter excursions about the operating point, thus permitting more accurate measurements and higher loop gains. Ng[40] has shown that in some particular systems, high perturbation frequencies approaching the system natural frequency can be used with better transient response and more accurate steady state performance. Roberts[34] claims that sinusoidal perturbation gives the best performance compared to square-wave and random telegraph wave perturbations.

The principle difficulty with sinusoidal or square-wave perturbation is the phase lags introduced by the system dynamics. These dynamic effects cause a reduction in the loop-gain and can also cause instability of the optimising loop. Phase compensation is generally not applicable as the dynamics of

the loop are dependent on the parameter settings. To keep the dynamic effects small, relatively low frequency perturbation (of the order of $\frac{1}{10}$th to $\frac{1}{100}$th the system natural frequency) are employed. When the system is subject to noise disturbances, for acceptable statistical accuracy in the measurement of the gradient, even slower perturbation rates become necessary.

Van der Grinten[41] has proposed a method of using stochastic signals as perturbation signals. In this technique, the impulse response of the system is measured by correlation methods from which the gradient of the parameter - performance characteristic is deduced. The impulse response measured is that which defines the dynamics from parameter to performance measure. Thus, the problem of dynamic lags can be overcome by this method. The main disadvantage of using truly random signals for perturbation is the statistical errors introduced due to finite measurement times.

To eliminate these statistical errors, the method reported in this thesis employs pseudo-random binary sequences as perturbation signals. This technique

was first proposed by Douce and Ng[42]. These pseudo-random binary sequences (abbreviated by PRBS) or 'Chain Codes' are periodic with an impulsive auto-correlation function. Their properties are summarised in Appendix A.1. The main advantage of using these signals is that noise-free estimates of the gradient can be obtained if measurements are made over an integral number of periods of the chain code. In this thesis, two methods of closing the adaptive loop are examined.

In the first method, adjustments to the parameter are made discontinuously once every period of the chain code. This necessitates the use of a sample-and-hold element. The step adjustments set up transients in the response of the process which is usually correlated with the perturbation signal. This introduces error terms to the subsequent measurements of the gradient. The effect of this on the response is particularly pronounced at high loop gains.

If the adjustment steps can be made smaller by making a number of small adjustments to achieve roughly the same amount of total parameter change in

a period of the chain code, it may be expected that the transient effects will be reduced. This technique then requires a method of obtaining a noise-free estimate of the gradient as many times as there are adjustments in a period to retain the advantages of the use of a PRBS.

In the second method of closing the adaptive loop investigated, a technique is proposed to adjust the parameter continuously. The use of a 'Running Averager' provides a continuous noise-free measure of the gradient and hence the parameter can be adjusted continuously. This method is shown to be superior to the first method. Errors due to output noise disturbances are smaller. An approximate stability analysis of the system is presented.

Extension of this technique to simultaneous optimisation of several parameters of a multi-parameter system requires a corresponding number of uncorrelated pseudo-random binary sequences to eliminate the effects of cross-coupling between the channels. Such signals also find important applications for the identification of multiple-input (and -output) systems. Unfortunately, all the known PRBS are correlated to one another. It

would be ideal if sequences which are uncorrelated could be found. The first step for this is to find methods of synthesising new sequences which satisfy the other specified properties such as impulsive auto-correlation function. In Section 9 of this thesis, two methods for the generation of new sequences have been examined. Some new sequences have been derived. Attempts have been made to generalise and to extend one of these methods.

2. DEVELOPMENT OF THE HILL-CLIMBING SYSTEM

In the hill-climbing method of optimisation, the information required is the gradient of the parameter-performance measure characteristic. This relationship is not explicitly known, in most cases. The gradient has to be measured at the working point. For small perturbations about the working point, a linear relationship between performance measure P and parameter K is assumed (Fig.14). This assumption is perfectly valid for small signals even though the transfer function between the point at which the perturbation is applied and the point of performance measure is non-linear.

In measuring $\frac{dP}{dK}$, for a small step change dK in K, the steady state change in P is to be evaluated. The form of the change in P depends of course on the system and the input signals but for optimisation, only the final value is required.

The theory of the technique relies on two well-known relationships of linear theory.

1. If y(t) is the response to an input signal x(t), then $\int y(t)\,dt$ is the response to an input signal $\int x(t)\,dt$.

2. If the input signal to a linear process has an impulsive auto-correlation function, then the cross-correlation function between the input and output gives the impulse response of the process.

Using these relationships an expression for the gradient can now be derived.

Consider the block diagram of the general extremum control system of Fig.15. The output signal $y(t)$ of the process is given by

$$y(t) = \int_{-\infty}^{+\infty} x(t-\tau_1)\, h(\tau_1)\, d\tau_1$$

The cross-correlation function between the perturbation $x(t)$ and the output $y(t)$ is given by

$$\phi_{xy}(\tau) = \lim_{T\to\infty} \frac{1}{2T} \int_{-T}^{+T} x(t)\, y(t+\tau)\, dt$$

Therefore

$$\phi_{xy}(\tau) = \lim_{T\to\infty} \frac{1}{2T} \int_{-T}^{+T} x(t) \int_{-\infty}^{+\infty} x(t+\tau-\tau_1)\, h(\tau_1)\, d\tau_1\, dt$$

Interchanging the order of integration, we get

$$\phi_{xy}(\tau) = \int_{-\infty}^{+\infty} h(\tau_1)\, \phi_{xx}(\tau-\tau_1)\, d\tau_1$$

Integrating both sides with respect to τ, we get

$$\int_{-\infty}^{t} \phi_{xy}(\tau)\, d\tau = \int_{-\infty}^{t} \int_{-\infty}^{+\infty} h(\tau_1)\, \phi_{xx}(\tau-\tau_1)\, d\tau_1\, d\tau$$

If the integral of $\phi_{xx}(\tau-\tau_1)$ is convergent, then the order of integration can be interchanged giving

$$\int_{-\infty}^{t} \phi_{xy}(\tau)\, d\tau = \int_{-\infty}^{+\infty} h(\tau_1) \int_{-\infty}^{t} \phi_{xx}(\tau-\tau_1)\, d\tau\, d\tau_1$$

For sufficiently large t, the integral of $\phi_{xx}(\tau-\tau_1)$ tends to a constant value. Then the right hand side of the above Equation can be considered as the product of the two integrals. Hence,

$$\int_{-\infty}^{+\infty} h(\tau_1)\, d\tau_1 = \frac{\int_{-\infty}^{t} \phi_{xy}(\tau)\, d\tau}{\int_{-\infty}^{t} \phi_{xx}(\tau-\tau_1)\, d\tau_1} \qquad \ldots\ldots (1)$$

As h(t) is the impulse response or response to a small pulse, the integral of h(t) is the step response of the system. The static gain which is the final value of the step response of the system for small steps at the working point is given by

$$\frac{\Delta y}{\Delta x} = \int_{-\infty}^{+\infty} h(t)\, dt = \frac{\int_{-\infty}^{+t} \phi_{xy}(\tau)\, d\tau}{\int_{+t} \phi_{xx}(\tau)\, d\tau} \qquad \ldots\ldots (2)$$

The static gain gives the slope of the performance index. Hence,

$$\frac{dP}{dK} = \frac{\int_{-\infty}^{+t} \phi_{xy}(\tau)\, d\tau}{\int_{-\infty}^{+t} \phi_{xx}(\tau)\, d\tau}$$

When the perturbation signal is a stationary random signal, $\int_{-\infty}^{t} \phi_{xx}(\tau)\, d\tau$ is a constant and therefore the slope is obtained by measuring the integral of the cross-correlation function only. Thus,

$$\frac{dP}{dK} = C' \int_{-T_1'}^{T_1} \phi_{xy}(\tau)\, d\tau \qquad \ldots\ldots (3)$$

where T_1' is such that $\int_{-\infty}^{-T_1'} \phi_{xy}(\tau)\, d\tau$ is small and T_1 is large enough such that the system has settled down. The choice of T_1 is also affected by the noise disturbances in the process.

The mechanisation for the evaluation of Equation (3) can be derived easily. From Equation (3),

$$\frac{dP}{dK} = I = C' \int_{-T_1'}^{T_1} \phi_{xy}(\tau)\, d\tau = C' \int_{-T_1'}^{T_1} \int_{-\infty}^{+\infty} x(t-\tau)\, y(t)\, dt\, d\tau$$

For optimisation, we are only interested in the

integral of the impulse response. The impulse response which has to be obtained by a process of deconvolution, need not be determined explicitly. By interchanging the order of integration in the above Equation and letting $T_1'=0$, we get

$$I = \int_{-\infty}^{+\infty} y(t) \left[\int_{0}^{T_1} x(t-\tau)\, d\tau \right] dt \qquad \ldots\ldots (4)$$

In Equation (4),

$$\int_{0}^{T_1} x(t-\tau)\, d\tau$$

is the 'Running average' or 'Moving average' of the signal x(t). Thus the slope is determined by taking the running average of the perturbation signal, multiplying this by the performance y and integrating with respect to time. The block diagram of the scheme is shown in Fig.16.

One of the main difficulties of this technique is the generation of accurate delayed versions of the random signal x(t). In addition, it is necessary to ensure that the statistical properties of the random signal remain constant.

Here lies the main advantages of using PRBS as perturbation signals. As the chain code is deterministic, statistical errors can be eliminated by

measuring the slope over one period of the chain code. The PRBS and its delayed versions can easily be generated using shift registers and simple logic circuits[57](Fig.36). The running average of the PRBS is easily obtained using reversible binary counters (Fig.37). More details about the mechanisation are discussed in Section 8.

3. SYSTEM WITH DISCONTINUOUS PARAMETER ADJUSTMENT

The schematic diagram of the system developed in the last Section is shown in Fig.16. Let us consider the slope S(t) at time t after the start of the optimisation process. S(t) is given by

$$S(t) = \frac{1}{T_i}\int_0^t x(t)\, y(t)\, dt$$

$$= \frac{1}{T_1 T_i}\int_0^t \left[\int_0^{T_1} x(t-\tau)\, d\tau \right] y(t)\, dt$$

$$= \frac{1}{T_1 T_i}\int_0^{T_1} \int_0^t x(t-\tau)\, y(t)\, dt\, d\tau$$

or

$$S(t) = \int_0^{T_1} \phi_{xy}(\tau)\, d\tau \qquad \text{only when } t=T \qquad \ldots\ldots (5)$$

$$= S(T)$$

Thus, it is seen from Equation (5) that if a sample-and-hold element is included after the integrator, a noise-free measurement of the gradient $\frac{dP}{dK}$ can be obtained once every period of the chain code. The parameter adjustment can then be made in steps at intervals of the period of the chain code.

When operating under closed-loop conditions, the output signal y(t) has two components, one due to the

perturbation x(t) and the other due to the adjustment. Assuming that both the step adjustment and the perturbation are small, each of these components of y can be considered separately and superposition then applied to determine the signal Z(t). The first component of y yields, after multiplication by r(t) and integration over time T, an estimate of the gradient at the present working point, K_n. This is the desired signal determining the magnitude of the next step adjustment. Thus the desired step adjustment is

$$\Delta K_{n+1} = C_s S_n(T)$$

where $S_n(T)$ is given by Equation (5) and C_s is a constant which includes the loop gain of the system. The second component varies with time and is produced as a result of the transient in y due to the previous (that is nth) step adjustment. Multiplication of this transient component with the running average r(t) gives the error component in $S_{n+1}(T)$. For a given process, this component is readily determined and can be shown to be given by

$$Z_1(t) = \alpha_n . \Delta K_n \qquad \ldots\ldots (6)$$

α_n, the 'Transient factor' is proportional to the gradient at the previous working point K_{n-1}.

The magnitude of the (n+1)th step is therefore,

$$\Delta K_{n+1} = C_s \left[S(t) + Z_1(t) \right] = C_s \left[S_n(T) + \alpha_n \Delta K_n \right]$$

If the initial point is on the left of the optimum, the gradient is negative and the adjustment step is positive. Hence

$$\Delta K_{n+1} = C_s \left[S_n(T) + \alpha_n . \Delta K_n \right]$$

On the otherhand, if the initial point is on the right of the optimum, the gradient is positive and the adjustment step is negative and $\alpha_n' = -\alpha_n$. Hence

$$\Delta K_{n+1} = - C_s \left[S_n(T) - \alpha_n . \Delta K_n \right]$$

Thus, it is seen that the form and speed of response from an initial offset in parameter value depends on which side of the optimum the initial point lies.

As a simple example, let us assume that the parameter-performance index characteristic is a modulus type curve. The sequence of steps from an initial setting to the left of the optimum, where the gradient is negative is

$$\Delta K_1 = C_s . S(T) = +e \quad \text{(which is a constant)}$$

$$\Delta K_2 = e + \alpha . \Delta K_1 = e + \alpha e$$

$$\Delta K_3 = e + \alpha . \Delta K_2 = e + \alpha(e + \alpha e)$$

and so on.

On the right of the optimum the gradient is positive, so that $\alpha' = -\alpha$. Thus,

$$\Delta K_1 = -e$$

$$\Delta K_2 = -e + \alpha' . \Delta K_1 = -e + \alpha e$$

$$\Delta K_3 = -e + \alpha' . \Delta K_2 = -e + \alpha(e - \alpha e)$$

and so on.

The response is aided by the transient from one side and opposed from the other side. Therefore, the response is faster in the one case than the ideal response and slower in the other. For values of α above a certain value, the slower response is also oscillatory and if $\alpha > 1$, the system is unstable, in this case. Typical response curves for three different values of α are shown in Fig.17.

3.1. Evaluation of Transient Factor α

For a given PRBS and a known process, the value of α can be determined as follows.

The running average signal $r(t)$ is a repetetive signal of period T, with discrete levels, the transitions occuring at the intervals λ. The amplitude of the wave-form depends upon the period over which the running average is taken. It is zero when the

running average is taken over a period of the chain code and is a maximum when taken over (very nearly) half the period. r(t) also has the property that $r_{\frac{T}{2} - T_2}(t)$ is approximately equal to $r_{\frac{T}{2} + T_2}(t)$. When the running average is taken over a period of $\frac{(N \pm 1)}{2}$ clock intervals of the chain code, all the even harmonics in the amplitude spectrum vanish. The odd harmonics will be attenuated by the reciprocal of their orders. Hence, for the purposes of this analysis, r(t) can be approximated to a good degree of accuracy by its fundamental component given by

$$r_1(t) = B \sin\left(\frac{\omega_c T_1}{2}\right) \sin(\omega_c t + \phi) \quad \ldots\ldots (7)$$

where B is a constant depending on the amplitude of the chain code. The phase angle ϕ is determined by the starting point of the chain code. The starting point is arbitrary.

Let the response in y to a small step adjustment ΔK in K be $g.\Delta K.q(t)$ where g is the gradient at the working point and q(t) is the unit step response of the process from parameter to performance. The output of the integrator due to this component of y is

$$Z_1(t) = \frac{1}{T_i} \int_o^T g.\Delta K.B \sin\left(\frac{\omega_c T_1}{2}\right).q(t).\sin(\omega_c t + \phi)\, dt$$

i.e.

$$Z_1(t) = \frac{\Delta K.g.B.\sin\left(\frac{\omega_c T_1}{2}\right)}{T_i} \int_0^T q(t).\ \sin(\omega_c t+\phi)\ dt$$

or $$Z_1(t) = \alpha\ .\ \Delta K \qquad \ldots\ldots (8)$$

For a given process with constant dynamics, it is possible to choose a starting point such that the value of α is negligibly small or equal to zero.

3.2. Response of a Particular System

The system shown in Fig.16 has been studied on the analogue computer. The chain code used is a 127 bit code described by the polynomial equation

$$D^7 \oplus D^3 \oplus 1 = 0$$

where $\oplus$ denotes modulo-2 addition and D is the delay operator. This is generated by a seven stage shift register. The running average is taken over a time T_1 equal to 64 clock periods. The process consists of a square law characteristic followed by a first order lag of time constant T_o. More details of the analogue computer mechanisation is discussed in Section 8. The time constant of the plant used in the analogue simulation is 0.3 seconds and the clock frequency of the chain code perturbation 200 cps. The magnitude of the perturbation used is 10 percent of the initial

misadjustment.

The variations in α as a function of the starting point (and hence $\emptyset$) are shown in Fig.18 where point A corresponds to the starting point when all but one of the shift register outputs are zero (1000000). The running average taken over 64 clock intervals of the chain code is also plotted.

The theoretical response can be calculated by determining the loop gain and the transient factor α. The loop gain is a function of the integral of the cross-correlation function derived in Equation (5). For the first-order plant considered in this simulation, it is shown in Appendix A.2 that

$$\int_0^{T_1} \emptyset_{xy}(\tau)d\tau = 0.634\ \lambda \qquad \ldots\ldots (9)$$

If the other loop gain constant of the adaptive loop is given by G_1, then the actual loop gain for a given set of loop constants is

$$G = 0.634\ \lambda\ G_1$$

α is obtained from Fig.18 for the particular starting point of the chain code used in the mechanisation. From these values, the theoretical response of the adaptive system can be calculated.

For three different values of the loop constants, the response curves have been calculated and plotted as shown in Fig.19. The practical response obtained for the same values of loop constants is also plotted. There is a good degree of agreement between the two illustrating the good degree of approximation to r(t) by the expression of Equation (7). The response on one side of the optimum is quite different to that on the other side. When the loop gain is adjusted to give the fastest response without overshoot, the response on the other side exhibits oscillations of quite large magnitude. The response is also much slower (Fig.19(c)).

For the first-order plant considered in the above example, it can be derived from Equation (8) as shown in Appendix A.3 that the transient factor α is zero when the starting point is chosen such that

$$\tan \phi = -\frac{2\pi T_o}{T}$$

This corresponds to the two points B and B' in Fig.18. If the chain code had been chosen to start at B or B', the transient effect would have been very much reduced. This is not always possible in practice, since the dynamics of the process are usually unknown

and may change with parameter setting. Moreover, the starting point of the chain code may be chosen from such other considerations as elimination or reduction of cross-correlation between the running average and signal frequency drift terms[48].

4. SYSTEM WITH CONTINUOUS PARAMETER ADJUSTMENT

It is seen from the last Section that the error signal in Z(t) is due to the transient in y(t) following the step adjustment in K. The effect of the transient is seen to be small when the loop gain is small. Thus, if the adjustment steps are kept small, the effect of the transient can be reduced.

Instead of making adjustments once every chain code period, if a large number of steps per period keeping each adjustment step small can be effected, then it may be expected to result in a smaller transient effect. This in other words means, a continuous parameter adjustment. When the parameter is continuously adjusted, the rate of change of K is small and hence the contribution of the time varying component of y(t) to Z(t) will become negligible.

For the continuous adjustment of the parameter K, the slope is required to be measured continuously. It was shown in the last Section that noise-free measurement of gradient is possible only once per period of the chain code. It is shown in this Section that by using a second running averager after the correlation multiplier, it is possible to obtain a noise-free estimate of the slope continuously.

Consider the schematic diagram shown in Fig.20. Let the signal at the output of the second running averager be $Z'(t)$.

$$Z(t) = \frac{1}{T_i} \int_{t_o}^{t} r(t)\, y(t)\, dt$$

$$Z'(t) = \frac{1}{T} \int_{t_o}^{t} Z(t)\, dt - \frac{1}{T} \int_{t_o}^{t} Z(t-T)\, dt$$

(By the definition of the running average)

or

$$Z'(t) = \frac{1}{TT_i} \int_{t_o}^{t} \left[\int_{t_o}^{t} r(t)y(t)dt - \int_{t_o}^{t} r(t-T)y(t-T)dt \right] dt$$

But

$$r(t) = \frac{1}{T_1} \int_{o}^{T_1} x(t-s)\, ds$$

Therefore

$$Z'(t) = \frac{1}{TT_i} \int_{t_o}^{t} \left[\int_{t_o}^{t} \left\{ \frac{1}{T_1} \int_{o}^{T_1} x(t-s)\, y(t)\, ds - \right. \right.$$

$$\left. \left. - \frac{1}{T_1} \int_{o}^{T_1} r(t-T-s)\, y(t-T)\, ds \right\} dt \right] dt$$

Interchanging the order of integration inside the square brackets, we get

$$Z'(t) = \frac{1}{T_i T} \int_{t_o}^{t} \left[\frac{1}{T_1} \int_{o}^{T_1} \left\{ \int_{t_o}^{t} x(t-s)\, y(t)\, dt - \right. \right.$$

$$\left. \left. - \int_{t_o}^{t} x(t-T-s)\, y(t-T)\, dt \right\} ds \right] dt$$

Simplifying the second term, we get

$$Z'(t) = \frac{1}{T_i T} \int_{t_o}^{t} \left[\frac{1}{T_1} \int_{o}^{T_1} \left\{ \int_{t_o}^{t-T} x(t-s)y(t)dt + \int_{t-T}^{t} x(t-s)y(t)dt - \right. \right.$$

$$\left. \left. - \int_{t_o-T}^{t-T} x(t-s)y(t)dt \right\} ds \right] dt$$

Since the integration starts at $t=t_o$, the third integral cancels with the first giving

$$Z'(t) = \frac{1}{T_i T} \int_{t_o}^{t} \left[\frac{1}{T_1} \int_{o}^{T_1} \left\{ \int_{t-T}^{t} x(t-s)\, y(t)\, dt \right\} ds \right] dt$$

$$= \frac{1}{T_i T} \int_{t_o}^{t} \left[\frac{1}{T_1} \int_{o}^{T_1} \phi_{xy}(s)\, ds \right] dt$$

i.e.

$$Z'(t) = \frac{1}{T_i T} \int_{t_o}^{t} S(t)\, dt \qquad \ldots\ldots (10)$$

Thus, it is seen from Equation (10) that a noise-free measurement of the gradient is obtained continuously. The parameter is adjusted at a rate proportional to the integral of the slope. Hence

$$K(t) \propto \int_{t_o}^{t} S(t)\, dt$$

Thus $$K(t) = Z'(t)$$

The variation in y as a result of the continuous adjustment of the parameter will produce an error term in the measured slope. An exact analytical expression for the response of the closed-loop is very difficult to obtain. It is possible however to predict the response by a step-by-step method. The method considers the response K(t) to be made up of small changes at intervals equal to the bit interval as would be the case in a digital mechanisation. Thus, in a system using a chain code of length N bits, there will be N step changes in K in any period T. Each (little step) produces an error in S(t). In the following analysis, the order of integration and the process of taking the running average in the system of Fig.20 are considered interchanged. Since these are linear operations, this procedure is valid.

Consider the step change δK_k in K at time t-kλ and the corresponding variation in y occuring at time t. This produces an error term in S(t) given by

$$Z'(t)_k = g_k.\delta K_k.\frac{B \sin(\frac{\omega_c T_1}{2})}{T} \int_o^{k\lambda} q(t).\sin(\omega_c t+\phi_k)\, dt$$

$$= \beta_k \cdot \delta K_k \qquad \ldots\ldots (11)$$

where ϕ_k is the phase angle of r(t). Assuming the system dynamics to be constant over the range of K considered in the time interval t-T to t, then at time t, the total error in S(t) due to the change in K over the past period T is given by

$$Z_1'(t) = \sum_{k=o}^{N} \beta_k \cdot \delta K_k$$

If N is large, then the summation can be replaced by an integration and letting $\frac{k}{N} = \xi$, then $Z_1'(t)$ becomes

$$Z_1'(t) = \frac{g.N.\delta K.B.\sin(\frac{\omega_c T_1}{2})}{T}\left\{\int_o^1 d\xi . \int_o^{N\lambda\xi} q(t).\sin(\omega_c t+2\pi\xi)dt\right\}$$

$\ldots\ldots$ (12)

where it is assumed that g is constant over the range of K considered and each step is of the same small amplitude.

Interchanging the order of integration, Equation (12) becomes

$$Z_1'(t) = \frac{g.N.\delta K.B.\sin(\frac{\omega_c T_1}{2})}{T} \int_0^T q(t).\int_{t/T}^{1} \sin(\omega_c t+2\pi\xi)d\xi.dt$$

$$= \frac{g.N.\delta K.B.\sin(\frac{\omega_c T_1}{2})}{2\pi T} \int_0^T q(t).(\cos 2\omega_c t - \cos \omega_c t)dt$$

or $$Z_1'(t) = \beta \cdot \delta K \qquad \ldots\ldots (13)$$

It is seen from Equation (13) that the error in S(t) in this system is dependent as in the system with discontinuous adjustment on the gradient g and step size δK.

The value of α in Equation (8) and β in Equation (13) can be calculated if the system dynamics are known. For a first-order plant, q(t) is given by

$$q(t) = 1 - e^{-t/T_o}$$

and hence α can be evaluated as

$$\alpha = \frac{g.B.\sin(\frac{\omega_c T_1}{2})}{T_i} \cdot \frac{\omega_c T_o^2(1-e^{-T/T_o})}{(1+\omega_c^2 T_o^2)} \cdot (\cos\phi + \frac{1}{\omega_c T_o}\sin\phi)$$

$$\ldots\ldots (14)$$

Similarly, β is given by

$$\beta = \frac{g.N.B.\sin(\frac{\omega_c T_1}{2})}{2\pi T} \cdot \frac{T_o(1-e^{-T/T_o})}{(1+\omega_c^2 T_o^2)} \cdot \left[\frac{1+\omega_c^2 T_o^2}{1+4\omega_c^2 T_o^2} - 1 \right]$$

..... (15)

For a loop gain such that the total desired adjustment in a period is equal in both the continuous and discontinuous adjustment systems (that is $\Delta K = N.\delta K$), the ratio of the errors in the two systems is given by

$$\frac{Z_1(t)}{Z_1'(t)} = \frac{\omega_c T_o(\cos \phi + \frac{1}{\omega_c T_o} \sin \phi) \cdot 2\pi N}{\frac{1+\omega_c^2 T_o^2}{1+4\omega_c^2 T_o^2} - 1}$$

For the system studied in Section 3.2, $\frac{T}{T_o} \approx 2$ and ϕ corresponds to the starting point A of the chain code (Fig.18). Hence

$$\frac{Z_1(t)}{Z_1'(t)} = \frac{8}{3}\pi^2 . N$$

Thus, from the above Equation, it is seen that the error in the system with continuous adjustment is very much smaller than the error $Z_1(t)$ in the system with discontinuous adjustment. The response can therefore be expected to be closer to the ideal response and the speed similar on both sides of the optimum.

4.1. Response of a Particular System

The response of the system with discontinuous adjustment has been illustrated in Section 3.2. The same process is used for investigating the response with continuous adjustment. The block diagram of the system is shown in Fig.20. The sample-and-hold unit of Fig.16 has been replaced by the running averager RA2. The analogue running averager has been developed from a capacitor-drum delay generator. The development and performance of this running averager is discussed in detail in Section 7 of the thesis.

Typical response curves are shown in Fig.21. These curves have been plotted for the same relative loop gains as those of Fig.19. The predictions of Section 4 are well borne out by the experimental results. The response is seen (Fig.21) to be similar on either side of the optimum. The theoretical response can be calculated by a step-by-step method as outlined in Appendix A.4. The calculated values of the response are also shown in Fig.21. The experimental values agree reasonably well with the theoretical response.

The variation in the speed of response measured by the time to reduce the off-set in parameter to one third of its initial value with loop gain is shown in Fig.22.

The response times of the system with discontinuous adjustment are seen to be significantly different on each side of the optimum (by a factor of about 3.5:1). The optimum can be reached in about 10-12 time constants of the plant without any significant overshoots or oscillations. As the loop gain is increased, the response becomes more oscillatory and for relative loop gains higher than 7.8, instability occurs. The system with continuous adjustment has a higher permissible loop gain before the system becomes unstable as compared to the system with discontinuous adjustment. Further stability analysis of the system is presented in Section 6.

4.2. Dynamic Compensation

When a digital computer is employed in the hill-climbing technique under discussion, the impulse response of the process from parameter adjustment to performance measure is normally computed first, by the cross-correlation technique. The gradient $\frac{\partial e_m}{\partial K}$ is obtained by integrating the computed impulse response. In the system with continuous adjustment, the computed impulse response is updated every clock interval of the perturbing chain code so that the gradient is determined continuously.

Since the impulse response is available, the change in y due to the step adjustment in parameter can be computed. The transient component in y due to the step change is then subtracted from the present value of y before cross-correlating y with the chain code to calculate the present value of the gradient. This eliminates the error term in the measured gradient. The same technique is repeated for all the subsequent steps. This procedure called 'Dynamic compensation' can be applied to the systems with both continuous and discontinuous adjustments. Thus, the main error in the evaluated gradient is eliminated and the system response approaches the response of the system with an ideal gradient computer.

4.2.1. Experimental Results

Application of dynamic compensation is possible only when a digital computer is used for optimisation. To evaluate the improvement in performance when dynamic compensation is applied, results have been obtained for a second-order process. The process consists of a square law characteristic followed by a second-order plant with an additional time delay of transfer function

$$H(p) = \frac{K_p \cdot e^{-p\tau}}{(1+pT_a)(1+pT_b)}$$

where $K_p = 0.25$, $\tau = 200$ msecs, $T_a = 100$ msecs, $T_b = 1$ sec.

The PRBS used for perturbation is the one of length 63 bits described by the polynomial equation

$$D^6 \oplus D^5 \oplus 1 = 0.$$

The clock frequency used is 8 c/s.

Typical response curves both for the continuous and discontinuous adjustment systems are shown in Fig.23. The response curves of Fig.23 are for the system, without dynamic compensation. The response of the discontinuous adjustment system is seen to be quite dissimilar from either side of the optimum as has already been illustrated for the first-order system in Fig.19.

The effect of applying dynamic compensation is shown in Fig.24. This shows the variation in speed of response as measured by the total adjustment in a given time from an initial offset as a function of the starting point of the chain code. For the system with discontinuous adjustment, it is seen that the application of dynamic compensation results in more similar response times from either side of the optimum. The system with continuous adjustment and without dynamic compensation is seen to be almost as good as the ideal system.

Application of dynamic compensation has only limited improvement in this case and hence may only be advantageous to apply when the loop gain of the system is relatively high.

(The experimental studies reported in Section 4.2.1 have been carried out by Dr. K.C. Ng, Dr. D.H. Stockwell and Mr. K.R. Morris on the hybrid computing fecility at the National Physical Laboratory. The author is grateful to them for this work).

5. EFFECT OF NOISE

5.1. General

In this Section, the effect of random disturbances on the hill-climbing systems discussed in Sections 3 and 4 is considered.

In all practical systems, the process may be subject to extraneous disturbances and measurement noise. The effect of these disturbances is to introduce measurement uncertainty onto the measured value of gradient. The effect of random disturbances on the performance of the adaptive system can be studied by applying noise signals to the output or input of the process. Fig.25 shows the schematic diagram of the adaptive system with the noise signal added to the output of the process. It is assumed that n(t) is a stationary random process.

The statistical errors in measurement in the presence of the output noise can be evaluated for the systems with discontinuous and continuous parameter adjustment. The variance in the output of the integrator and the running averager respectively is calculated. It is shown that if the noise is band-limited, the system with continuous parameter adjustment has a lower variance.

5.2. Evaluation of Variance

Let the noise signal n(t) have a zero mean value and an auto-correlation function given by

$$\phi_{nn}(\tau) = \sigma_{nn}^2 \, e^{-\tau/T_f} \qquad \ldots\ldots (16)$$

For a linear system with random input, the relationship between the auto-correlation functions of the output and input signals is given by[49]

$$\phi_{oo}(\tau) = \int_{-\infty}^{+\infty} \phi_{ii}(\tau-t)\, \phi_{HH}(t)\, dt$$

If the input signal has zero mean, then the mean square value or the variance of the output fluctuations is given by

$$D^2 = \phi_{oo}(o) = \int_{-\infty}^{+\infty} \phi_{ii}(t)\phi_{HH}(t)dt \qquad \ldots\ldots (17)$$

From Equation (17), the variance at the output of any linear device can be calculated if the impulse response of the transfer function and the auto-correlation function of the input signal are known.

5.2.1. Variance of System with Discontinuous Adjustment

The adaptive system with discontinuous adjustment is shown in Fig.25(a). The input signal to the multi-

plier has two components - the signal component due to response of the system and the noise component. When the signal component is multiplied by the running average r(t) and integrated, the resulting signal gives a measure of the gradient. When the noise signal is multiplied by r(t) and integrated, the resulting signal contributes to the fluctuations with variance D^2. If r(t) and n(t) are uncorrelated, the auto-correlation function of the output of the multiplier is given by

$$\phi_{z_\gamma z_\gamma}(t) = \phi_{rr}(t)\,\phi_{nn}(t) \qquad \ldots\ldots (18)$$

If r(t) and n(t) are correlated, then $\phi_{z_\gamma z_\gamma}(t)$ involves the fourth moment terms of r(t) and n(t). It can be easily shown that the variance of the fluctuations at the output of the integrator (Fig.25(a)) is given by[50]

$$D^2 = \frac{2T_m}{T_i^2}\int_0^{T_m}\left(1-\frac{\tau}{T_m}\right)\text{Covariance}\left\{Z_\gamma(o), Z_\gamma(\tau)\right\}\,d\tau$$

where

$$\text{Covariance}\left\{Z_\gamma(o), Z_\gamma(\tau)\right\} = \phi_{z_\gamma z_\gamma}(\tau) - \left(E\{Z_\gamma\}\right)^2$$

$E\{Z_\gamma\}$ is the mean value of the random signal.

If the mean value is zero, then

$$D^2 = \frac{2T_m}{T_i^2}\int_0^{T_m}\left(1-\frac{\tau}{T_m}\right)\phi_{z_\gamma z_\gamma}(\tau)\,d\tau \qquad \ldots\ldots (19)$$

If $\phi_{z_\nu z_\nu}(\tau)$ is known, then the variance can be evaluated from Equation (19). For the evaluation of $\phi_{z_\nu z_\nu}(t)$, it is seen from Equation (18) that the auto-correlation function of the running average is required to be determined.

The running average signal is a periodic signal with a periodic auto-correlation function. When the running average is taken over 64 clock periods as has been done in the system of Fig.25, the auto-correlation function of r(t) can be shown to be

$$\left.\begin{aligned}
\phi_{rr}(\tau) &= \frac{\sigma_{cc}^2\lambda}{T_r^2}\left[-\tau + \frac{T}{4}\right] \qquad \text{for } 0<\tau<\frac{(N-1)\lambda}{2} \\
&= \frac{\sigma_{cc}^2\lambda}{T_r^2}\left[\frac{(N+1)\lambda}{2} + \frac{T}{4}\right] \quad \text{for } \tau=\frac{(N+1)\lambda}{2} \\
&= \frac{\sigma_{cc}^2\lambda}{T_r^2}\left[\tau - \frac{3}{4}T\right] \qquad \text{for } \frac{(N+1)\lambda}{2}<\tau<N\lambda
\end{aligned}\right\} \quad \ldots\ldots (20)$$

Equation (20) is plotted in Fig.26. It is seen that it has a triangular wave-form.

Since the period of r(t) is the chain code period, the upper limit of the integration in Equation (19) is T. From Equations (16) through (20), the variance

of the fluctuations at the output of the integrator is given by

$$D^2 = \frac{2.\sigma_{cc}^2.\sigma_{nn}^2.\lambda.T}{(T_i T_r)^2}\left[\int_0^{T/2} e^{-\tau/T_f}.(1-\frac{\tau}{T})(-\tau+\frac{T}{4})\,d\tau + \int_{T/2}^{T} e^{-\tau/T_f}.(1-\frac{\tau}{T})(\tau-\frac{3}{4}T)\,d\tau\right]$$

Evaluating the above integral and simplifying, we get

$$D^2_{S.H.} = \frac{2.\sigma_{cc}^2.\sigma_{nn}^2.T^4}{N(T_i T_r)^2}\left[e^{-T/2T_f}(d^2-4d^3) + e^{-T/T_f}(\frac{d^2}{4}+2d^3) + (\frac{d}{4}+2d^3-\frac{5}{4}d^2)\right] \quad \ldots\ldots (21)$$

where $d = \frac{T_f}{T}$.

The variance can thus be evaluated from Equation (21).

5.2.2. Variance of System with Continuous Adjustment

The block diagram of the adaptive system with continuous adjustment is shown in Fig.25(b). In the system with discontinuous adjustment (Fig.25(a)), the signals at points A and B are the same when t = T,2T,... whereas in the system with continuous adjustment, the

signal at point B_1 is the signal at A_1 averaged over a past period of the chain code. This averaging acts as additional filtering of the fluctuations and the resulting variance may be expected to be smaller than that obtained fron Equation (21) for the system with discontinuous adjustment.

The impulse response of the integrator and running averager combination H(t) is given by

$$H(t) = \mathcal{L}^{-1}\left[\frac{1}{p^2}\left(1 - e^{-pT}\right)\right] \qquad \ldots\ldots (22)$$

The auto-correlation function of H(t) is given by

$$\left.\begin{aligned} \phi_{HH}(\tau) &= \frac{1}{(T_i T_r')^2} \cdot (T-\tau)^2 \cdot \frac{(2T+\tau)}{6}, \quad \text{for } 0<\tau\leq T \\ &= 0 \qquad\qquad\qquad\qquad\qquad\qquad \text{for } |\tau|>T \end{aligned}\right\} \qquad \ldots\ldots (23)$$

As before, the variance is given by

$$D^2 = \frac{\sigma_{cc}^2 \cdot \sigma_{nn}^2 \cdot \lambda}{3(T_i T_r T_r')^2}\left[\int_0^{T/2} (2T+\tau)(T-\tau)^2\left(\frac{T}{4}-\tau\right) e^{-\tau/T_f}\, d\tau + \int_{T/2}^{T} (2T+\tau)(T-\tau)^2\left(\tau-\frac{3}{4}T\right) e^{-\tau/T_f}\, d\tau\right]$$

Evaluating the above integral, we get

$$D^2_{R.A.} = \frac{\sigma_{cc}^2 . \sigma_{nn}^2 . T^6}{12N(T_i T_r T_r')^2} \left[e^{-T/2T_f} . d^2(5-36d+72d^2+192d^3) \right.$$

$$\left. - e^{-T/T_f} . d^3(6+78d+96d^2) + d(2-11d+24d^2+6d^3-96d^4) \right]$$

..... (24)

The variance in the two systems can thus be evaluated from Equations (21) and (24). The calculated values are plotted in Fig.27 as a function of the ratio $\frac{T_f}{T}$.

It is seen that when the ratio $\frac{T_f}{T} < 1$, the variance in the system with continuous adjustment is lower by a factor of 2 to 3 compared to the system with discontinuous adjustment. This means that when the noise band-width is large compared to the perturbation signal band-width, the noise performance of the system with continuous adjustment is superior to that of the system with discontinuous adjustment.

The variance has been experimentally measured for the process comprising the square law device followed by a first-order transfer function $\frac{1}{1+pT_o}$. The noise signal used is obtained by passing a PRBS through a first-order low pass filter of time constant T_f. Further details of this are discussed in Section 8.

The measured values of the variance agree quite well with the calculated values for both systems.

5.3. System Response in the Presence of Noise

In the presence of output noise, the measured slope has a standard deviation which can be calculated from Equations (21) and (24). The stability and the accuracy of parameter adoption is affected due to noise. Typical response curves for the practical system described in Section 4.1 in the presence of output noise is shown in Fig.28. It is seen that when the noise to signal ratio is comparatively high, the parameter excursion about the optimum is large. Though the initial noise to signal ratio is 1:23, it becomes 1:1 when the parameter reaches 20 per cent of the optimum for the system of Fig.28(a). The effect of noise is most pronounced in the region of the optimum when the noise power becomes comparable to or larger than that of the signal power. The speed of adaptation roughly remains the same as that for the system free from noise disturbances. The peak to peak value of the parameter excursion about the optimum is seen to be about half for the system with continuous parameter adjustment as compared to the system with discontinuous adjustment when the loop gain is the same for both the systems.

6. STABILITY OF THE SYSTEM WITH CONTINUOUS ADJUSTMENT

6.1. General

The adaptive system considered in Section 4 is a closed loop system, and hence instability may exist. An exact analysis of system stability is difficult and no general method has been developed. Even for the simplest cases, the differential equations of the system are non-linear and time varying.

Under certain assumptions, an approximate stability analysis may be carried out. Such an approximate analysis for the system with continuous parameter adjustment is presented in this Section. The analytical technique only applies to the particular class of system investigated.

When the loop gain of the adaptive system is increased to too high a value to achieve a faster response, the response becomes erratic and oscillatory and the system may become unstable. The value of the loop gain is to be properly chosen to give a satisfactory response.

Consider the block diagram shown in Fig.29(a). Under closed-loop operating conditions, the parameter changes in small discrete steps after each adjustment.

For a small step change δK in the parameter K, the output of the non-linearity is given by

$$\delta y'(t) = \mu \left[\delta K^2 + 2K_i \delta K + 2\delta K . x(t) \right] u(t) \quad \ldots\ldots (25)$$

$$y(t) = \int_0^\infty h(\tau)\ \delta y'(t-\tau)\ d\tau$$

$$m(t) = r(t) \int_0^\infty h(\tau)\ \delta y'(t-\tau)\ d\tau$$

The running average of m(t) is taken over a period of the chain code and hence g(t) is given by

$$g(t) = \int_0^T m(t-s)\ ds$$

$$= \int_0^T r(t-s) \int_0^\infty h(\tau)\ \delta y'(t-s-\tau)\ d\tau$$

Substituting for $\delta y'(t)$ from Equation (25), we get

$$g(t) = \int_0^T r(t-s) \int_0^\infty A_k\ h(\tau)\ u(t-s-\tau)\ d\tau\ ds\ +$$

$$\int_0^T r(t-s) \int_0^\infty B_k\ h(\tau)\ x(t-s-\tau)\ u(t-s-\tau)\ d\tau\ ds$$

where

$$A_k = \mu(\delta K^2 + 2K_i \delta K) \quad , \quad B_k = 2\mu\delta K$$

or $$g(t) = g_1(t) + g_2(t)$$

$g_1(t)$ can be expressed as

$$g_1(t) = A_k \int_0^T r(t-s) \int_0^{t-s} h(\tau)\, d\tau\, ds$$

or

$$g_1(t) = A_k \int_{t-T}^{t} r(\tau_1) \int_0^{\tau_1} h(\tau)\, d\tau\, d\tau_1 \quad \ldots\ldots \quad (26)$$

$g_2(t)$ can be expressed as

$$g_2(t) = \int_0^T \int_0^{T_1} x(t-s-\tau_2)\, d\tau_2 \int_0^{\infty} B_k h(\tau)\, x(t-s-\tau)\, u(t-s-\tau)\, d\tau\, ds$$

Interchanging the order of integration, we get

$$g_2(t) = B_k \int_0^{T_1} d\tau_2 \int_0^{T} x(t-s-\tau_2)\, ds \int_0^{\infty} h(\tau)\, x(t-s-\tau)\, u(t-s-\tau)\, d\tau$$

If the order of integration and multiplication is interchanged,

$$g_2(t) = B_k \int_0^{T_1} d\tau_2 \int_0^{\infty} h(\tau)\, d\tau \int_0^{T} x(t-s-\tau)\, x(t-s-\tau_2)\, u(t-s-\tau)\, ds$$

This can be rearranged and simplified to give

$$g_2(t) = B_k \int_0^{T_1} d\tau_2 \int_0^{\infty} h(\tau) d\tau \int_0^{t-\tau} x(v)\, x(v+\tau-\tau_2)\, dv \,, \qquad \text{for } t<T+\tau$$

$$= B_k \int_0^{T_1} d\tau_2 \int_0^{\infty} h(\tau)\, \phi_{xx}(\tau-\tau_2)\, d\tau \,, \qquad \text{for } t>T+\tau$$

..... (27)

Equations (26) and (27) give expressions for the output of the running averager for a small step change in parameter. If $g(t)$ can be evaluated explicitly, then the forward loop of the adaptive system can be represented by an equivalent linear small signal transfer function. The stability analysis can then be carried out by well known techniques applicable to linear systems. For simplicity, let us first consider the system neglecting system dynamics.

6.2. System without Dynamics

If the system dynamics are neglected, then impulse response $h(\tau)$ can be represented by an impulse function

$$h(\tau) = \delta(\tau)$$

Substituting the above for $h(\tau)$ into Equations (26) and (27), the expressions for $g_1(t)$ and $g_2(t)$ are

$$g_1(t) = A_k \int_{t-T}^{t} r(\tau_1)\, d\tau_1$$

$$g_2(t) = B_k \int_{0}^{T_1} d\tau_2 \cdot \int_{0}^{t} x(v)\, x(v-\tau_2)\, dv \qquad \text{for } t<T$$

..... (28)

$g_1(t)$ is zero since it is the integral of the running average over a period of the chain code. Hence

$$g(t) = B_k \int_{0}^{T_1} d\tau_2 \cdot \int_{0}^{t} x(v)\, x(v-\tau_2)\, dv \qquad \text{for } t<T$$

..... (29)

The first integration in Equation (29) which is with respect to τ_2 can be replaced by a summation over the range $T_1(=n_1\lambda)$ since $x(t)$ is a discrete signal. This results in

$$g(t) = B_k \cdot \int_{0}^{t} x(v) \cdot x(v)\, dv + B_k \cdot \sum_{j=\lambda}^{n_1\lambda} \int_{0}^{t} x(v) \cdot x(v-j)\, dv$$

..... (30)

In Equation (30), the first term is the product of the chain code with itself integrated over time t. Since x takes the values ± 1, the integral over time t is a ramp function the slope of which depends upon B_k. The second term of Equation (30) is not easy to evaluate.

It represents a randomly varying signal in the interval $t<T$. At $t = T = N\lambda$

$$g(T) = B_k \cdot \int_0^T x(v).x(v).dv + B_k \cdot \sum_{j=\lambda}^{n_1\lambda} \int_0^T x(v).x(v-j).dv$$

$$= B_k \cdot T + B_k \cdot \sum_{j=\lambda}^{n_1\lambda} \phi_{xx}(j) \qquad \ldots\ldots (31)$$

The auto-correlation function $\phi_{xx}(\tau)$ is zero except at $\tau = o$ and hence

$$g(t) = B_k \cdot T \qquad \text{for } t \geqslant T \qquad \ldots\ldots (32)$$

Thus, after a step change in parameter, the output of the running averager reaches a steady value at the end of one period of the chain code.

The variation of g(t) is shown in Fig.29(b). If the random fluctuations are neglected, this is identical to the step response of a running averager. Hence, in the absence of system dynamics, the small signal transfer function from point P to Q (Fig.29(a)) can be represented by a running averager.

6.3. System with Dynamics

When the system dynamics are included, the expression for $g(t)$ becomes more complicated to evaluate. $g_1(t)$ is given by Equation (26) and it is again zero for all t. $g_2(t)$ is given by Equation (27) which can be simplified to give

$$g_2(t) = B_k \int_0^{\infty} h(\tau)\, d\tau \sum_{j=0}^{j=n_1\lambda} \int_0^{t-\tau} x(v)\, x(v+\tau-j)\, dv \qquad \text{for } t < T+\tau$$

$$= B_k \int_0^{T_1} h(s)\, ds \qquad \text{for } t > T+\tau \qquad \ldots\ldots (33)$$

or this can be written as

$$g_2(t) = B_k \int_0^{\infty} d\tau \int_0^{t-\tau} h(\tau)\, d\tau \; + \; B_k \int_0^{\infty} h(\tau)\, d\tau \sum_{j=\lambda}^{j=n_1\lambda} \int_0^{t-\tau} x(v)\, x(v+\tau-j)\, dv \qquad \text{for } t < T+\tau$$

$$= B_k \int_0^{T_1} h(s)\, ds \qquad \text{for } t > T+\tau$$

If the random variations represented by

$$\sum_{j=\lambda}^{j=n_1\lambda} \int_0^{t-\tau} x(v)\, x(v+\tau-j)\, dv$$

are assumed to be small and neglected, then $g_2(t)$ can be represented by the step response of the running averager and the plant transfer function in cascade. Then the small signal transfer function from point P to Q (Fig.29(a)) can be represented by the plant transfer function in cascade with the running averager. This can be seen to be valid from physical considerations as follows.

Consider the block diagram shown in Fig.29(a). When an impulse δK_o (of duration λ) is applied at P, the effect of this is to move the working point along the square law characteristic in the affected direction. As a result, the input signal $\mu(K_i+x(t)+\delta K_o)^2$ to the plant has a component which is the modulated chain code. The response to this is important as all the other terms effectively contribute to only a change in the gain. The response of the plant due to this signal is the modulated impulse response of the plant. The multiplication of y(t) and r(t) is equivalent to the multiplication of the plant response by the chain code x(t) and its successive delayed versions

$\left[\text{upto } x(t-n_1\lambda)\right]$ and summation of the multiplier outputs. The output of the multipliers corresponds to the successive ordinates of the modulated impulse response at time intervals $o,\lambda,2\lambda,\ldots,n_1\lambda$. The output of the multipliers depends on the instant at which the impulse is applied. The ensemble average of the output of the multipliers is a time function which is the impulse response h(t) of the plant. Therefore, for small signals, the transfer function from P to P_1 can be represented by the transfer function of the process dynamics. Thus, the small signal transfer function from P to Q can be represented by the plant transfer function in cascade with the running averager.

Fig.30(a) shows the schematic diagram of the approximate linear model which can be analysed for stability.

For a first-order plant $\frac{1}{1+pT_o}$, the Nyquist diagram is shown in Fig.30(b)*. From the Nyquist plot, it is found that the system becomes unstable for

$$G \geqslant 3.45$$

The practical value obtained for the adaptive system

---

* The running averager has a frequency response as shown in Fig.35.

of Section 4.1 is

$$G \geqslant 3.72$$

For the application of this method of approximate stability assessment, only an estimate of the impulse response or frequency response of the plant is required. The method is not limited to low order plants in principle, though experimental results have not been obtained for higher order plants. The method can be applied to systems with time delays also.

7. THE ELECTRO-MECHANICAL RUNNING AVERAGER

7.1. General

It was shown in Section 2 that the mechanisation for the evaluation of the integral of the cross-correlation function requires the generation of the 'Running average' or 'Moving average' of the perturbation signal.

The running average R(t) of a function of time U(t) over an interval of time T_r is defined as

$$R(t) = \int_{o}^{T_r} U(t-s)\, ds = \int_{t-T_r}^{t} U(s)\, ds \qquad \ldots\ldots (34)$$

where U(t-s) is the delayed version of the function U(t). Equation (34) can also be written as

$$R(t) = \int_{-\infty}^{t} U(s)\, ds - \int_{-\infty}^{t} U(s-T_r)\, ds \qquad \ldots\ldots (35)$$

By the definition of Equations (34) and (35), the running average R(t) at time t of the signal U(t) is the integral of the signal over the interval $(t-T_r)$ to t. That is, it is equal to the integral of U(t) minus the integral of the delayed signal $U(t-T_r)$.

In Section 4, it was shown that two running averagers are required (Fig.20) for the mechanisation of the adaptive system with continuous parameter adjustment. The first running averager is easy to implement digitally since the two-level signal and its delayed version are obtained by logic circuits, and the difference signal (±1 or 2 or zero) can be added to a reversible digital counter. Also, this counter need have quite a small capacity as can be seen for example, from Fig.37.

The second running averager is much more difficult to realise however, since the input analogue signal is not confined to discrete amplitude levels. A new method of generating the running average of an analogue signal using an electro-mechanical device has been developed. In this Section, the development and operation of this running averager is described.

According to the definition of Equation (35), the mechanisation for the computation of R(t) is shown schematically in Fig.31.

From Fig.31, the impulse response of the running averager can be expressed as

$$h_r(t) = u(t) - u(t-T_r) \qquad \ldots\ldots (36)$$

Thus, the impulse response of the running averager has a box-car wave-form.

7.2. Methods of Simulation

The method of simulation of the running average as represented in Fig.31 requires the delayed version of the time function. When the signal whose running average is required is discrete, delayed versions of the function can easily be generated as discussed earlier. But when the signal is a continuous function of time, the generation of delayed versions are not very easy and accurate. The delayed versions of such time functions can be obtained by conventional techniques such as electronic delay circuits or magnetic tape delay lines. With these methods, precise unity gain setting for the delay block (Fig.31) is difficult. If the gain is not exactly unity, the residual difference, when integrated, results in considerable deviations from the correct running average at the output of the integrator. This is a serious limitation on the accuracy obtainable by this method.

If the delayed versions are obtained using the R.C. network approximation based upon Taylor's expansion of $U(t-T_r)$, the amplitude and phase distortion will be

excessive. An alternative but rather expensive method is to convert the analogue signal into a digital signal. The delayed versions are then readily obtained and the running average computed using reversible binary counters. A D-to-A converter is then used to obtain the analogue running average signal. The accuracy here is dependent on the A-to-D and D-to-A converters used, and the number of past values maintained in the store.

The electro-mechanical running averager described below has the advantages of low cost and simplicity. No complicated equipment or circuitry is involved. It is particularly useful when analogue signals are involved.

7.3. Principle of Operation

The principle of operation of this running averager is the capability of a capacitor drum to generate delayed versions of the time function. The performance of the capacitor drum as a delay generator is described first, before describing the running averager proper.

A number of capacitors are connected at one end each to a commutator segment on a rotating drum and at the other ends to a common point. Two brushes are

provided on the commutator. The input voltage (a function of time) is connected to one of the brushes, the other brush is taken to the input of a high input-impedance amplifier. The common point of the capacitors is earthed.

When a commutator is in contact with the input brush through its connected commutator segment, the input voltage charges the capacitor to the instantaneous value of the input voltage. The capacitor moves on with its full charge until it comes in contact with the next brush when the charge on the capacitor causes the output voltage of the amplifier to rise to a value proportional to the stored charge. If the leakage is negligible, the output voltage is the same as the instantaneous value of the input voltage, but delayed by a time interval equal to the time taken by the capacitor to move from one brush to the other. Similarly, successive capacitors delay the successive instantaneous values of the input voltage and the voltage at the output of the amplifier is thus a delayed version of the input voltage. The length of the delay is conveniently varied by varying the speed of rotation of the drum.

The capacitor drum described above can be used in

a novel manner to realise Equation (35) and generate the running average.

This is best illustrated by considering the arrangement shown in Fig.32. The voltage whose running averager is required is connected to a brush on the drum. The common point of the capacitors is taken to the virtual earth of an electronic integrator. The capacitors are charged to the instantaneous value of the input voltage U(t) as they pass under the brush in turn. After a complete revolution, when the first capacitor again comes under the brush, it is charged to the new value of the input voltage at that instant of time and thus the previous charge is automatically erased.

If U(t) is an impulse $A_1.u_o(t_o)$ occuring at $t=t_o$, the capacitor which is in contact with the brush at $t=t_o$ gets charged to the value

$$q_i = A_1.C$$

where C is the value of the capacitance.

At point A, the virtual earth of the amplifier

$$i_i = i_o$$

Therefore, $$q_i = q_o$$

Hence the output voltage V_o is given by

$$V_o = -\frac{A_1 C}{C_1}$$

After one full revolution, when the same capacitor passes through the brush again the original charge is erased and hence the output voltage falls to zero. Thus the impulse response is a constant of magnitude $\frac{A_1 C}{C_1}$ from t_o to $t_o+n\Delta t$ and zero for all other values of t, where $n\Delta t$ is the time required for one complete revolution.

Thus, the successive values of the input signal is remembered over the time required for one revolution. The output of the integrator is the average value of the input signal over the last period, that is, it is the running average of the input signal over this period.

7.4. Construction of the Running Averager

Fig.33 shows the practical set-up of the running averager. The capacitors are connected between two copper-laminate discs on which the desired number of conducting segments (commutator segments) has been etched. Low leakage high stability polystyrene capacitors are used. In the unit built, 127 such

condensers (each 1000 pf) are employed. The capacitor drum is driven by a servo-motor. Since the time over which the running average is taken is the time required for one complete revolution of the drum, the running average of the signal over a wide range of time intervals can be obtained by driving the drum at the appropriate speed.

As stated in Section 4.1, this running averager has been particularly developed for use as RA2 in Fig.20. In this application, the running average is taken over exactly one period of the chain code. To achieve correct synchronisation, the clock pulses for the shift register generating the perturbation signal is generated by the same shaft that drives the capacitor drum. This is done by arranging a circular aluminium disc with 127 equally spaced holes on its pheriphery to be driven from the shaft of the capacitor drum. The holes in the rotating disc allow light from a light source to energise a photo-transistor whose output is shaped to give a square wave signal. Hence in one revolution of the disc, 127 clock pulses are generated. Thus, the period of the chain code is synchronised to the revolutions of the drum.

A photograph of the complete running averager is shown in Fig.34.

7.5. Frequency Response of the Running Averager

By transforming Equation (36), the frequency response $H_r(j\omega)$ of the running averager is obtained as

$$H_r(j\omega) = \frac{T_r \cdot \sin \frac{\omega T_r}{2}}{\frac{\omega T_r}{2}} \cdot \angle - \frac{\omega T_r}{2} \qquad \ldots\ldots (37)$$

This is plotted in Fig.35 where the practical values obtained are also shown. It is seen that the experimental and theoretical values agree quite closely. The error is within 2.5 percent in the low frequency range.

8. SPECIAL COMPUTING ELEMENTS

The experimental work on the adaptive systems described in Sections 3 and 4 were carried out on a special purpose analogue computer which employed chopper stabilised computing amplifiers. In this Section, the special circuitry employed are described.

The PRBS used in the experiments is of 127 bit length and is generated by a seven stage feed back shift register. The delayed signal $x(t-64\lambda)$ required for generating the running average is obtained at the output of a not-equivalent gate, the inputs to which are the signals from the second and fourth stages of the shift register. The block diagram of the arrangement is shown in Fig.36. The clock pulses for the chain code generator are generated by the analogue running averager as described in Section 7.4.

The chain code and its delayed version are gated to obtain the ADD and SUBTRACT pulses as shown in Fig.37(a) which form the inputs to the reversible binary counter generating the running average of the chain code. The running average is a discrete level signal whose amplitude does not exceed eight levels and hence four counters are adequate for the purpose.

The flow diagram of the arrangement is shown in Fig.37(b).

The multiplication of the running average r(t) by the response y(t) is carried out by a hybrid multiplier. The multiplier is a switching arrangement formed by the six diode bridge, shown in Fig.38(a). The multiplier built can handle upto ±20v with a switching error of less than 5 mv. The integral of the multiplier output is the required measure of the slope $\frac{dP}{dK}$.

The response of the adaptive loop depends on the starting point of the chain code as discussed in Section 3. In the mechanisation, further logic circuitry ensures that the starting point corresponds to the state 1000000 of the shift registers.

All the gates, flip flops and other circuitry are semi-conductor circuits.

The parameter is wired-in as a coefficient potentiometer which is set by a low inertia R.P.C. system the input of which is the output of the integrator. The output shaft position of the R.P.C. is obtained from the second gang of the two gang potentiometer.

The noise signal used for the measurement of

variance as described in Section 5 is obtained by passing a PRBS through a first-order low pass filter. The bandwidth of the filter is chosen such that the amplitude probability distribution of the resulting wave-form is Gaussian[51]. The PRBS used is the one of length 2043 generated by an 11 stage feed back shift register.

9. METHODS OF SYNTHESIS OF NEW BINARY SEQUENCES

9.1. General

The hill-climbing technique described in Sections 3 and 4 can be readily extended to the simultaneous adjustment of parameters of a multi-parameter system, if uncorrelated PRBS can be generated. All the known quadratic residue and m-sequences are correlated to one another. Godfrey et al[52] have described modifications to the known m-sequences to obtain uncorrelated sequences. The instrumentation of these modifications in practical applications is difficult.

There are many applications for sequences which have approximately an impulsive auto-correlation function and uncorrelated to one another or to the existing sequences. In a search for such new sequences, two methods of synthesis are examined in this Section. Some new sequences have been derived by using one of these techniques. Unfortunately, these sequences are not uncorrelated to any of the known sequences of the same length.

9.2. Method of Synthesis using a Non-linearity

A well known relationship between the auto-corre-

lation functions of the input and output signals of a bang-bang non-linearity for Gaussian input signals exists[53] which is given by

$$\rho_{ii}(\tau) = \sin\left[\frac{\pi}{2} \cdot \phi_{oo}(\tau)\right] \quad \ldots\ldots (38)$$

Fromthis relationship, for any desired form of the auto-correlation function of the output of the non-linearity, the auto-correlation function of the input signal can be obtained. From the Wiener-Khintchine relationships, the power spectrum of the Gaussian input signal can be calculated. If the signal with such a power spectrum can be generated, then the desired two-level sequence is readily obtained.

Let us now consider a few desired forms of the output auto-correlation function.

(i) The auto-correlation function of the output signal X(t) is assumed to be periodic and as shown in Fig.39(a). $\phi_{XX}(\tau)$ is defined over a period $N\lambda$ by

$$\phi_{XX}(\tau) = 1 - \frac{|\tau|}{\lambda} \qquad \text{for } |\tau| < \lambda$$

$$= 0 \qquad \text{for } \tau > \lambda$$

Fourier transformation of $\phi_{LL}(\tau)$ gives, using Equation (38)

$$\Phi'_{LL}(\omega) = 2\int_{0}^{\lambda} \sigma^{2}_{LL} \cdot \sin\left[\frac{\pi}{2}(1-\frac{\tau}{\lambda})\right] \cos \omega\tau \, d\tau$$

which after integration results in

$$\Phi'_{LL}(\omega) = \frac{\frac{\pi}{\lambda}\cdot\sigma^{2}_{LL}}{(\frac{\pi}{2\lambda})^{2} - \omega^{2}} \cos \omega\lambda$$

The input signal L(t) is periodic. The power spectrum is hence discrete with a harmonic separation equal to the period of the output sequence. The input power spectrum is given by

$$\Phi_{LL}(\omega) = 2\pi \cdot \sum_{r=-\infty}^{+\infty} \alpha_{r} \cdot \delta(\omega - r\omega_{c})$$

where

$$\alpha_{r} = \frac{1}{N\lambda} \Phi'_{LL}(\omega) \Big]_{\omega=r\omega_{o}}$$

in which

$$\omega_{o} = \frac{2\pi}{N\lambda}$$

Hence

$$\Phi_{LL}(\omega) = \frac{2\pi\cdot\sigma^{2}_{LL}}{N\lambda} \cdot \sum_{r=-\infty}^{+\infty} \frac{\pi/\lambda}{(\frac{\pi}{2\lambda})^{2} - (r\omega_{o})^{2}} \cdot \cos r\omega_{o}\lambda \cdot \delta(\omega - r\omega_{o}) \quad \ldots\ldots (39)$$

It is seen from Equation (39) that the power spectrum becomes negative for values of $\omega > \frac{3\pi}{2\lambda}$. Hence the signal with this power spectrum is physically unrealisable. Thus, a two level periodic sequence with a triangular form of auto-correlation function cannot be synthesised by this technique.

(ii) If the auto-correlation function of the output sequence is assumed to have an auto-correlation function of that of a PRBS (triangular with a negative bias for $\tau > \lambda$), it can be derived as in (i) that the power spectrum cf the input signal becomes negative and hence the signal is physically unrealisable.

(iii) The auto-correlation function of the output sequence is assumed to be of the exponential form and periodic with period $N\lambda$. It is given by

$$\phi_{XX}(\tau) = e^{-\frac{|\tau|}{\lambda}}$$

Therefore

$$\phi_{LL}(\tau) = \sigma_{LL}^{2} \cdot \sin\left[\frac{\pi}{2} \cdot e^{-\frac{|\tau|}{\lambda}}\right]$$

The Fourier transformation of $\phi_{LL}(\tau)$ is given by

$$\Phi'_{LL}(\omega) = \int_{-\frac{N\lambda}{2}}^{+\frac{N\lambda}{2}} \sigma_{LL}^{2} \cdot \sin\left[\frac{\pi}{2} \cdot e^{-\frac{|\tau|}{\lambda}}\right] e^{-j\omega\tau} \cdot d\tau \qquad \ldots\ldots (40)$$

But

$$\sin\left[\frac{\pi}{2} \cdot e^{-\frac{|\tau|}{\lambda}}\right] =$$

$$\frac{\pi}{2} \cdot e^{-\frac{|\tau|}{\lambda}} - \left(\frac{\pi}{2}\right)^{3} \cdot \frac{1}{\angle 3} \cdot e^{-\frac{3|\tau|}{\lambda}} + \left(\frac{\pi}{2}\right)^{5} \cdot \frac{1}{\angle 5} \cdot e^{-\frac{5|\tau|}{\lambda}} - + \ldots$$

Substituting for $\sin\left[\frac{\pi}{2} \cdot e^{-\frac{|\tau|}{\lambda}}\right]$ and evaluating the integral of Equation (40) and simplifying, we get

$$\Phi'_{LL}(\omega) = 2\lambda.\sigma_{LL}^{2} \cdot \sum_{k=0}^{k=\infty} \frac{(-1)^{k} \cdot \left(\frac{\pi}{2}\right)^{2k+1}}{\angle 2k+1 \left[(2k+1)^{2}+\omega^{2}\lambda^{2}\right]}$$

$$\left[(2k+1) + e^{-\frac{N}{2}(2k+1)} \left[\omega\lambda.\sin\frac{N\omega\lambda}{2} - (2k+1).\cos\frac{N\omega\lambda}{2}\right]\right]$$

If N is large, which is generally true, $\exp(-\frac{N}{2})$ becomes extremely small and hence the second term

inside the brackets can be neglected. Therefore

$$\Phi'_{LL}(\omega) = 2\lambda.\sigma^2_{LL}.\sum_{k=0}^{k=\infty} \frac{(-1)^k.(\frac{\pi}{2})^{2k+1}}{\underline{/2k}\left[(2k+1)^2+\omega^2\lambda^2\right]}$$

The auto-correlation function of the input signal is periodic. In a similar way as derived in (i) above, the power spectrum of the input signal is given by

$$\Phi_{LL}(\omega) = \frac{2\pi}{N\lambda}.2\lambda.\sigma^2_{LL}.\sum_{r=-\infty}^{+\infty}\sum_{k=0}^{\infty} \frac{(-1)^k.(\frac{\pi}{2})^{2k+1}}{\underline{/2k}\left[(2k+1)^2+r^2\omega_o^2\lambda^2\right]}\delta(\omega-r\omega_o)$$

Truncating the infinite series into N terms,

$$\Phi_{LL}(\omega) = \frac{4\pi.\sigma^2_{LL}}{N}.\sum_{r=-N}^{+N}\sum_{k=0}^{\infty} \frac{(-1)^k.(\frac{\pi}{2})^{2k+1}}{\underline{/2k}\left[(2k+1)^2+r^2\omega_o^2\lambda^2\right]}\delta(\omega-r\omega_o)$$

..... (41)

This power spectrum is always positive and hence the corresponding signal is physically realisable in theory. As an example, assuming that the output sequence is periodic and of length 31 bits, the power spectrum of Equation (41) is plotted in Fig.40. A time function with this discrete spectrum is to be generated to synthesise the sequence.

But unfortunately, it is not possible to generate Gaussian repetitive signals and hence it has not been possible to synthesise any new sequences by this method.

9.3. Method of Synthesis using Impulse Trains

A suitably selected impulse train when integrated results in a two level sequence. It is a well known property[49] that the auto-correlation function of the input signal to the integrator is the negative second derivative of the auto-correlation function of the signal at the output of the integrator. If the form of the auto-correlation function of the output is specified, then by the above property, the auto-correlation function of the input impulse train can be derived. Knowing the auto-correlation function, it may then be possible to synthesise the actual input impulse train.

For the successful application of this method, the following essential properties must be satisfied.

(i) The number of impulses in the input impulse train must be even.

(ii) All impulses must be of equal magnitude.

(iii) The impulses must alternate in sign.

(iv) The variable to be chosen to give the desired auto-correlation function is the time spacing between successive impulses.

The general arrangement of generating sequences by this method is shown in Fig.41(a). The general form of the output auto-correlation function considered for synthesis and the corresponding input auto-correlation functions are shown in Fig.41(b) and (c).

9.3.1. Necessary Conditions for the Existence of Sequences

It is not always possible to generate sequences of a given auto-correlation function. It is shown in Appendix A.5 that if the auto-correlation function of the output sequence consists of successive straight line sections with increasing slopes (for $\tau>0$), such sequences cannot be synthesised. If the desired auto-correlation function consists of a number of straight line sections with decreasing slopes as shown in Fig. 41(b), then some necessary (but not sufficient) conditions for the existence of the sequence can be derived.

Condition (1)

A relation between the number of 'Ones' and the length of the sequence can be derived as follows:

Let the sequence be of length N and the number of 'Ones' in the sequence be m. The desired auto-correlation function of the sequence is shown in Fig. 41(b) where $s_1 > s_2 - s_1 > s_3 - s_2 \ \ldots$.

The total contribution of the m 'Ones' to the sum of the ordinates of the output auto-correlation over a period is m^2. Thus,

$$m + 2(m-s_1) + 2(m-s_2) + \ldots + 2(m-s_{r-1}) + (N-2r+1)(m-s_r) = m^2$$

Therefore

$$m^2 - m - 2m(r-1) + m(2r-1) + 2(s_1 + s_2 + \ldots + s_{r-1}) = -Ns_r + (2r-1)s_r + Nm$$

Therefore $$N = \frac{m^2 + 2(s_1+s_2+\ldots+s_{r-1}) - s_n(2r-1)}{m - s_r} \qquad \ldots\ldots (42)$$

For a specified auto-correlation function of the sequence, the combination of N and m are determined to satisfy the equality of Equation (42).

Condition (2):

A relationship between the d.c. bias of the auto-correlation function and the number of 'Ones' and the length of the sequence can be derived as follows:

In the auto-correlation function of Fig.41(b), let the d.c. level of the auto-correlation function be D_c for values of delay $> r\lambda$ where r is the number of straight line sections and λ the event time. D_c is always an integer.

Then, for a shift of $r\lambda$, $\phi_{XX}(r\lambda) = D_c$

for a shift of $(r+1)\lambda$, $\phi_{XX}((r+1)\lambda) = D_c$

. . . .

for a shift of $(N-r)\lambda$, $\phi_{XX}((N-r)\lambda) = D_c$

Sum of these values gives

$$\sum_{k=1}^{N-r} \phi_{XX}(k\lambda) = (N - 2r + 1)D_c$$

For any 'One', the contribution to the sum of the auto-correlations is (m-r).

The total contribution from m 'Ones' to the sum of auto-correlations is m(m-r). Hence

Hence,

$$(N - 2r + 1)\, D_c = m(m-r)$$

Therefore $D_c = \frac{m(m-r)}{N-2r+1} =$ integer ..... (43)

Condition (3) :

The different groups of ones (and hence zeros) in the sequence can be chosen to satisfy certain conditions. These conditions which are given below are the relationships between the number of groups of 'Ones' and the magnitudes of the auto-correlation function for different delays which can be readily derived.

(i) The number of groups of 'Ones' m_1 is given by

$$\phi_{XX}(o) - \phi_{XX}(\lambda) = m_1$$

(ii) $\phi_{XX}(\lambda)$ = number of 'Ones' in groups with greater than one 'One' - the number of groups with greater than one 'One'.

(iii) $\phi_{XX}(2\lambda)$ = number of 'Ones' in groups with greater than two 'Ones' - 2(number of groups with greater than two 'Ones') + (the number of groups of the form 101).

(iv) $\phi_{XX}(3\lambda)$ = number of 'Ones' in groups with greater than three 'Ones' - 3(number of groups with

greater than three 'Ones') + the number of groups of the form 1001 + the number of groups of the form 1101 + 2(number of groups of the form 11011).

This can be extended to cover auto-correlations for delays of 4λ, 5λ, etc.

If there are r straight line sections in the desired auto-correlation function, then r of these conditions are necessary for the synthesis of the sequence.

9.3.2. The Actual Synthesis

It is again emphasised that all the above conditions given are only necessary conditions and hence the actual synthesis of the sequences involves a trial and error procedure.

Now, an example of synthesising these new sequences using the above conditions is given.

Example 1: Let the desired auto-correlation function be the one shown in Fig.42(a). It has two straight line sections of slope 2 and 1 respectively.
From Equation (42), we have

$$N = \frac{m^2 + 2s_1 - 3s_2}{m - s_2}$$

If we assume that $k_1 = 2$ and $k_2 = 3$ as in Fig.42(a), then

$$N = \frac{m^2 - 5}{m - 3} \qquad \ldots\ldots (44)$$

From Equation (43), the d.c. level is given by

$$D_c = \frac{m(m - 2)}{N - 3} \qquad \ldots\ldots (45)$$

Trying out various values of m to satisfy Equation (45), it is seen that m = 4 satisfies Equations (44) and (45) giving $N = 11$ and $D_c = 1$.

Therefore $\phi_{XX}(o) = 4$ and $\phi_{XX}(\lambda) = 2$

Hence

$$\phi_{XX}(o) - \phi_{XX}(\lambda) = 2 = \text{number of groups of 'Ones'.}$$

There are two possibilities — these groups can occur in the form ...001001110... or ..00011000110... From (3) (iii) above, it is seen that no groups of 101 is admissible and the arrangement ...001001110... satisfies all the conditions. The actual sequence that has the auto-correlation function of Fig.42(a) is 10011100000. The impulse train generating this sequence is shown in Fig.42(b).

In a similar way to that shown in the above example, three more new sequences have been obtained. These are

(2) $N = 15$, $X(t) = 101100111000000$

(3) $N = 20$, $X(t) = 10011000111100000000$

(4) $N = 25$, $X(t) = 1000110000111110000000000$

The generating impulse trains and the auto-correlation functions of these sequences are shown in Fig.43.

9.3.3. Power Spectrum of the New Sequences

By Fourier transformation of the auto-correlation function, the power spectrum of the sequences can be derived easily. Considering the sequence to be of levels +1 and -1 instead of +1 and 0, the power spectrum of the sequence with an auto-correlation function of the form shown in Fig.44(a) is obtained as follows. From Fig.44(a)

$$\phi_{XX}(\tau) = N - \frac{s_1 |\tau|}{\lambda} \qquad \text{for } |\tau| < \lambda$$

$$= (N-s_1) - \frac{(|\tau|-\lambda)(s_2-s_1)}{\lambda} \qquad \text{for } \lambda < |\tau| < 2\lambda$$

$$= N - s_2 \qquad \text{for } |\tau| > 2\lambda$$

Fourier transformation of $\phi_{XX}(\tau)$ is given by

$$\Phi'_{XX}(\omega) = \frac{1}{N\lambda} \int_{-\frac{N\lambda}{2}}^{\frac{N\lambda}{2}} \phi_{XX}(\tau) \cos \omega\tau \, d\tau$$

Evaluating this integral, we get the power spectrum $\Phi_{XX}(\omega)$ as

$$\Phi_{XX}(\omega) = \left[(N - s_2) + \frac{s_1}{N} + \frac{3(s_2-s_1)}{N}\right] \delta(f)$$

$$+ \sum_{\substack{r=-\infty \\ r\neq 0}}^{r=\infty} \left\{ \frac{s_1}{N} \left[\frac{\sin \frac{\pi r}{N}}{\frac{\pi r}{N}} \right]^2 + \frac{3(s_2-s_1)}{N} \left[\frac{\sin \frac{\pi r}{N}}{\frac{\pi r}{N}} \right]^2 \right.$$

$$\left. - \frac{(s_2-s_1)}{N} \cdot \frac{4\pi^2 r^2}{N^2} \cdot \left[\frac{\sin \frac{\pi r}{N}}{\frac{\pi r}{N}} \right]^4 \right\} \delta(f-rf_o)$$

..... (46)

where $f_o = \frac{1}{N\lambda}$

The power spectrum is discrete with a harmonic separation equal to the repetition frequency of the sequence. This power spectrum has been plotted for the sequence of length 15 (No.(2) above) in Fig.44(b). For comparison, the power spectrum of a maximal length

PRBS of the same length is also plotted. It is seen that the power spectra of the two are similar. The new sequence has more power concentrated in the lower frequencies compared to the PRBS.

These new sequences are unfortunately not uncorrelated with the known m-sequences or quadratic residue sequences of the same length. Hence from the point of view of synthesising uncorrelated sequences this procedure is not very promising. Binary sequences have applications in other fields such as telecommunications. Perhaps, sequences with a desired autocorrelation function have some applications in these fields.

10. CONCLUSIONS

A hill-climbing technique using pseudo-random binary sequences as perturbation signals has been studied. Two methods of closing the adaptive loop have been examined. In one case, a noise-free measurement of the gradient is obtained once every period of the perturbation signal leading to a system with discontinuous adjustment of the parameter. The step adjustments to the parameter excite the process transients and these transients give rise to error terms in the measured gradient during subsequent steps. As a result of this, the response of the adaptive loop is dissimilar from either side of the optimum. Theoretical analysis agrees with the experimental results obtained.

To overcome these transient effects, a new method of closing the adaptive loop has been proposed. In this method, a noise-free measurement of the gradient is continuously obtained resulting in a continuous adjustment (once every clock interval) of the parameter. It has been shown that the effect of transients in this system is very much reduced, resulting in a superior system response. It has been shown that application of 'Dynamic Compensation' further improves

the performance, particularly when the loop gain is relatively high.

The effect of noise disturbances in the form of an additive noise signal at the output of the process has been evaluated. It has been shown that the system with continucus parameter adjustment has a better noise performance compared with the system having discontinuous adjustment.

An approximate stability analysis of the system with continuous parameter adjustment is given.

An inexpensive and novel analogue running averager has been developed. Its performance has been found to be satisfactory. It has applications where ever running averages of continuous functions are required.

Extension of this hill-climbing technique to the simultaneous adjustment of multi-parameter systems requires uncorrelated chain codes as perturbation signals. It has been found necessary to look for new sequences which may possess this property. In an attempt to synthesise new codes, two methods have been examined. The first method has been found to be unsuccessful. Using the second method, some new sequences have been derived. Attempts have been made to

generalise this method. The method has been found to be unpromising as the new sequences derived are not uncorrelated to other existing sequences.

11. APPENDICES

A.1. Properties of Pseudo-Random Binary Sequences

Various aspects of the theory of PRBS and other sequences have been published in the literature[43,44]. The properties of the PRBS and their particular advantages for application in the field of adaptive control are summarised in this Section.

1. There are at least two ways of generating PRBS. One makes use of the theory of quadratic residues and the other is based on the properties of digital filters and their maximal length null sequences. The maximal length sequences or m-sequences can be easily generated using shift register circuits (Fig.36).

2. For an n-stage shift register the m-sequence is repetetive and has a period $(2^n-1)\lambda$ where λ is the clock period.

3. Each state of the binary shift register generating the sequence has a unique predecessor (within one period).

4. If the two states of the PRBS are +1 and -1, the sequence has a unique shift and multiply property. Because of this property, delayed versions of the

sequence can be generated very easily.

5. In each period of the sequence the number of 'Ones' exceeds the number of 'Minus Ones' by one only.

6. In each period of the sequence, there will be twice as many runs of 'Ones' or 'Minus Ones' of length r as those runs of length r+1 except that there are no runs of n 'Minus Ones' or (n-1) 'Ones'.

7. The number of different m-sequences obtainable from an n-stage shift register is given by $\frac{\phi(2^n-1)}{n}$ where $\phi(m)$ is Euler's Phi function defined as the number of integers s such that $o < s < m$ and s is prime to m.

8. For the generation of an m-sequence , the corresponding characteristic polynomial must be irreducible and primitive.

9. The amplitude probability density function of an m-sequence x(t) of +1 and -1's consists of two impulse of magnitudes

$$\frac{2^{n-1}}{2^n-1} \quad \text{and} \quad \frac{2^{n-1}-1}{2^n-1}$$

centred at $x = +1$ and $x = -1$ respectively.

10. The auto-correlation function of a PRBS is periodic with the same period as the sequence. For a sequence

of magnitude +a and -a, the auto-correlation function is as shown in Fig.49. For large N and small clock period, this auto-correlation function approximates to that of white noise. The auto-correlation function for the first period can be shown to be

$$\left.\begin{aligned} \phi_{xx}(\tau) &= a^2\left[1 - \left|\frac{\tau}{\lambda}\right|\frac{2^n}{2^n-1}\right] \qquad \text{for } |\tau| < \lambda \\ &= -\frac{a^2}{2^n-1} \qquad \text{for } |\tau| \geq \lambda \end{aligned}\right\} \quad \ldots\ldots \text{(A.1)}$$

The negative bias from the auto-correlation function can be removed if the code values are assigned $(1+\epsilon)$ and $-(1-\epsilon)$ instead of +1 and -1 where

$$\epsilon = \frac{(N+1)^{\frac{1}{2}} - 1}{N}$$

11. The power density spectrum can be derived using the Wiener-Khintchine theorem. From Equation (A.1), it can be shown that[57]

$$\Phi_{xx}(\omega) = \frac{a^2}{N^2}\delta(\omega) + \frac{N+1}{N}\left[\frac{\sin\frac{r\pi}{N}}{\frac{r\pi}{N}}\right]^2 \delta(\omega - r\omega_c)$$

$$r = -\infty, \ldots, -2, -1, 1, 2, \ldots, +\infty \text{ and } r \neq 0$$

$\ldots\ldots$ (A.2)

where

$\delta(\omega - r\omega_c)$ = Impulse function at $\omega = r\omega_c$.

It is seen from Equation (A.2) that $\Phi_{xx}(\omega)$ is a discrete spectrum with a harmonic separation of $\frac{f_c}{N}$ c.p.s. Nulls occur at integral multiples of clock frequency f_o. The bandwidth of $\Phi_{xx}(\omega) \simeq \frac{0.32}{2\pi} N\omega_c$.

A.2. Gain of Adaptive Loop

The gradient $\frac{dP}{dK}$ is proportional to the integral of the cross-correlation function between the perturbation $x(t)$ and the response of the process $y(t)$. The loop gain is the product of the integral of the cross-correlation function $\phi_{xy}(\tau)$ and the other loop constants. The expression to evaluate this integral is derived in this Section.

It is well known that the cross-correlation function between the input and the output signals of a process is equal to the convolution of the auto-correlation function of the input signal and the impulse response of the process.

Hence

$$\phi_{xy}(s) = \int_0^\infty \phi_{xx}(s-\tau)\, h(\tau)\, d\tau$$

The integral of $\phi_{xy}(s)$ is given by

$$\int_{-\infty}^{+\infty} \phi_{xy}(s)\, ds \simeq \int_{-\infty}^{+T_1} \phi_{xy}(s)\, ds$$

$$= \int_{-\infty}^{T_1} \left[\int_{0}^{\infty} \phi_{xx}(s-\tau)\, h(\tau)\, d\tau \right] ds \qquad \ldots\ldots \text{(A.3)}$$

The integral inside the square brackets of Equation (A.3) is to be evaluated for all the different configurations of $\phi_{xx}(s-\tau)$. The second integral of (A.3) is over all s.

The auto-correlation function of x(t) is shown in Fig.49. By shifting the d.c. level of the chain code, the auto-correlation function $\phi_{xx}(\tau)$ is given by

$$\phi_{xx}(\tau) = \frac{N+1}{N}\left(1-\frac{\tau}{\lambda}\right) \qquad \text{for } \tau \leq \lambda$$

$$= \frac{N+1}{N}\left(1+\frac{\tau}{\lambda}\right) \qquad \text{for } -\lambda \leq \tau \leq 0$$

$$= 0 \qquad \text{for other values of } \tau.$$

The integral of Equation (A.3) can be evaluated as

the sum of the following four integrals for different configurations and over all s.

(i) $s < 0$ and $s+\lambda > 0$, $\phi_{xx}(s-\tau)$ lies entirely in the second quadrant. Therefore

$$I_1 = \int_{-\infty}^{-\lambda} \phi_{xy}(s)\, ds = 0.$$

(ii) $-\lambda < s < 0$,

$$I_2 = \int_{-\lambda}^{0} \left[\int_{0}^{s+\lambda} h(\tau)\, (1+ \tfrac{s-\tau}{\lambda})\, d\tau \right] ds.$$

(iii) $0 < s < \lambda$,

$$I_3 = \int_{0}^{\lambda} \left[\int_{0}^{s} (1+\tfrac{\tau-s}{\lambda})h(\tau)d\tau + \int_{s}^{s+\lambda} (1+\tfrac{s-\tau}{\lambda})h(\tau)d\tau \right] ds.$$

(iv) $s-\lambda \geq 0$,

$$I_4 = \int_{+\lambda}^{T_1} \left[\int_{s-\lambda}^{s} (1+\tfrac{\tau-s}{s})h(\tau)d\tau + \int_{s}^{s+\lambda} (1+\tfrac{s-\tau}{\lambda})h(\tau)d\tau \right] ds.$$

Hence

$$\int_{-\infty}^{T_1} \phi_{xy}(s)\, ds = I = \frac{N+1}{N} (I_1 + I_2 + I_3 + I_4) \qquad \ldots\ldots (A.4)$$

For the first-order plant considered in Section 3.2,

$$h(\tau) = \frac{1}{T_o} \cdot e^{-\tau/T_o} \qquad \ldots\ldots (A.5)$$

Evaluating the integrals of Equation (A.4) using Equation (A.5), we get

$$I = \int_{-\infty}^{T_1} \phi_{xy}(s)\, ds = \frac{N+1}{N}\left[\lambda + \frac{T_o^2}{\lambda}.e^{-T_1/T_o}\left\{2-e^{-\lambda/T_o}-e^{+\lambda/T_o}\right\}\right]$$

$\ldots\ldots (A.6)$

For $T_1 = 64\lambda$, $T_o = \frac{T}{2}$, $T = 127\lambda$, the values used in the practical simulation of Section 3.2, from Equation (A.6), we get

$$I = 0.634\,\lambda \qquad \ldots\ldots (A.7)$$

A.3. Relationship between the Starting Point of the Chain Code and the Transient Factor α

The transient factor α is given by Equation (8) as

$$\alpha = \frac{g.B.\sin\frac{\omega_c T_1}{2}}{T_i} \int_o^T q(t).\sin(\omega_c t + \phi)\, dt$$

For the first-order plant,

$$q(t) = (1 - e^{-t/T_o}) \qquad \ldots\ldots (A.8)$$

Hence

$$\alpha = \frac{g.B.\sin\frac{\omega_c T_1}{2}}{T_i} \int_0^T (1-e^{-t/T_o}) \sin(\omega_c t+\phi)\, dt$$

The first term when integrated over a period of the chain code becomes zero. Evaluating the other integral,

$$\alpha = \frac{g.B.\sin\frac{\omega_c T_1}{2}}{T_i}\left[\frac{1}{(\omega_c^2+\frac{1}{T_o^2})}\left[\omega_c\cos\phi+\frac{1}{T_o}\sin\phi\right]\left[1-e^{-T/T_o}\right]\right] \quad \ldots\ldots (A.9)$$

$\alpha = 0$, when $\omega_c \cos\phi = -\frac{1}{T_o}\sin\phi$

$$\text{or} \quad \tan\phi = -\omega_c T_o = -\frac{2\pi T_o}{T} \quad \ldots\ldots (A.10)$$

A.4. Calculation of the Theoretical Response for the System with Continuous Parameter Adjustment

Though the parameter is adjusted quasi-continuously (in N small discrete step adjustments in a period of the chain code), the effect of the transient due to these small step adjustments will still be present. In calculating the response of the system the effect of these transients has to be considered. A digital computer programme has been written to calculate the

response for a first-order process. The method is general and can be used for higher order plants also. The step-by-step procedure adopted for this computation is described in this Section.

Let $q'(t)$ be the transient component in the response following a unit step adjustment in parameter and G_1' the other loop constants of the adaptive system. The multiplication of $q'(t)$ by the sinusoidal approximation of $r(t)$ and integration gives the error due to a step adjustment. As the gradient is measured by averaging over a past period of the chain code, the total error at the end of the rth step consists of error contributions from the previous (r-1) step adjustments. If $r > N$, then the error contributions from the past N adjustments only is considered.

If δK_o, δK_1, ... , δK_r are the magnitudes of the first, second, ... , and (r+1)th step changes in parameter, the error after say pth adjustment is given by

$$e_p = G_1' \sum_{m=o}^{p-1} \delta K_m . \int_o^{(p-m)\lambda} q'(t).\sin(\omega_c t+\phi+m\theta)\, dt, \text{ for } p<N \qquad \ldots\ldots (A.11)$$

and

$$e_p = G_1' \sum_{m=o}^{p-1} \delta K_m . \int_o^{(p-m)\lambda} q'(t).\sin(\omega_c t+\phi+m\theta)\, dt$$

$$- G_1' \sum_{m=o}^{p-1-N} \delta K_m . \int_o^{(p-m-N)\lambda} q'(t).\sin(\omega_c t+\phi+m\theta)\, dt \quad \text{for } p>N$$

..... (A.11)

where ϕ is the phase angle of $r(t)$ and $\theta = \frac{2\pi}{N}$.
It is seen from Equation (A.11) that for every rth adjustment step, r integrals have to be evaluated. If the order of the plant is high, $q'(t)$ is a complicated expression and the evaluation of Equation (A.11) becomes very lengthy.

However, for the process considered in Section 4.1, a square law device followed by a first-order plant, $q'(t)$ is given by

$$q'(t) = - e^{-t/T_o}$$

Since $q'(t)$ is a simple exponential, the error terms can be computed with relative ease.

Consider Fig.50. The error component due to the step change in parameter at the rth clock interval is

given by the integral representing the product of the hatched areas. This is given by

$$I_r = G_1' \cdot e^{-\frac{(r-1)T}{NT_o}} \cdot \int_{\frac{(r-1)T}{N}}^{\frac{rT}{N}} e^{-t/T_o} \cdot \sin(\omega_c t+\phi)\, dt \qquad \ldots\ldots \text{(A.12)}$$

The transient will be negligibly small at the end of a period of the chain code after a step disturbance, as the response will have settled during this interval. Hence only N numbers of these integrals of Equation (A.12) are required to be calculated. Since $q'(t)$ is exponential, these N I's need be evaluated over successive clock intervals only once and stored. The error contributions due to the previous (r-1) steps can be calculated in an easy way by weighting the stored I's in an exponential manner. If $a_1, a_2, \ldots, a_r$ are the ordinates of the exponential at the successive clock periods (Fig.50), then the error terms $e_1, e_2, \ldots, e_r$ are given by

when $r < N$:

$$e_1 = (I_1 a_1)\delta K_o$$

$$e_2 = (I_1 a_1 + I_2 a_2)\delta K_o + (I_2 a_1)\delta K_1$$

$$e_3 = (I_1a_1+I_2a_2+I_3a_3)\delta K_o+(I_2a_1+I_3a_2)\delta K_1+(I_3a_1)\delta K_2$$

. . . . . .

$$e_r = (I_1a_1+\ldots+I_ra_r)\delta K_o+(I_2a_1+\ldots+I_ra_{r-1})\delta K_1 + \ldots + (I_ra_1)\delta K_{r-1} \quad \ldots\ldots \text{(A.13)}$$

when $r > N$:

$$e_r = (I_{r-N+1}a_{r-N+1} +\ldots+ I_ra_r)\delta K_o + (I_{r-N+1}a_{r-N} +\ldots+ I_ra_{r-1})\delta K_1 +\ldots + (I_{r-N+1}a_1 +\ldots+ I_ra_N)\delta K_{r-N} + (I_{r-N+2}a_1 +\ldots+ I_ra_{N-1})\delta K_{r-N+1} \ldots + (I_ra_1)\delta K_{r-1} \quad \ldots\ldots \text{(A.14)}$$

In this expression all a_r's for $r > N$ will be zero, thus reducing the computation considerably. The step changes in parameter δK_o, δK_1, ... , δK_r are to be computed to evaluate e_1, e_2, ... , e_r. These are dependent on the adjustment steps and these can be successively calculated as follows.

Let the initial misadjustment in parameter be $(K_o - K_{opt})$. Let g_o, g_1, ... , g_r be the gradients at the parameter values of K_o, K_1, ... , K_r. If the

other loop constants are given by G_1, the step adjustments N_o, N_1, ... , N_r are given by

$$N_o = - g_o G_1 \qquad \delta K_o = g_o N_o$$

This first step is error free.

$N_1 = - g_1 G_1 + e_1$ where $e_1 = I_1 a_1 \cdot \delta K_o$, $\delta K_1 = g_1 N_1$

$N_2 = - g_2 G_1 + e_2$

.....

$$N_r = - g_r G_1 + e_r , \quad \delta K_r = g_r N_r \qquad \text{..... (A.15)}$$

e_r is calculated from either Equation (A.13) or Equation (A.14).

For the system considered in Section 4.1,

$$g_r = 2 \sqrt{\mu} K_r , \quad \sqrt{\mu} = \frac{1}{50} , \quad T_o = 0.3 \text{ secs},$$

$$\frac{T}{T_o} = 2.115 , \quad K_o = 17.5\text{v}, \quad G_1 = \frac{0.0906}{127} .$$

The programme to evaluate e_r and the adjustment steps N_r is written in Algol and run on Elliot 803 Computer. The response is plotted in Fig.21.

A.5. Proof that Certain Types of Auto-Correlation Functions are Unrealisable

In Section 9.3, two level sequences with an auto-correlation function made up of straight line sections was considered. The desired auto-correlation function must be made up of straight line sections such that $g_k < g_{k-1}$ (Fig.41(b)).

Consider the form of the auto-correlation function shown in Fig.51(a) in which $g_2 > g_1$. The first and second derivatives of the auto-correlation function are shown in Fig.51(b) and (c). It is seen from Fig.51(c) that $\phi_{YY}(t)$ is positive both for $t = +\lambda$ and $t = -\lambda$. This is possible only if there are consecutive positive or negative impulses in the impulse train which is inadmissible for a two-level signal. Hence two-level sequences that have an auto-correlation function such that $g_k < g_{k+1}$ are unrealisable.

A.6. The Published Papers

RECENT ADVANCES IN A HILL-CLIMBING TECHNIQUE.

By K.C. Ng*, K.K. Murthy*, D.H. Stockwell++, K.R. Morris+.

Introduction

The use of pseudo-random binary sequences or chain codes as test signals in control systems has been widely reported. [1, 2, 3]. Its use in optimisation has been described by Douce and Ng [4] who investigated its application in a hill-climbing scheme first proposed by van der Grinten [5]. The response of their system is discussed in this paper and a new arrangement is proposed which overcomes the limitation of their original system. To facilitate the discussions in the paper, a brief review of the technique will be given first.

In hill-climbing, the information required is the gradient of the performance - parameter characteristic. For small perturbations about the working point we assume a linear relationship between performance measure P and parameter value K. For optimisation, we wish therefore to determine the value of $\frac{dP}{dK}$ at the working point. Van der Grinten has shown that when a broad-band stationary random signal is used as the perturbation in parameter value, an estimate of the gradient $\frac{dP}{dK}$ is given to within a constant factor, by the integral

$$I = \int_{-\infty}^{\infty} h(\tau)\, d\tau = \int_{-\infty}^{\infty} \phi_{xy}(s)\, ds$$

$h(\tau)$ is the impulse response of the process from parameter K to performance measure P. $x(t)$ is the perturbation and $y(t)$ is the performance signal.

In practice, this integral is evaluated over a time T_1 where T_1 is large enough such that the process has settled sufficiently to the steady state. The choice of T_1 is also affected by the noise disturbance in the process.

The system investigated by Douce and Ng is reproduced in figure 1. The perturbation used is a chain code of length 127. The integration is performed over 63 bit intervals, that is over a time $T_1 = 63\lambda$ where $T_1 \simeq T_0$, the major time constant of the process. Thus

$$\frac{dP}{dK} = \int_0^{T_1} \phi_{xy}(s)\, ds = \int_0^{T_1} \int_{-\infty}^{\infty} x(t-s)\, y(t)\, dt\, ds$$

$$= \int_{-\infty}^{\infty} y(t) \left\{ \int_0^{T_1} x(t-s)\, ds \right\} dt.$$

---

* School of Engineering Science, University of Warwick.
\+ N.P.L. Teddington, Autonomics Division.
++ National Coal Board, Cheltenham.

This expression is mechanised by taking the running average

$$r(t) = \frac{1}{T_1}\int_0^{T_1} x(t-s)\,ds$$

multiplying this by y(t) and integrating the result with respect to time. The running average operation is performed using a reversible binary counter, the digital output of which forms one input of a hybrid multiplier.

Now consider the signal Z(t) at time t after the start of the optimisation process.

$$Z(t) = \frac{1}{T_i}\int_0^{t} r(t)\ \ y(t)\,dt$$

$$= \frac{1}{T_i T_1}\int_0^{t}\left\{\int_0^{T_1} x(t-s)\,ds\right\} y(t)\ \ dt$$

$$= \frac{1}{T_i T_1}\int_0^{T_1}\int_0^{t} x(t-s)\,y(t)\,dt\ \ ds.$$

$$Z(t) = \frac{1}{T_i T_1}\int_0^{T_1} \phi_{xy}(s)\,ds \quad \text{only}$$

$$= Z(T)$$

when $t = T$ or $t = nT$. (1)

A sample-and-hold element is thus included so that noise-free measurements of the gradient $\frac{dP}{dK}$ can be obtained, once per chain code cycle.

2. Response of the Closed-Loop System

When the loop is closed, the parameter K is adjusted in steps at intervals of T, the chain code period. The variation in y has two components, one due to the perturbation x(t) and the other due to the adjustment. Assuming that both the step adjustment and the perturbation are small, each of these components of y can be considered separately and superposition then applied to determine the signal Z(t).

The first component of y yields, after multiplication by r(t) and integration over time T, an estimate of the gradient at the present working point, K_n. This is the desired signal determining the magnitude of the next step adjustment. Thus the desired step adjustment is

$$\Delta K_{n+1} = c\, Z(t)$$

where Z(t) is defined by expression (1)

The transient in y as a result of the n^{th} adjustment step will produce, after multiplication by r(t), an error component in Z(t). For a given process this component is readily determined and can be shown to be given by

$$Z_1(t) = \alpha_n \Delta K_n$$

α_n, the transient factor, is proportional to the gradient at the previous working point K_{n-1}. The magnitude of the $(n+1)^{th}$ step is therefore

$$\Delta K_{n+1} = c\left[Z(t) + Z_1(t)\right]$$
$$= c\left[Z(t) + \alpha_n \Delta K_n\right]$$

The form and speed of response from an initial offset in parameter value thus depends on which side of the optimum the initial point lies. For example, assuming a modulus-type characteristic, the sequence of steps from an initial setting to the left of the optimum, where the gradient is negative, is

$$\Delta K_1 = c.Z(T) = +\theta \quad \text{(a constant)}$$

$$\Delta K_2 = \theta + \alpha \Delta K_1 = \theta + \alpha\theta$$

$$\Delta K_3 = \theta + \alpha \Delta K_2 = \theta + \alpha(\theta + \alpha\theta).$$

and so on.

On the right of the optimum the gradient is positive, so that $\alpha' = -\alpha$. Thus

$$\Delta K_1 = -\theta$$

$$\Delta K_2 = -\theta + \alpha' \Delta K_1 = -\theta + \alpha\theta.$$

$$\Delta K_3 = -\theta + \alpha' \Delta K_2 = -\theta + \alpha(\theta - \alpha\theta).$$

and so on.

The response is therefore faster in the one case than the ideal response and slower in the other. For values of α above a certain value, the slower response is also oscillatory and if $\alpha > 1$, the system is unstable in this case.

2.1. Evaluation of α

For a given chain code and a known process, the value of α can be determined as follows. The running average signal r(t) is a repetitive signal of period T, with discrete levels, the transitions occurring at the intervals $n\lambda$ where λ is the chain code bit interval. For the purpose of this analysis, it can be approximated to a good degree of accuracy by the sinusoidal signal

$$r_1(t) = B \sin\left(\frac{\omega_c T_1}{2}\right) \sin\left(\omega_c t + \phi\right) \qquad (2)$$

where B is a constant depending on chain code length and peak amplitude, $\omega_c = \frac{2\pi}{T}$ and T_1 is the running average time. ϕ is determined by the starting point of the chain code. This starting point is arbitrary.

Let the response in y to a small step adjustment ΔK in K be $g.\Delta K.q(t)$ where g is the gradient at the working point and q(t) is the unit step response of the process from parameter to performance. The output of the integrator due to this component of y is

$$Z_1(t) = \frac{1}{T_i}\int_0^T g.\Delta K.\ B \sin\left(\frac{\omega_c T_1}{2}\right).q(t) \sin(\omega_c t + \phi)\, dt$$

$$= \Delta K.\ \frac{g\ B \sin\left(\frac{\omega_c T_1}{2}\right)}{T_i} \cdot \int_0^T q(t) \sin(\omega_c t + \phi)\, dt$$

$$= \alpha.\Delta K. \qquad (3)$$

For a given process with constant dynamics it is possible to choose a starting point such that the value of α is negligibly small or equal to zero.

As an example, consider the system shown in figure 1. The chain code used is a 127 bit code described by the polynomial equation $D^7 \oplus D^3 \oplus 1 = 0$ ($\oplus$ denoting modulo-two addition and D is the delay operator) and generated by a seven-stage feedback shift-register generator. T_1 equals 63λ. The process consists of a square-law characteristic followed by a first-order lag of time constant T_o.

The variations in r(t) and in α as a function of the starting point (and hence ϕ) are shown in figure 3, where the point A corresponds to the starting point when all but one of the shift-register outputs are zero.

For the values of loop constants given, the behaviour of the system is shown by the typical response curves in figure 4 in which theoretical curves are plotted to illustrate the good degree of accuracy in the approximation to r(t) by expression 2. Note that the response on one side of the optimum is vastly different from that on the other. When the loop gain is adjusted so that response on one side is fastest without overshoot, the response on the other side exhibits quite large oscillations and is also exceedingly slow.

In this example, the chain code period could have been chosen to start at the point B (figure 3). This is not always possible in practice, since the dynamics of the process are usually unknown and may change with parameter setting.

3. Continuous Parameter Adjustment

It is seen that the error signal in Z(t) is due to the transient in y(t) following the step adjustments in K. This effect may be reduced

by continuous instead of discontinuous adjustments in K. y will contain a component varying continuously with time. If the rate of change of K is small, the contribution of this component to Z(t) is negligible.

Continuous adjustment of K requires continuous measurement of the gradient as K is adjusted. For noise-free measurements it is necessary to continuously evaluate Z(t) over a period T. This is achieved by inserting a second running averager RA2 after the multiplier. The signal at the output of this averager is

$$Z'(t) = \frac{1}{T}\int_0^T m(t-\gamma)\, d\gamma$$

where $m(t) = r(t).y(t)$

$$\therefore \quad Z'(t) = \frac{1}{T}\int_0^T \left\{ \frac{1}{T_1}\int_0^{T_1} x(t-\gamma-s)ds \right\} y(t-\gamma)\, d\gamma.$$

$$= \frac{1}{T\,T_1}\int_0^T d\gamma \int_0^{T_1} x(t-\gamma-s)\, y(t-\gamma)\, ds.$$

$$= \frac{1}{T\,T_1}\int_0^{T_1} ds \int_0^T x(t-\gamma-s)\, y(t-\gamma)\, d\gamma.$$

$$= \frac{1}{T\,T_1}\int_0^{T_1} \phi_{xy}(s)\, ds. \qquad (4)$$

A noise-free measurement of the gradient is available continuously. The sample-and-hold is now redundant. The parameter is adjusted continuously such that

$$K(t) = \frac{1}{T_i}\int_0^t Z'(t)\, dt. \qquad (5)$$

The variation is y as a result of the continuous adjustment of the parameter will produce an error term in Z'(t). An exact analysis of the closed-loop system is not possible at present. It is possible however to predict the response by a step-by-step method. The method considers the response K(t) to be made up of small changes at intervals equal to the chain code bit interval. Thus in a system using a 127 bit chain code, there will be 127 step changes in K in any period T. Each (little) step change produces an error in Z'(t).

Consider the step change δK_k in K and the corresponding variation in y occurring at time $t = k\lambda$. This produces an error in Z'(t) given by

$$Z'(t)_k = \xi_k . \delta K_k . \frac{B \sin\left(\frac{\omega_c T_1}{2}\right)}{T} \int_0^{k\lambda} q(t) . \sin(\omega_c t + \phi_k)\, dt$$

$$= \beta_k . \delta K_k . \qquad (6)$$

where ϕ_k is the phase angle of $r_1(t)$ at time $t - k\lambda$ measured with respect to $q(t)$. Assuming that the dynamics is constant over the range of K considered in the time interval $t - T$ to t, then at time t, the total error in $Z'(t)$ due to the change in K over the past period T is

$$Z'_1(t) = \sum_{k=1}^{N} \beta_k . \delta K_k$$

where N = number of bits in the chain code and $N\lambda = T$.

If N is large then the summation can be replaced by an integration and letting $k/N = \zeta$, then $Z'_1(t)$ becomes

$$Z'_1(t) = \xi . \delta K . NB \sin\left(\frac{\omega_c T_1}{2}\right) \left\{ \int_0^1 d\zeta \int_0^{N\lambda\zeta} q(t) \sin(\omega_c t + 2\pi\zeta)\, dt \right\} \qquad (7)$$

where it is assumed that ξ is constant over the range of K considered and each step is of the same small amplitude.

Interchanging the order of integration, equation (7) becomes

$$Z'_1(t) = N\xi . \delta K . B \sin\left(\frac{\omega_c T_1}{2}\right) \int_0^T q(t) \int_{\frac{t}{T}}^1 \sin(\omega_c t + 2\pi\zeta)\, d\zeta\, dt$$

$$= N\xi . \delta K . B \sin\left(\frac{\omega_c T_1}{2}\right) \int_0^T q(t)(\cos 2\omega_c t - \cos \omega_c t)\, dt \qquad (8)$$

$$= \beta . \delta K .$$

The error in Z(t) in this system is dependent, as in the original system, on the gradient ξ and on the step δK. For a loop gain such that the total desired adjustment in a period T is equal in both systems (that is, $\Delta K = N . \delta K$), the error $Z'_1(t)$ is in general very much smaller than $Z_1(t)$ in the original system, (by a factor of the order of N). The response will therefore be very close to the ideal response and the speed of response will be similar on both sides of the optimum.

3.1. Dynamic Compensation

When a digital computer is employed in this hill-climbing technique, the impulse response $h(\tau)$ is determined first and the gradient is then computed

by integrating the impulse response. In the continuous system, the impulse response is updated every bit interval so that the gradient can be determined continuously.

Since the impulse response is available, the response in y following a step change in parameter can be determined. If this is subtracted from the new values of y before performing the cross-correlation, the error term in Z(t) is eliminated. This method, called dynamic compensation, can be applied to the original and the continuously adjusted system. The system with dynamic compensation approaches the ideal configuration for this hill-climbing technique.

4. Experimental Results

The response of the original system has been illustrated in section 2. The same process is used for investigating the new method. The sampler-and-hold element in figure 2 is replaced by an analogue running averager developed from a capacitor-drum delay generator[6].

Typical responses are shown in figure 5, which shows response curves on both sides of the optimum for loop gains of the same value as in figure 4. The predictions of section 4 are well borne out by the experimental results. The variation in speed of response, measured by the time to reduce the offset in parameter to one-third of the initial value, with loop gain is shown in figure 6. The response times of the system with discontinuous adjustment are significantly different on each side of the optimum (by a factor of about 3.5). The response of the new system is similar on both sides of the optimum. The fastest time to optimise, to within 5% of the optimum parameter setting in both systems, is about 10 T_0. The system with continuous adjustment has a higher limiting value of loop gain before the system becomes unstable.

Both methods have been applied to a second process consisting of a square-law characteristic followed by a transfer function

$$H(p) = \frac{k\epsilon^{-p\tau}}{(1+pT_a)(1+pT_b)}$$

where $k = 0.25$, $\tau = 200$ msec, $T_a = 100$ msec and $T_b = 1$ sec. The chain code used is a 63 bit code generated by the equation $D^6 \oplus D^5 \oplus 1 = 0$. The chain code clock frequency is 8 c/s so that $\lambda = \frac{1}{8}$ sec.

The results, obtained using the hybrid computing facilities of the N.P.L., are summarised in figure 7. This shows the variation in speed of response, as measured by the total adjustment in a given time from an initial offset, as a function of the starting point for the system with step adjustment of parameter. The speed of response of the system with continuous adjustment is also shown for comparison.

The results of applying dynamic compensation are clearly shown in figure 7. It is seen that the system with continuous adjustment is almost as good as the ideal system. For very high gains, it may be advantageous to apply dynamic compensation.

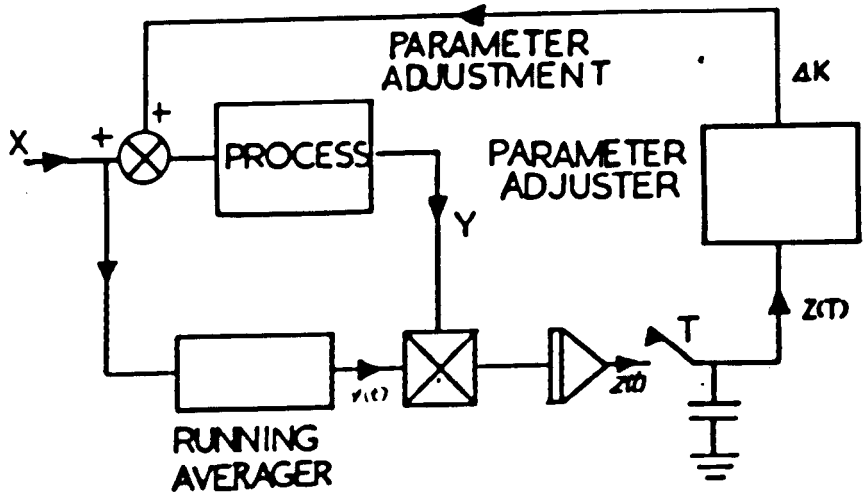

Fig.1. Schematic Diagram of the Original System.

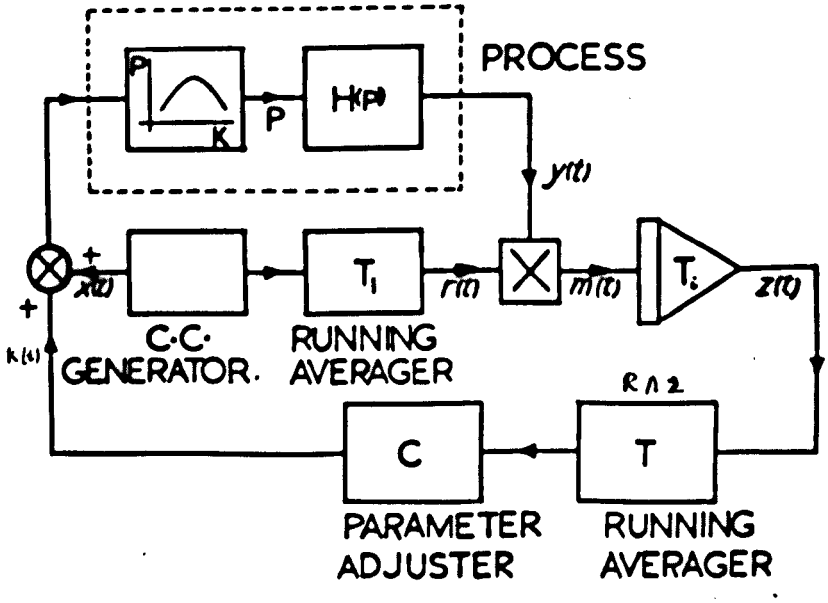

Fig.2. Schematic Diagram of the New System.

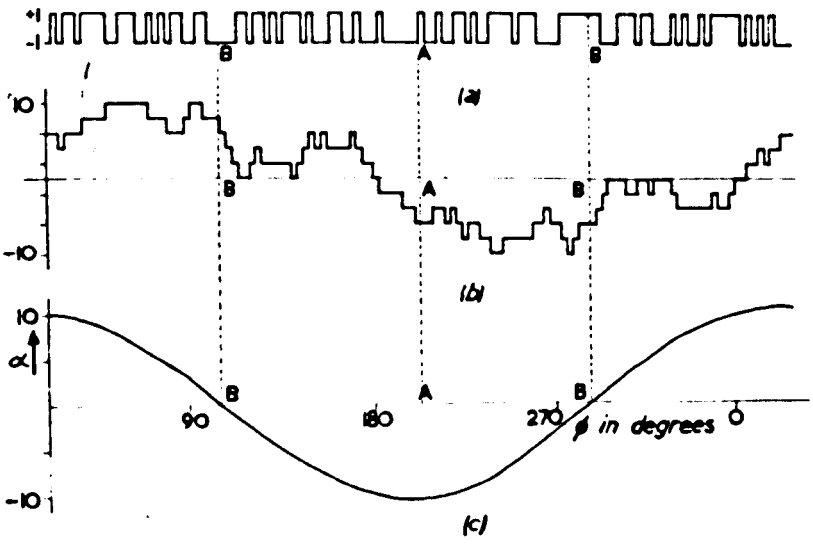

Fig. 3. (a) 127 bit chain code.
(b) Running Average of chain code.
(c) Plot of α vs φ.

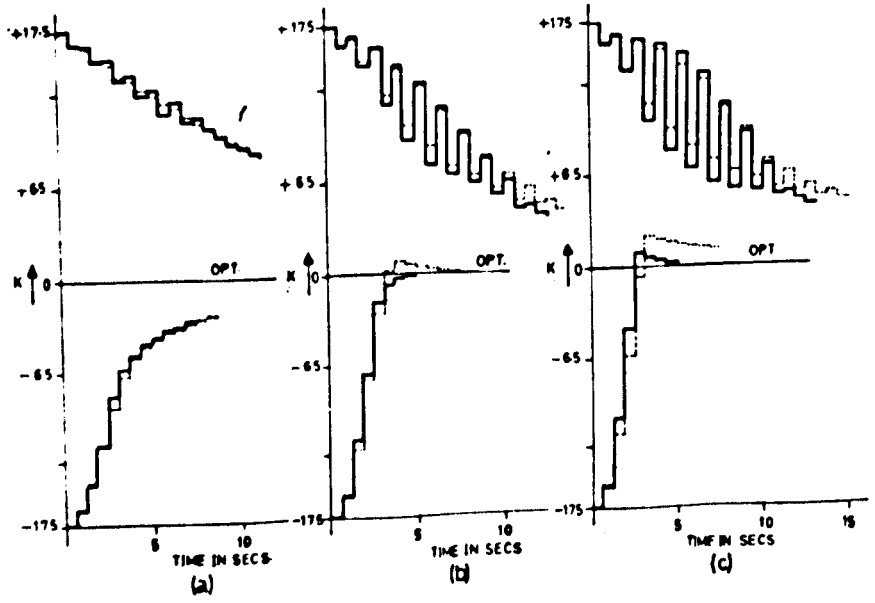

Fig.4. Response of the system with discontinuous (step) adjustment. ---- Theoretical. —— Practical.

(a) Loop gain = 3.34.
(b) Loop gain = 4.65.
(c) Loop gain = 5.20.

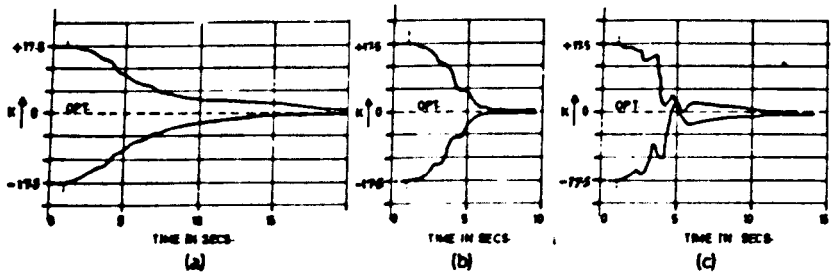

Fig.5. Response of the system with Continuous Adjustment.
(a) Loop gain = 3.34.
(b) Loop gain = 4.65.
(c) Loop gain = 5.20.

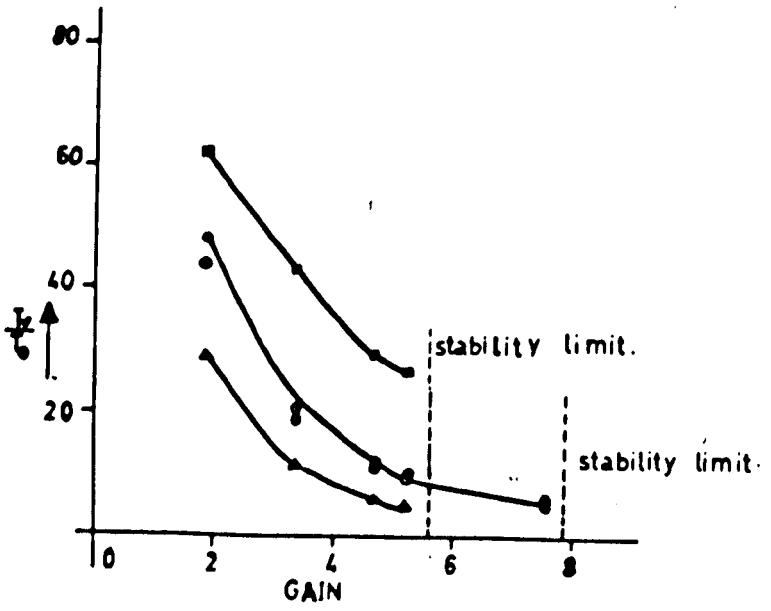

Fig.6. Plot of response time vs gain.

Step adjustment (from +ve side)
Step adjustment (from -ve side)
Continuous adjustment (from +ve side)
Continuous adjustment (from -ve side)

$t_{\frac{1}{3}}$ = time to reduce parameter offset to $\frac{1}{3}$ of initial value.

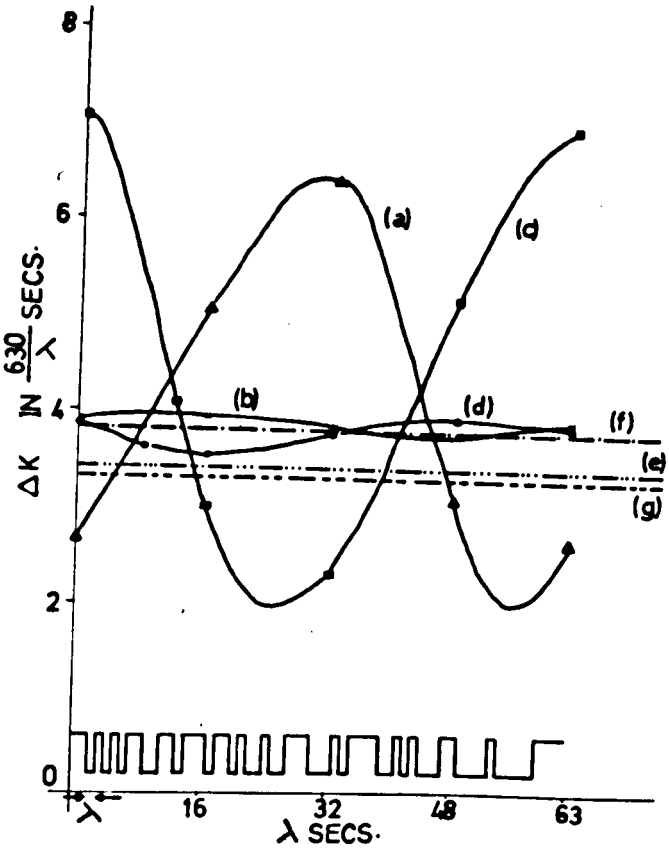

Fig.7. Speed of response vs starting point.

Discontinuous (step) adjustment.

(a) $K_{initial} > K_{opt}$. Without dynamic compensation.

(b) $K_{initial} > K_{opt}$. With dynamic compensation.

(c) $K_{initial} < K_{opt}$. Without dynamic compensation.

(d) $K_{initial} < K_{opt}$. With dynamic compensation.

Continuous adjustment

(e) $K_{initial} > K_{opt}$. Without dynamic compensation.

(f) With dynamic compensation (for both values of $K_{initial}$.)

(g) $K_{initial} < K_{opt}$. Without dynamic compensation.

$\lambda = 1/3$ sec.)

An Electromechanical Running Averager

By K. C. Ng, Ph.D. and K. K. Murthy, M.E.

A new electromechanical running averager is described. It is inexpensive, simple in construction and reliable in operation. It is particularly useful when the running average of signals are required to be simulated on an analogue computer.

(Voir page 203 pour le résumé en français: Zusammenfassung in deutscher Sprache auf Seite 210)

IN certain analogue computer applications, the 'moving average' or the 'running average' of a functon of time is required. The running average $R(t)$ of a function of time $x(t)$ over an interval of time T is defined as:

$$R(t) = \int_0^T x\,(t-s)\,ds = \int_{t-T}^{t} x(s)\,ds \quad \ldots\ldots\ldots (1)$$

where $x(t-s)$ is the delayed version of the function $x(t)$.

An example of a practical situation where the realization of equation (1) on the analogue computer is desired is the determination of the integral of cross-correlation function between two signals in a particular adaptive control system[1].

$$\text{Let } I = \int_0^T \phi_{xy}\,(s)ds \quad \ldots\ldots\ldots\ldots (2)$$

where $\phi_{xy}(t)$ is the cross-correlation function between two signals $x(t)$ and $y(t)$.

Equation (2) can be written as:

$$I = \int_0^T \int_{-\infty}^{+\infty} y(t)\,x(t-s)dt\,ds \text{ (from the definition of } \phi_{xy}(t))$$

Changing the order of integration gives:

$$I = \int_{-\infty}^{+\infty} y(t)\,\{\int_0^T x(t-s)ds\}\,dt \quad \ldots\ldots\ldots (3)$$

In equation (3), $\int_0^T x(t-s)ds$ is the running average of $x(t)$ over time T which is required to be simulated on the analogue computer for the determination of I.

This article explains a new method of obtaining the running average using a simple electromechanical system.

Equation (1) can be written as:

$$R(t) = \int_{-\infty}^{t} x(s)ds - \int_{-\infty}^{t} x(s-T)\,ds \quad \ldots\ldots\ldots (4)$$

By the definition of equations (1) and (4), the running average $R(t)$ at time t of the signal $x(t)$ is the integral of the signal over the interval $(t-T)$ to t. That is, it is equal to the integral of $x(t)$ minus the integral of the delayed signal $x(t-T)$. The mechanization for the computation of $R(t)$ is shown schematically in Fig. 1.

From Fig. 1, the impulse response of the running averager can be expressed as:

$$h(t) = u(t) - u(t-T) \quad \ldots\ldots\ldots\ldots (5)$$

where $u(t)$ is the unit step function and $u(t-T)$ is the delayed step function.

Thus, the impulse response of the running average has a box car waveform.

Methods of Simulation

The method of simulation of the running average as represented in Fig. 1 requires the delayed version of the time function. The accuracy with which the running average can be simulated largely depends upon the accuracy with which the delayed signal can be generated.

The delayed versions of time functions can be obtained by conventional techniques such as electronic delay circuits or magnetic tape delay lines. With these methods, precise unity gain setting for the delay block (Fig. 1) is difficult. If the gain is not exactly unity, the residual difference when integrated results in considerable deviations from the actual running average at the output of the integrator. This is a serious limitation on the accuracy obtainable by this method.

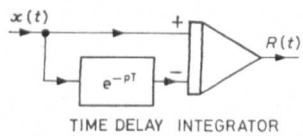

Fig. 1. Arrangement for averager

An alternative but rather expensive method is to convert the analogue signal into a digital signal. The delayed versions are then readily obtained and the computations of the running average is easily performed using reversible binary counters. A digital to analogue convertor is then used to obtain the analogue running average signal. The accuracy here is dependent only on the analogue to digital and digital to analogue convertors used.

The electromechanical running averager described in the next section has the advantages of low cost and simplicity. No complicated equipment or circuits are involved. It is particularly useful when analogue signals are involved.

Principle of Operation and Construction

The principle of operation of this is the capability of a capacitor drum to generate delayed versions of the time function. The performance of the capacitor drum as a delay unit is described first, before describing the running averager proper.

A number of capacitors are connected at one end each to a commutator segment on a rotating drum and at the other ends to a common point. Two brushes are provided on the commutator at diametrically opposite points. The input voltage (a function of time) is connected to one of the brushes, the other brush is taken to the input of a high input-impedance amplifier. The common point of the capacitors is earthed.

When a capacitor is in contact with the input brush through its connected commutator segment, the input voltage charges the capacitor to the instantaneous value of the input voltage. The capacitor moves on with its full charge until it comes in contact with the next brush when the charge on the capacitor causes the output voltage of the amplifier to rise to a value proportional to the stored charge. If the leakage is negligible, the output

* The University of Warwick.

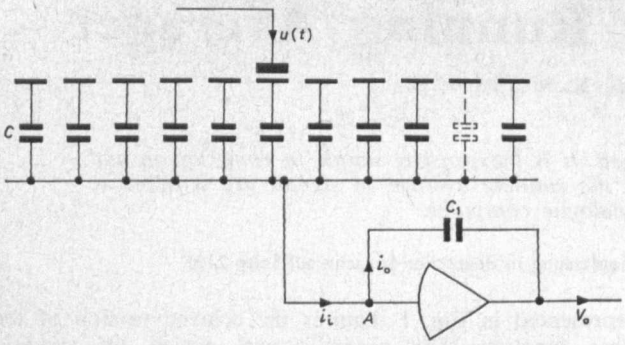

Fig. 2. Principle of the running averager

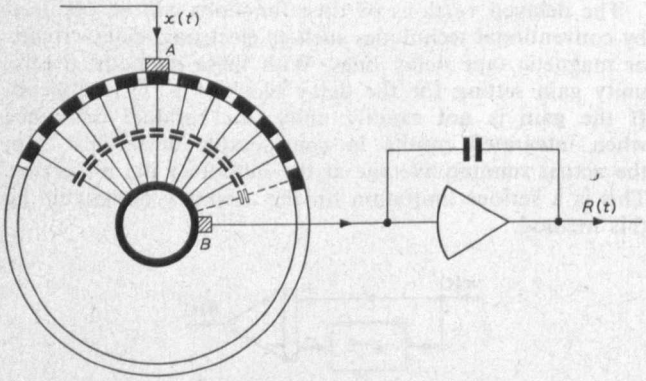

Fig. 3. Practical arrangement of running averager

voltage is the same as the instantaneous value of the input voltage, but delayed by a time interval equal to the time taken by the capacitor to move from one brush to the other. Similarly, successive capacitors delay the successive instantaneous values of the input voltage and the voltage at the output of the amplifier is thus a delayed version of the input voltage. The length of the delay is conveniently varied by varying the speed of rotation of the drum.

The capacitor drum described can be used to realize equation (4) and generate the running average.

This is best illustrated by considering the arrangement shown in Fig. 2. The voltage whose running average is required is connected to a brush on the drum. The common point of the capacitors is taken to the virtual earth of an electronic integrator. The capacitors are charged to the instantaneous value of the input voltage $u(t)$ as they pass under the brush in turn. After a complete revolution, when the first capacitor again comes under the brush, it is charged to the new value of the input voltage at that instant of time and thus the previous charge is automatically erased.

If $u(t)$ is an impulse $A_1 u_0(t_0)$ occurring at $t = t_0$, the capacitor which is in contact with the brush at $t = t_0$ gets charged to the value:

$$q_i = A_1 C \quad \ldots\ldots\ldots\ldots\ldots\ldots (7)$$

where C is the value of the capacitance.

At point A, the virtual earth of the amplifier.

$$i_i = i_o$$

$$\therefore\ q_i = q_o$$

Hence the output voltage V_o is given by:

$$V_o = \frac{-A_1 C}{C_1} \quad \ldots\ldots\ldots\ldots\ldots\ldots (8)$$

After one full revolution, when the same capacitor passes through the brush again the original charge is erased and hence the output voltage falls to zero. Thus the impulse response is a constant of magnitude $-A_1C/C_1$ from t_0 to $t_0 + n\Delta t$ and zero for all other values of t, where $n\Delta t$ is the time required for one complete revolution.

Thus, the successive values of the input signal is remembered over the time required for one revolution. The output of the integrator is the average value of the input signal over the last period, i.e. it is the running average of the input signal over this period.

Fig. 3 shows the practical set-up of the running averager. The capacitors are connected between two copper laminate disks on which the desired number of conducting segments (commutator segments) has been etched. Low leakage, high stability polystyrene capacitors are used. In the unit built, 127 such capacitors are employed. The capacitor drum is driven by a servo-motor. Since the time over which the running average is taken is the time required for one complete revolution of the drum, the running average of the signal over a wide range of time intervals

Fig. 4. Frequency response of the averager for a delay $s = 40$msec

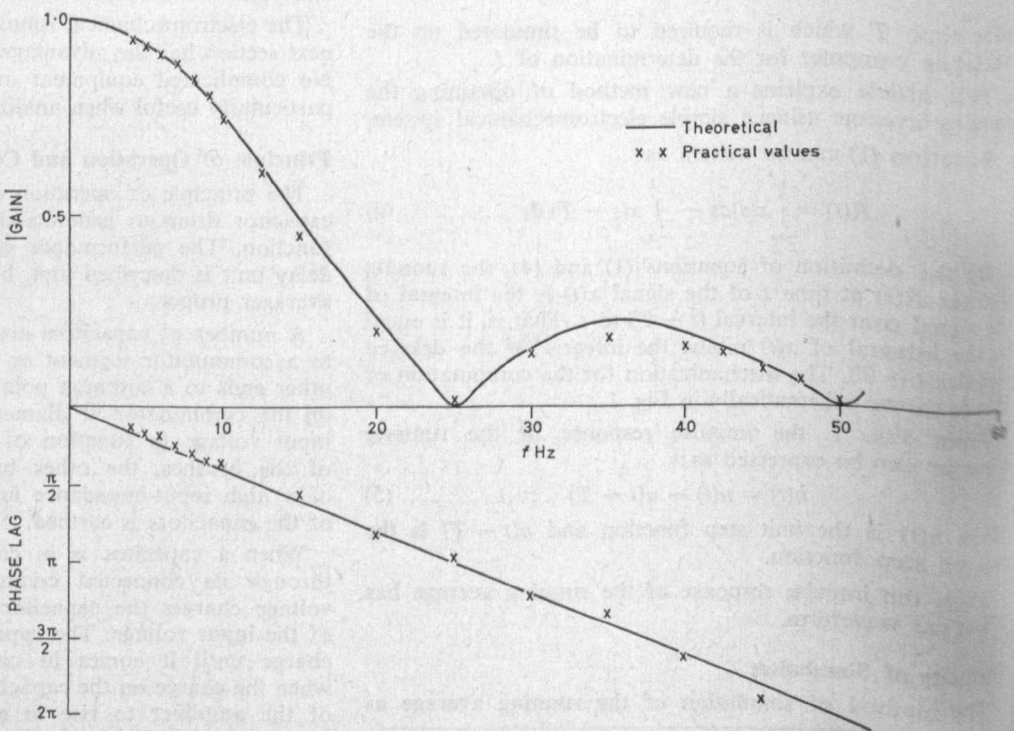

can be obtained by driving the drum at the appropriate speed.

Frequency Response of the Running Averager

By transforming equation (5), the frequency response function $H(j\omega)$ of the running averager is obtained as

$$H(j\omega) = \frac{T \sin(\omega T/2)}{\omega T/2} \angle -(\omega T/2) \quad \ldots\ldots\ldots (9)$$

This is plotted in Fig. 4 where the practical values obtained are also shown. It is seen that the experimental and theoretical values agree quite closely.

Conclusions

The running averager described is simple to construct and reliable in operation. The accuracy is limited by the number of capacitors used and in the experimental unit 127 discrete elements perform satisfactorily. The accuracy also depends upon the leakage in the capacitors and brush ripple. For the experimental unit, the error is within 2·5 per cent in the low frequency range. Six of these units are now under construction for use in a multi-channel adaptive computer financed by a Ministry of Technology Research Contract.

Acknowledgment

One of the authors (K. K. Murthy) wishes to thank the Commonwealth Scholarship Commission in the U.K. for the Scholarship Award for higher studies in this country.

REFERENCE

1. Douce, J. L., Ng, K. C. The Use of Pseudo-random Signals in Adaptive Control. I.F.A.C. (Teddington) Symposium, 1965.

The Belfast Flight Simulator

A flight simulator, designed and manufactured by Miles Electronics Ltd of Shoreham, Sussex, has now been put into operation at the RAF Transport Command Squadron Station at Brize Norton for flight training with the Short S.C.5 Belfast aircraft.

This transport aircraft is a 4-turboprop machine having a maximum payload of over 35 tons with a speed of 306 knots and a range of 5300 miles. As a trooper aircraft it can carry 250 men.

The simulator (Fig. 1) is equipped with a cockpit motion system providing sensations of movement to the crew of three which are representative of the movements of the aircraft during flight. The system is free to move in roll, pitch and heave.

All aspects of the aircraft's operation are faithfully simulated. The noise system provides the sounds of engines, propellers, wind noises, alternators, the noise of tyres on the run-way and of the wheels running over the joints in the concrete taxi-tracks. Even such things as the thud of the undercarriage going down when it is lowered and the difference in noise when the flaps are operated, are simulated.

In addition to full simulation of all the aircraft systems, the Belfast is fitted with the Smiths Autoland system, similar to the one used on Trident aircraft operated by British European Airways. This simulator is the first to be fully equipped for practising automatic landings so that pilots can become familiar with the operation of the aircraft while on automatic flight.

Simulated aircraft failures of the various systems, including the Autoland system, can be introduced at will by the instructor. The aircrew can then practise the emergency procedures necessary to maintain control under all combinations of these failures.

To provide practice in world wide flying the Belfast simulator is provided with a radio navigation simulation system which is capable of producing synthetic signals representing 60 ground radio stations simultaneously. When the aircrew tune from one or other airborne receivers to a ground radio beacon they will receive the proper identification signal and information automatically from the simulator computer. The computer calculates the position of the radio station and of the aircraft and varies the signal strength as the aircraft gets further away from the radio station.

This vital facility is provided by a special purpose digital computer of Miles design and manufacture. To ensure that the coverage is really world-wide a facility is provided for changing the programme of radio stations by the simple insertion of a punched programming tape, thus an exercise which has been concerned with flying in Europe in the morning can be replaced with a North American flight in the afternoon.

The instructors' positions (Fig. 2) are completely comprehensive and in addition to the radio aids and faults selectors, contain all the controls and instruments necessary to efficiently conduct and predefine the exercises. These positions are ergonomically designed and contain automatic devices to record the situations existing at crucial points in the exercise such as landing.

Within the next few months the simulator will be equipped with a synthetic vision system to allow pilots to practise day and night landings at an airfield in visual conditions under reduced visibility. The display to the pilots will be provided by a 3-barrel colour projection television system with projectors mounted under the front of the fuselage and the image back projected on to a screen mounted in front of the pilots' windscreen. An ultra light weight mirror is placed in front of the projectors to reflect the picture on to the back of the screen.

Fig. 1. The Belfast Three-axis Simulator weighing approximately 8000lb

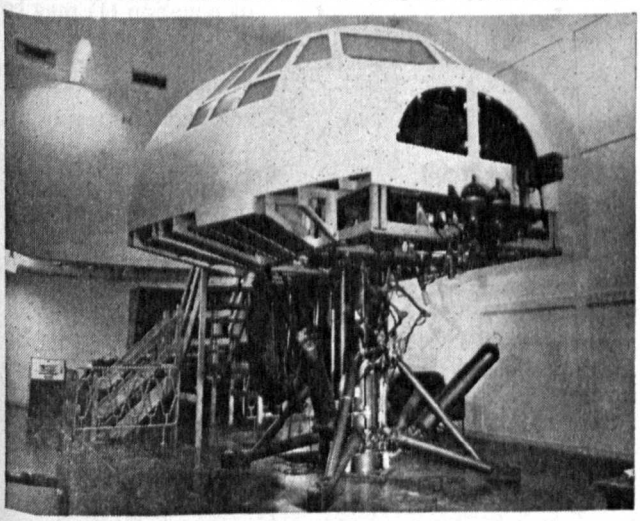

Fig. 2. The Instructors' Control Desk showing the several tape recorders and the maps of the routes of the simulated flight

Determination of Non-linearity by Analogue Simulation

By G. W. Holbrook*, B.Sc., M.Sc., Ph.D., and J. S. Collins†, B.Eng., M.Eng.

The majority of non-linear devices can be described by a power series relating output and input currents or voltages. The coefficients of the earlier and significant terms may be obtained by synthesizing the output waveform of the device by means of a sequence of integrating circuits, using a ramp input signal. The output of each integrator circuit may be used to provide a direct plot of the corresponding coefficient over a range of bias voltages.

(Voir page 203 pour le résumé en français: Zusammenfassung in deutscher Sprache auf Seite 210)

NON-LINEAR devices which exhibit a continuous and single valued relationship between input voltage and output current can generally be described by an infinite power series of the type:

$$I = a_o + a_1V + a_2V^2 + a_3V^3 + \text{etc.} \quad \ldots\ldots \quad (1)$$

While a number of methods exist for determining this describing power series, the majority of these require a large number of measurements which are usually followed by a tedious calculation. Addtionally, any of these methods which depend upon a d.c. measurement often require that the device be held, over the period of the measurement, in a steady condition which is beyond its normal continuous power rating. This is of particular consequence in semiconductor devices which are susceptible to even small temperature changes above the normal.

Methods[1] which depend upon the measurement of the harmonics, generated with a single sine wave input signal, require a knowledge of the relative phase as well as amplitude of each harmonic with respect to the fundamental. While the amplitude of harmonics may easily be determined, phase measurements of higher harmonics represent a distinct problem.

The following paragraphs describe a method of obtaining the first few significant coefficients of the describing series, directly and under dynamic operating conditions. It will be appreciated that the degree of significance of the coefficients will depend upon the degree of non-linearity of the device and also on the amplitude of the input voltage which is contemplated. Additionally, the method described below is limited in use to non-linear devices which are resistive in nature and thus exhibit no 'hysteresis loop' in their characteristics.

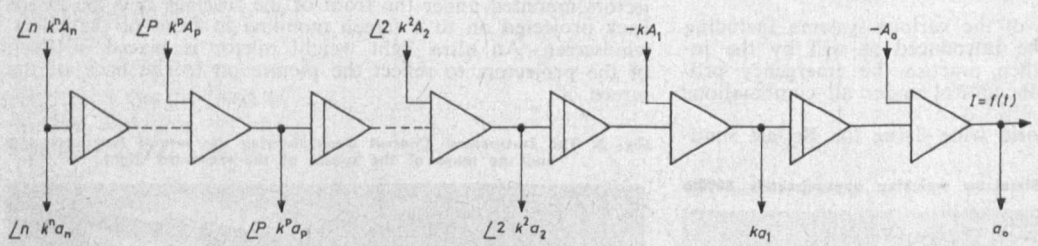

Fig. 1. Arrangement of integrators

Waveform Synthesis

This method depends essentially on synthesizing a waveform which will match the output waveform of the device in question. Synthesis is achieved by a number of successive integrations performed by electronic integrating circuits whose initial conditions can be adjusted to provide an optimum match. In order to integrate voltages and currents, with respect to time, a linear sawtooth signal is used as the input to the non-linear device allowing the input signal to be written as:

$$V = V_o + kt$$

where V_o is the input steady-state bias and k is a scaling factor. If equation (1) is rewritten as a Taylor's series:

$$I = \sum_{p=o}^{n} A_p (V - V_o)^p \quad \ldots\ldots \quad (2)$$

where:

$$A_p = 1/P!\ \frac{d^pI}{dV^p}\bigg|_{V=V_o}$$

then:

$$I(t) = \sum_{p=o}^{n} k^pA_pt^p \quad \ldots\ldots \quad (3)$$

where:

$$d^pI/dt^p = P!\ k^pA_p$$

Such a series can be generated using a number of operational amplifiers, connected alternately as adders and integrators as indicated in Fig. 1. At any time, t_1,

$$I(t) = \sum_{p=o}^{n} k^pa_p\ (t - t_1)^p$$

Thus coefficients of equation (1) can be written as:

$$\left.\begin{aligned} a_o &= A_o + kA_1t_1 + k^2A_2t_1^2 - - - - k^nA_nt_1^n \\ ka_1 &= kA_1 + 2k^2A_2t_1 + 3k^3A_3t_1^2 - - - - nk^nA_nt_1^{n-1} \\ 2!\ k^2a_2 &= k^2A_2 + 6k^3A_3t_1 - - - - n(n-1)\ k^nA_nt^{n-2} \\ n!\ k^na_n &= n!\ k^n\ A_n \end{aligned}\right\} \quad \ldots\ldots \quad (4)$$

A comparison of equation (4) with Fig. 1 indicates that the total input to the integrator establishes the value of:

$$P!\ k^pa_p \text{ for } t = t_1$$

Thus, providing that the output of the integrating circuits matches the output of the non-linear device, when it is driven with a ramp signal, the coefficients of equation (1) may be read off, for any point in the operating region, as the input to the corresponding integrator.

Typical Test Circuit

In order to establish a match between the output waveform of the non-linear device and the waveform as generated by the integrators, a visual comparison of the differences between these two signals may be made on a c.r.o. This is achieved as shown in Fig. 2.

The control device, on which depends the basic timing of the whole system, provides the energizing and reset current of all of the s.p.d.t. relay contacts in the system. Additionally, it provides a triggering pulse for the c.r.o. Amplifier No. 1, connected as an integrator, produces a ramp signal of kt to the non-linear device, via the biasing voltage V_o and also drives the X axis of the XY plotter

* *Nova Scotia Technical College, Canada.*
† *Northern Electric Co. Ltd, Canada.*

P A R T III

FREQUENCY RESPONSE OF LINEAR SAMPLED-DATA SYSTEMS

SUMMARY

While designing the electronic sample and hold for the adaptive system of Section 3 (Part II) of this thesis, the frequency response of the S and H was investigated. It was found that at certain sampling frequencies, the standard text book approach gave rise to erroneous results. In this part of the thesis, the correct frequency response of the sample and hold at these frequencies is derived. This result has a particular importance in stability assessment.

1. INTRODUCTION

Frequency response methods are invaluable for analysing and synthesising of linear, time invariant control systems. Sampled-data systems cannot be handled in an exact manner using these techniques however, since a sinusoidal input signal does not produce a sinusoidal output. However, if the output signal is approximated by its component of input frequency, useful information can be obtained in many cases of practical importance. The common approach to this approximate analysis is significantly in error. The correct expression for the frequency response of the sample-and-hold is derived.

A typical sampled-data system consists of a sampler followed by a zero-order hold and the plant transfer function. The text books[54,55] on sampled-data systems derive the frequency response function of the hold as a continuous function plotted in Fig.45. The same plot except for a scale factor also represents the transfer function of the sample-and-hold unit if only the fundamental component of the output of the hold is considered[56].

If $G_{sh}(j\omega)$ is the frequency response function of the sample-and-hold, then the quoted result is

$$G_{sh}(j\omega) = \frac{\sin \frac{\omega T_s}{2}}{\frac{\omega T_s}{2}} \angle -\frac{\omega T_s}{2} \qquad \ldots\ldots (1)$$

This representation of the transfer function of sample-and-hold gives good results when the ratio of the sampling frequency to input signal frequency is large. However, when this frequency ratio is small and in particular when $\frac{\omega_s}{\omega} = \frac{2}{n}$ where $n = 1, 2, \ldots$, the frequency response function is no longer single valued as predicted by Equation (1) and plotted in Fig. 45.

When the input frequency is simply related to the sampling frequency ($\omega = \frac{n\omega_s}{2}$), the gain of the sample-and-hold unit depends upon the phase relationship between the input sinusoid and the sampling pulses. This is not exhibited in Fig. 45, but can readily be deduced. The effect will be discussed in detail for $\omega = \frac{\omega_s}{2}$ which is the most important practical case, since system instability can always occur at this frequency.

2. DERIVATION OF $G_{sh}(j\omega)$ AT $\omega = \frac{\omega_s}{2}$

The transfer function of the sample-and-hold taking into account the phase angle between input and sampling wave-forms is derived as follows.

By definition, the gain of S and H is given by

$$G_{sh}(j\omega) = \frac{\text{Fundamental Component of the Output of the Hold}}{\text{Magnitude of Sinusoidal Input}}$$

At the input frequency of $\omega = \frac{\omega_s}{2}$, the output of the sampler is a series of alternate pulses of amplitude A sin ϕ, and the output of the hold is thus a square wave whose amplitude depends on ϕ, the phase angle between the reference zero of the input signal and the instant of commencement of sampler action, as shown in Fig.46. The output signal from the data hold has a magnitude m(t) which is a maximum when $\phi = \pm 90^{\circ}$ and zero when $\phi = 0$ or $\pm 180^{\circ}$ (Fig.46). The fundamental component of m(t) is, by Fourier analysis,

$$X_o = A_1 \cos \omega t + B_1 \sin \omega t$$

where

$$A_1 = \frac{1}{\pi} \int_0^{2\pi} m(t) \cos \omega t \, d\omega t$$

$$= \frac{4A}{\pi} \sin^2 \phi$$

and

$$B_1 = \frac{1}{\pi} \int_0^{2\pi} m(t) \sin \omega t \, d\omega t$$

$$= - \frac{4A}{\pi} \sin \phi . \cos \phi .$$

Thus,

$$X_o = \frac{4A}{\pi} \sin \phi \sin (\omega t - \phi) \qquad \ldots\ldots (2)$$

from which it follows that

$$G_{sh}(j\omega) = \frac{4}{\pi} \sin \phi . e^{-j\phi} \qquad \ldots\ldots (3)$$

Thus, it is seen from Equation (3) that $G_{sh}(j\omega)$ is not equal to $\frac{2}{\pi}$ as predicted by Equation (1), but can take any value between 0 and $\frac{4}{\pi}$ depending on the phase angle ϕ (which can vary in the range $0 \leq \phi \leq 180^\circ$). Also the phase of $G_{sh}(j\omega)$ is equal to $-\phi$ and not a constant angle $-\frac{\pi}{2}$ as predicted by Equation (1).

Similarly it can be shown that $G_{sh}(j\omega)$ varies with ϕ in the same manner at input frequencies $\omega = \frac{n\omega_s}{2}$ where $n = 3,5,7,\ldots$. These frequencies are precluded from the discussion by the sampling theorem, however, and are not of significant interest in feed-back control systems.

It is easily shown that Equation (3) represents a circle in the $G(j\omega)$ plane with centre $(0, -\frac{2}{\pi})$ and radius $\frac{2}{\pi}$, as shown in Fig.47.

3. STABILITY ANALYSIS

The stability of a closed-loop continuous system can be predicted by plotting the Nyquist diagram of the open-loop frequency response function and checking for encirclement of the -1 point. Neglecting harmonics and intermodulation terms, the technique can be used as an approximate method for the stability assessment of a sampled-data system.

If the transfer function of the plant is $G_p(p)$, then the open-loop frequency response function $G(j\omega)$ is

$$G(j\omega) = G_{sh}(j\omega) \cdot G_p(j\omega) \qquad \ldots\ldots (4)$$

where $G_{sh}(j\omega)$ is the frequency response function of the sample-and-hold. In plotting the Nyquist diagram from Equation (4), care must be taken to use Equation (3) for the frequency response function of the sample-and-hold at $\omega = \frac{\omega_s}{2}$. Otherwise, erroneous stability predictions can result. When $\omega = \frac{\omega_s}{2}$, from Equations (3) and (4), it is seen that the Nyquist plot can lie anywhere on the circle of radius $\frac{2}{\pi} \left|G_p(\frac{j\omega_s}{2})\right|$ passing through the origin with its centre on the line through the origin at an angle of $\left[-90^\circ + \text{Arg.}\, G_p(\frac{j\omega_s}{2})\right]$. If this circle encloses the

-1 point, then instability is predicted. This is illustrated by considering the following examples. The results are compared to those obtainable from the Z-transform method which of course gives exact solutions.

Example 1:

Let $$G_p(p) = \frac{K}{1+T_1 p}$$

From Equations (1) and (4), we get, using the quoted transfer function for the sample-and-hold,

$$G(j\omega) = \frac{K}{(1+\omega^2 T_1^2)^{1/2}} \cdot \frac{\sin \frac{\omega T_s}{2}}{\frac{\omega T_s}{2}} \angle -\frac{\omega T_s}{2} - \tan^{-1}\omega T_1 \quad \ldots\ldots (5)$$

It is clear from Equation (5) that for any $\omega < \frac{\pi}{T_s}$, the Nyquist plot of $G(j\omega)$ cannot encircle the -1 point, thus predicting the stability of the closed loop system for all K. Thus, the instability that is observed at half sampling frequency is not predicted.

Using the procedure described above, the more accurate open-loop frequency response locus may be used. For $\omega \neq \frac{n\omega_s}{2}$, this locus is identical to the original curve. For $\omega = \frac{\omega_s}{2}$, when the gain of the continuous portion is $R\angle\phi$, say, the overall gain is

represented not by a point but by a circle of radius R and centre $R\angle\phi$, as shown in Fig.48. The particular point along this circle which is effective depends on the phase angle between the input sinusoid and the sampling pulses. The circle passes through the (-1,0) point for K = 2.73, for the example under consideration. This compares reasonably well with the exact result, $K \leq 2.17$ given by the Z-transform method.

Example 2:

Let $$G_p(p) = \frac{K(1+T_2p)}{p(1+T_1p)} \qquad T_2 > T_1$$

From Equations (1) and (4),

$$G(j\omega) = \frac{\sin\frac{\omega T_s}{2}}{\frac{\omega T_s}{2}} \cdot \frac{K(1+\omega^2T_2^2)^{1/2}}{\omega(1+\omega^2T_1^2)^{1/2}} \angle \frac{\omega T_s}{2} - \frac{\pi}{2} - \tan^{-1}\omega T_1 + \tan^{-1}\omega T_2$$

For any value of $\omega \leq \frac{\pi}{T_s}$, the phase angle of $G(j\omega)$ cannot reach $-\pi$ and hence $G(j\omega)$ cannot encircle the -1 point predicting stability for all K. As in the previous example, using the above procedure, it can be worked out for the representative values say, $T=1=T_1$, $T_2=2$, the phase angle of $G(j\omega)$ becomes $-\pi$ when $\phi = 98.6^\circ$. This corresponds to the stability limit of K = 1.3.
The Z-transform method gives $K \leq 1.03$.

4. CONCLUSIONS

It has been shown that the conventional frequency response function of the sample-and-hold unit is in serious error when frequencies of $\frac{n\omega_s}{2}$ have importance. By considering the response to these input frequencies in detail, a more accurate response function may be derived, with a pronounced effect on the predicted stability of closed-loop sampled-data systems. As the order of the system increases, it may be expected that the accuracy of the technique will improve, with the increased attenuation of harmonic components. Although the method is only approximate, it may prove valuable for rapid estimation of system behaviour and for providing a physical insight into some phenomenon observed in sampled-data systems. The predicted instability in the above analysis is due to the phase sensitivity of the output of the hold at $\omega = \frac{\omega_s}{2}$. This is a phenomenon which is neglected in the Z-transform analysis. In the Z-transform method, the gain of the zero-order hold is taken as constant since perfect reconstruction is assumed. But, as has been shown, this is not true at $\omega = \frac{\omega_s}{2}$. The gain is a function of the phase angle ϕ and the instability predicted in the above analysis is due to this phenomenon only.

REFERENCES

1. Oldenburger, R. "Optimum Non-linear Control". A.S.M.E. Trans., Vol. 79, 1957. p. 527.

2. McDonald, D. "Non-linear Techniques for Improving Servo Performance". National Electronics Conference 6, 1950. p. 400.

3. Hopkin, A.M. "A Phase-Plane Approach to the Compensation of Saturating Servo-mechanisms". A.I.E.E. Trans., Vol. 70, 1951. p. 631.

4. Uttley, A.M. and Hammond, P.H. "The Stabilisation of On-Off Servo-mechanisms". Automatic and Manual Control, 1951 Cranfield Conference, 1952. p. 285.

5. Flugge-Lotz, I. "Discontinuous Automatic Control". (book) Princeton University Press, 1953.

6. West, J.C.,Douce, J.L. and Naylor, R. "The Effect of the Addition of Some Non-linear Elements on the Transient Performance of a Simple R.P.C. System Possessing Torque Limitation". Proc. I.E.E. 101, 1954. p. 156.

7. Kalman, R.E. "Analysis and Design Principles

of Second and Higher-Order Saturating Servo-mechanisms". A.I.E.E. Trans., Vol. 74, Part II, 1955. p. 294.

8. Bogner, I. and Kazda, L.F. "An Investigation of the Switching Criterion for Higher-Order Servo-mechanisms". A.I.E.E. Trans., Vol. 73, Part II, 1954. p. 118.

9. Bellman, R., Gliksberg, I. and Gross, O. "On the Bang-Bang Control Problem". Quart. Appl. Maths. 14, 1956.

10. Rozoncer, L.I. "L.S. Pontryagin's Maximum Principle in the Theory of Optimum Systems". Automation and Remote Control, Parts I - III, 20, 1959.

11. Lasalle, J.P. "The Time Optimal Control Problem". In: Contributions to the Theory of Non-linear Oscillations, Vol. V, Princeton University Press, 1960.

12. Tsien, H.S. "Engineering Cybernetics". Mcgraw Hill, 1954.

13. West, J.C. and Nikiforuk, P.N. "The Frequency Response of a Servo-mechanism Designed for

Optimum Transient Response". A.I.E.E. Trans., Part II, 1956. p. 234.

14. Bushaw, D.W. "Optimal Dis-continuous Forcing Terms". In: Contributions to the Theory of Non-linear Oscillations, Vol. IV, Princeton University Press, 1958.

15. Kazda, L.F. "Errors in Relay-Servo Systems". A.I.E.E. Trans., Vol. 72, Part II, 1953. p. 323.

16. Stout, T.M. "Effects of Friction in an Optimum Relay Servo-mechanism". A.I.E.E. Trans., Vol. 72, Part II, 1953. p. 329.

17. Graham, D. and McRuer, D. "Analysis of Non-linear Control Systems". John Wiley & Sons, 1961.

18. Dorato, P. "On Sensitivity in Optimal Control Systems". I.E.E.E. Trans. on Automatic Control, Vol. A.C. 8, 1963. p. 256.

19. Rohrer, R.A. and Sobral, M. "Sensitivity Considerations in Optimal System Design". I.E.E.E. Trans. on Automatic Control, Vol. A.C. 10, Jan. 1965. p. 43.

20. Aseltine, J.A., Mancini, A.R. and Sarture, C.W. "A Survey of Adaptive Control Systems". I.R.E. Trans. on Automatic Control, Vol. A.C. 6, 1958.

21. Stromer, P.R. "Adaptive or Self-Optimising Control Systems; A Bibliography". I.R.E. Trans. on Automatic Control, Vol. A.C. 4, 1959.

22. Levin, M.J. "Methods of Realisation of Self-Optimising Systems". I.S.A. paper-2-58, A.S.M.E. Instruments and Regulators Conference, 1958.

23. Jacobs, O.L.R. "A Review of Self-Adjusting Systems in Automatic Control". Jour. Electronics and Control, Vol. 10, 1961.

24. Anderson, G.W., Buland, R.N. and Cooper, G.R. "Use of Cross-Correlation in an Adaptive Control System". Proc. Natl. Electronics Conference, Vol. 15, 1959.

25. Margolis, M. and Leondes, C.T. "A Parameter Tracking Servo for Adaptive Control Systems". I.R.E. Trans. on Automatic Control, Vol. A.C. 4, Nov. 1959. p. 104.

26. Popov, E.P., Loskutov, G.M. and Yusopov, R.M. "One Self-Adjusting Control System without Test Disturbance Signals". I.F.A.C. Congress (Basle), 1963.

27. Draper, C.S. and Li, Y.T. "Principles of Optimalising Systems and an Application to the Internal Combustion Engine". A.S.M.E. Publication, New York, 1951.

28. Grensted, P.E.W. and Jacobs, O.L.R. "Automatic Optimisation". Trans. S.I.T., Vol. 13, No. 3, 1961. p. 203.

29. Feldbaum, A.A. "Problems in the statistical Theory of Systems of Automatic Optimisation". Proc. I.F.A.C. Congress (Moscow), 1960.

30. Gibson, J.E. "Self-Optimising or Adaptive Control Systems". Automation and Remote Control, Vol. 2, Butterworth and Co., (Publishers) Ltd., London, 1961.

31. Norkin, K.B. "On One Method of Automatic Search for the Extremum of a Function of Many Variables". Automation and Remote Control, Vol. 22, No. 5, 1961.

32. McGrath, R.J. and Rideout, V.C. "A Simulator

Study of a Two-Parameter Adaptive System". Trans. I.R.E. on Automatic Control, A.C. 6, 1, Feb. 1961.

33. Blackman, P.F. "Extremum-Seeking Regulators". Proc. Symposium on Adaptive Processes, Imperial College, London, 1961.

34. Roberts, J.D. "Extremum or Hill-Climbing Regulation:- A Statistical Theory Involving Lags, Disturbances and Noise". Proc. I.E.E. Vol. 112, No. 1, Jan. 1965. p. 137.

35. Eveleigh, V.W. "General Stability Analysis of Sinusoidal Perturbation Extrema Searching Adaptive Systems". Proc. I.F.A.C. Congress (Basle), 1963.

36. Douce, J.L. and King, R.E. "A Self-Optimising Non-Linear Control System". Proc. I.E.E., Vol. 108, Part B, No. 40, July, 1961, p. 441.

37. Hammond, P.H. and Duckenfield, M.J. "Automatic Optimisation by Continuous Perturbation of Parameters". Automatica, Vol. 1, No. 2/3, August, 1963. p. 147.

38. Nightingale, J.M. "Parameter-Perturbation Adaptive Control Systems with Imposed

Constraints". Proc. I.E.E., Vol. 109, May, 1962. p. 539.

39. Douce, J.L. and Bond, A.D. "The Development and Performance of a Self-Optimising System". Proc. I.E.E., Vol. 10, No. 3, 1963. p. 619.

40. Ng, K.C. "High Frequency Perturbation in Hill-Climbing Systems". Proc. I.E.E., Vol. 111, No. 11, Nov. 1964. p. 1907.

41. Van der Grinten, P.M.E.M. "The Application of Random Test Signals in Process Identification". Proc. I.F.A.C. Congress (Basle), Butterworth and Co., (Publishers) Ltd., 1963.

42. Douce, J.L. and Ng, K.C. "The Use of Pseudo-Random Signals in Adaptive Control". I.F.A.C. Symposium (Teddington), 1965. Published by the Instrument Society of America.

43. Golomb, S.W. "Digital Communication Systems". John Wiley and Sons, 1965.

44. Elspas, B. "The Theory of Autonomous Linear Sequential Networks". Trans. I.R.E., Vol. C.T. 6, March, 1959. p. 45.

45. Taylor, W.K. "An Experimental Control System with Continuous Automatic Optimisation". Proc. I.F.A.C. Congress (Moscow), Butterworth and Co., (Publishers) Ltd., 1960.

46. Briggs, P.A.N., Hammond, P.H., Hughes, M.T.G. and Plumb, G.O. "Correlation Analysis of Process Dynamics using Pseudo-Random Binary Test Perturbations". Advances in Automatic Control Conference (I.Mech.E.), Nottingham, 1965.

47. Izawa, K. and Furuta, K. "Simultaneous Identification of Multi-input and-output Systems". Proc. I.F.A.C. Symposium (Tokyo), 1965. p. 229.

48. Douce, J.L., Ng, K.C. and Walker, A.E.G. "System Identification in the Presence of Ramp Disturbance". Electronic Letters, July, 1966.

49. Lee, Y.W. "Statistical Theory of Communication". John Wiley and Sons, 1960.

50. Korn, G.A. "Random Process Simulation and Measurements". Mcgraw-Hill, New York, 1966.

51. Roberts, P.D. and Davis, R.H. "Statistical Properties of Smoothed Maximal-Length Linear Binary Sequences". Proc. I.E.E., Vol. 113, Jan. 1966.

52. Briggs, P.A.N. and Godfrey, K.R. "Pseudo-Random Signals for the Dynamic Analysis of Multi-Variable Systems". Proc. I.E.E., Vol. 113, July, 1966.

53. Solodovnikov, V.V. "Introduction to the Statistical Dynamics of Automatic Control Systems". Dover Publications, New York, 1960.

54. Ragazzini, J.R. and Franklin, G.F. "Sampled-Data Control Systems". Mcgraw-Hill, New York, 1958.

55. Kuo, B.C. "Analysis and Design of Sampled-Data Control Systems". Prentice Hall, 1963.

56. Brown, R.G. and Murphy, G.J. "An Approximate Transfer Function for the Analysis and Design of Pulsed Servos". Trans. A.I.E.E., Vol. 72, Part II, 1953.

57. Hampton, R.L.T. "A Hybrid Analog-Digital Pseudo-Random Noise Generator". E.E.S.

Report No. 1, University of Arizona, 1963-64.

58. Paul, R.J.A. "Simulation of Rational Transfer Functions with Adjustable Coefficients". Proc. I.E.E., Vol. 110, April, 1963.

59. Private Correspondence with Dorato, P. of the Polytechnic Institute of Brooklyn, New York.

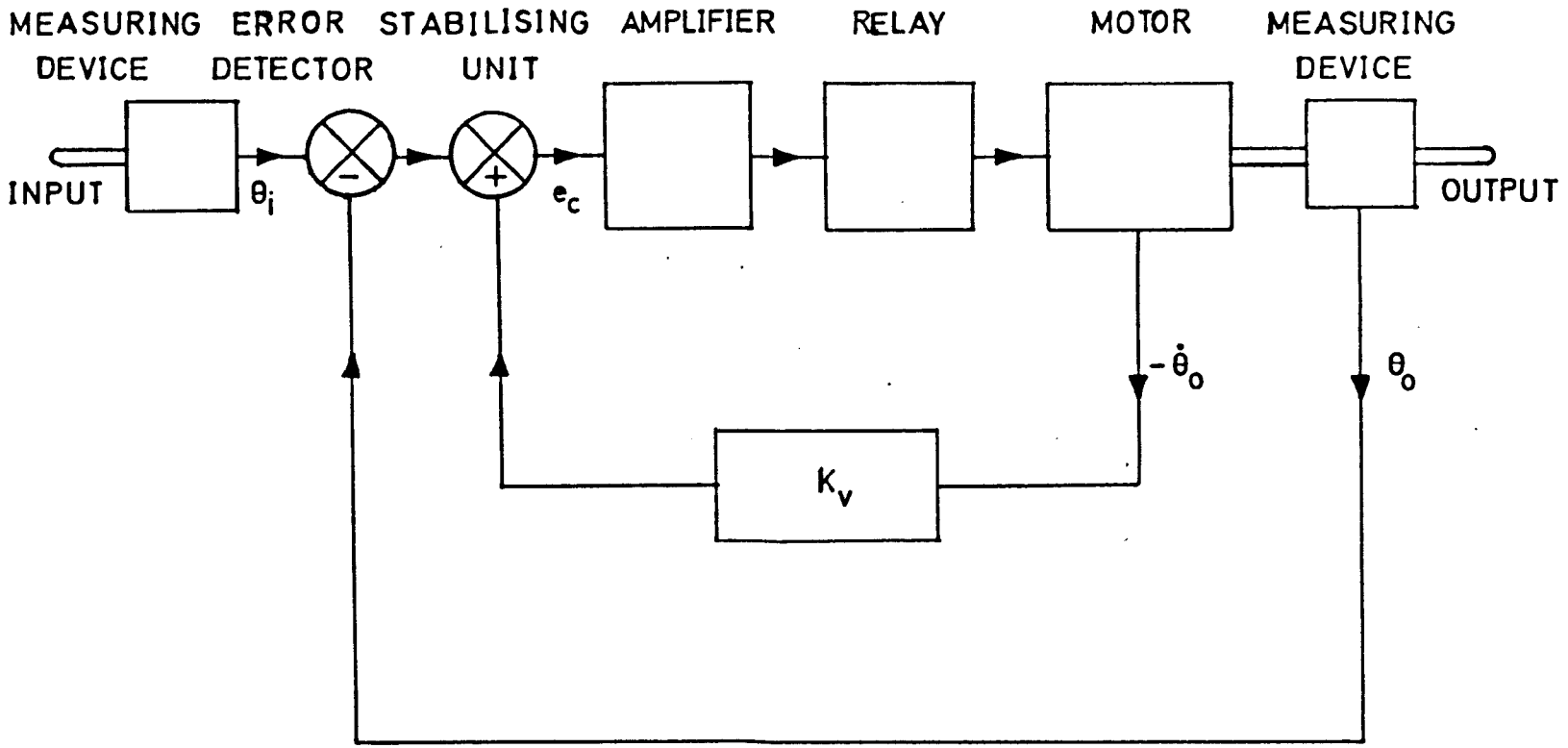

FIG. 1 THE BLOCK DIAGRAM OF THE GENERAL SYSTEM

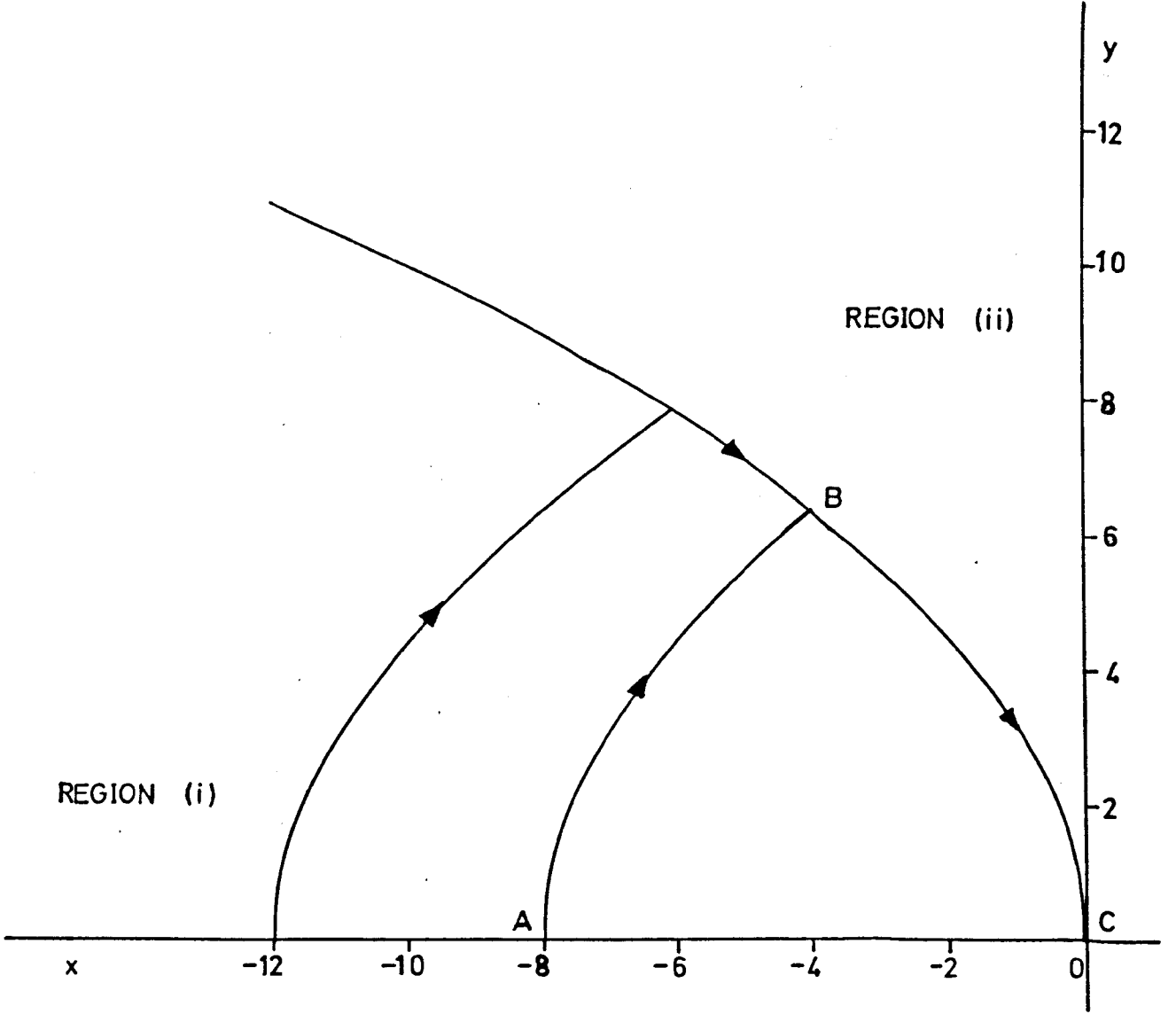

FIG. 2 THE OPTIMUM SWITCHING TRAJECTORY

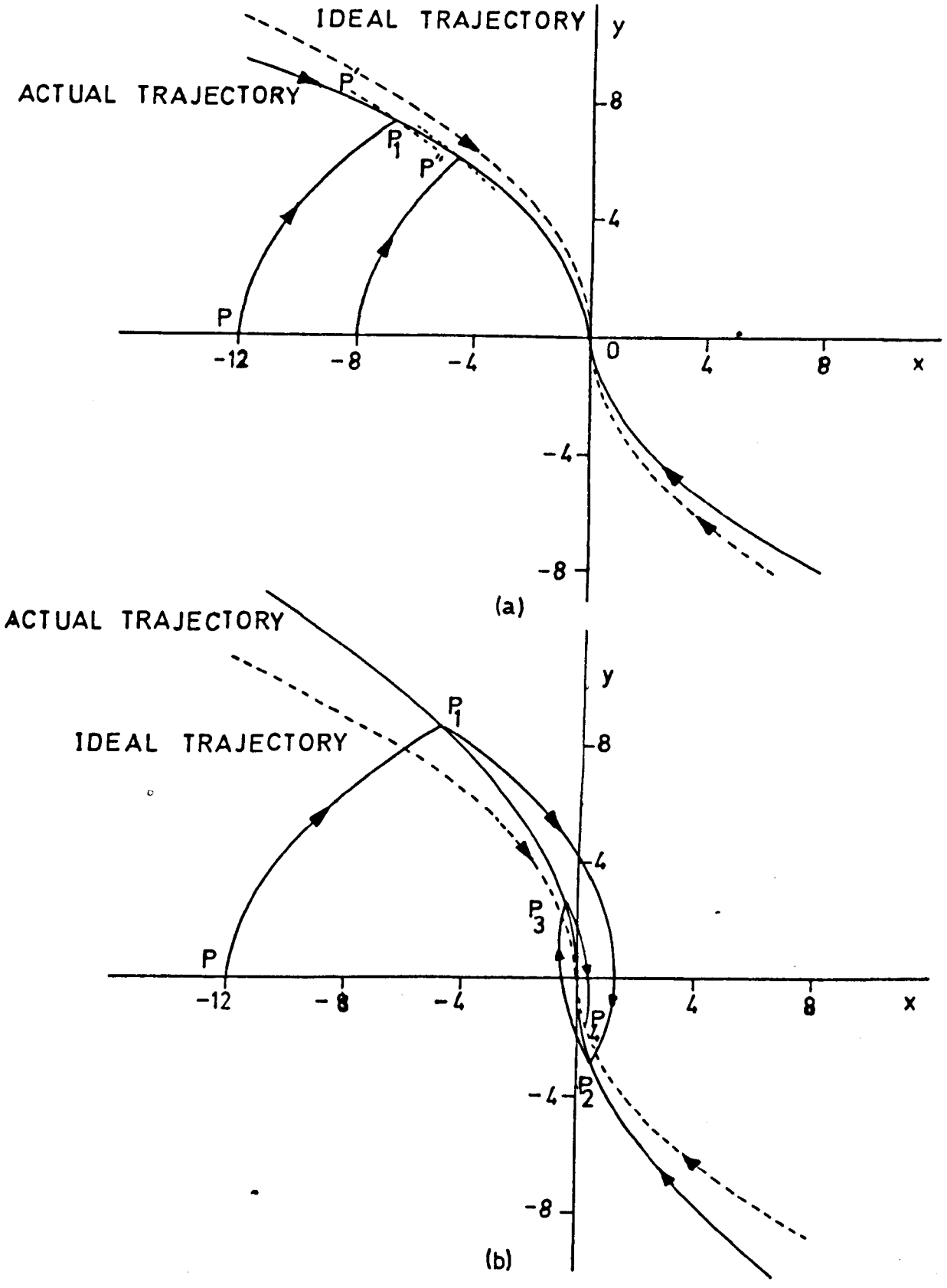

FIG. 3 ERRORS IN THE SWITCHING CURVE

(a) ACTUAL TRAJECTORY NEARER THE x-AXIS

(b) ACTUAL TRAJECTORY NEARER THE y-AXIS

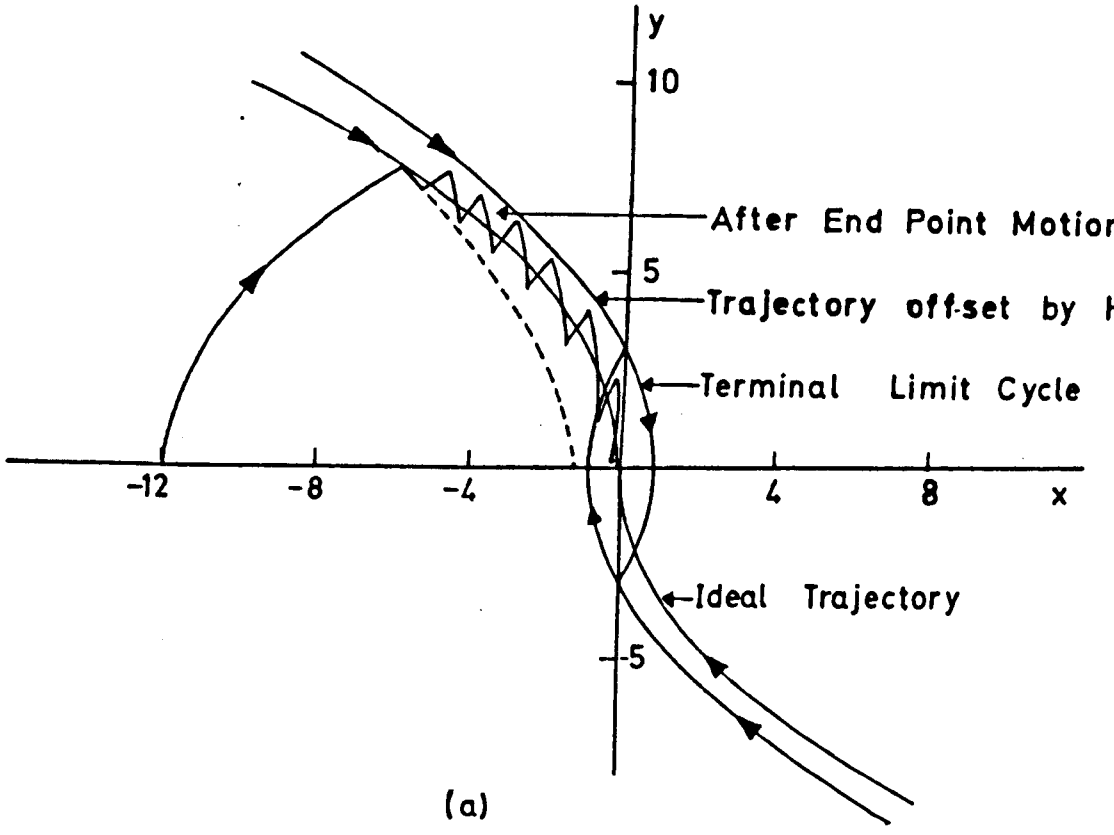

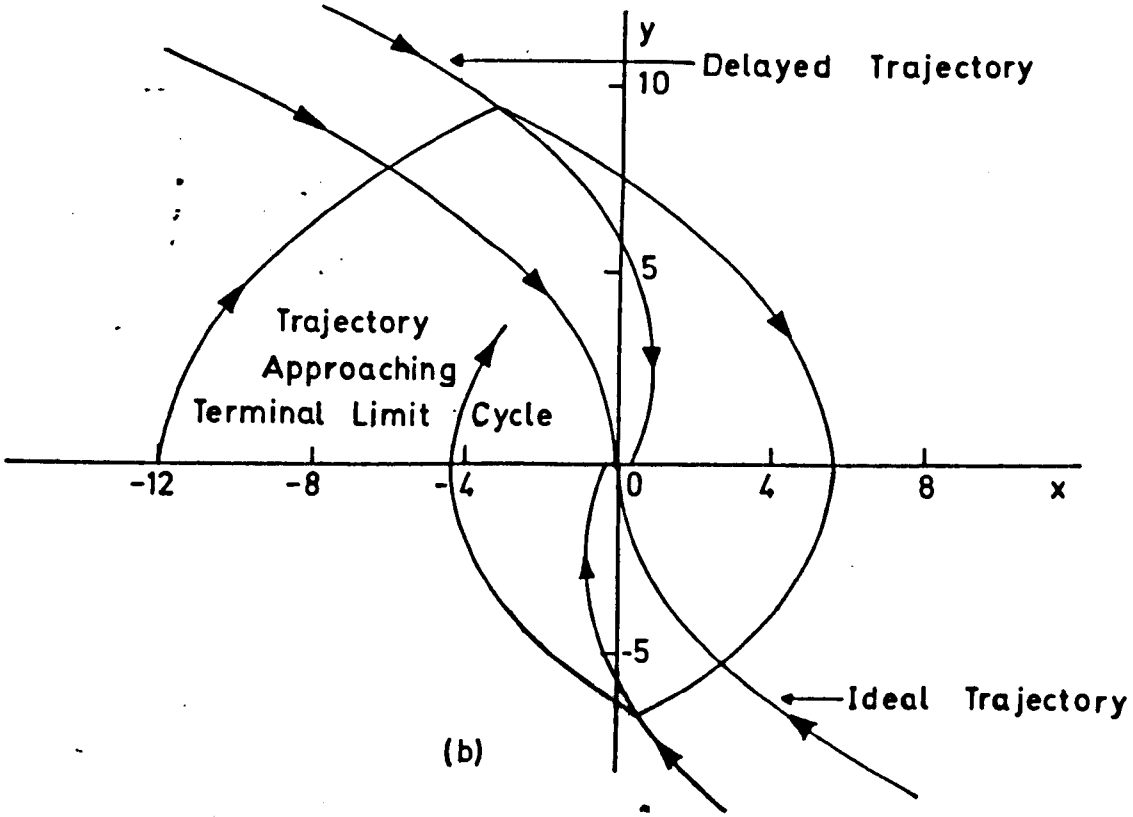

FIG. 4 OPERATION UNDER NON-IDEAL CONDITIONS

(a) EFFECT OF COULOMB FRICTION AND HYSTERESIS

(b) EFFECT OF TIME DELAY

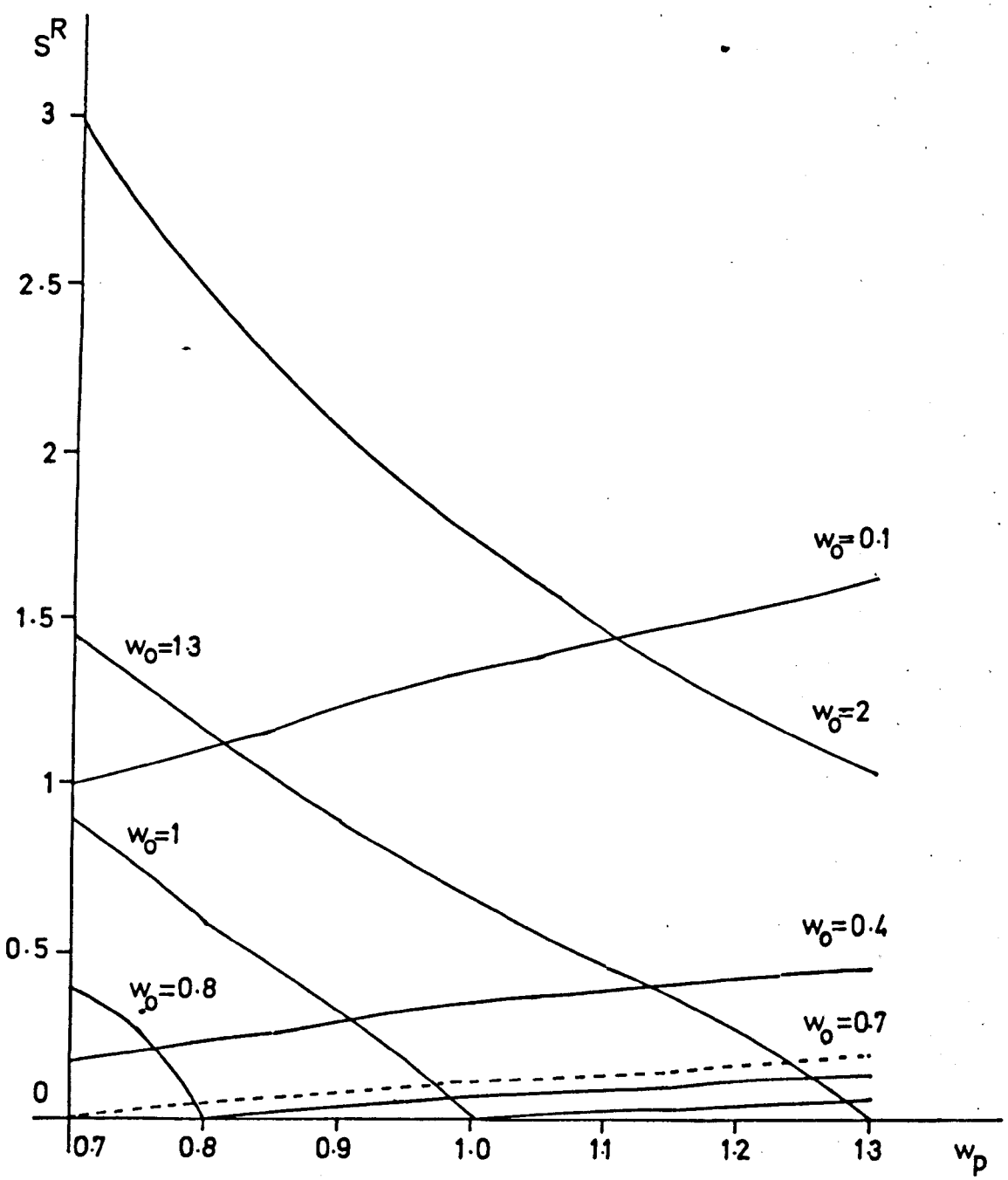

FIG. 5 VARIATION OF RELATIVE SENSITIVITY

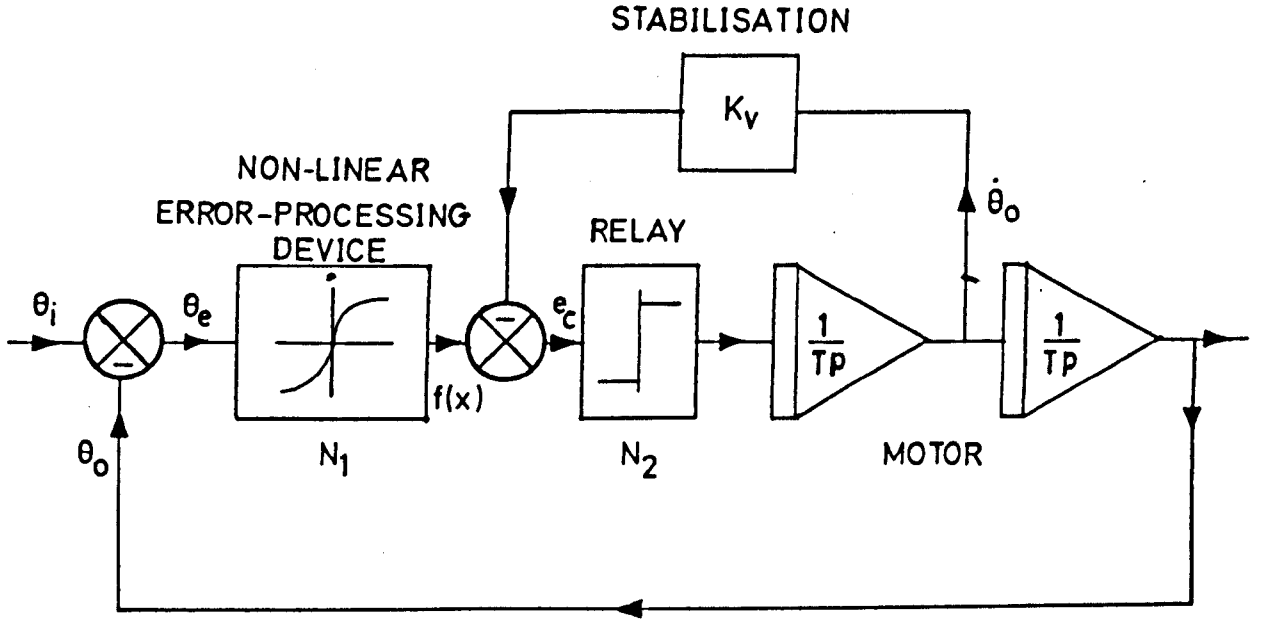

(a)

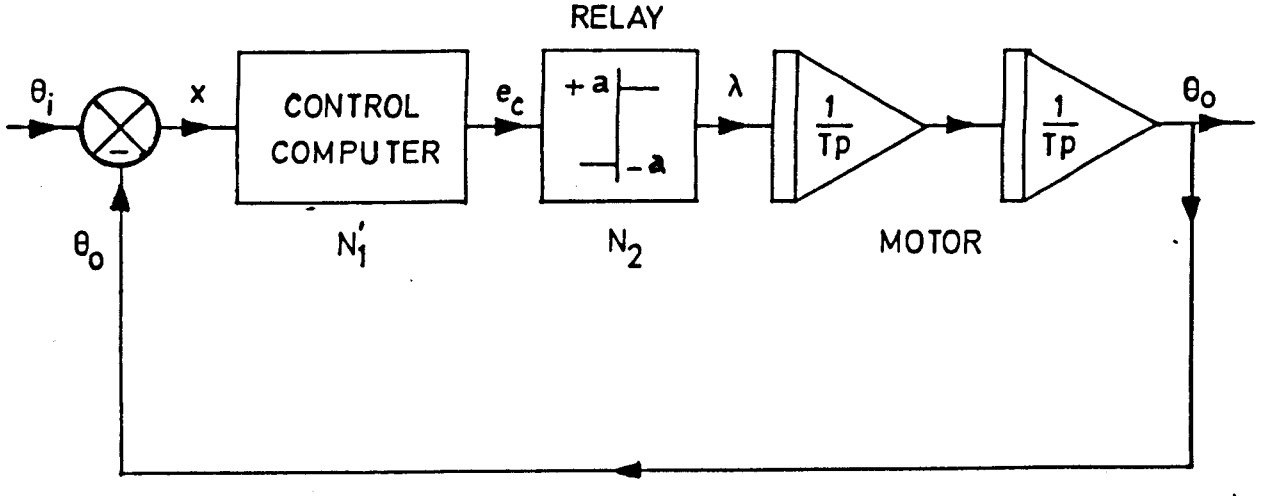

(b)

FIG. 6 SYSTEM STABILITY

(a) THE BLOCK DIAGRAM OF THE OPTIMAL SYSTEM

(b) THE BLOCK DIAGRAM OF THE EQUIVALENT SYSTEM

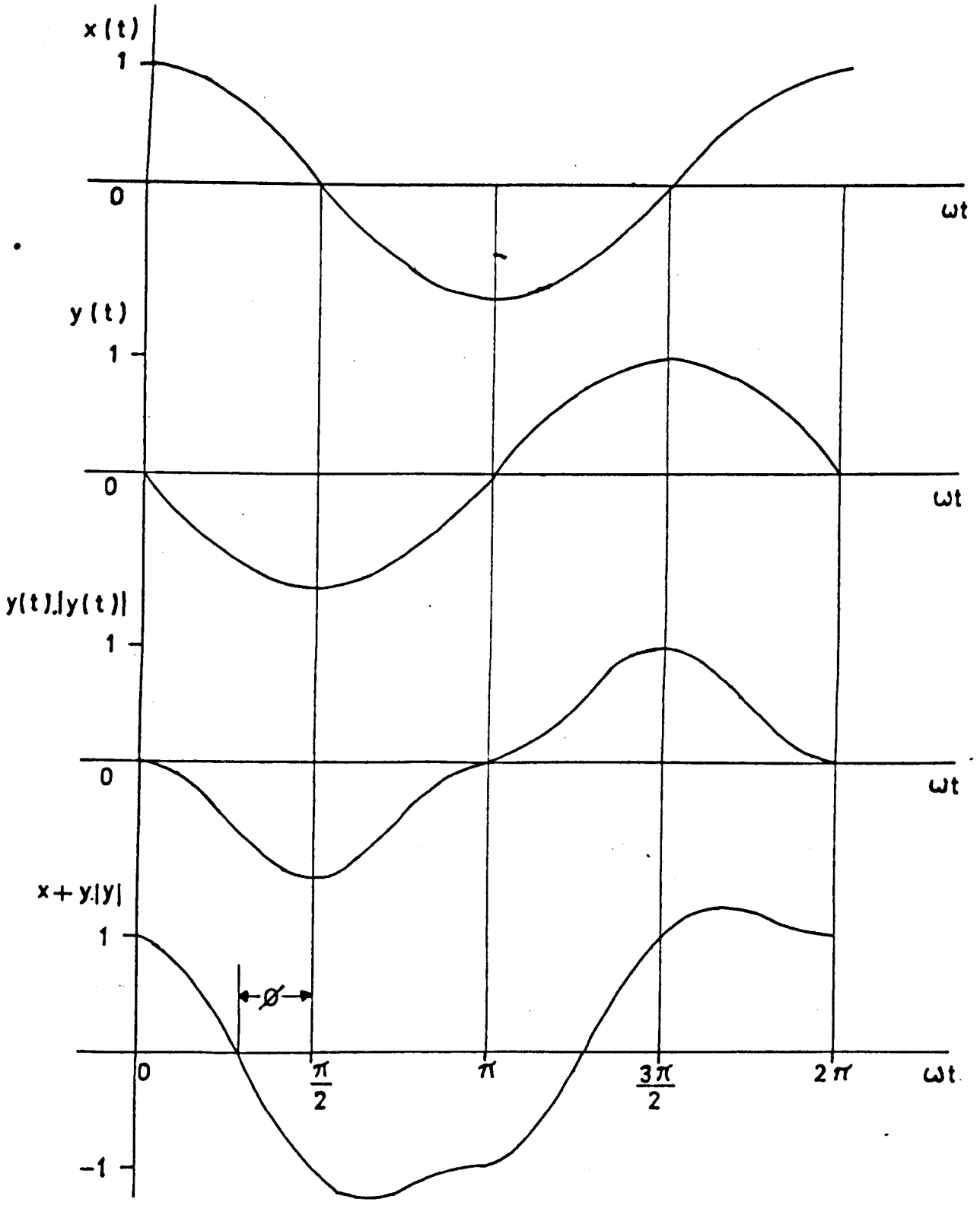

FIG. 7 PHASE ANGLE OF THE DESCRIBING FUNCTION

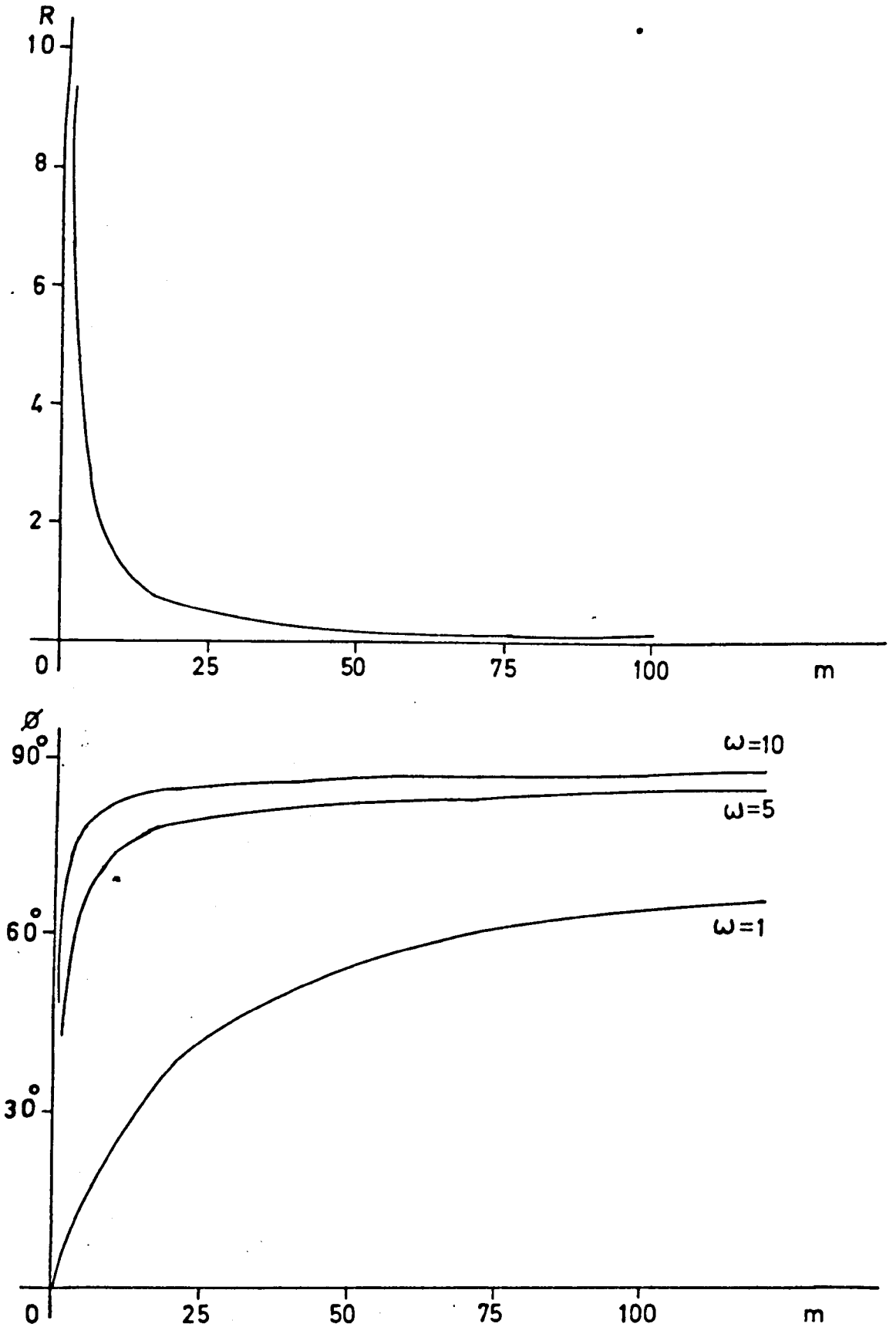

FIG. 8 MAGNITUDE AND PHASE ANGLE OF THE DESCRIBING FUNCTION N(m)

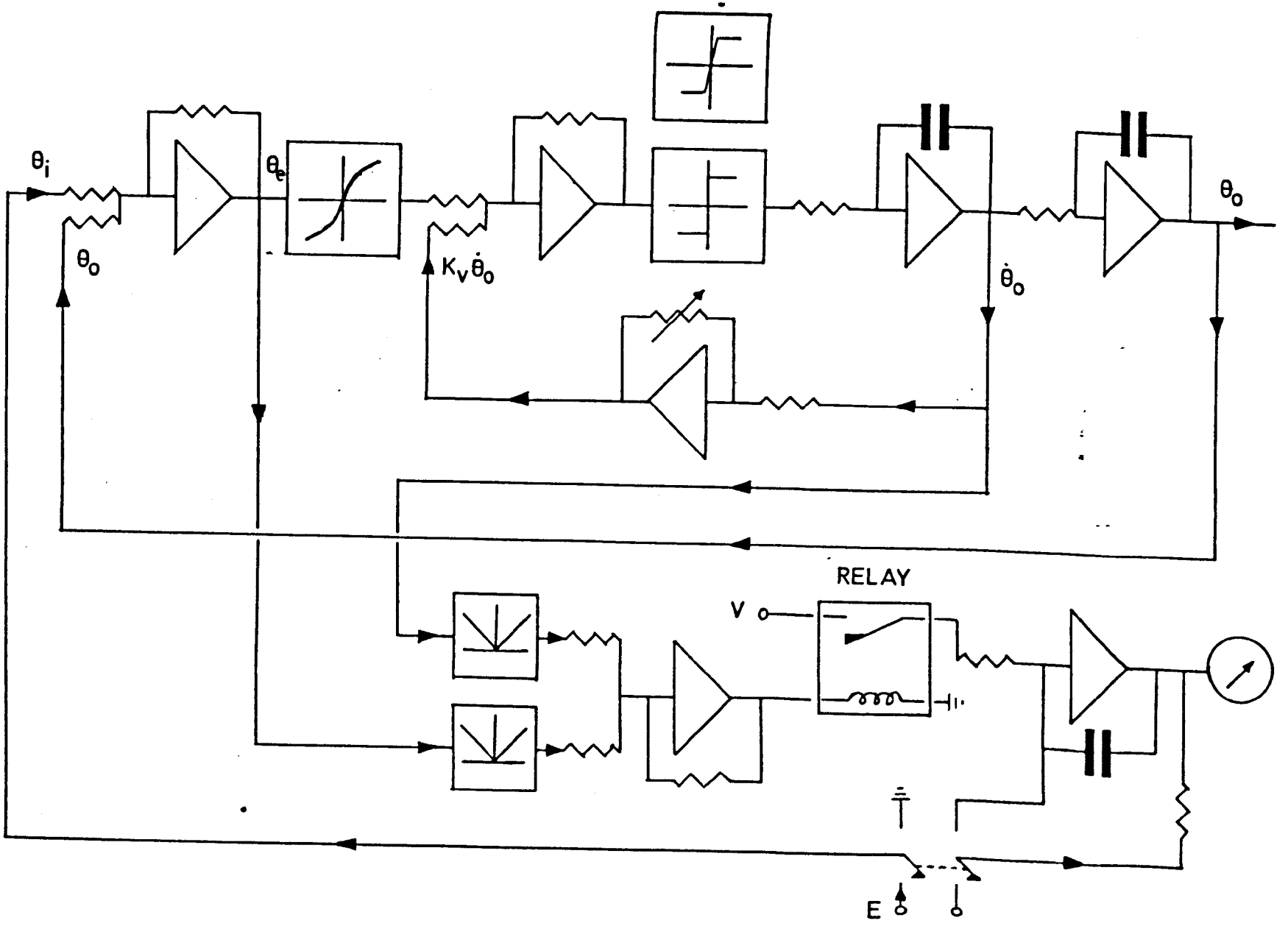

FIG. 9 ANALOGUE SIMULATION OF THE SYSTEM

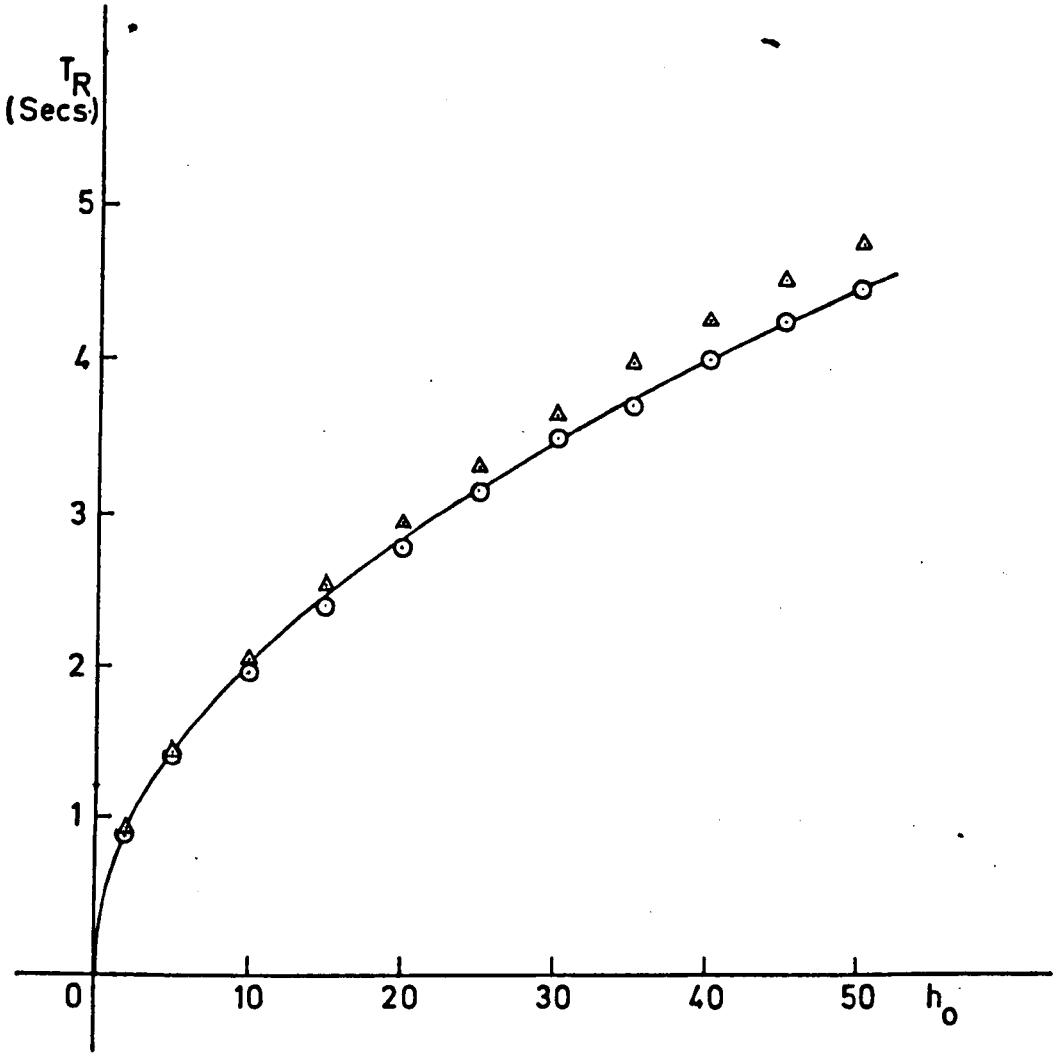

FIG. 10 VARIATION OF RESPONSE TIME WITH INPUT

— THEORETICAL BANG BANG

⊙ PRACTICAL BANG BANG

△ SYSTEM WITH LIMITER

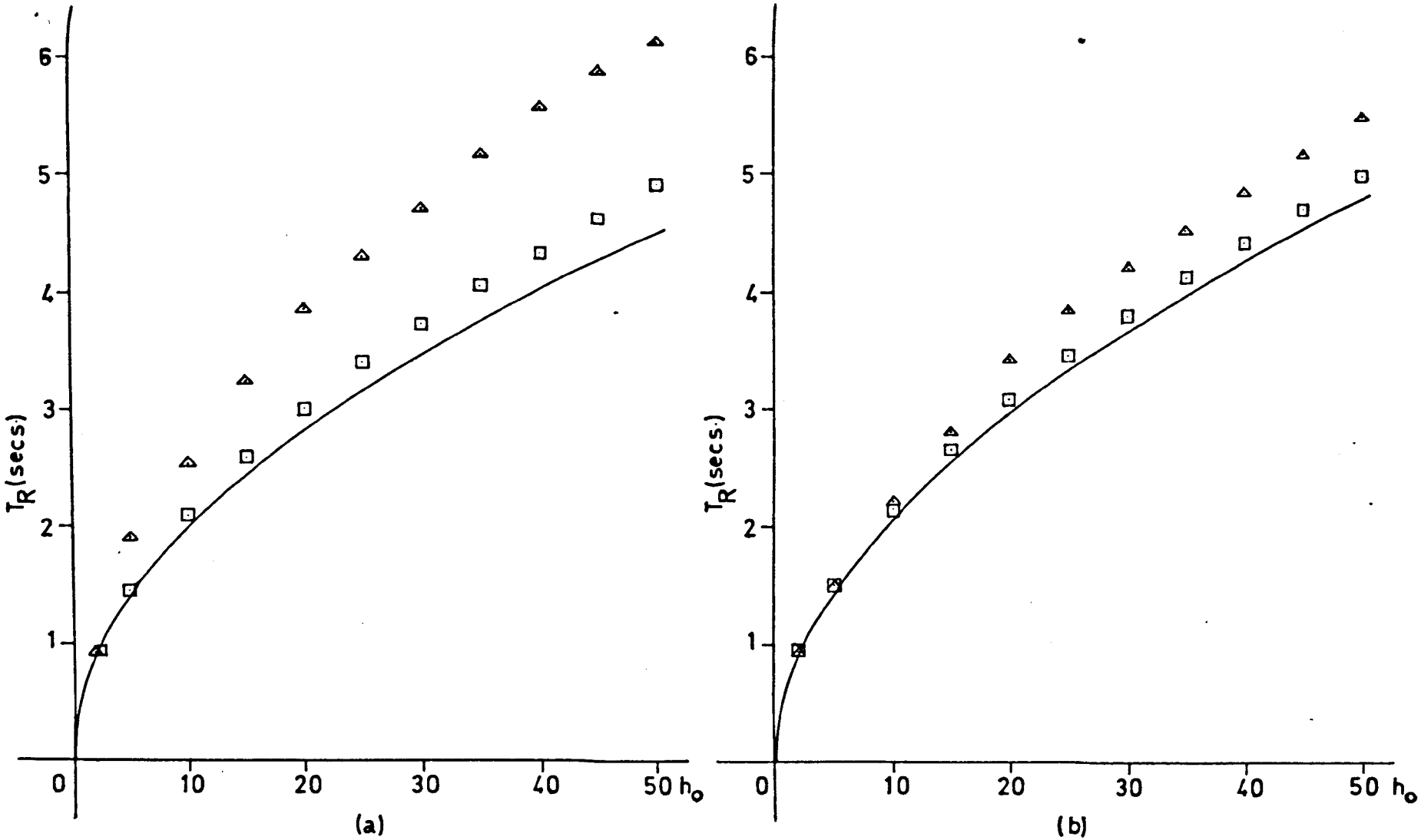

FIG. 11 VARIATION OF RESPONSE TIME WITH INPUT

(a) BANG BANG CONTROLLER (b) CONTROLLER WITH LIMITER

— CRITICAL GAIN FACTOR FOR STABILISER

⊡ CRITICAL GAIN FACTOR + 10 %

△ CRITICAL GAIN FACTOR — 10 %

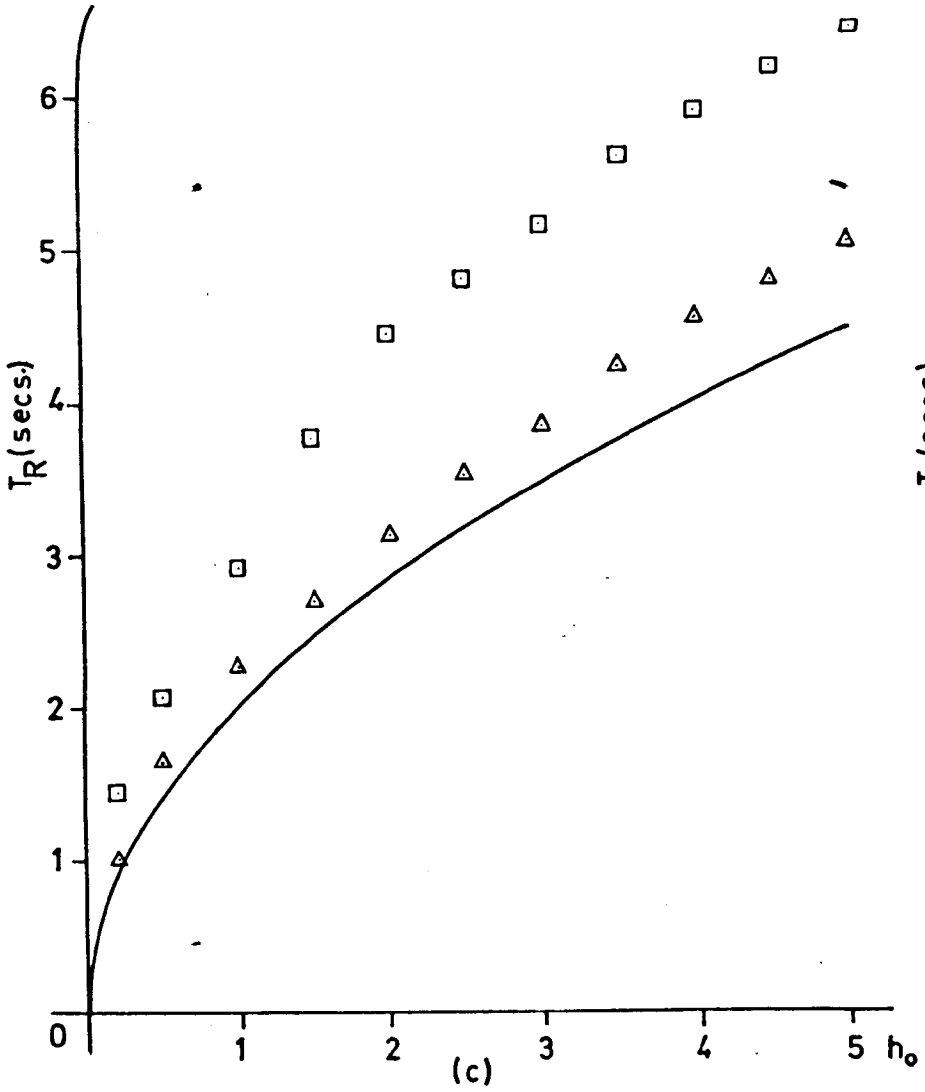

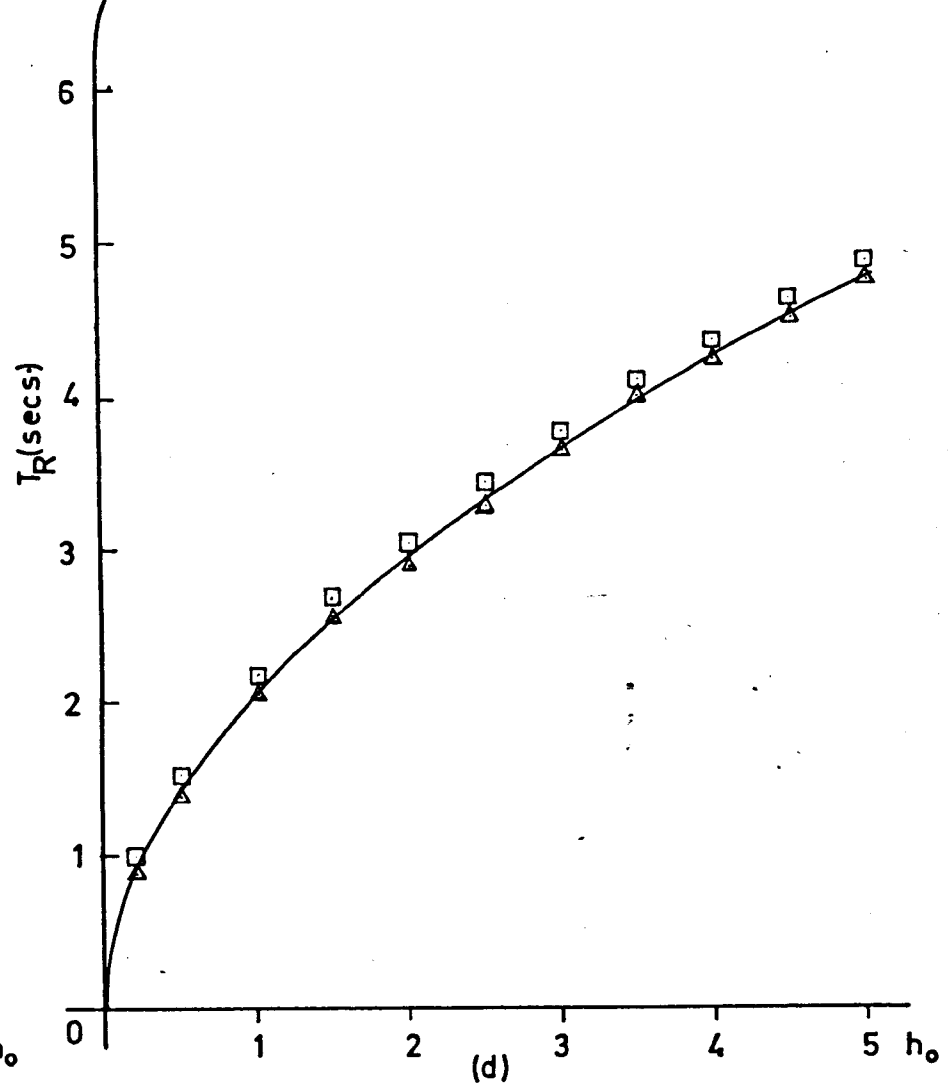

FIG. 11 VARIATION OF RESPONSE TIME WITH INPUT

(c) BANG BANG CONTROLLER (d) CONTROLLER WITH LIMITER

— IDEAL RESPONSE

⊡ RESPONSE WITH A LAG $\frac{1}{1+pT_1}$ WITH THE MOTOR

△ ——— DO ——— WITH THE ERROR DETECOR

T_1=0·1 sec. T=1 sec.

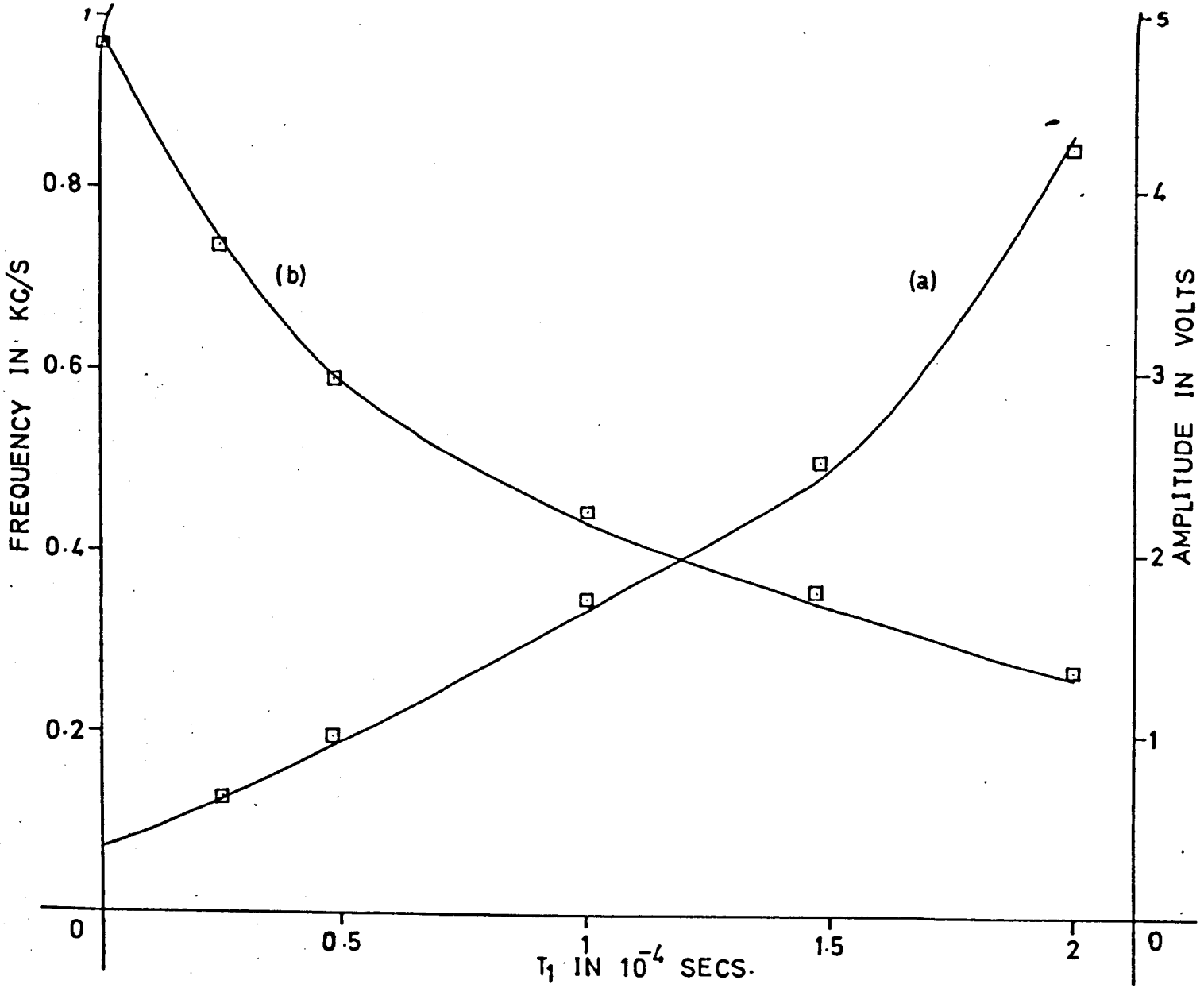

FIG. 12 PLOT OF LIMIT CYCLE AMPLITUDE AND FREQUENCY
(a) AMPLITUDE (b) FREQUENCY
⊡ EXPERIMENTAL POINTS. $T_D = 0.8 \times 10^{-4}$ SECS.

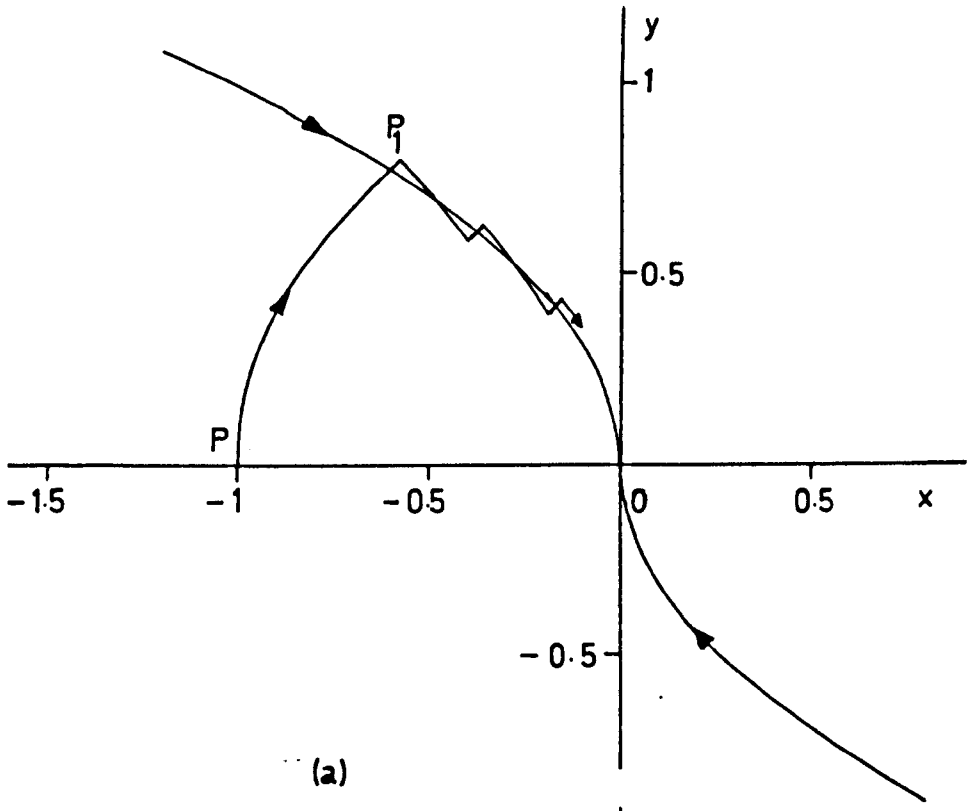

(a)

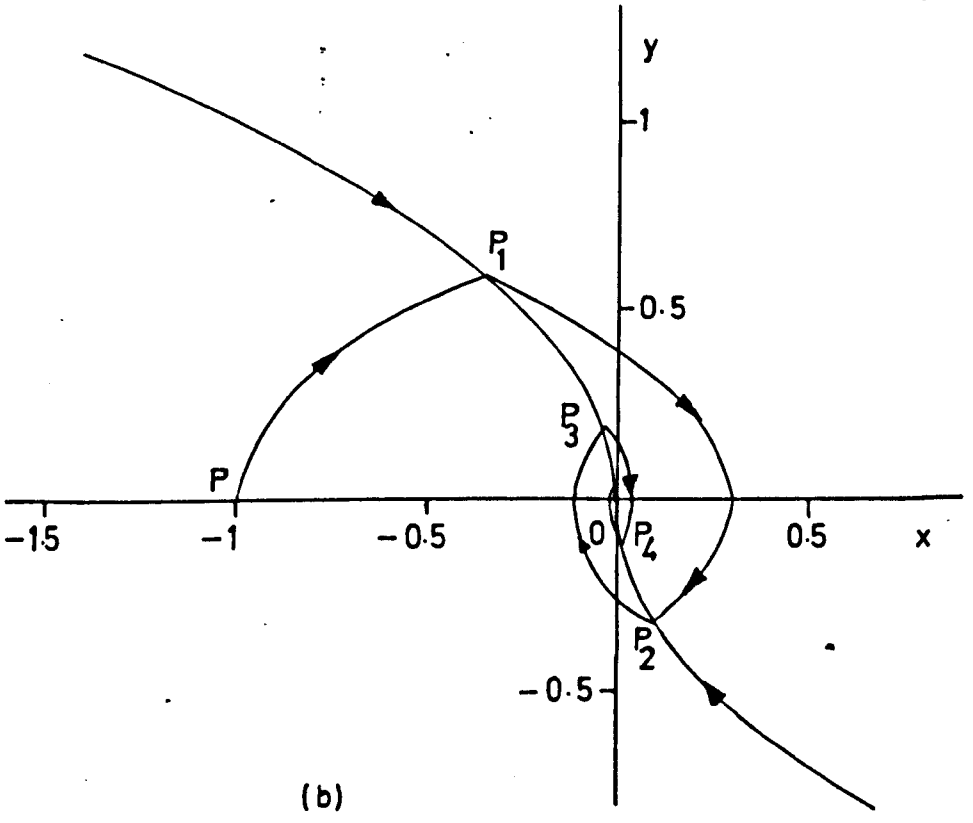

(b)

FIG. 13 PHASE PLANE TRAJECTORIES

(a) $w_p > w_o$

(b) $w_p < w_o$

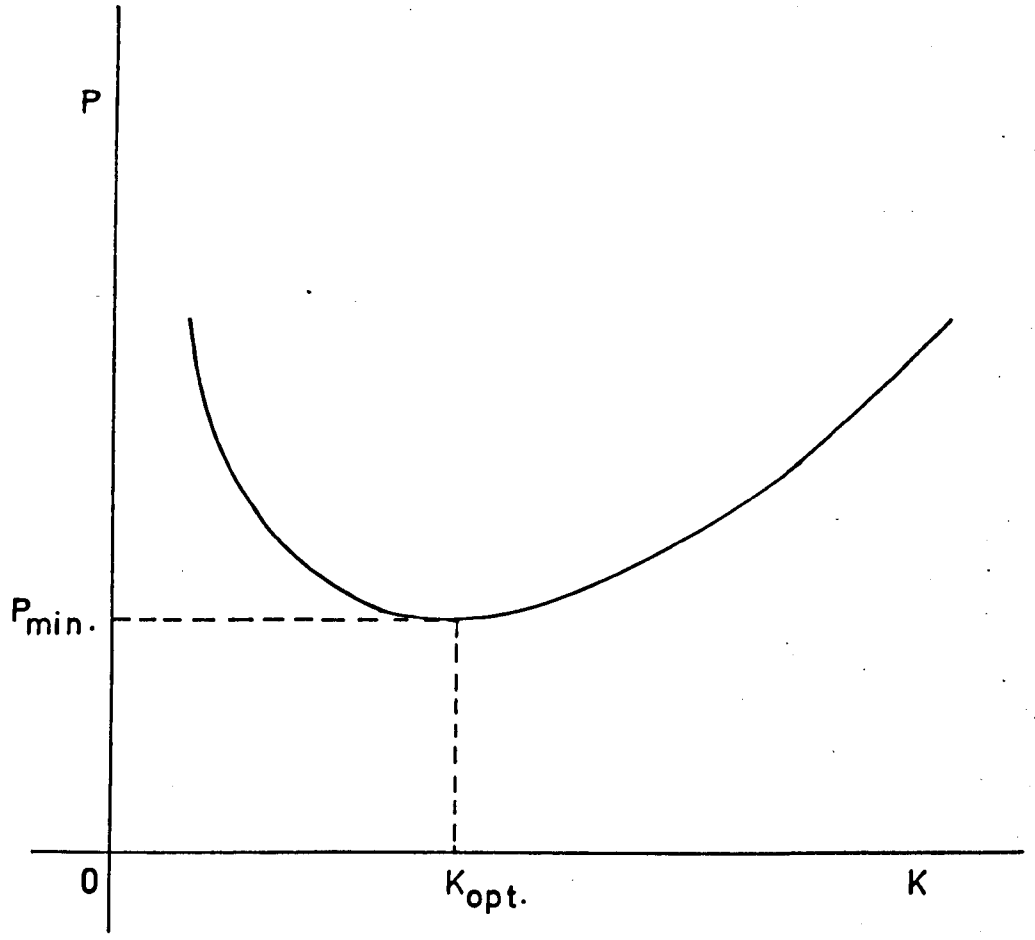

FIG. 14 PERFORMANCE MEASURE CHARACTERISTIC

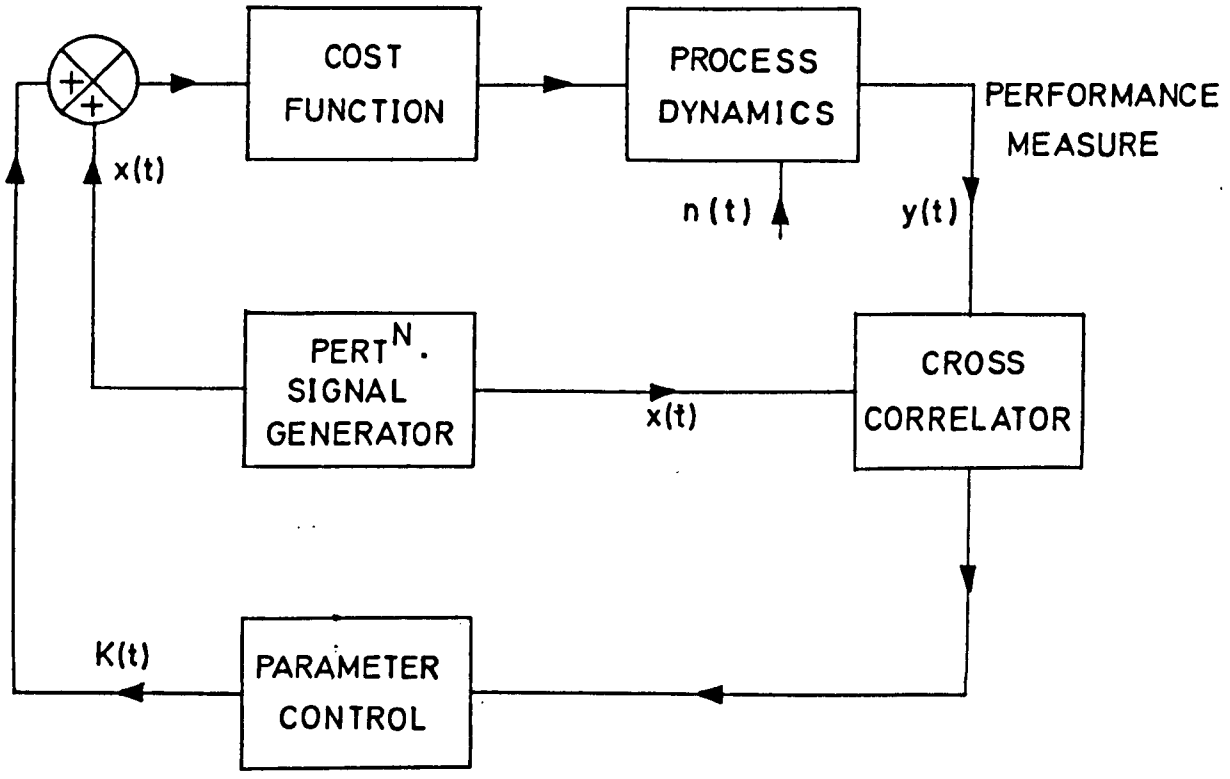

FIG. 15 THE GENERAL EXTREMUM SYSTEM

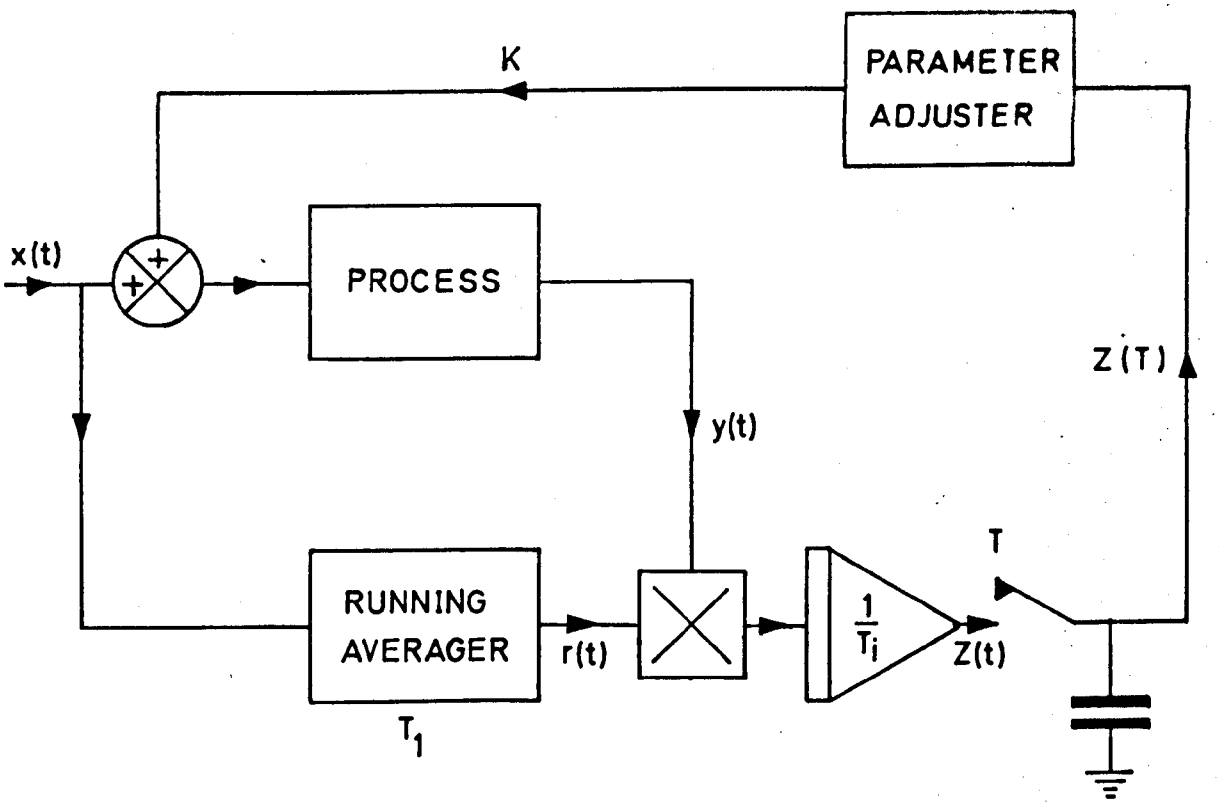

FIG. 16 SCHEMATIC DIAGRAM OF THE HILL CLIMBING SYSTEM WITH DISCONTINUOUS ADJUSTMENT

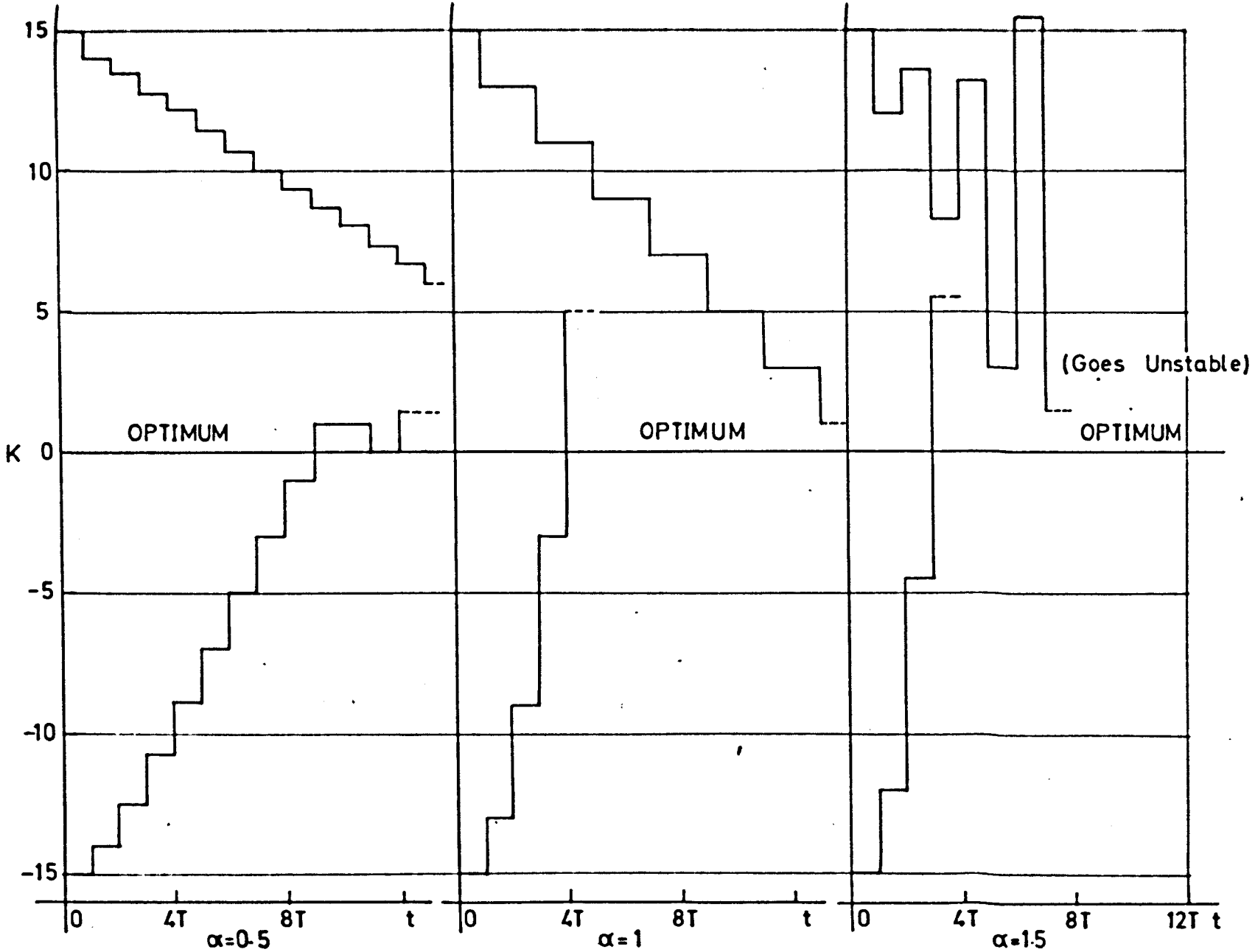

FIG. 17 SYSTEM RESPONSE FOR DIFFERENT VALUES OF α

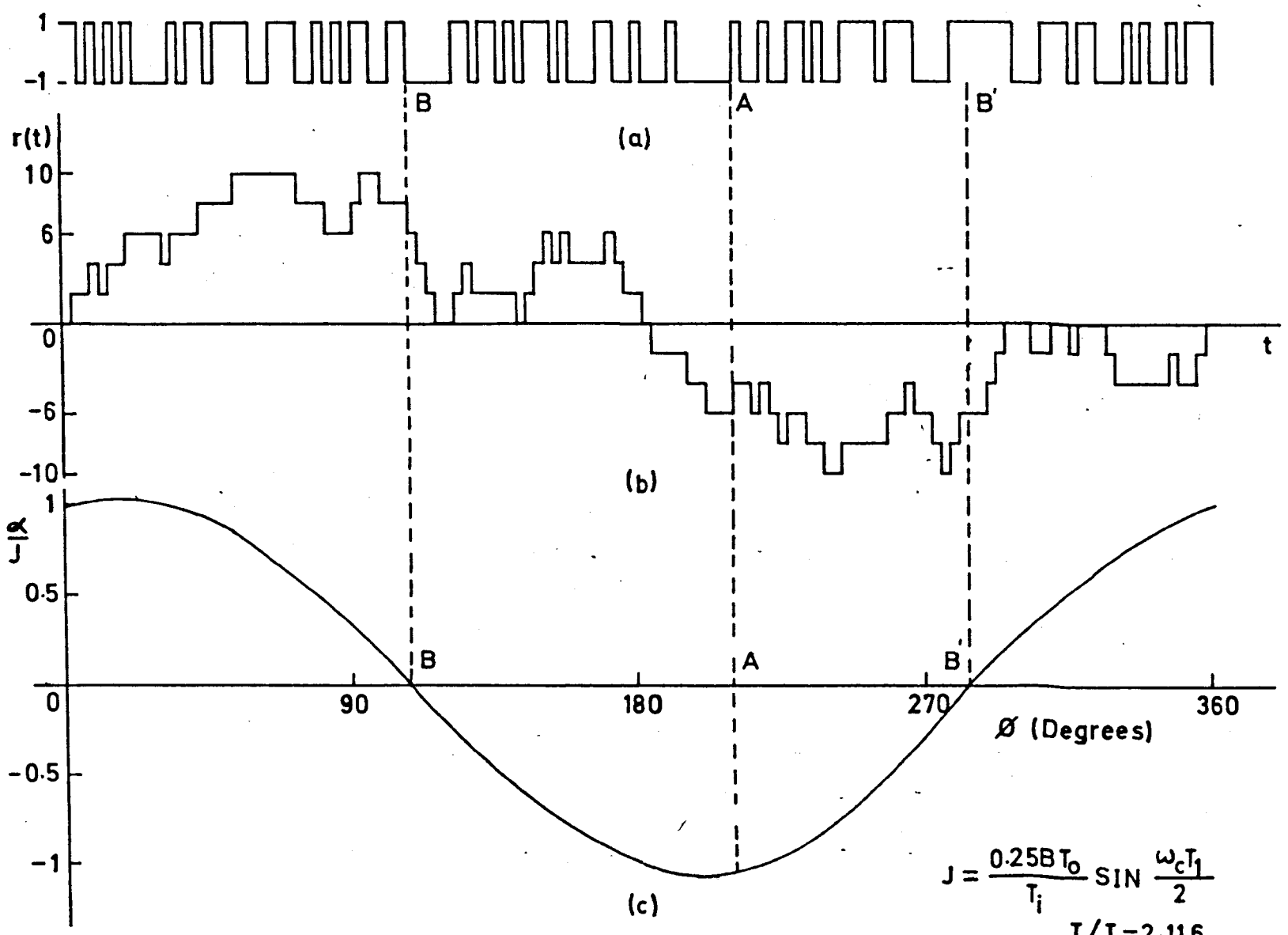

FIG. 18

(a) 127 BIT PRBS (b) RUNNING AVERAGE OVER 64 BITS (c) PLOT OF α VS ϕ

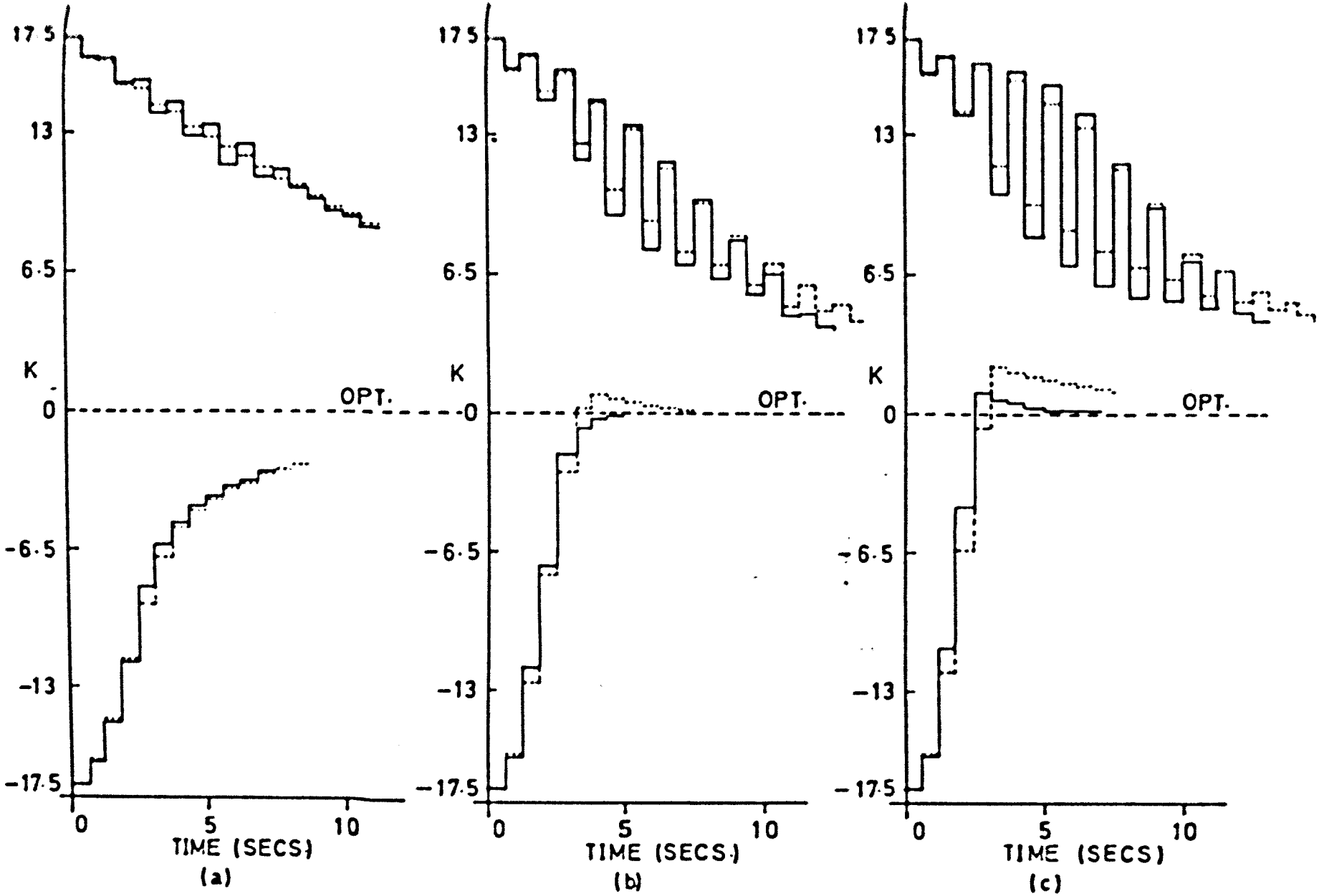

FIG. 19 RESPONSE OF THE SYSTEM WITH DISCONTINUOUS ADJUSTMENT

(a) RELATIVE LOOP GAIN = 3·34
(b) RELATIVE LOOP GAIN = 4·65
(c) RELATIVE LOOP GAIN = 5·20

—— PRACTICAL

----- THEORETICAL

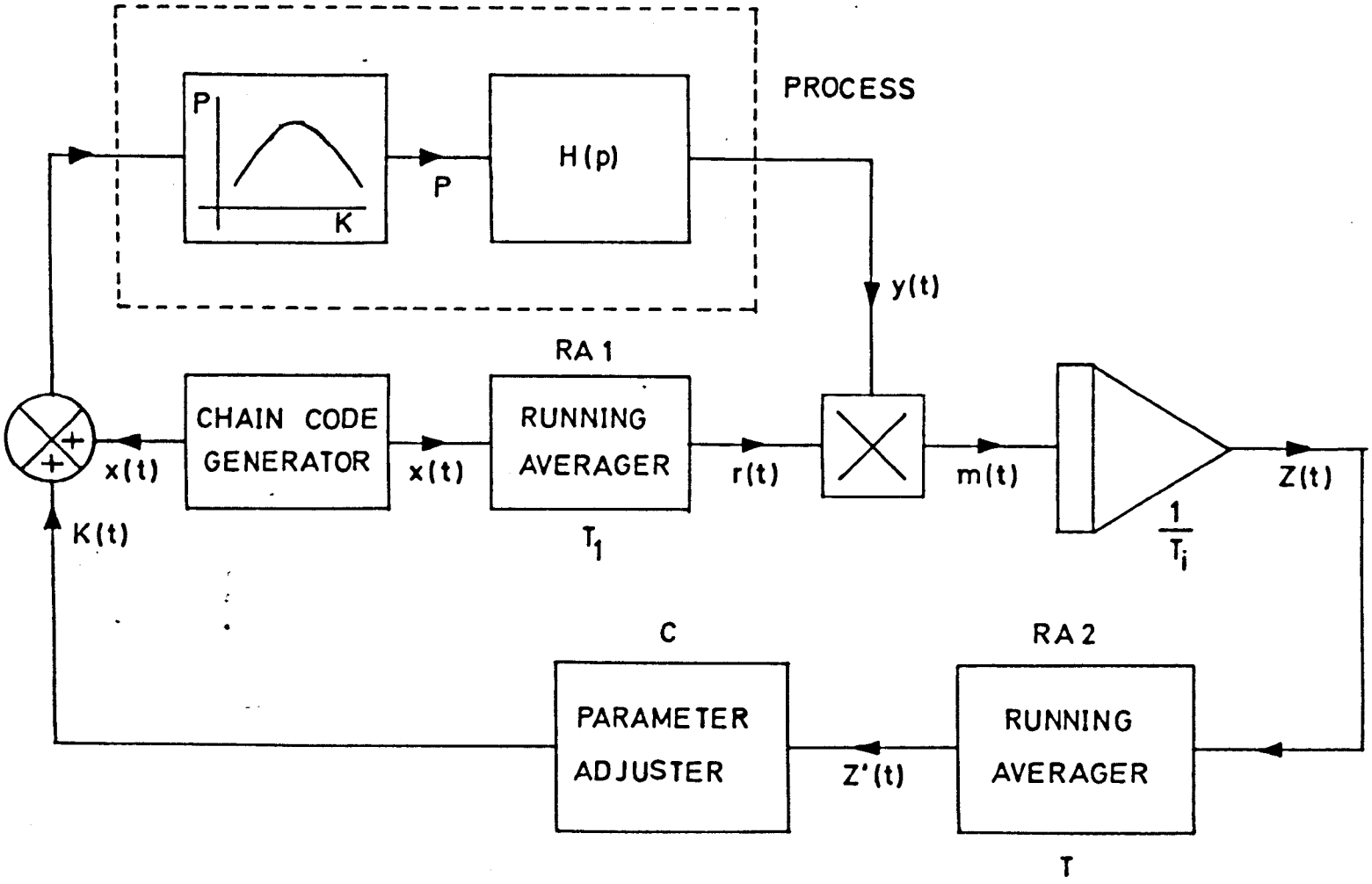

FIG. 20 BLOCK DIAGRAM OF THE SYSTEM WITH CONTINUOUS PARAMETER ADJUSTMENT

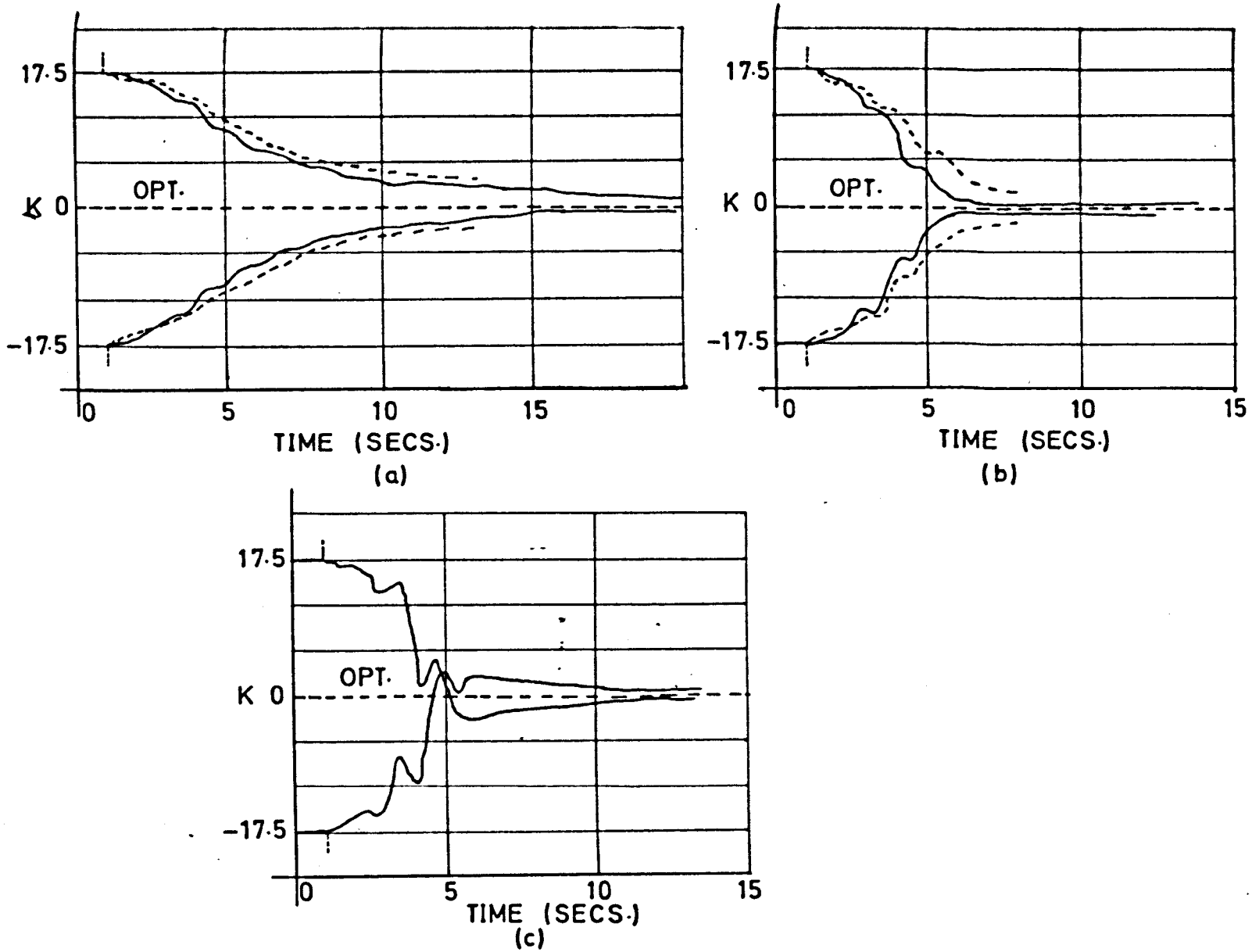

FIG. 21 RESPONSE OF THE SYSTEM WITH CONTINUOUS ADJUSTMENT

(a) RELATIVE LOOP GAIN = 3·34 —— PRACTICAL

(b) RELATIVE LOOP GAIN = 4·65 ---- THEORETICAL

(c) RELATIVE LOOP GAIN = 5·20

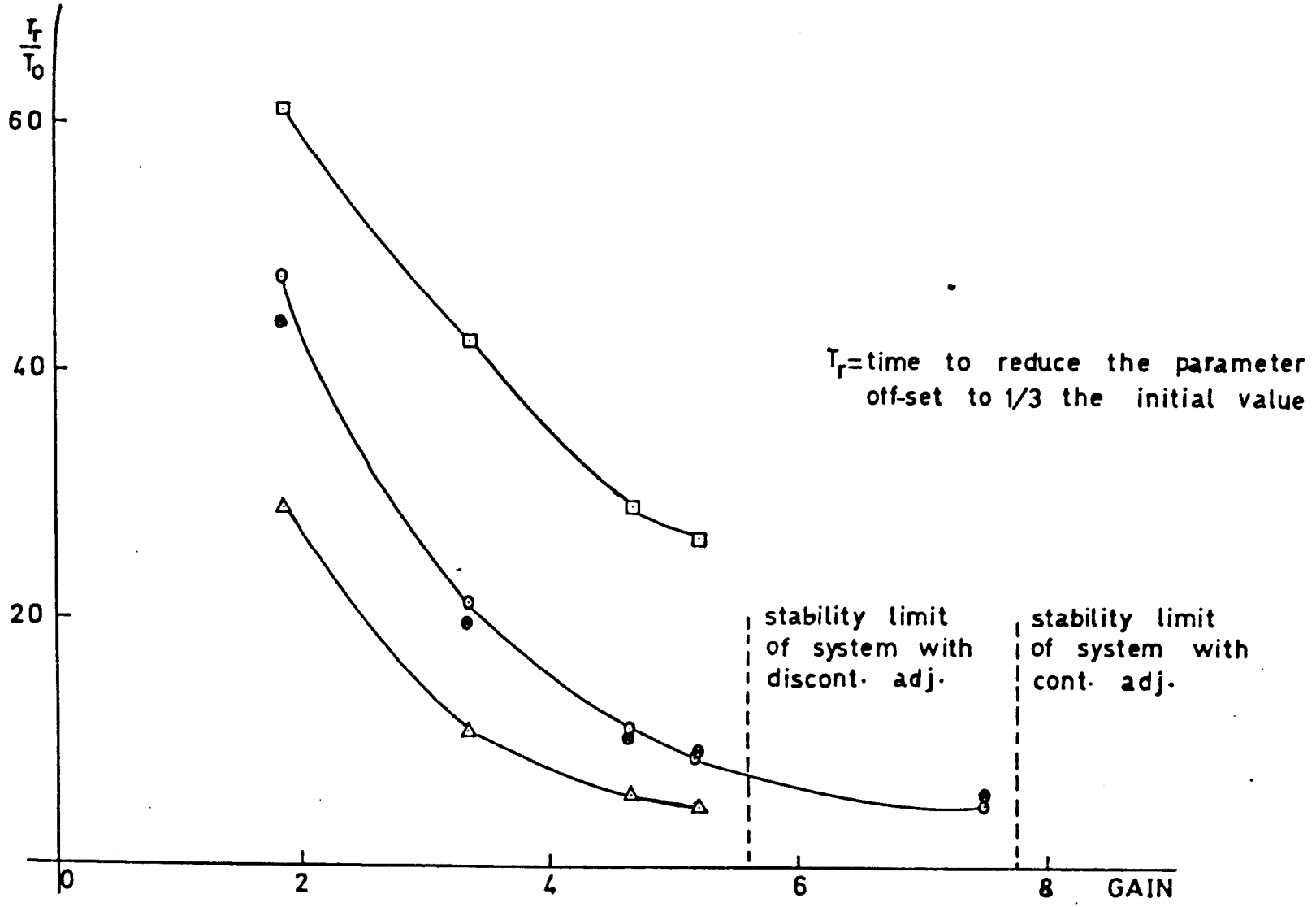

FIG. 22 PLOT OF RESPONSE TIME VS LOOP GAIN

—□— DISCONT. ADJUSTMENT (FROM +VE SIDE)

—△— DISCONT. ADJUSTMENT (FROM —VE SIDE)

—○— CONT. ADJUSTMENT (FROM +VE SIDE)

⊗ CONT. ADJUSTMENT (FROM —VE SIDE)

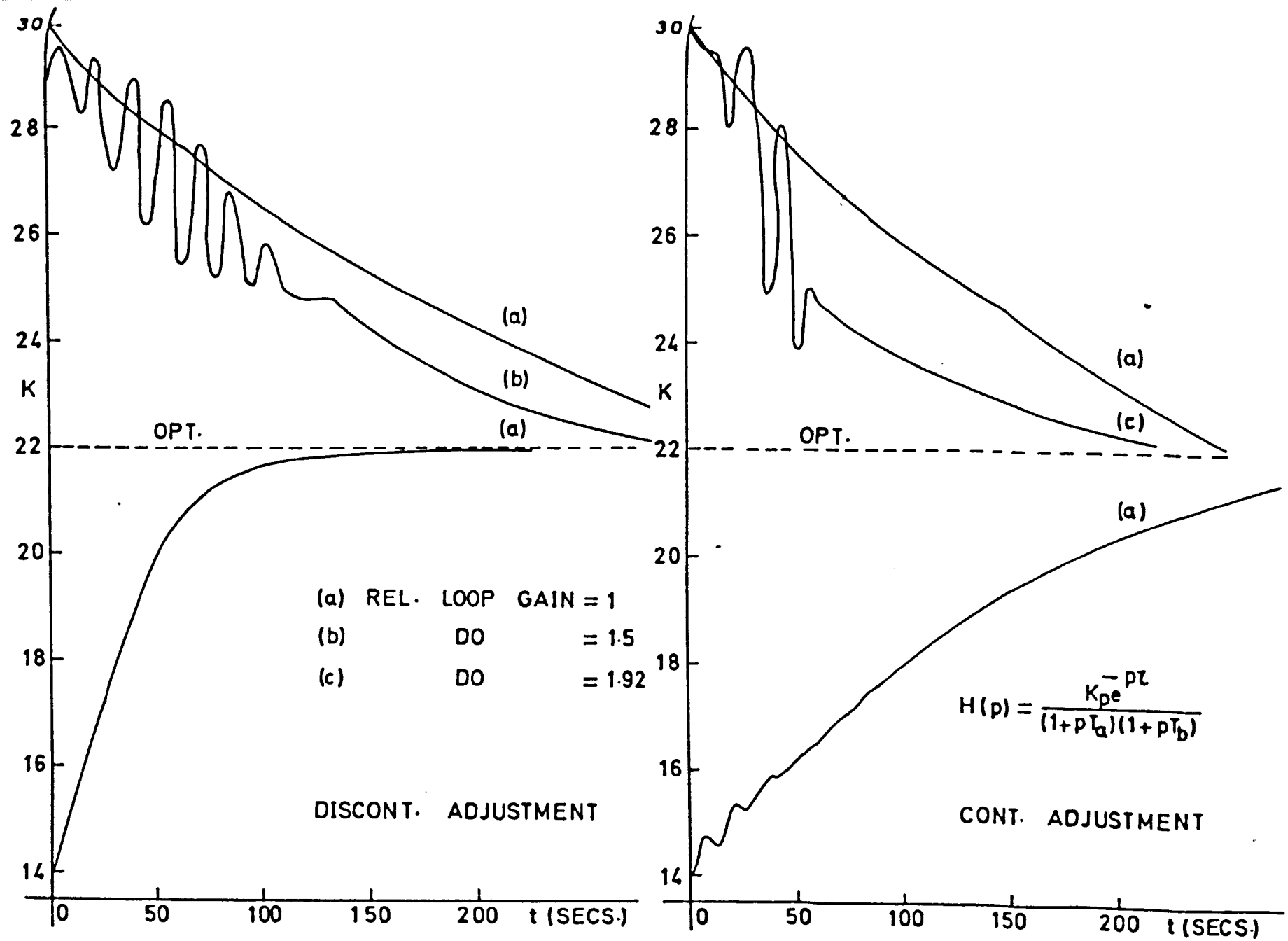

FIG. 23 RESPONSE OF THE SYSTEM WITH THE PLANT H(p)

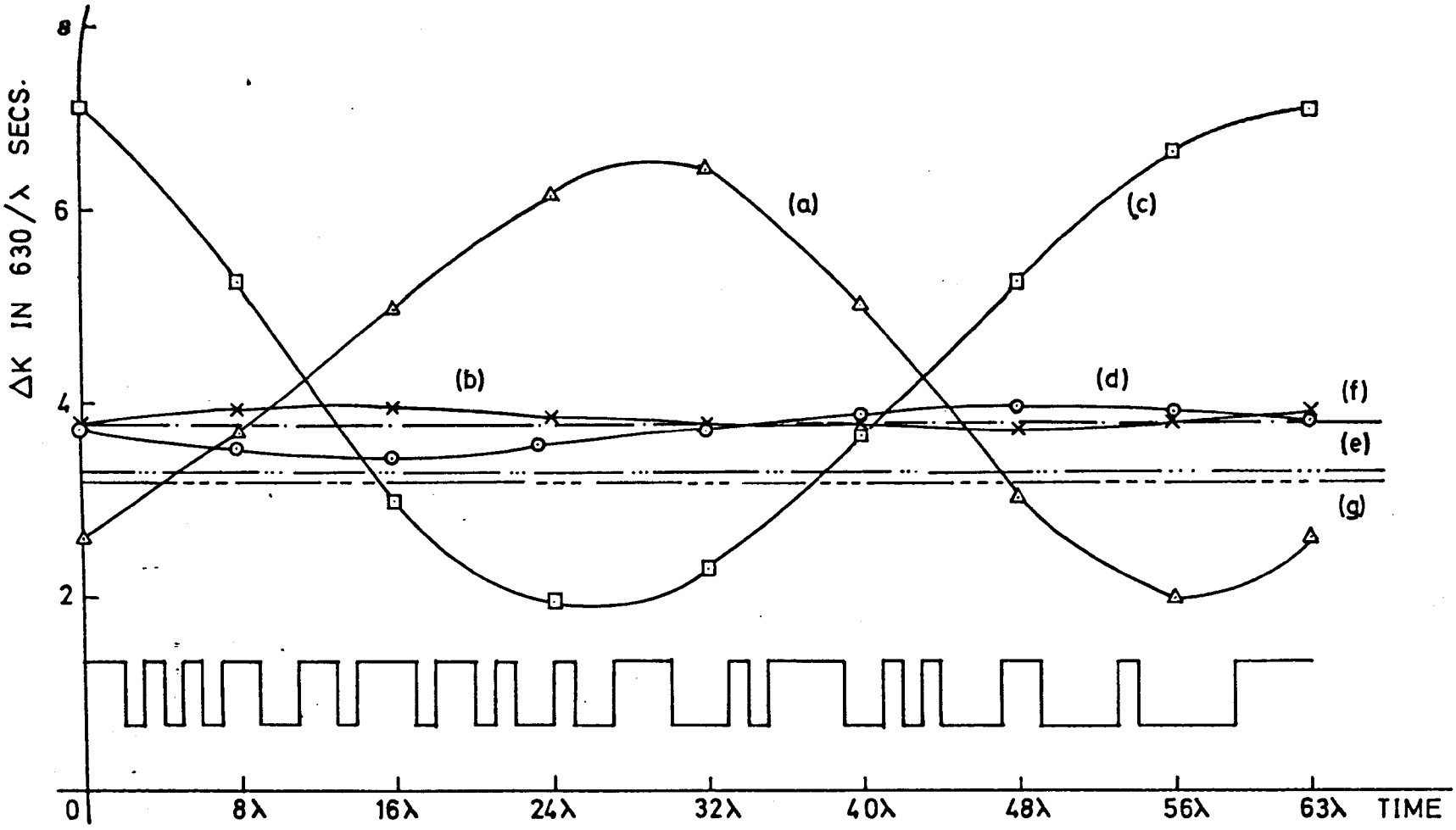

FIG. 24 SPEED OF RESPONSE VS STARTING POINT

DISCONTINUOUS ADJUSTMENT

(a) $K_{initial} > K_{opt.}$ without dynamic compensation

(b) do with dynamic compensation

(c) $K_{initial} < K_{opt.}$ without dynamic compensation

(d) do with dynamic compensation

$\lambda = 0.125$ sec.

CONTINUOUS ADJUSTMENT

(e) $K_{initial} > K_{opt.}$ without dynamic comp.

(f) do with dynamic comp.

(g) $K_{initial} < K_{opt.}$ without dynamic comp.

(h) do with dynamic comp-

(h) is same as (f)

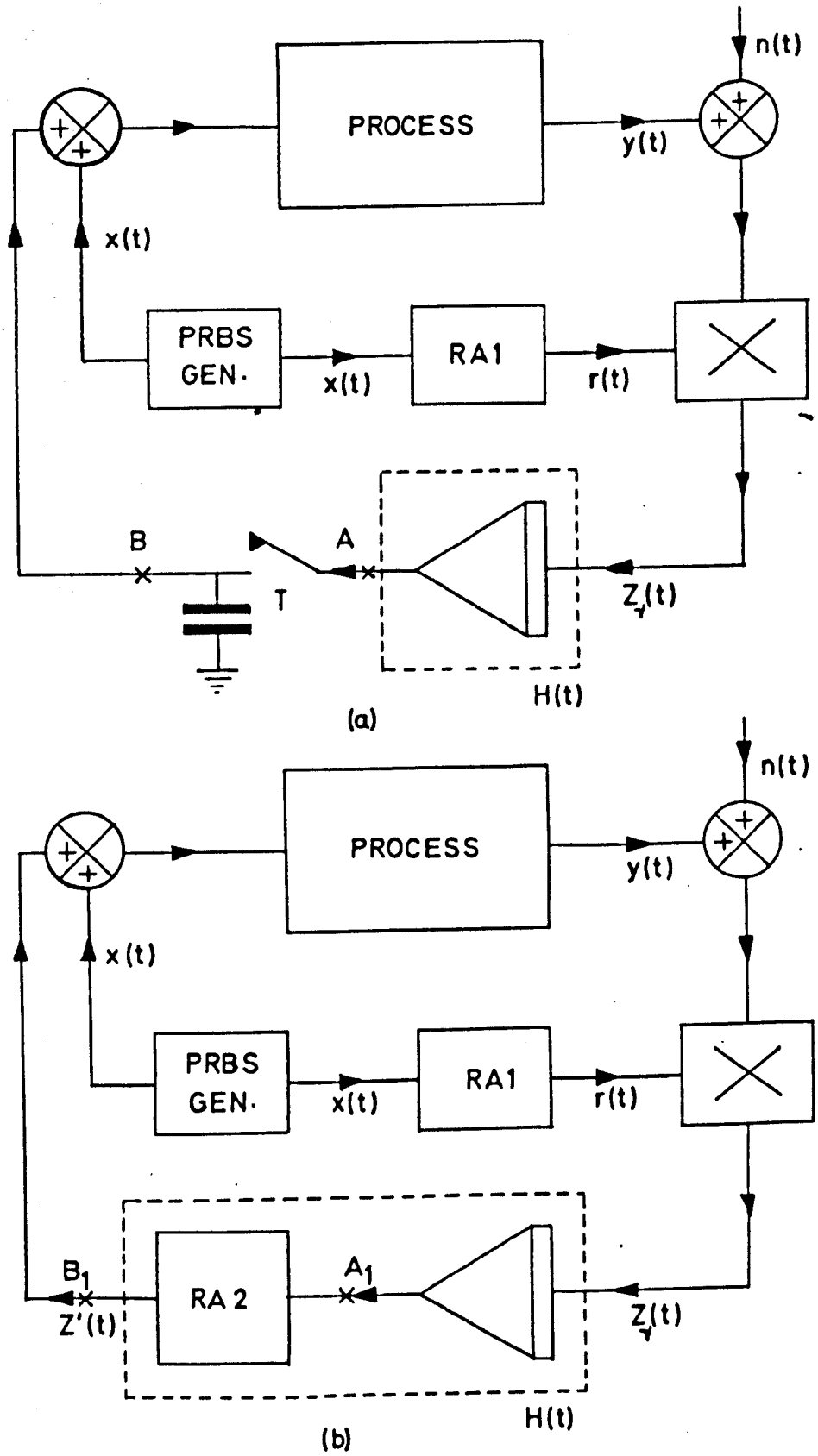

FIG. 25 SCHEMATIC DIAGRAM OF THE SYSTEM WITH OUTPUT NOISE

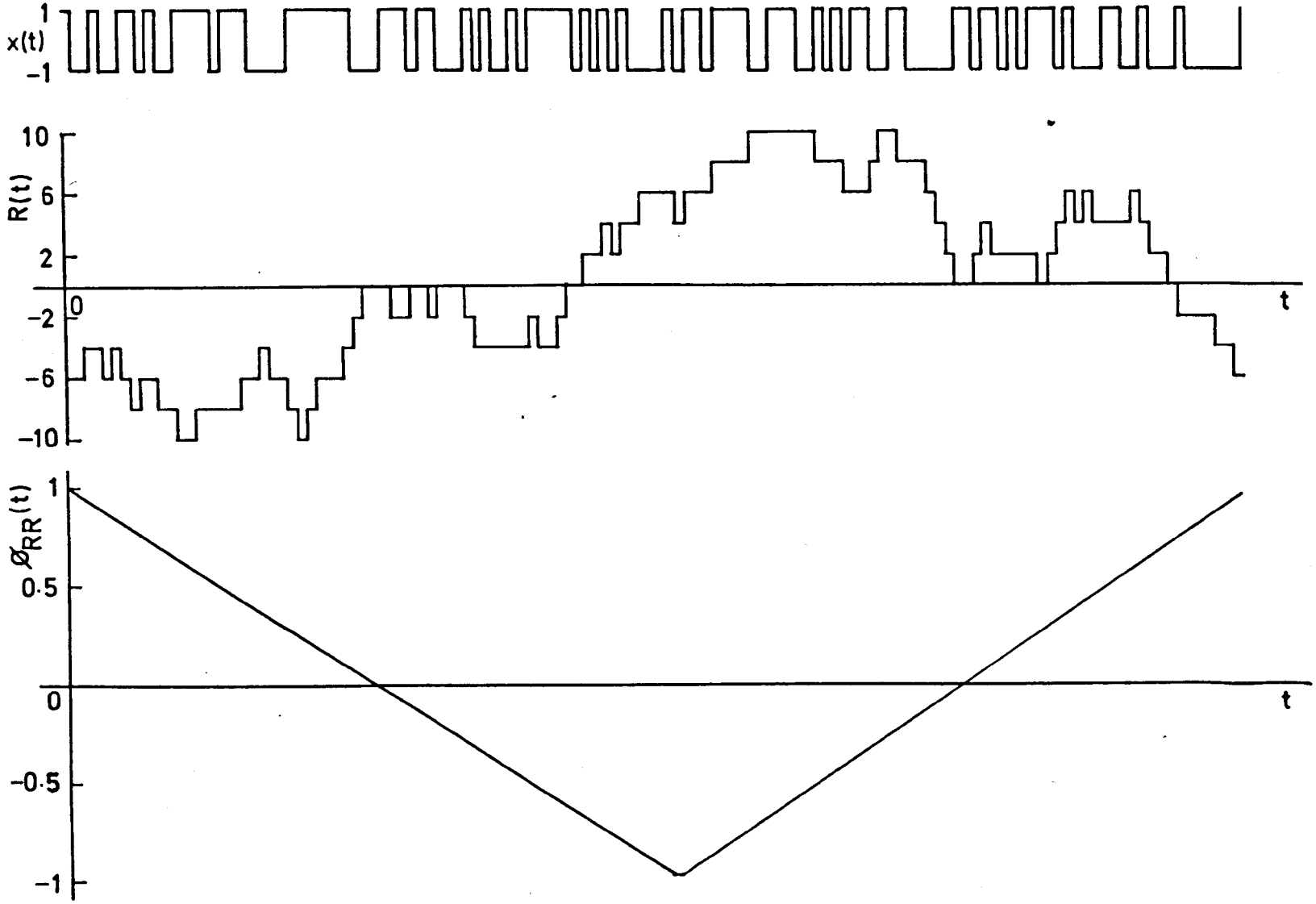

FIG. 26 AUTOCORRELATION FUNCTION OF THE RUNNING AVERAGE

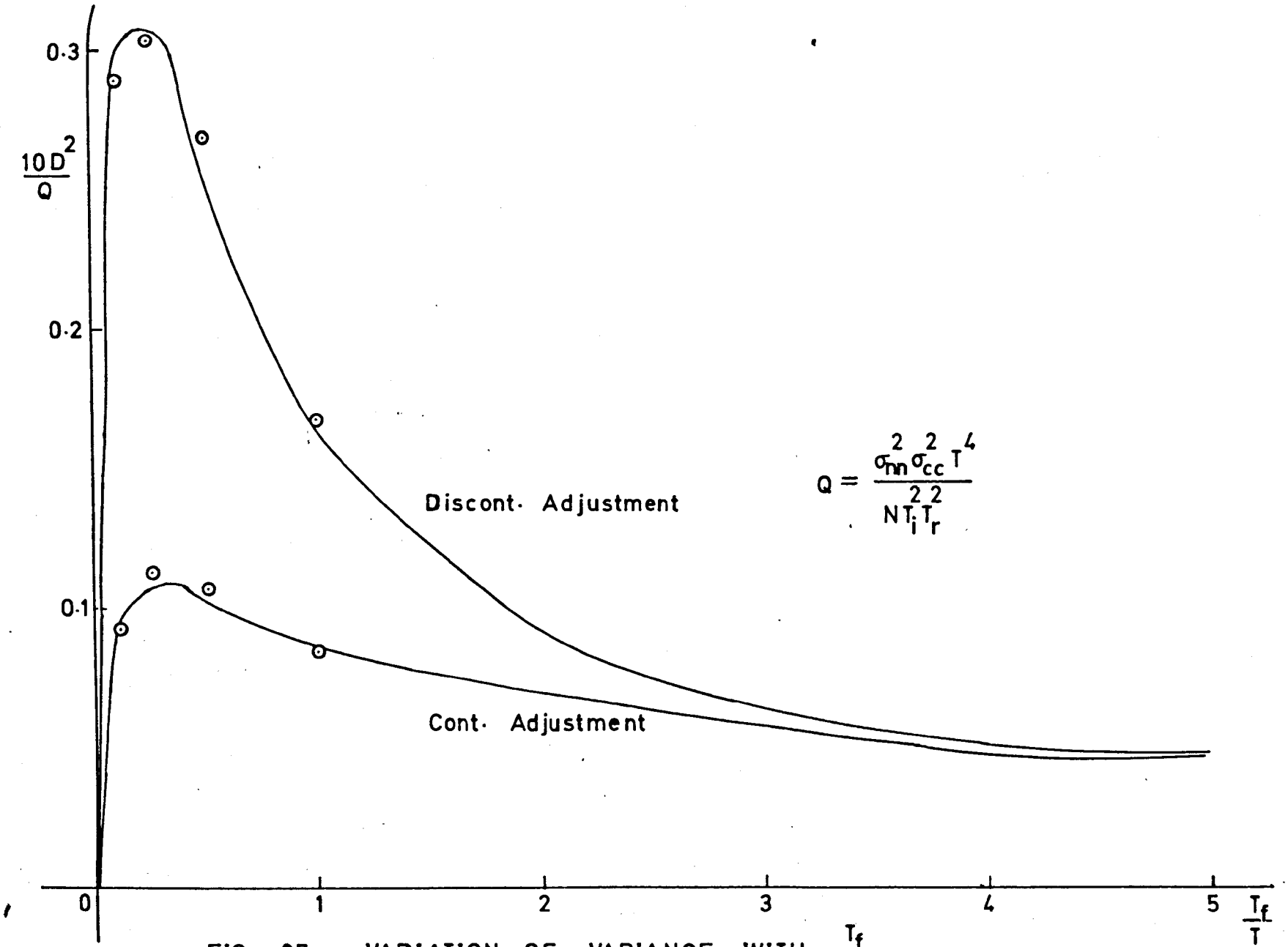

FIG. 27 VARIATION OF VARIANCE WITH $\frac{T_f}{T}$
⊙ PRACTICAL POINTS

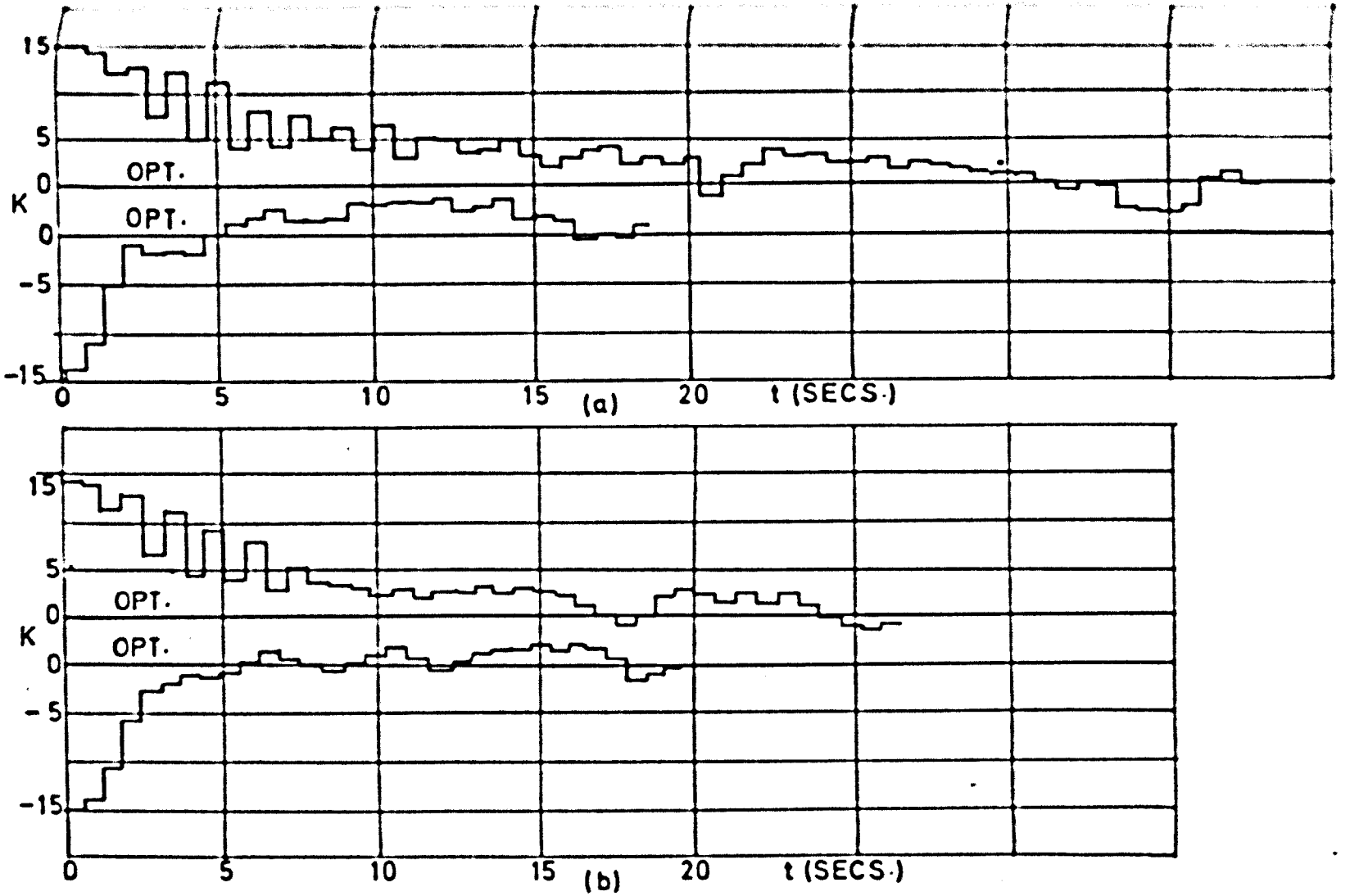

FIG. 28 RESPONSE OF THE SYSTEM WITH OUTPUT NOISE DISCONTINUOUS ADJUSTMENT

(a) Relative Loop Gain = 4·65; Initial $\frac{\text{Noise}}{\text{Signal}}$ Ratio = $\frac{1}{23}$

(b) do do = $\frac{1.83}{100}$

$T_1/T = 0.63$

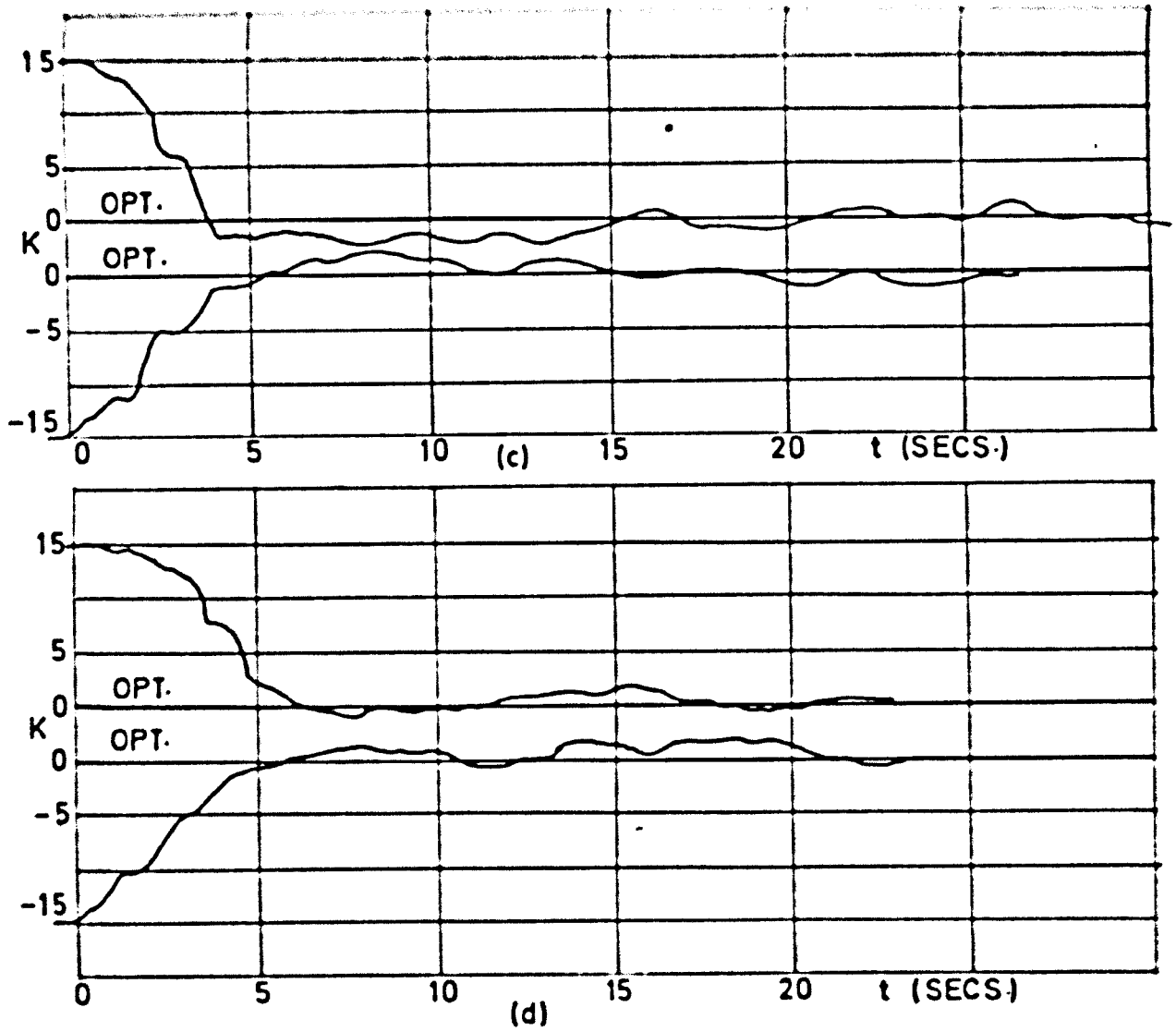

FIG. 28 RESPONSE OF THE SYSTEM WITH OUTPUT NOISE CONTINUOUS ADJUSTMENT

(c) Relative Loop Gain = 4.65 ; Initial $\frac{\text{Noise}}{\text{Signal}}$ Ratio $= \frac{1}{23}$

(d) do do $= \frac{1.83}{100}$

$T_f / T = 0.63$

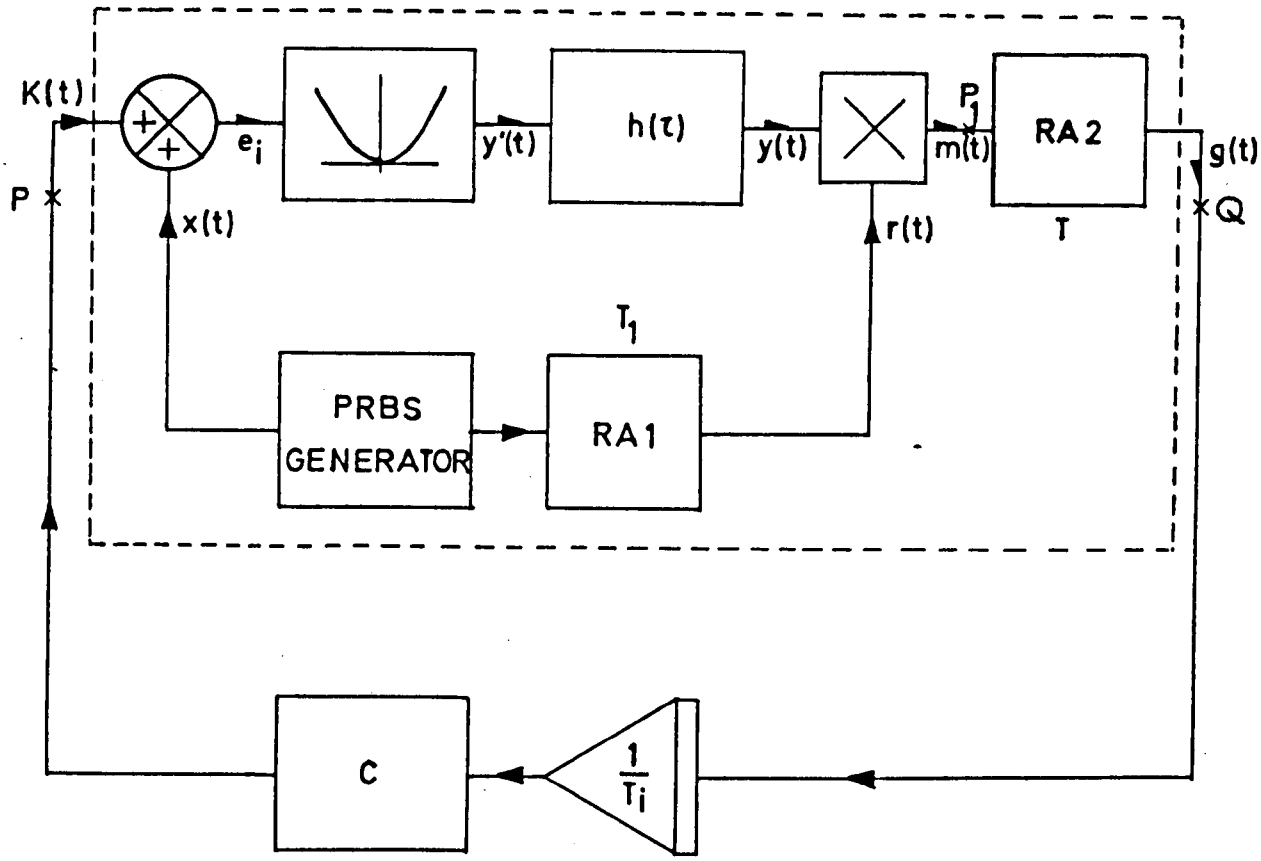

(a)

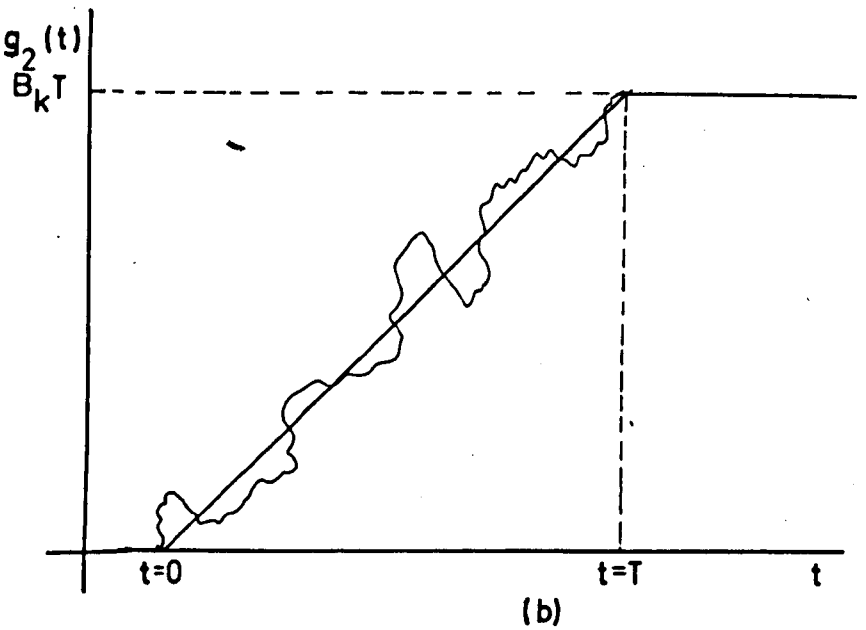

(b)

FIG. 29 STABILITY ANALYSIS OF THE SYSTEM WITH CONTINUOUS ADJUSTMENT

(a) THE BLOCK DIAGRAM (b) VARIATION OF $g_2(t)$

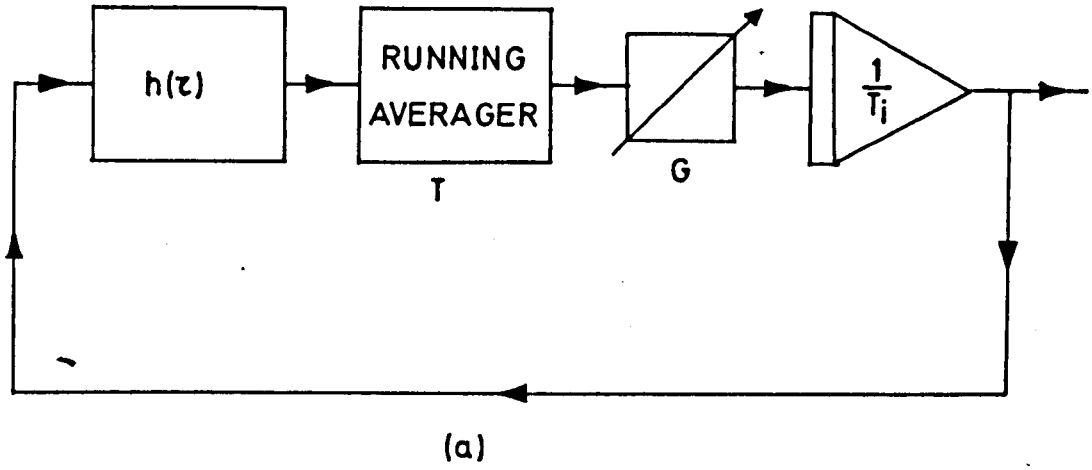

(a)

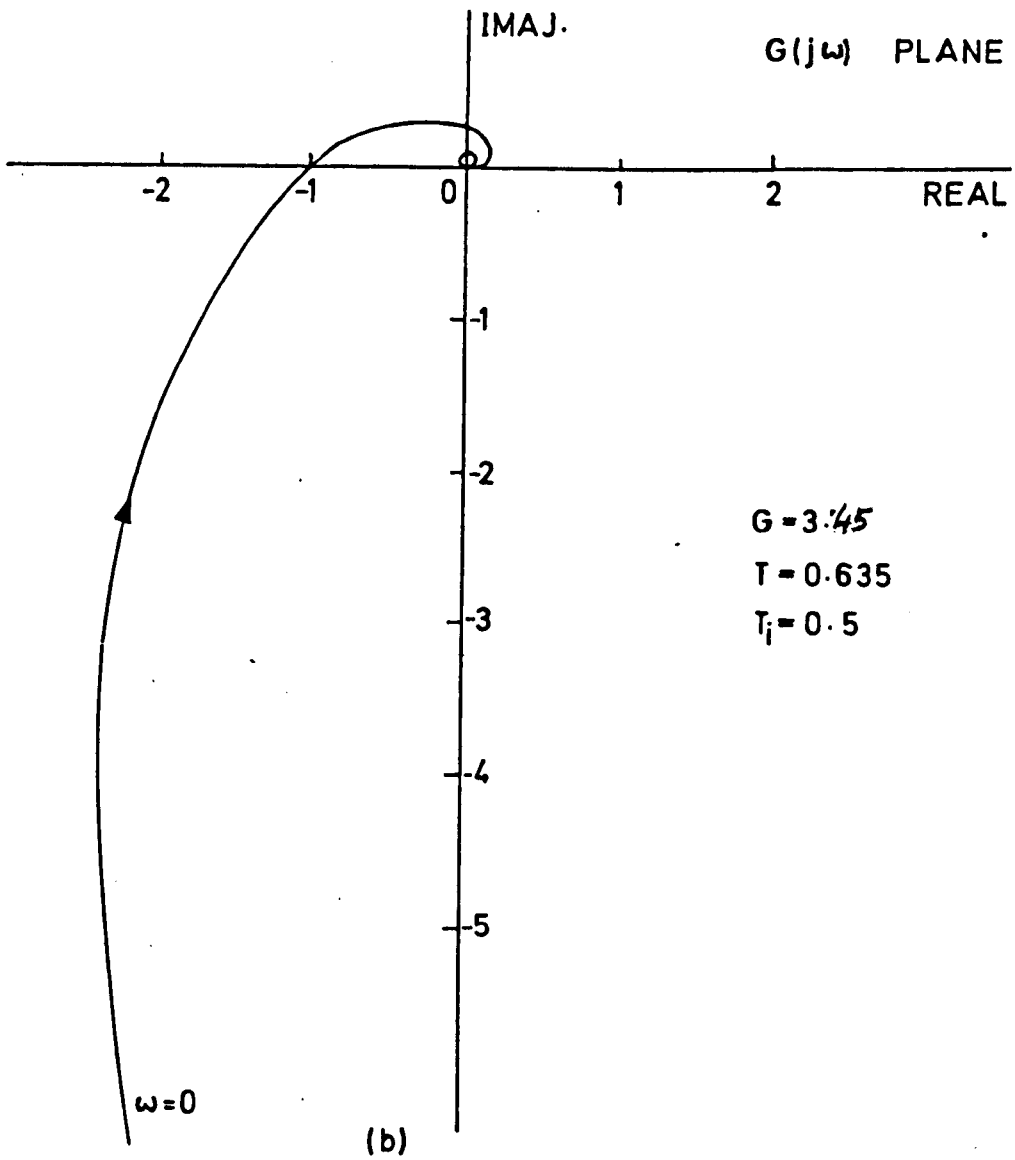

(b)

FIG. 30 STABILITY OF THE SYSTEM WITH CONTINUOUS ADJUSTMENT

(a) BLOCK DIAGRAM OF THE LINEARISED MODEL

(b) THE NYQUIST DIAGRAM

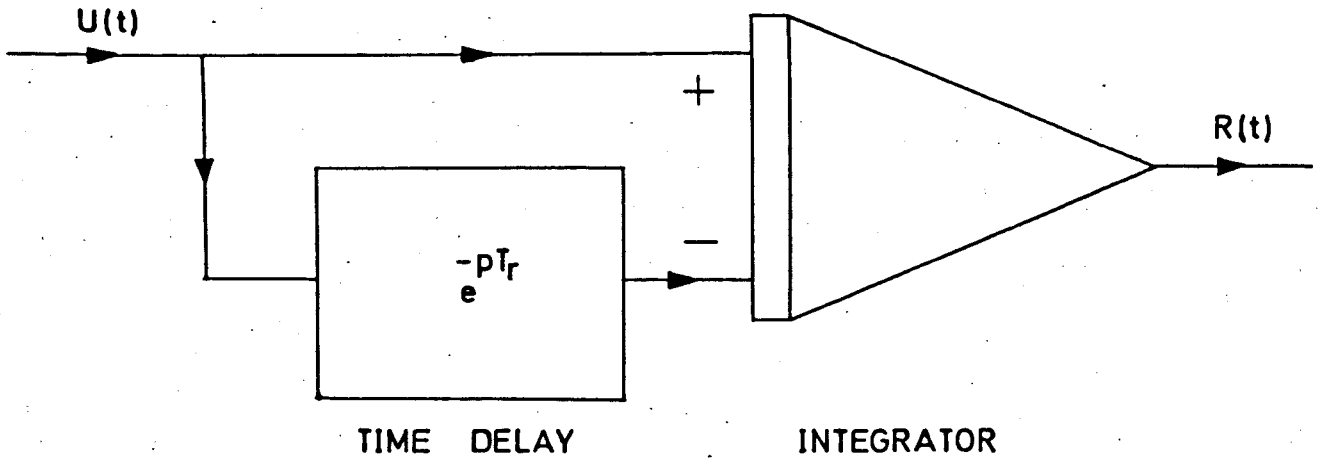

FIG. 31 ARRANGEMENT FOR THE GENERATION OF RUNNING AVERAGE

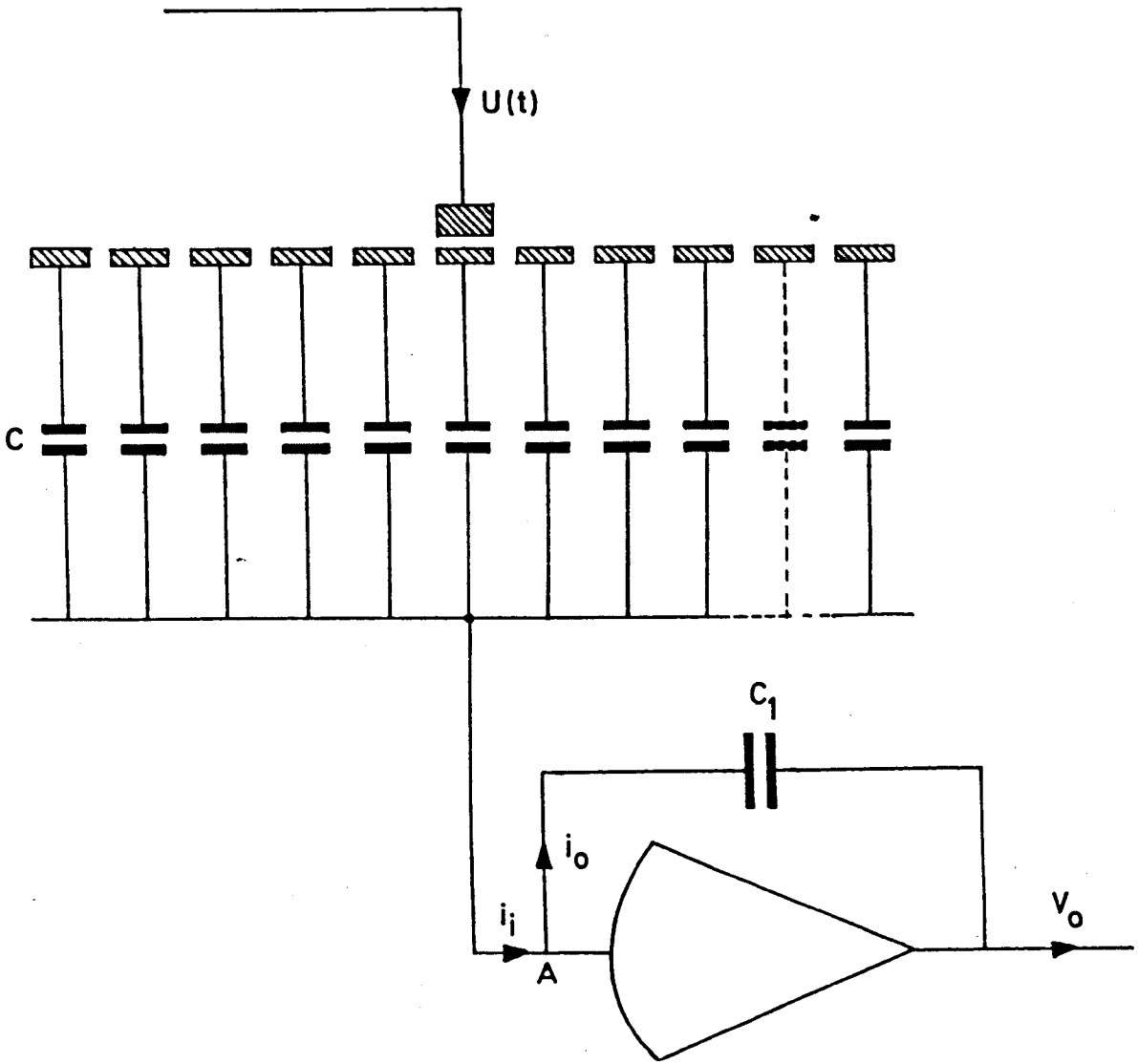

FIG. 32 PRINCIPLE OF THE ELECTRO-MECHANICAL RUNNING AVERAGER

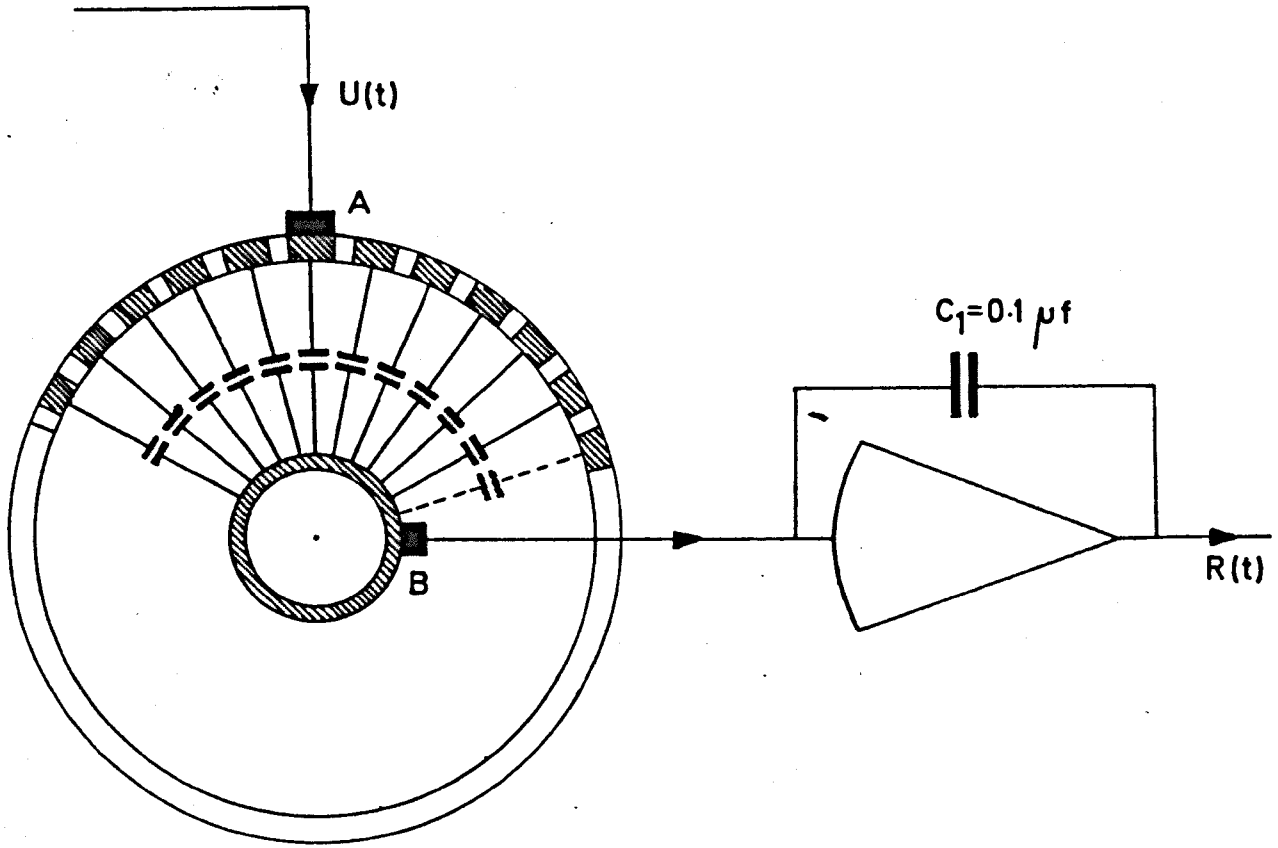

FIG. 33 PRACTICAL ARRANGEMENT OF THE RUNNING AVERAGER

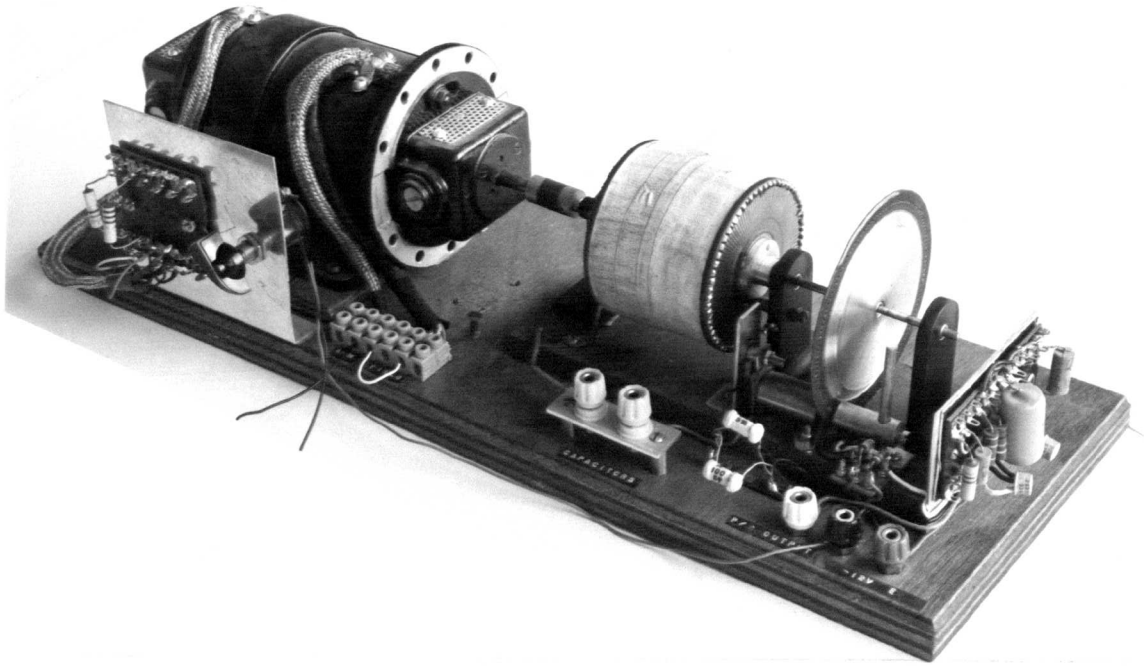

FIG. 34 PHOTOGRAPH OF THE ELECTRO-MECHANICAL RUNNING AVERAGER

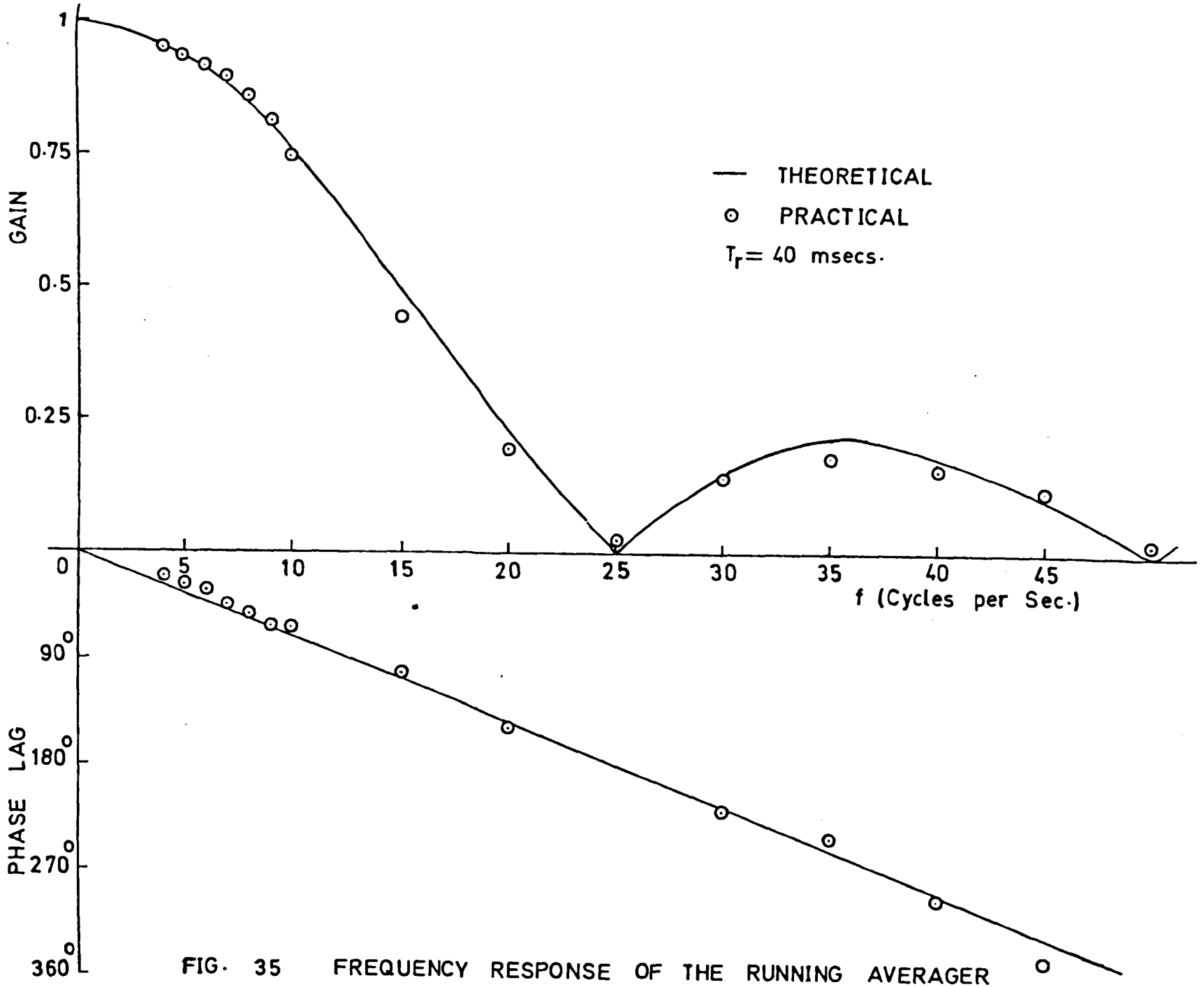

FIG. 35 FREQUENCY RESPONSE OF THE RUNNING AVERAGER

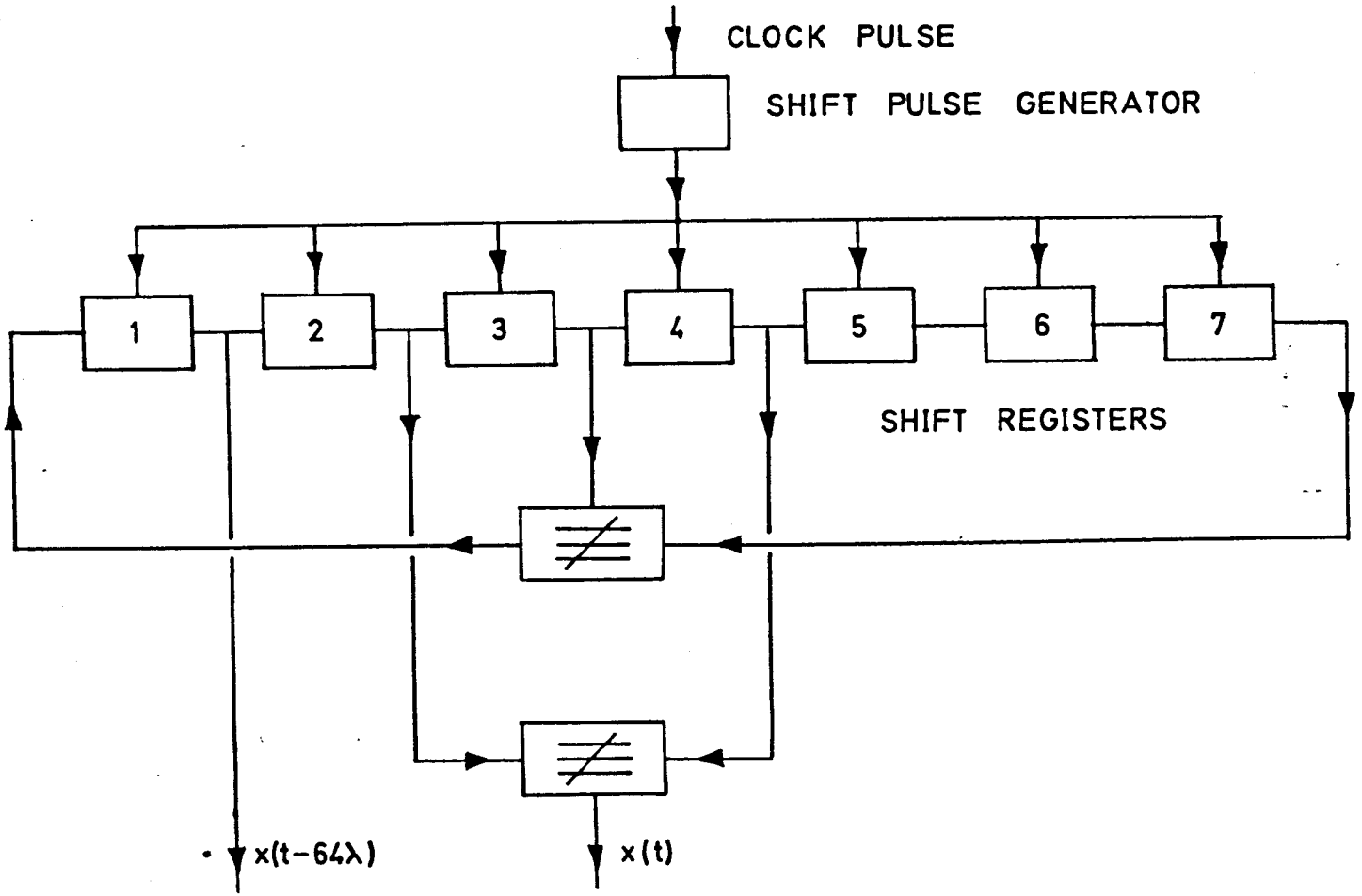

FIG. 36 GENERATION OF PRBS AND ITS DELAYED VERSION

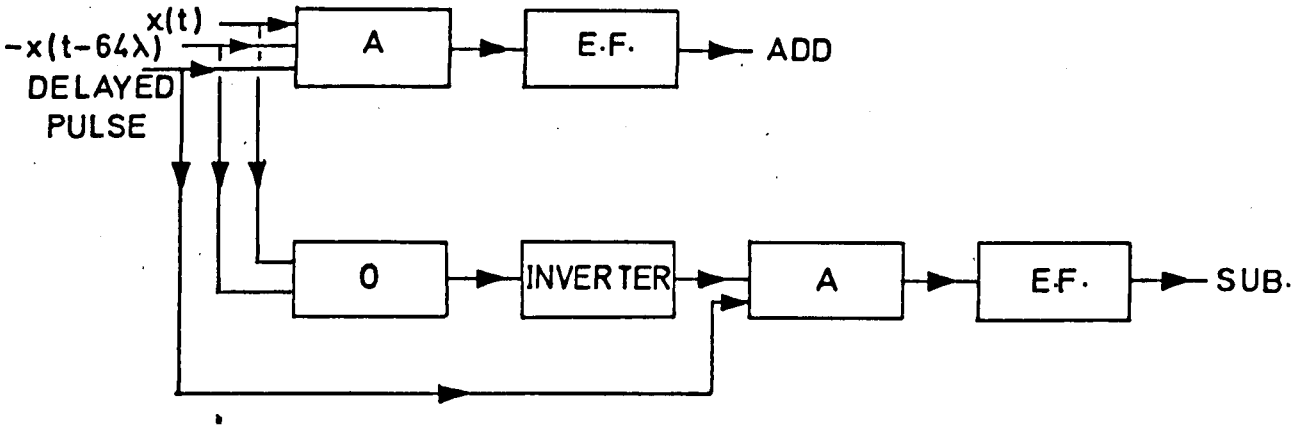

(a)

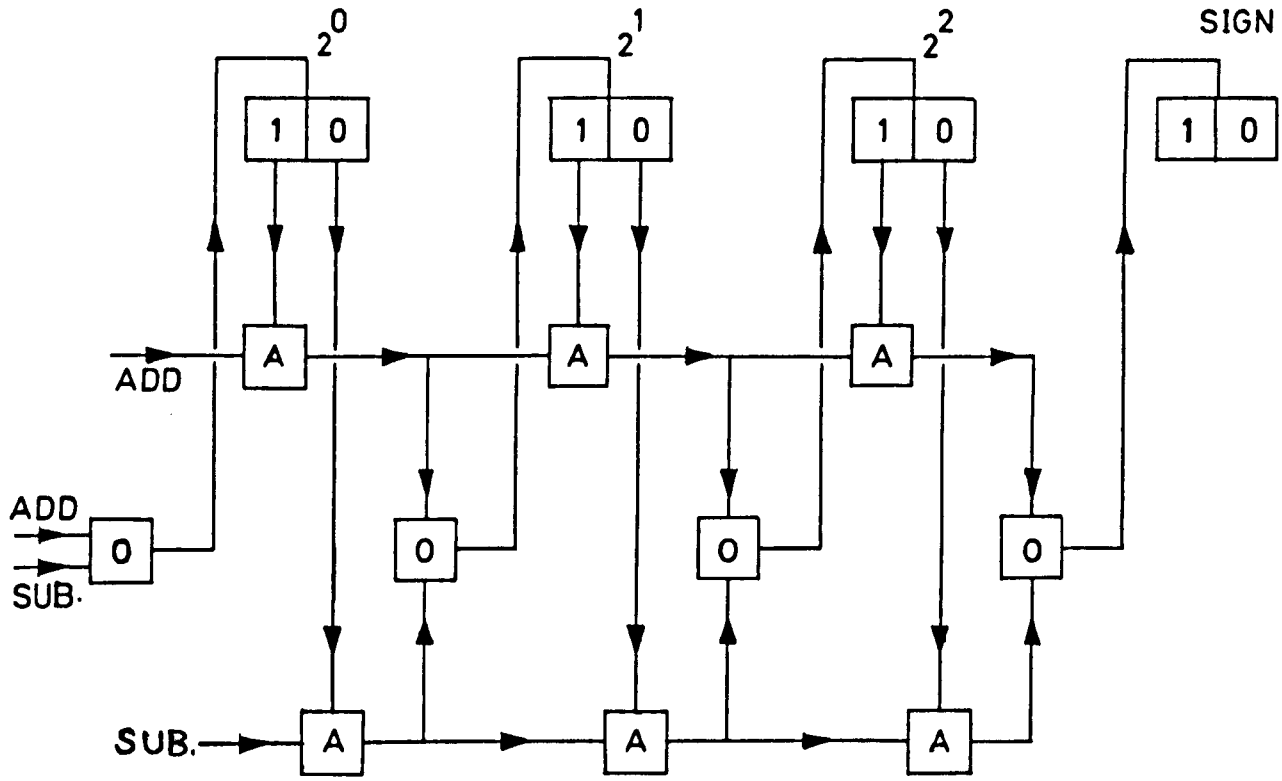

A—AND gate 0—OR gate E.F.—Emitter Follower

FIG. 37 RUNNING AVERAGER

(a) GENERATION OF ADD AND SUBTRACT PULSES

(b) FLOW DIAGRAM OF THE BINARY COUNTER

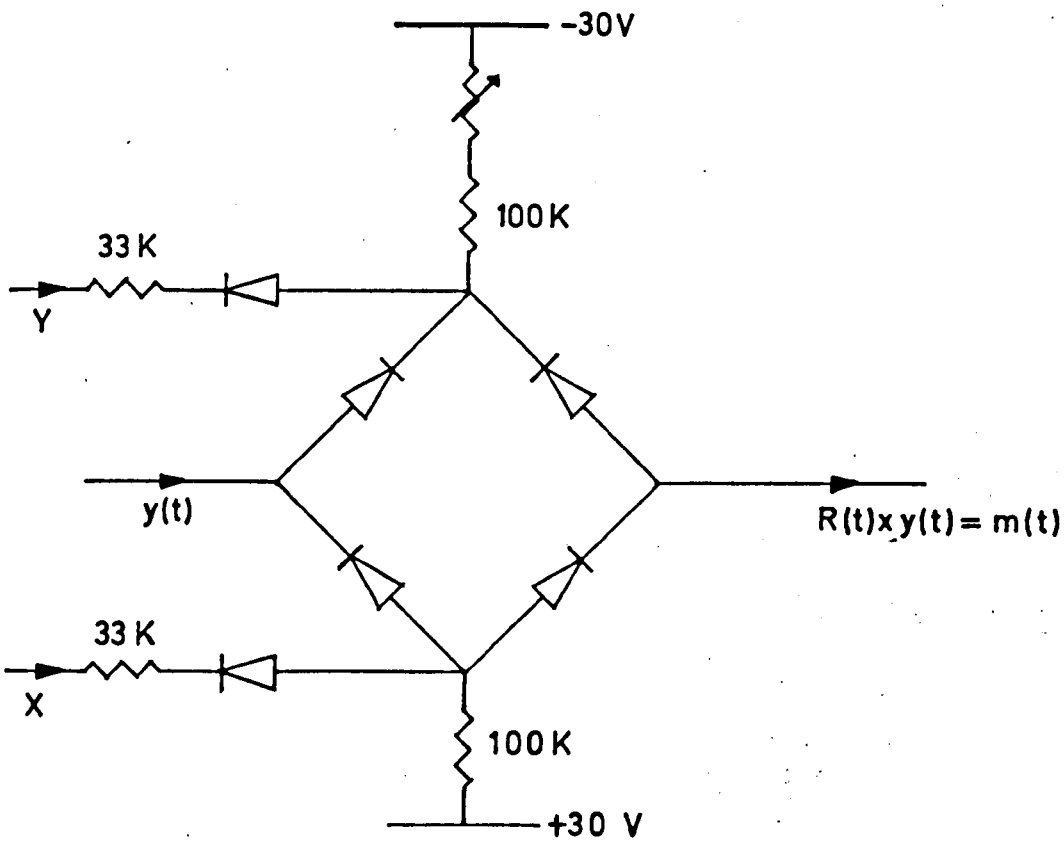

(a)

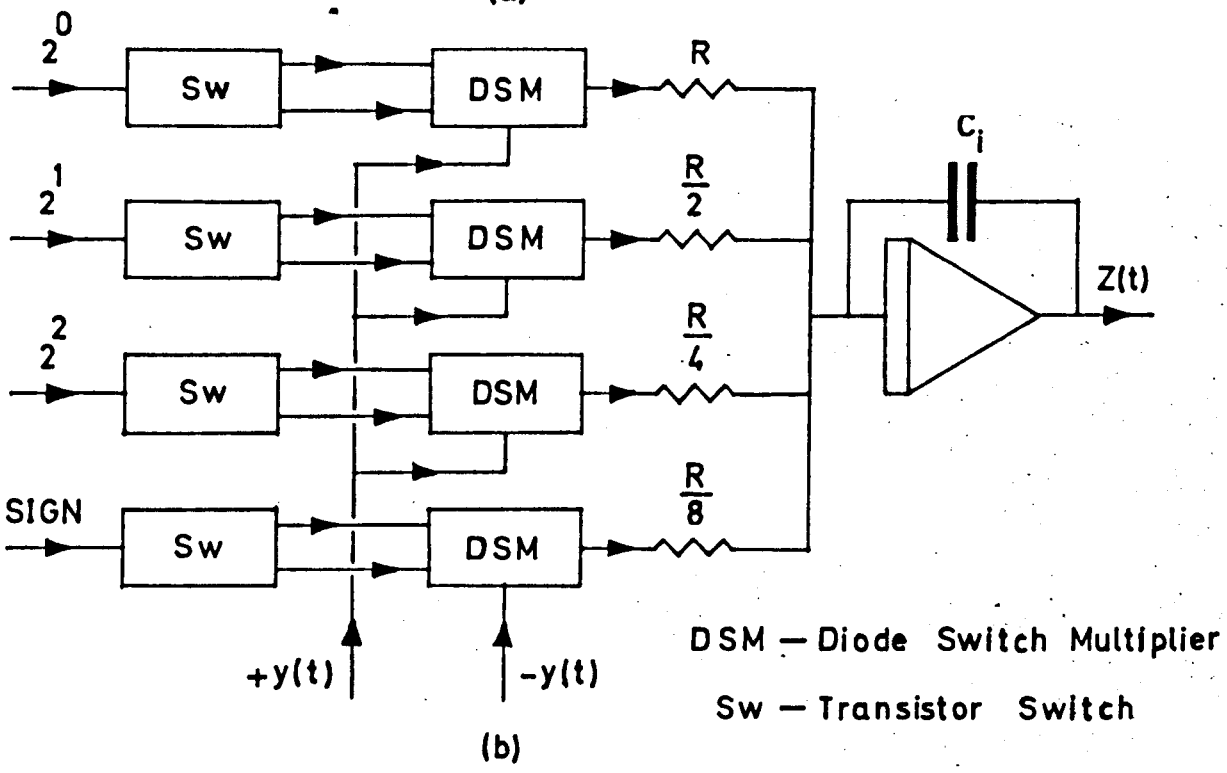

(b)

FIG. 38

(a) THE HYBRID DIODE SWITCH MULTIPLIER

(b) COMPLETE MECHANISATION FOR THE MEASUREMENT OF SLOPE

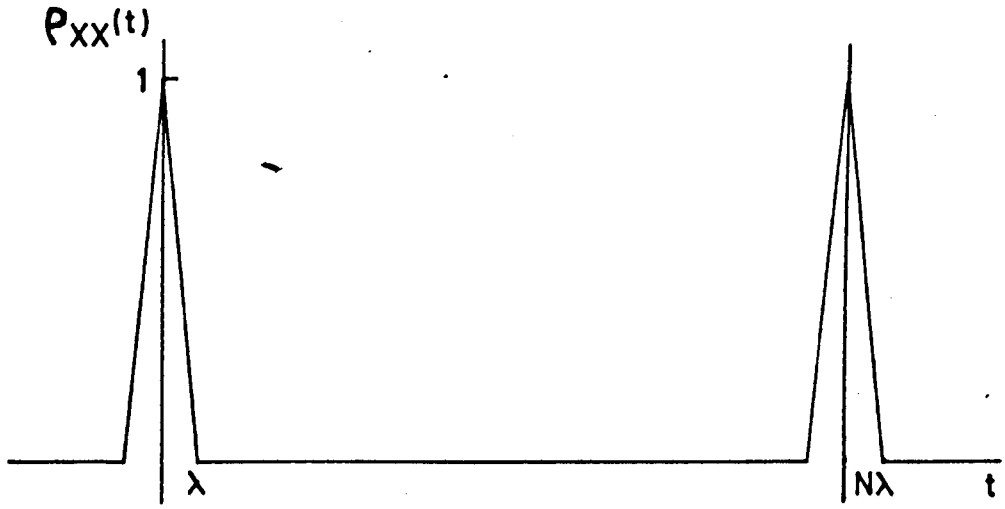

(a)

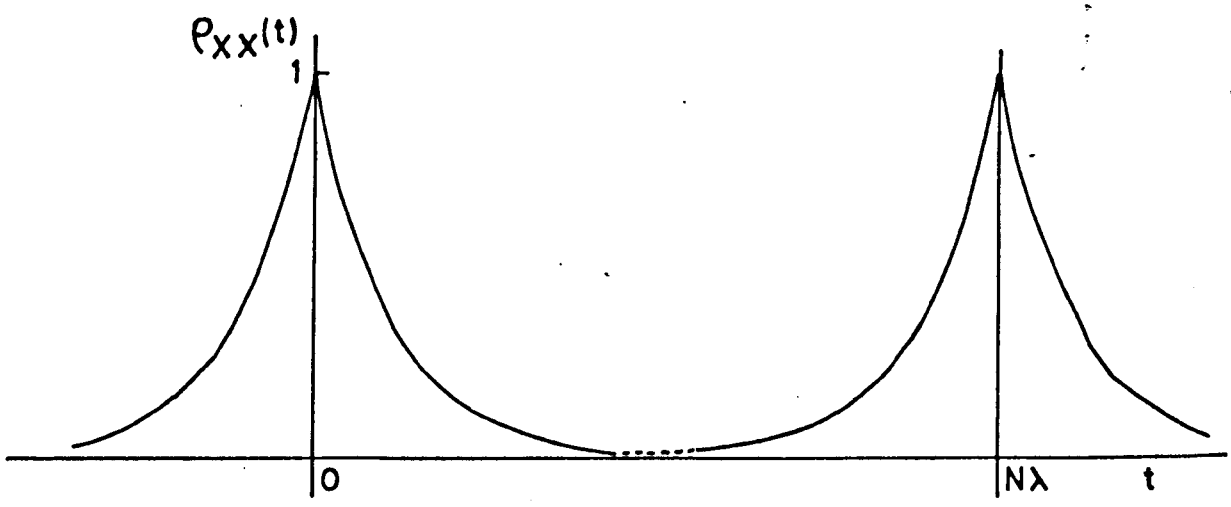

(b)

FIG. 39 DESIRED FORMS OF AUTOCORRELATION FUNCTION FOR THE TWO-LEVEL SEQUENCE

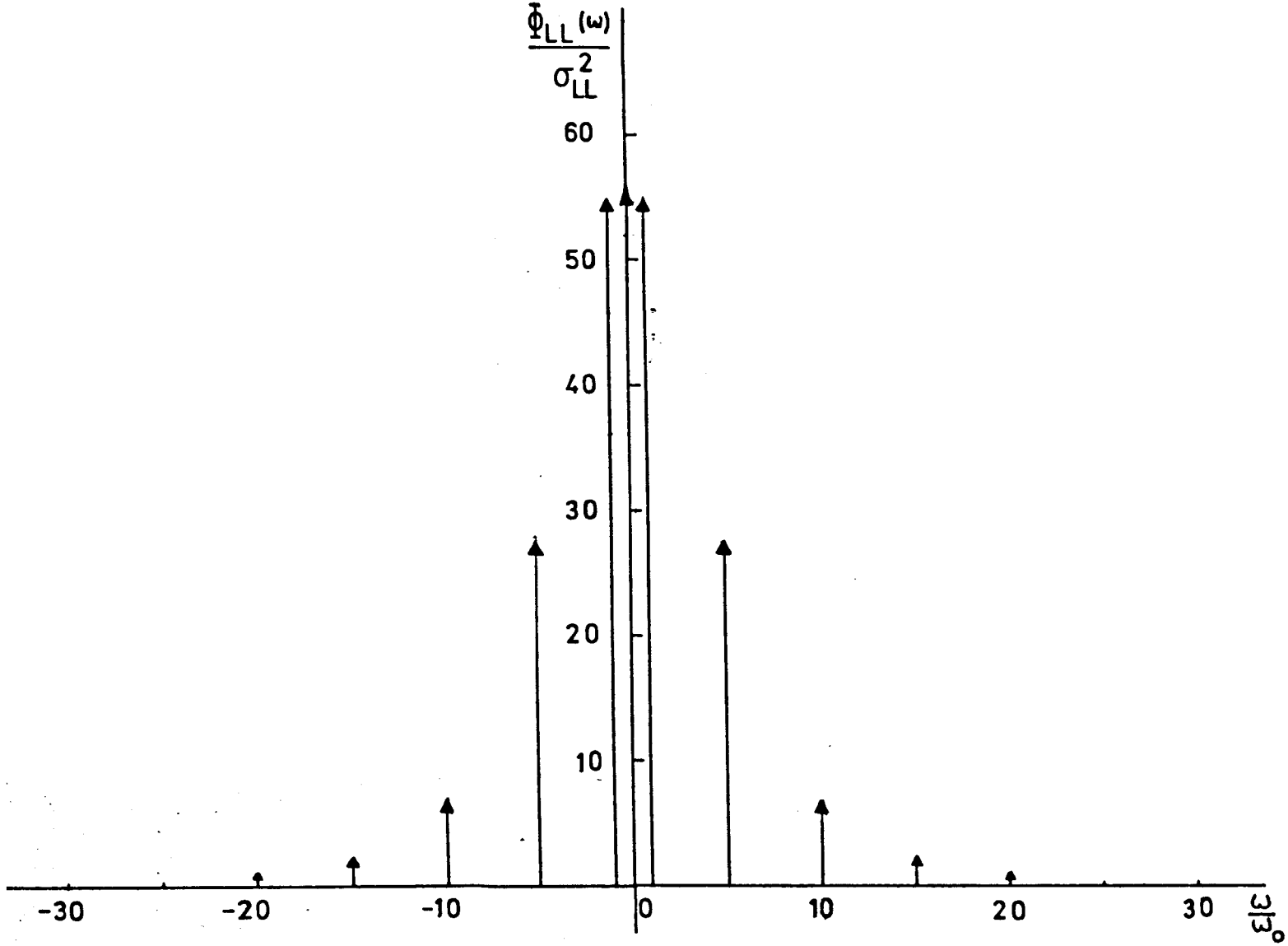

FIG. 40 POWER SPECTRUM OF THE INPUT SIGNAL TO THE NON-LINEARITY (N=31)

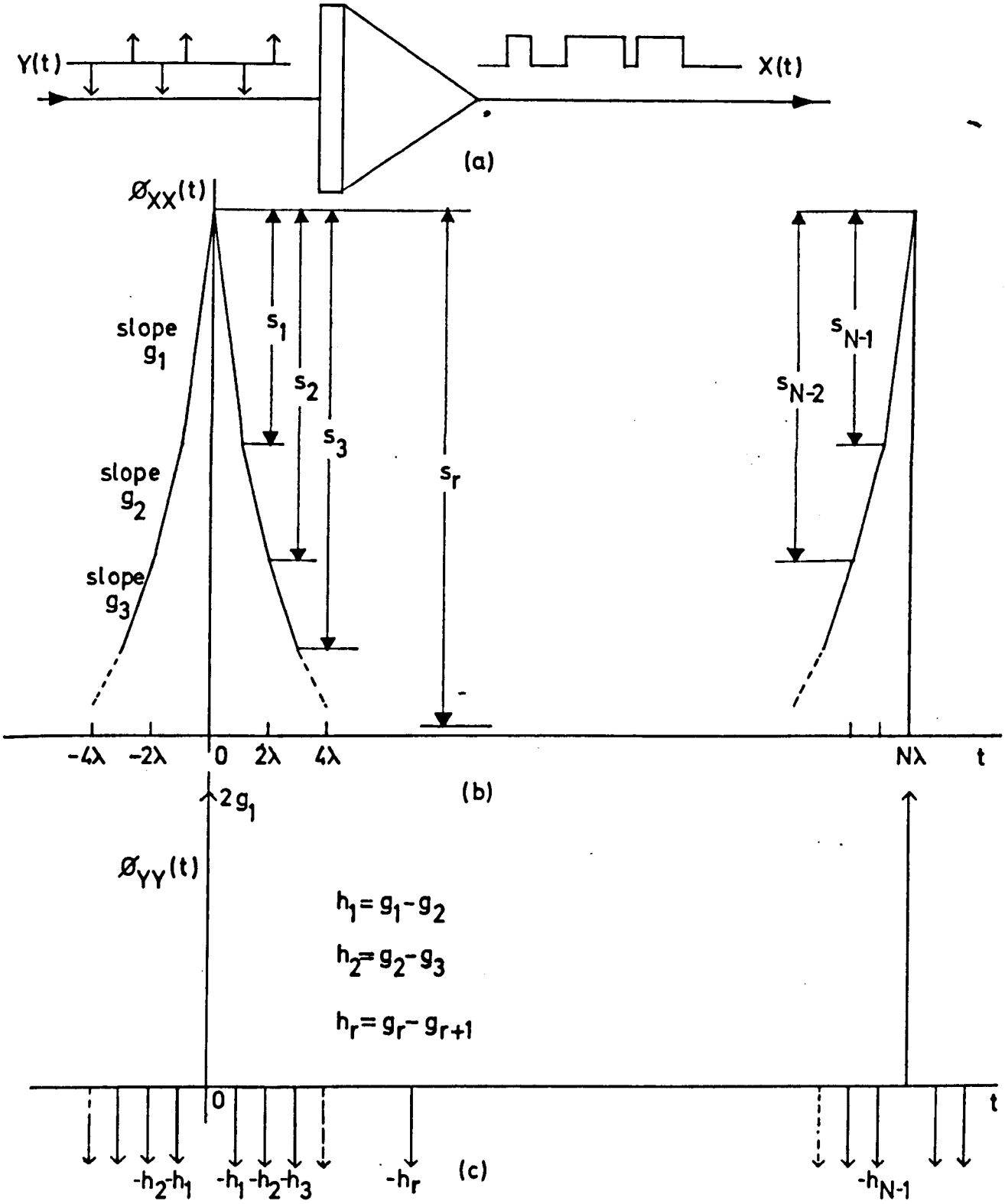

FIG. 41 SYNTHESIS OF NEW SEQUENCES

(a) GENERAL ARRANGEMENT FOR GENERATION

(b) FORM OF THE OUTPUT AUTOCORRELATION FUNCTION

(c) CORRESPONDING INPUT AUTOCORRELATION FUNCTION

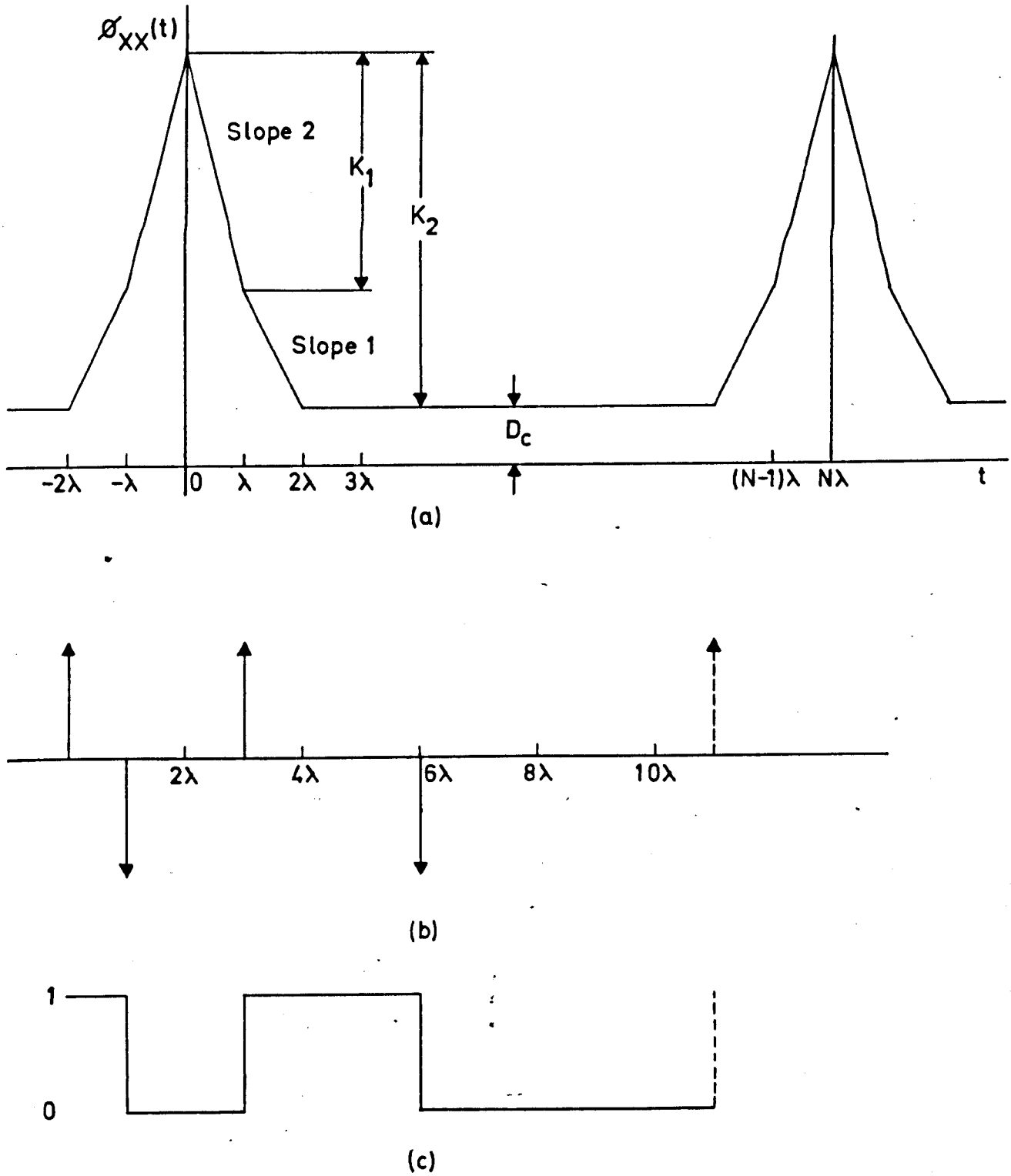

FIG. 42 SYNTHESIS OF BINARY SEQUENCE OF EXAMPLE 1

(a) DESIRED AUTOCORRELATION FUNCTION

(b) THE GENERATING IMPULSE TRAIN

(c) THE TWO-LEVEL SEQUENCE

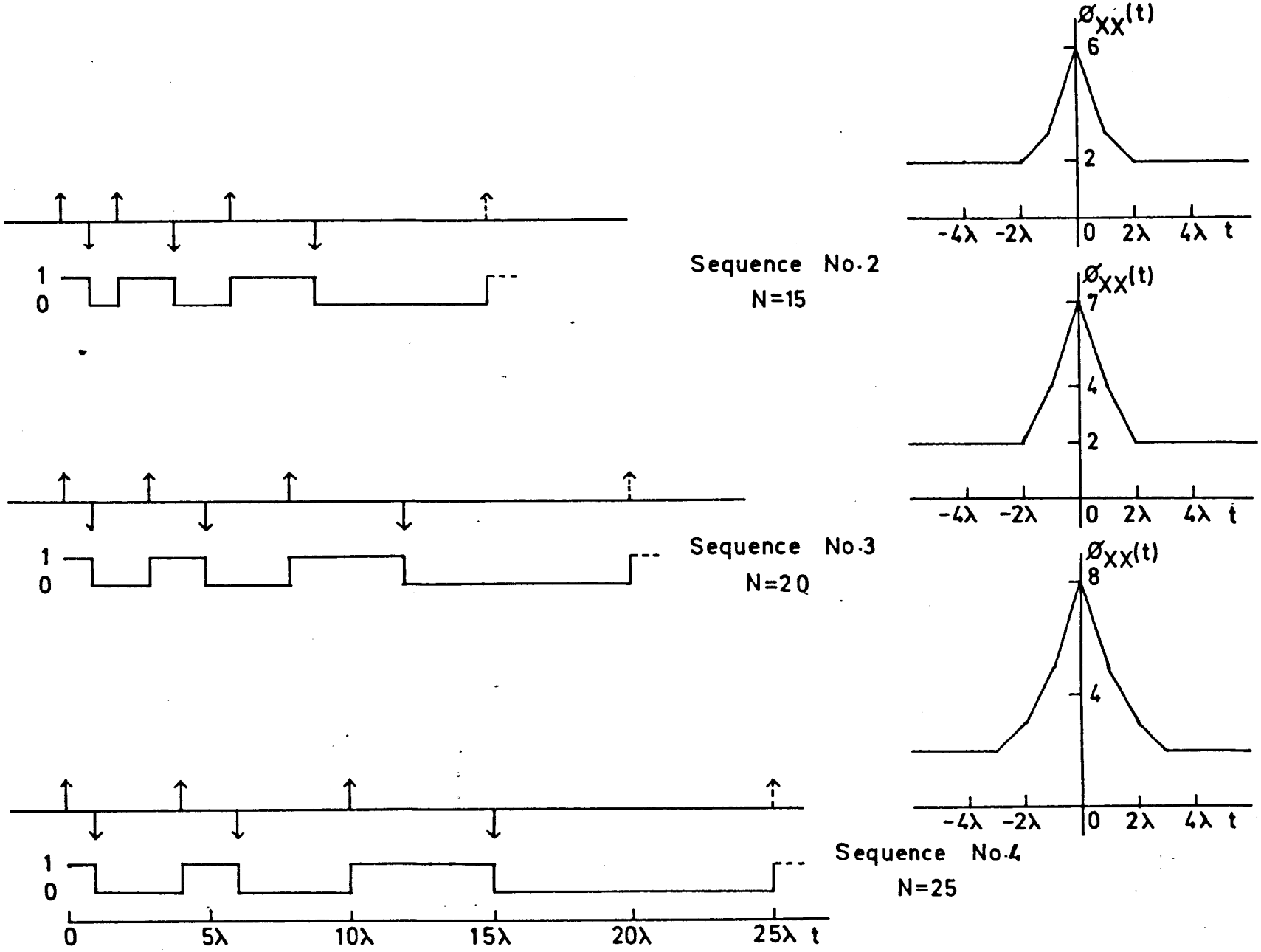

FIG. 43 AUTOCORRELATION FUNCTION AND THE IMPULSE TRAINS OF NEW SEQUENCES

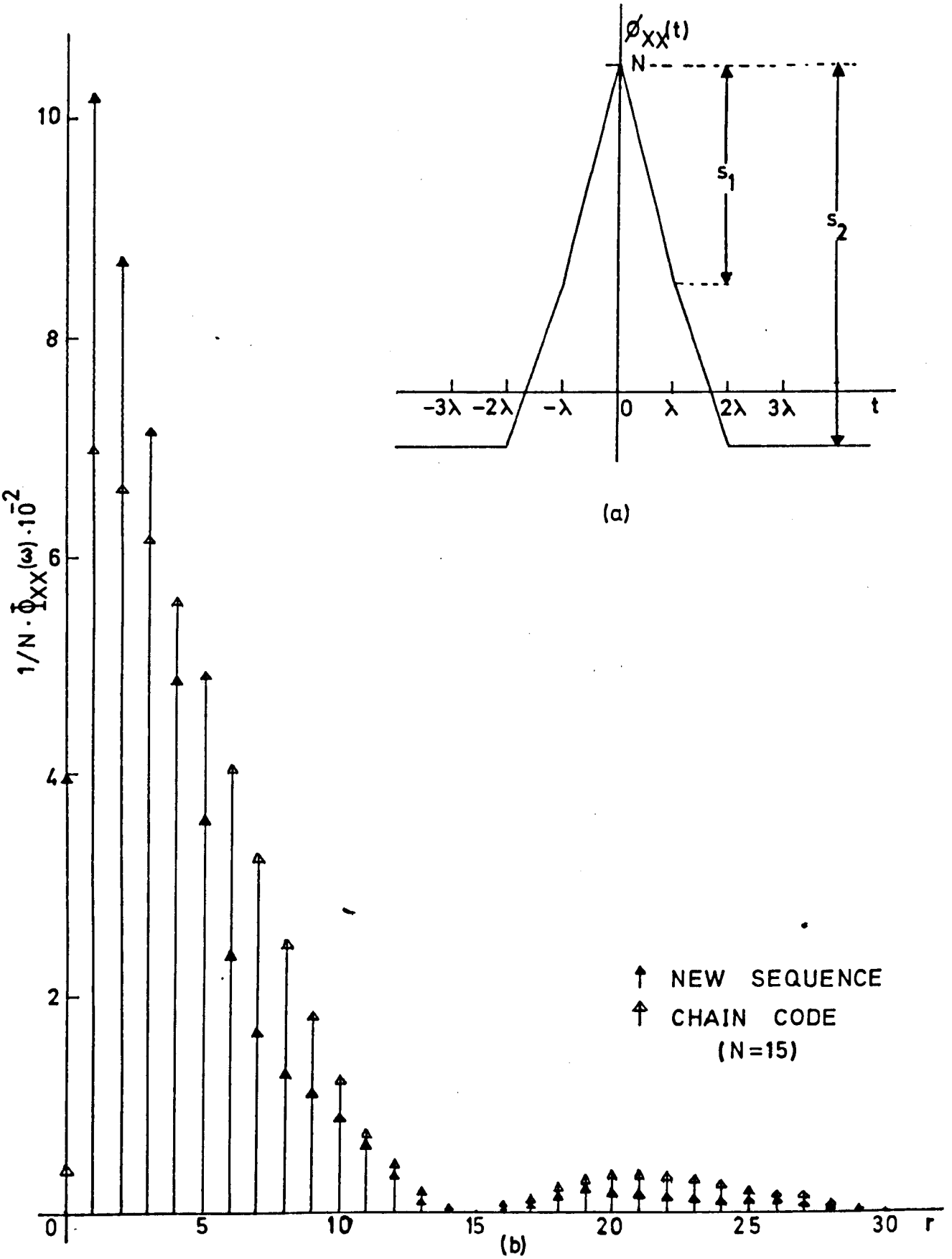

FIG. 44 POWER SPECTRUM OF THE NEW SEQUENCE

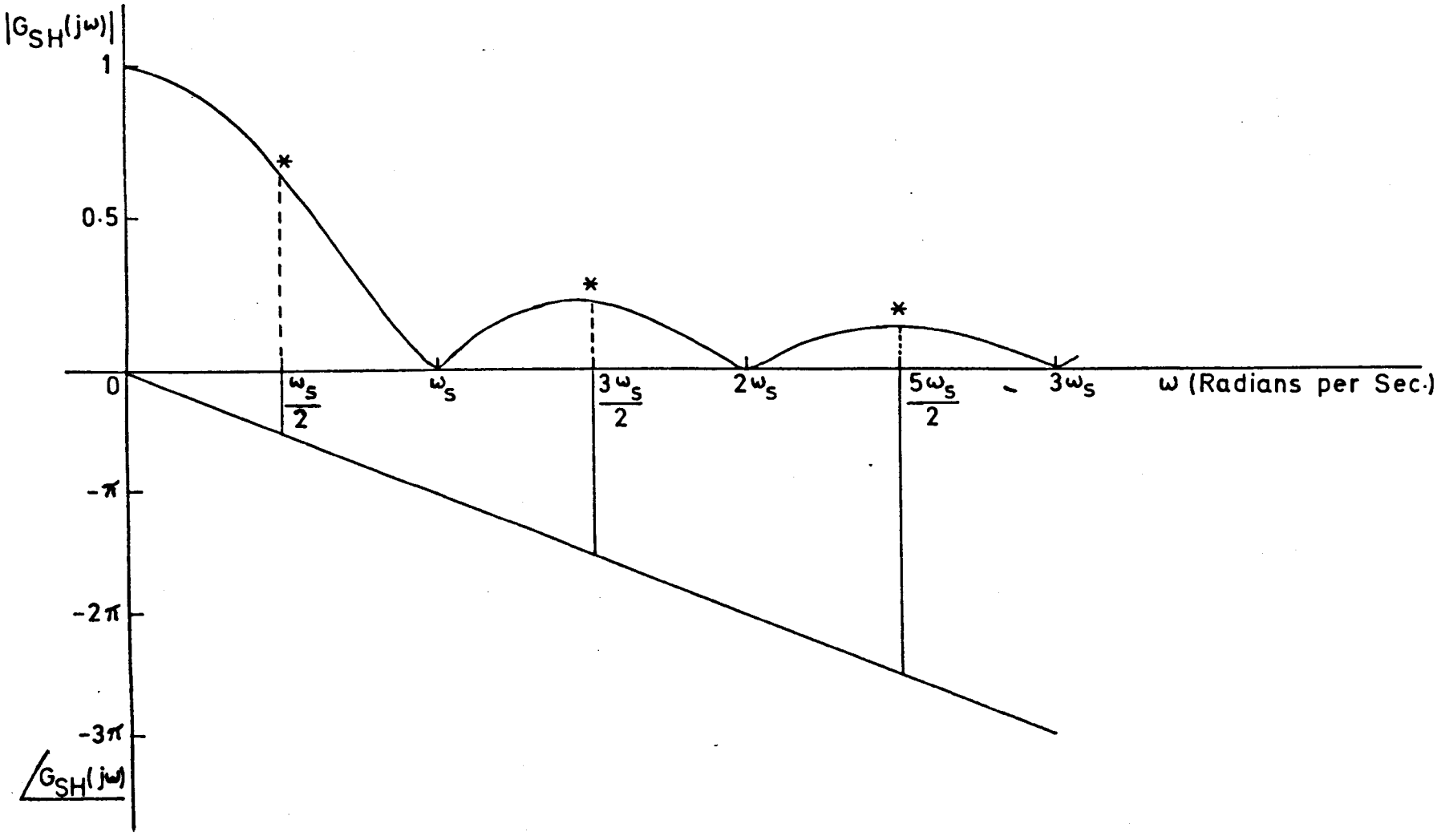

FIG. 45 QUOTED FREQUENCY RESPONSE OF SAMPLE AND HOLD
* Points of Discontinuity

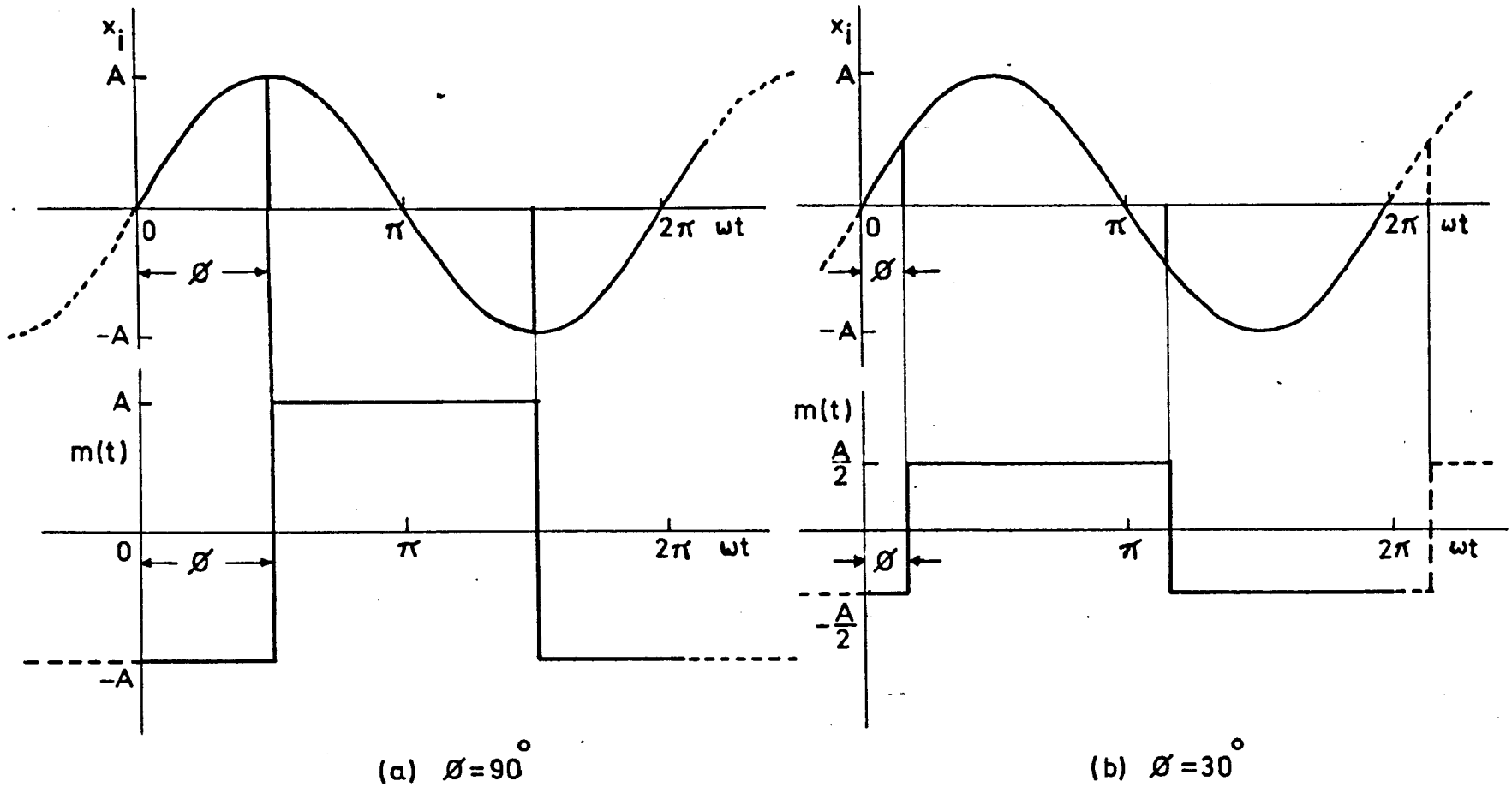

FIG. 46 OUTPUT OF SAMPLE AND HOLD FOR $\omega = \frac{\omega_s}{2}$

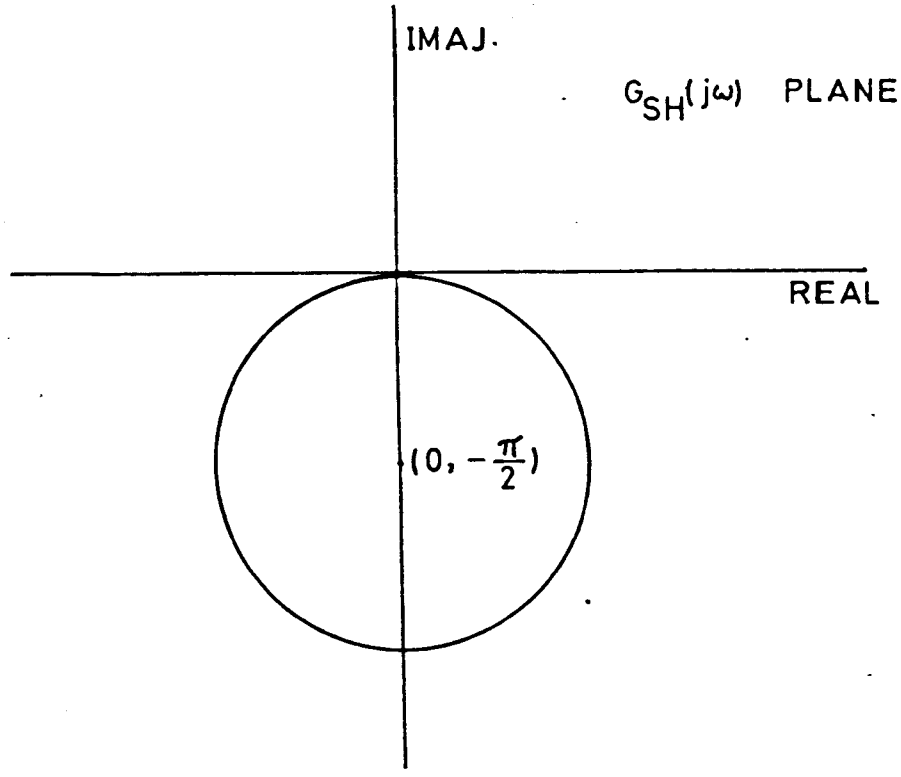

FIG. 47 RESPONSE ON THE COMPLEX PLANE FOR $\omega = \frac{\omega_s}{2}$

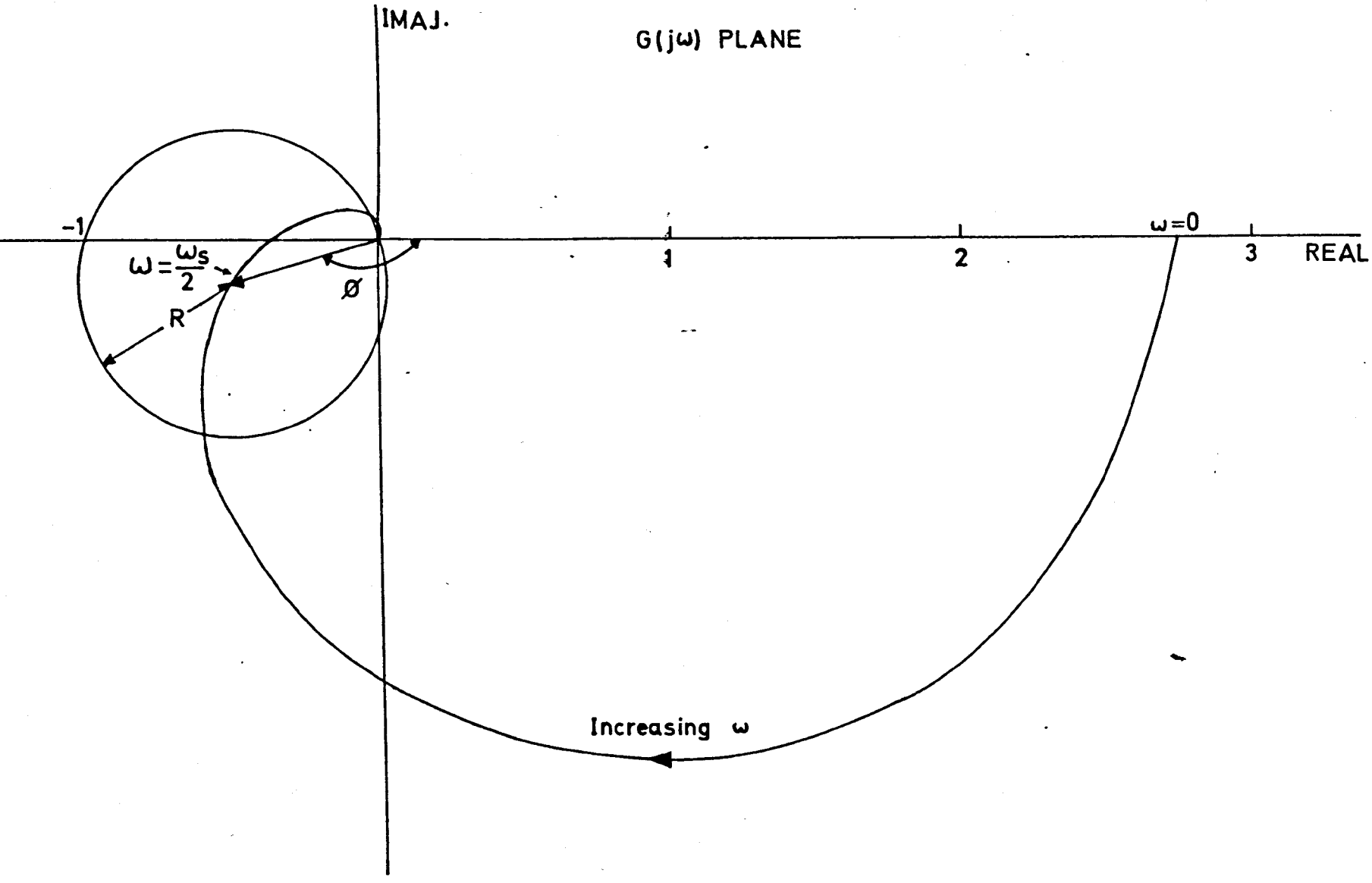

FIG. 48 NYQUIST PLOT OF THE SYSTEM WHEN $G_p = \frac{K}{1+T_1 p}$

$T_1 = T_s = \frac{2\pi}{\omega_s} = 1 \cdot \quad K = 2.73$

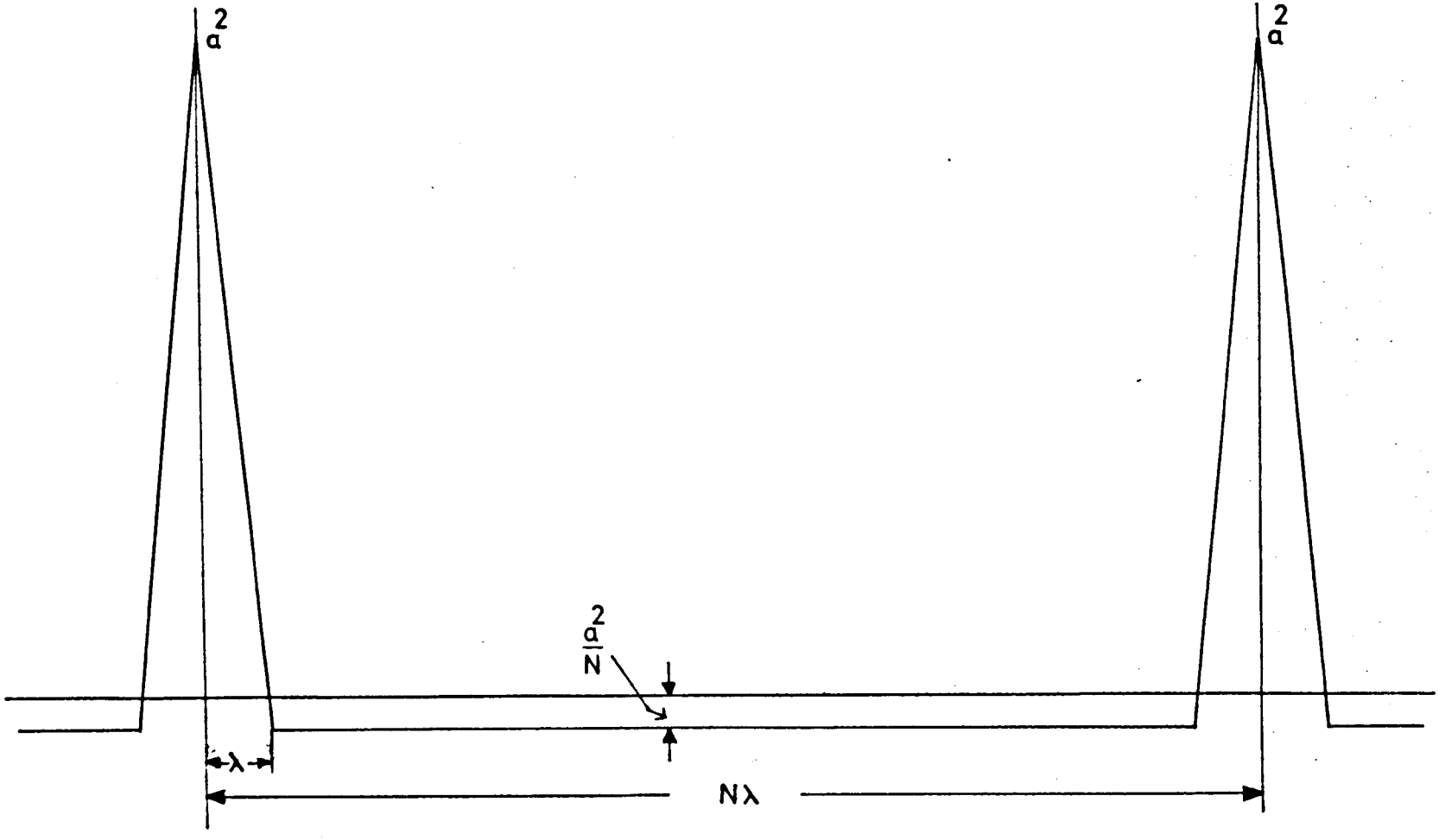

FIG. 49 AUTOCORRELATION FUNCTION OF PRBS

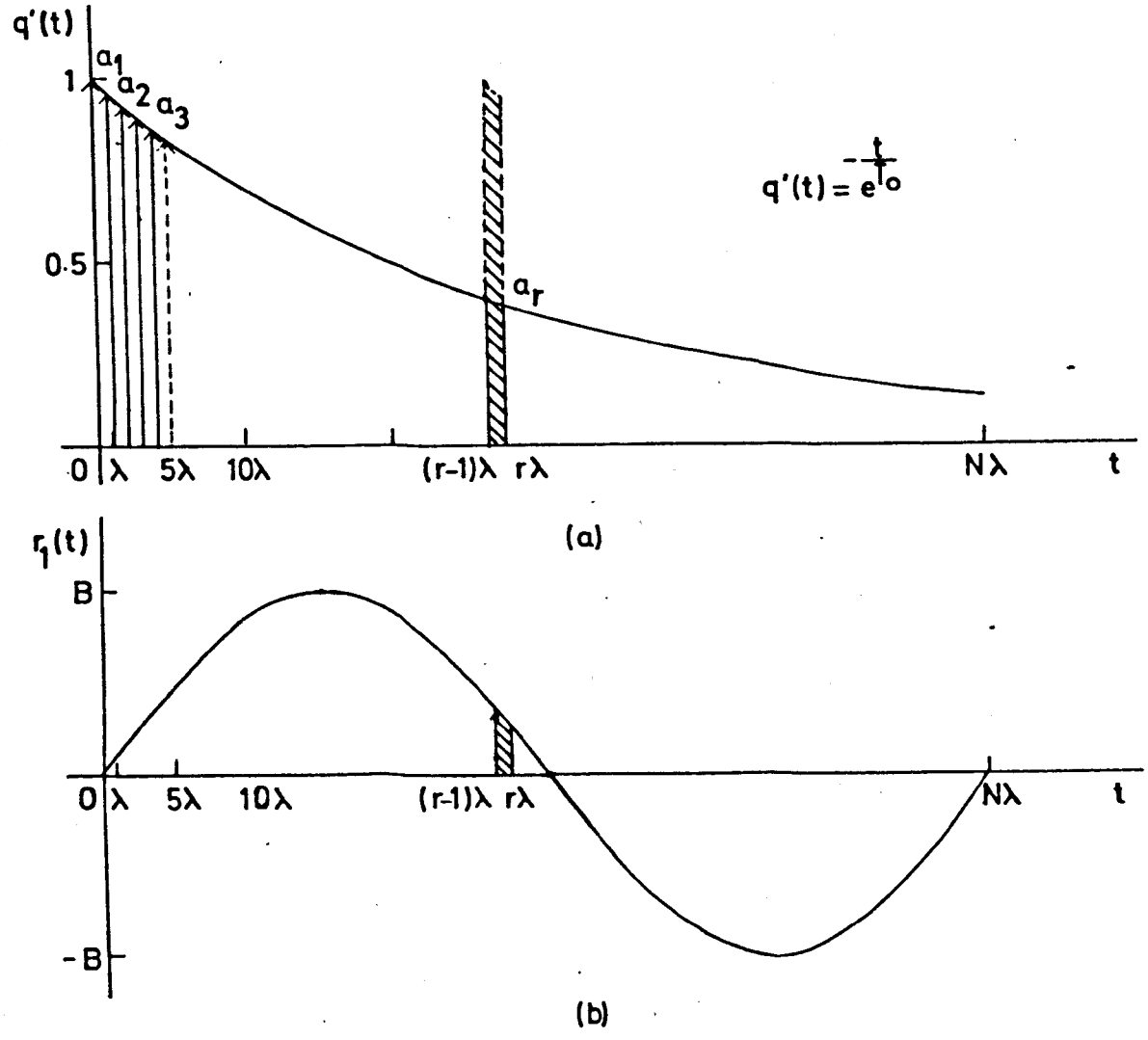

FIG. 50 CALCULATION OF SYSTEM RESPONSE

(a) PLOT OF q'(t)

(b) PLOT OF THE SINUSOIDAL APPROXIMATION OF r(t)

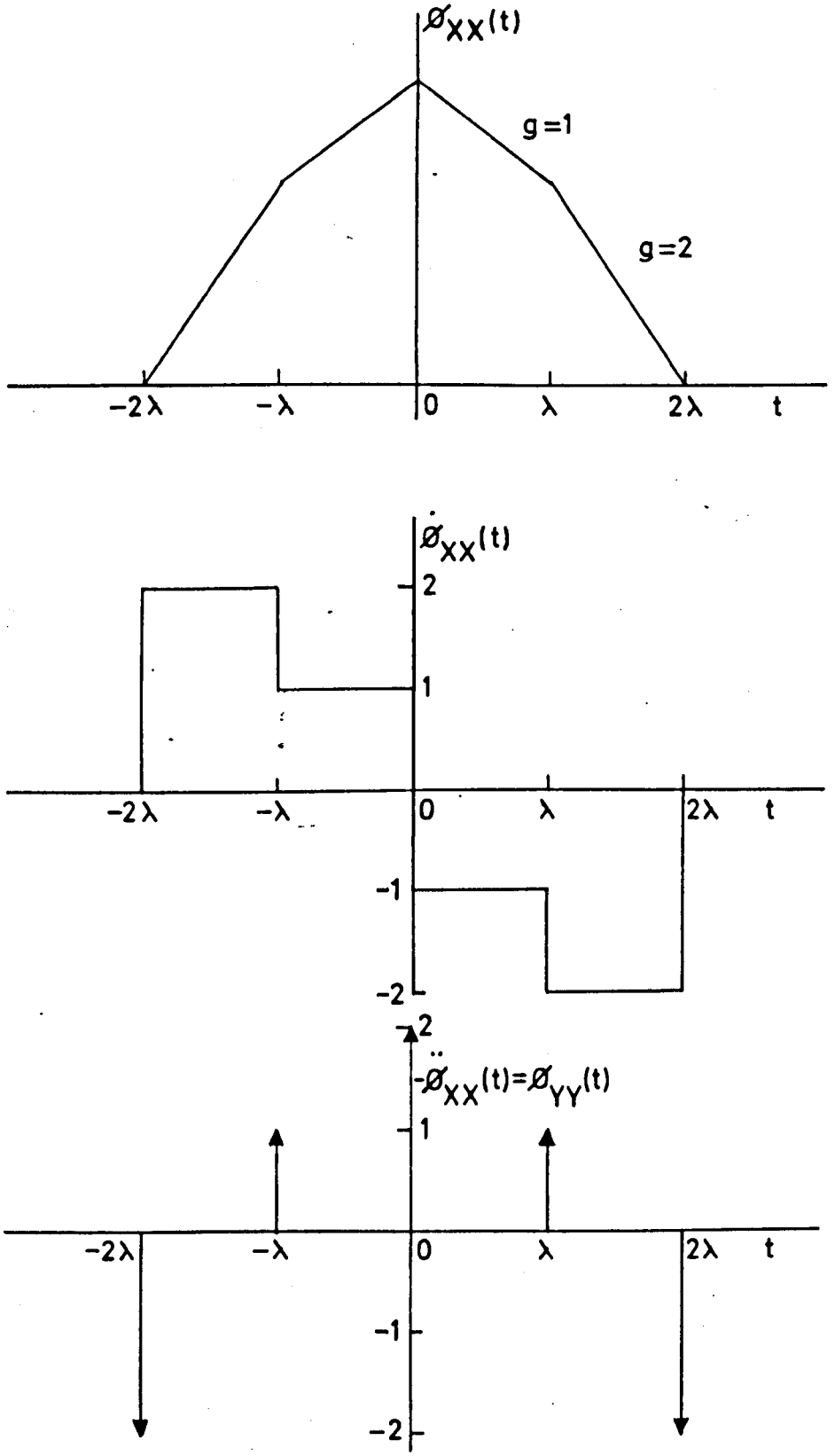

FIG. 51 OUTPUT AND INPUT AUTOCORRELATION FUNCTIONS

Simultaneous equation model

$$\underset{(18,1763)}{Mri = 16,6920} \underset{(0,632)}{- 0,6557\ W1960} \underset{(1,823)}{- 2,972\ Wi} \underset{(0,00236)}{+ 0,00094\ R1960}$$

$$\underset{(0,180101)}{+ 0,08012\ IDj} \underset{(0,0197)}{+ 0,00728\ Ri}$$

$$\underset{(1,57731)}{Wi = 3,16187} \underset{(0,00098)}{+ 0,0007904\ U1960} \underset{(0,3225)}{+ 0,02435\ Mri} \underset{(0,00564)}{- 0,00143\ Ri}$$

$$\underset{(71,8439)}{Ri = -16,3797} \underset{(1,20782)}{+ 9,37910\ Mri} \underset{(0,148192)}{+ 0,215564\ Ti}$$

LIST OF REFERENCES

(1) MIYAMI R. — Population migration away from agriculture in Japan
ECONOMIC DEVELOPMENT AND CULTURAL CHANGE
(1966 - 67) Vol.15 pp.185

(2) OECD — Geographic and Occupational Mobility of rural manpower
Documentation in agriculture and food, 75 Nov. 1964.

(3) LEWIS W.A. — Economic Development with unlimited supplies of labour.
The Manchester School (22)
1954 pp.139 - 91

(4) FEI J.C. & RANIS G. — A theory of Economic Development
American Economic Review
Vol.51 1961 pp.533 - 565

(5) JORGENSON D.W. — Surplus agricultural labour and the development of a rural economy
OXFORD ECONOMIC PAPERS
1967 pp.288

(6) JOHNSTON B.F. & MELLOR J.W. — The role of agricuture in economic development
A.E.R. 1961 Vol.51 pp.566 - 593

(7) WOYTINSKY W.S. & WOYTINSKY E.S. — World Population and Production Trends and Outback.
Newyork 1953 pp.153 - 157

(8) PROF. ENOS — Research on Agricutural Income Distribution in Turkey (1962)
Unpublished report under the supervision of State Planning Organization.